ABSTRACT

MARKS, ODESSA. Generation of Severe Combined Immunodeficient (SCID) Pigs: A Novel Large Animal Model for Human Stem Cell Research. (Under the direction of committee chair Jorge A. Piedrahita, PhD).

Pigs are an excellent large animal model for studies of human disease because of their similarities to humans in organ size and physiology. Developing pigs with severe combined immunodeficiency (SCID) would offer a powerful tool for human biomedical research. I report the generation of a "double knockout" SCID pig containing inactivating mutations in the genes encoding interleukin-2 receptor subunit gamma (IL2RG) and recombination activating gene 1 (RAG1) using transcription activator-like effector nucleases (TALENs). SCID pigs have no functional T, B, or NK lymphocytes and have an atrophic, non-functional thymic remnant, with loss of lymph nodes and Peyer's patches. Their spleens lack germinal centers and red/white pulp differentiation. Serum IgM, IgG, and IgA are absent in SCID pigs.

Allogeneic bone marrow transplantation (BMT) with T cell depleted porcine bone marrow was performed on SCID pigs. Intravenous BMT led to transient reconstitution of only the T cell lineage, while intraosseous BMT reconstituted T cells, B cells, and low levels of NK cells. Engrafted T cells after allogeneic BMT predominantly displayed an activated, memory phenotype, likely due to the absence of a functional thymus and extrathymic differentiation of peripheral T cell progenitors. Transplanted pigs that showed strong B cell repopulation also expressed plasma IgM and IgG up to WT levels, but not IgA. While irradiation led to earlier engraftment following allogeneic BMT, it was also quite toxic to the pigs, while higher levels of late engraftment were achieved without irradiation.

To generate SCID pigs reconstituted with human lymphocytes, human CD34+ cells were transplanted into SCID pigs, leading to successful engraftment with human T cells,

which repopulated the blood, spleen, thymus, and bone marrow, as well as human B cells, which repopulated the blood and spleen. *In utero* intrahepatic transplantation of human donor cells was significantly more effective than postnatal intraosseous transplantation. Engrafted human T cells predominantly expressed a naïve phenotype, with lineage marker expression largely consistent with normal thymic T cell development. Human IgM was present in the plasma, reflecting the presence of functional B cells. These findings constitute the first successful construction of a "humanized" SCID pig reconstituted with a human immune system. The humanized pig represents a powerful new animal model for numerous biomedical disciplines, particularly for the development of novel approaches to human transplantation and stem cell therapy.

Generation of Severe Combined Immunodeficient (SCID) Pigs: A Novel Large Animal Model for Human Stem Cell Research.

by
Odessa Amanda Marks

A dissertation submitted to the Graduate Faculty of
North Carolina State University
in partial fulfillment of the
requirements for the degree of
Doctor of Philosophy

Comparative Biomedical Sciences

Raleigh, North Carolina

2014

APPROVED BY:

_____

Jorge Piedrahita, PhD
Committee Chair

_____
Luke Borst, DVM, PhD

_____
Paul Hess, DVM, PhD

_____
Sam Jones, DVM, PhD, DACVIM

_____
Shila Nordone, PhD

DEDICATION

To my grandmother, Mavis Stewart, the completion of my dissertation is the fulfillment of a promise I made to you many years ago. I pray that as you look down from heaven, you are smiling. Please know that you are forever my greatest inspiration. Thank you for giving our family the gift of "the circle."

To my brother, Geramy Marks, thank you for showing me that the only limit to our aspirations is in our ability to dream far beyond what is expected of us. Whatever I have is yours, and I will forever be in awe of your kindness and love. Please remember to never limit your own heart's aspirations.

To my husband, Joshua Lacsina, you are God's perfect reflection of love for me. You are my heart's joy. You give me strength when I am tired, and ask more of me when I think I have done my best. I am honored to be your wife.

I love you with my whole heart: OAC!

To my mother, Celeste Marks, your prayers, love and unbreakable faith give me the strength I needed to keep pressing forward. Because you first believed in me I believed I could accomplish all things through Him who strengthens me.

BIOGRAPHY

Odessa Amanda Marks was born in Guyana, South America. Her family home was 10 minutes from the beach, which, as a young child, she would visit frequently with her parents. She loved the beach so much that her father had sand relocated from their favorite beach to cover part of their lawn. A few years later, Odessa's parents, Celeste and Michael Marks, and her brother, Geramy, immigrated to Brooklyn in New York City, so that both she and her brother could be educated in America. Odessa enjoyed a happy childhood, and pursued numerous interests as she grew into her adult life, including cheerleading, modeling, and founding a modeling agency. Odessa's grandmother, Mavis Stewart, insisted that both she and her brother attain the highest levels of academic achievement, saying, "Education is the key to any door you wish to enter." Those words were forever instilled in Odessa's heart, and guided Odessa as she pursued a degree in biology at Eastern University, a private Christian school near Philadelphia, PA. The first time she met with her college mentor, Dr. David Wilcox, Odessa told him that she wanted to graduate with a Bachelor of Science degree in 3 years with honors. Odessa accomplished her college goal and was awarded a research scholarship to study at Dartmouth University, where she worked with MCF-7 breast cancer cells, her first introduction to mammalian cell culture. In 2004, Odessa was accepted to Duke's Postbaccalaureate Research Education Program (PREP), where she discovered the function of single nucleotide polymorphisms (SNPs) that regulate alternative splicing of the mRNA for TNNI3K, a heart-specific kinase that modulates the phenotype of a mouse model of dilated cardiomyopathy. While at Duke, she met and started dating her future husband, Joshua Lacsina, as he was starting his first lab rotation of graduate school in 2005.

In 2006, Odessa began her PhD studies at the North Carolina State University College of Veterinary Medicine (CVM) through the Comparative Biomedical Sciences Graduate Program. Her initial work focused on the S2 accessory protein of equine infectious anemia virus in the laboratory of Dr. Fred Fuller. In 2007, she was awarded the George H. Hitchings New Investigator Award in Health Research, from the Triangle Community Foundation. In 2010, Odessa joined the laboratory of Dr. Jorge Piedrahita and began to work on the generation of SCID pigs in 2011. During her graduate studies, Odessa served as a two term President of the NCSU CVM Graduate Student Association and was twice awarded the annual Academic Achievement Award from the NCSU Association for the Concerns of African American Graduate Students (ACAAGS).

In 2014, Odessa completed her graduate studies and married Joshua, her fellow sweetheart in science and life. Their honeymoon brought Odessa back to the Caribbean for the first time since she left Guyana, as the newlyweds enjoyed the quiet beaches of Providenciales in Turks and Caicos. Shortly after returning, Odessa moved from Raleigh to Seattle, WA with her husband, Joshua. Together, they will be living in Naivasha, Kenya for a year starting in June 2015. While there, Odessa hopes to pursue postdoctoral research at the intersection of molecular biology and global health. Her long-term research focuses are vaccine development, and, inspired by both her graduate research and the words of her grandmother, organ production and tissue repair in regenerative medicine.

ACKNOWLEDGMENTS

To my pet cat, Kitty, who played the critical role in my first ever scientific experiment. Now, as an adult, I am forever thankful you lived. You were the catalyst of my scientific curiosity.

To my many research mentors from college and beyond: Dr. David Wilcox and Dr. Maria E. Fichera at Eastern Univeristy, to Dr. William North at Dartmouth College where I received my first research scholarship. At Duke University, to Dr. Kenneth Kreuzer with PREP, Dr. Mariano Garcia-Blanco and Dr. Douglas Marchuk, with whom I published my first scientific manuscript. At the North Carolina State University College of Veterinary Medicine, to Dr. Prema Arasu, who was the first person at NCSU to believe in me, see my potential, and give me the opportunity to pursue my lifelong dream of becoming a scientist. To Dr. Fred Fuller, who introduced me to the field of virology, to Dr. Shila Nordone and Dr. Isbel Gimeno. Thank you for being great mentors and role models to me.

To Jorge Piedrahita, for welcoming me into your laboratory, for helping me to take my first tentative steps into the wonders of the regenerative medicine field. One of my favorite moments occurred during one of the allogeneic transplantation experiments, when I was exhausted from working continuously for almost 48 hours. I was processing pig bone marrow and by the end of the experiment I did not have enough viable cells to transplant into the double knockout SCID pigs. You came into the cell culture room where I had been working and I gave you the bad news. You asked if I had any frozen bone marrow saved that I could use and I replied that I had some frozen H2B-GFP bone marrow. You saw the fatigue and frustration on my face and said to me, “I know that you are tired, but these are the

moments that your science means the most." Those words inspired me to complete the isolation and intraosseous transplantation that night. I don't know if you knew this, but the oldest living double knockout transplanted SCID piglet at 97 days was the piglet that received that H2B-GFP bone marrow after our talk in the cell culture room all those tiring nights ago. Thank you for teaching me that lesson in life and as a scientist.

To all the Piedrahita lab members, past members Dr. Shengdar Tsai, Dr. Steve Bischoff, Dr. Sehwon Koh, Dr. Ling Guo, Ashley Sough, and Liz Selisker, thank you for teaching me about science and life. And to the present members Demeterio Dichoso, Xia Zhang, Sean Simpson, Bruce Collins, Jaewok Chung, Dr. Renan Sper, and Hannah Reynolds, I am so thankful for your many days and nights of helping me to manage the enormous task of taking care of all of the SCID pigs, I could not have completed this project without your help, I am forever grateful.

To Dr. Gabriel McKeon, Dr. Charles Long, Maria Stone, and all of the LAR staff who cared for my SCID piglets. To Dr. Barb Sherry, for assistance with the Western blotting experiments. To Dr. Liara Gonzalez, thank for your helping me to remember to have fun and for verifying the loss of lymph nodes in my SCID piglets. To Sitka Eguiluz thank you for your help and for being so awesome. To Dr. Steve Suter, for providing Neupogen for our transplantation experiments. To Dr. Charles Gersbach from Duke University for the pSSA plasmid that was used for TALEN functional screening. To Dr. Jeffrey Platt at the University of Michigan for the mobilized human hematopoietic cells.

To the Duke Catholic Center, for offering me a faith home and a lovi ng community. To Fathers Joe Vetter, John McDonagh, and Mike Martin, and to Catherine Preston and the

community of Catholic graduate students at Duke. And special thanks and appreciation to Father John McDonagh for officiating the Sacrament of Marriage for me and my new husband, Joshua Lacsina.

To my best friends and sisters: Lakiema McNeill, Sarah Billeter, Atiya Lamptey, Sherry Marks, Masani Marks, Monique Marks, Mandy Ducreay, Keisha Findley, and Rashida Mengi, thank you for your love, prayers, and friendship.

To my new family, the Lacsina, Andens, and Quiambaos. To Mom Teresa and Pa Rene, thank you for your love, support and prayers, I am grateful for all that you do for Josh and I.

To my family: Emily Arnold, Ethan Arnold, Anika London, Geramy Marks, Sherry Marks, Naomi Marks, Maya Marks, Mikey Marks, Masani Marks, Monique Marks, Stevin Marks, Sharmy Simmons Rasheed, Arron Rasheed, Peggy Simmons, Oneal Simmons, Elizabeth Stewart, and Aubrey Stuart, I am truly blessed to have you in my life.

To my parents Michael Marks and Celeste Marks, thank you for your overwhelming love and support. This is as much your accomplishment as it is mine; thank you and I love you.

To my husband, Joshua Lacsina, I will love you forever and thanks for “being sure.” I am so thankful that God created us for each other.

To my Lord and Savior, Jesus Christ, all of my accomplishments are a testament and service to you and the path you have given to me. Thank you for giving me the gift of science. To God be all the glory! Amen!!

TABLE OF CONTENTS

LIST OF FIGURES

LIST OF TABLES

CHAPTER 1: INTRODUCTION

1.1. "Humanized" animal models for the study of human physiology and disease.

Animal models are essential tools for biomedical research and the development and testing of novel therapeutic agents. While direct studies of human subjects and clinical trials are ultimately needed to validate discoveries made in animal models, the range of experimentation possible with humans is limited by ethical considerations, in addition to being both resource and time intensive. With the wide availability of molecular tools for transgenesis and targeted genomic mutation in mammalian organisms, *in vivo* studies in animal models allow for mechanistically detailed and relatively rapid testing of hypotheses and provide an avenue for preclinical safety testing before embarking on potentially risky and costly human trials. The challenge, then, is to develop animal models that are similar enough to human physiology to be predictive of how diseases and novel therapies will behave in human subjects.

One major success in making a more "physiologic" animal model is the development of human hemato-lymphoid system mice, termed "humanized" mice (Rongvaux et al., 2013), in which the murine immune system is replaced with human hematopoietic cells. This allows the unparalleled opportunity to investigate the human immune system *in vivo* in a model organism that can be readily and precisely manipulated experimentally. To facilitate engraftment of the xenotransplanted human immune system, the endogenous murine immune system must be eliminated; this is accomplished via targeted mutations (a.k.a. "knockouts") of genes essential to the early development of the immune system, producing immunodeficient mice. In the following sections, I will review how these genetically

immunodeficient mice were developed and subsequently utilized to produce humanized mice. I focus on the inactivation of two essential and widely conserved genes that are necessary for lymphocyte development: IL2RG and RAG1. I will then discuss the limitations of using humanized mice, and the prospects for developing a human hemato-lymphoid system large animal model – specifically, the pig – that more accurately recapitulates human physiology.

1.2. Of humanized mice and men: mice with severe combined immunodeficiency and engraftment with human hematopoietic cells.

In 1983, a mutation in the PRKDC gene (protein kinase, DNA activated, catalytic polypeptide) was found to cause the absence of mature B and T cells in CB-17 mice, known thereafter as *scid* (severe combined immunodeficiency) mice (Bosma et al., 1983). Five years later, multiple groups reported the successful engraftment of human peripheral blood mononuclear cells (PBMCs), fetal hematopoietic tissue, and hematopoietic stem cells (HSCs) into *scid* mice (Lapidot et al., 1992; McCune et al., 1988; Mosier et al., 1988), however engraftment was at a low level and did not reconstitute a functional human immune system. One reason for the poor engraftment in *scid* mice was the persistence of natural killer (NK) cells, which inhibit human hematopoietic cell engraftment (Christianson et al., 1996). This was addressed by crossing the *scid* mutation onto the non-obese diabetic (NOD) mouse background; NOD-*scid* mice have intrinsically lower levels of NK cell activity as well as impairments in innate immunity (Shultz et al., 1995), both of which improved engraftment with human PBMCs and HSCs (Hesselton et al., 1995; Lowry et al., 1996; Pflumio et al., 1996).

Another barrier to *scid* mouse engraftment with human cells was the spontaneous generation of murine B and T cells later in the life of the mouse. To address this, knockout mice were developed with functional inactivation of recombination-activating gene 1 (RAG1) or RAG2. These genes encode the RAG1/2 enzymes that catalyze site-specific V(D)J recombination and thereby produce the sequence diversity in immunoglobulins (Igs) from B cells and the T cell receptor (TCR) on T cells to generate a lymphocyte repertoire that can respond to a diverse range of antigens with high specificity (McBlane et al., 1995; de Villartay et al., 2003). The RAG1 and RAG2 proteins are encoded on adjacent genes and work synergistically by binding the recombination signal sequences adjacent to each gene segment participating in the V(D)J recombination reaction and thereby directing the location of DNA cleavage (Oettinger et al., 1990) (Bassing et al., 2002). The RAG1/2 proteins assembled within the synaptic complex cleave DNA, with non-adjacent sequences processed and repaired by the non-homologous end joining pathway to complete the recombination event. Naturally occurring mutations in RAG1 or RAG2 in humans result in the loss of all T and B cells (Schwarz et al., 1996), or Omenn syndrome, in which T cells are autoreactive due to the deficiency in V(D)J recombination (Villa et al., 1998). Mice with inactivating mutations in either RAG1 or RAG2 lack mature T and B cells, but only show limited engraftment with human hematopoietic cells due to the persistence of NK cells (Mombaerts et al., 1992; Shinkai et al., 1992).

The needed breakthrough to improve human cell engraftment came with the development of SCID mice bearing homozygous mutations of the interleukin-2 receptor γ-chain (IL2RG), also known as the common cytokine-receptor γ-chain. IL2RG is a shared

common subunit that is a necessary component of the cytokine receptors for IL-2, IL-4, IL-7, IL-9, IL-15, and IL-21 (Sugamura et al., 1996). Signaling through IL2RG occurs via the association of its cytoplasmic tail with JAK3, such that mutations in IL2RG that disrupt the JAK3 interaction lead to more severe immunodeficiency (Russell et al., 1994). Because IL2RG is necessary for the signaling of numerous cytokines, knockout of IL2RG in mice severely impairs the development of B and T cells, and completely eliminates NK cells due to their dependence on IL-15 (Cao et al., 1995; DiSanto et al., 1995; Ohbo et al., 1996). There are naturally occurring human mutations of IL2RG, which is located on the human X chromosome and therefore causes X-linked SCID (Puck et al., 1993). Unlike IL2RG knockout mice, which lack all lymphocyte lineages, human X-linked SCID patients have diminished T cells in their peripheral blood and normal B cell numbers, but the B cells are non-functional, highlighting the differences in IL2RG function between humans and mice (Noguchi et al., 1993). IL2RG knockout mice were crossed into both the NOD-*scid* and NOD-RAG2-/- backgrounds, both of which showed the highest levels of engraftment of human PBMCs and HSCs seen for any of the humanized mouse models as well as development of functional human blood and immune systems (Ishikawa et al., 2005; Ito et al., 2002; Shultz et al., 2005; Traggiai et al., 2004).

The goal of transplantation when making humanized mice is to direct human HSCs to a supportive microenvironmental niche within the SCID mouse (Shultz et al., 2012). Approaches differ between research groups, including administration of donor cells via intravenous (Ishikawa et al., 2005), intrahepatic (Traggiai et al., 2004), intraosseous

(Mazurier et al., 2003), and *in utero* (Schoeberlein et al., 2004) routes, however head-to-head comparisons of engraftment protocols are lacking for humanized mice.

1.3. Limitations in mouse models and the advantages of swine as a novel large animal model for human immunology.

Despite the wealth of knowledge gained from experiments with humanized mice, there are still limitations in the translatability of that knowledge to human immunology and biomedicine. Mice have diverged extensively from humans to the point that there are major differences in numerous aspects of innate and adaptive immunity between the two species (Mestas and Hughes, 2004). Some particularly divergent immunologic features include the percentages of different immune effector cells, the tissue distribution of Toll like receptor (TLR) expression, cell surface markers, immunoglobulin classes, interleukins, the regulation of Th1 and Th2 signaling and differentiation, and the phenotypes of various genetic knockouts, including IL2RG, discussed previously (Mestas and Hughes, 2004). A recent high profile article raised particular concern that genomic responses to inflammation are very different between mice and humans (Seok et al., 2013), however a recent reanalysis of that data set called that conclusion into question and actually suggests strong interspecies correlation for specific functional classes of genes (Takao and Miyakawa, 2014). The small size and short lifespan of mice make it challenging to perform surgical procedures and experiments over a protracted time course that requires serial collections of blood or tissue. There is thus an urgent need for a humanized large animal model that better mirrors human physiology and immune function.

Pigs are an excellent model organism for biomedical research because of their similarities to humans in size, anatomy, physiology, and metabolism (Lunney, 2007). Pigs are genetically more closely related to humans than mice and share a more similar chromosome structure (Hart et al., 2007; Jørgensen et al., 2005; Sun et al., 1999; Wernersson et al., 2005). With their longer lifespan of 10 to 20 years, pigs are better suited for studies that require long-term follow-up over a clinically relevant time frame, including cancer, stem cell biology, and transplantation. Several disease processes progress similarly between humans and pigs, including cardiovascular disease and infections that are shared by both species. As a large animal experimental model, pigs offer the advantages of reaching early sexual maturity (by 5 to 8 months), having a variety of breeds, a short generation interval of 12 months with breeding in all seasons (Wolf et al., 2000), and large litters, containing 10 to 12 piglets on average (Aigner et al., 2010). Standardized practices for pig housing, feeding, and hygiene are well-developed with regularly updated consensus guidelines. With an increasing number of well-defined porcine cell lines, molecular tools, pig-specific microarrays (Meurens et al., 2012), and publication of a complete draft of the pig genome (Groenen et al., 2012), the pig model has recently become much more accessible to precise experimental manipulation. The emergence of techniques allowing targeted modification of the pig genome has resulted in a surge of novel porcine models of human diseases, including Alzheimer's disease (Kragh et al., 2009), Huntington's disease (Uchida et al., 2001), retinitis pigmentosa (Kraft et al., 2005; Petters et al., 1997), cardiovascular disease (Hao et al., 2006), cystic fibrosis (Rogers et al., 2008a, 2008b; Stoltz et al., 2013), and type 2 diabetes (Renner et al., 2010).

In comparing the pig, mouse, and human immune systems, the pig was the more similar organism to human for >80% of measured immunologic parameters compared to <10% for mice (Dawson, 2011). All the major immune cell populations described in humans and mice are present in pigs (Meurens et al., 2012). Humans and pigs both have high percentages of peripheral blood neutrophils (50 to 70%), in contrast to mice (Fairbairn et al., 2011). Porcine orthologs have been identified for all the human cytokines that mediate Th1, Th2, Th17, and Treg differentiation, function, and signaling (Käser et al., 2011; Kiros et al., 2011; Murtaugh et al., 2009). The human neutrophil chemoattractant, IL-8, has a direct pig ortholog while mice have no such homolog (Fairbairn et al., 2011). While the expression of TLRs 7 and 9 is limited to plasmacytoid dendritic cells (DCs) in humans and pigs, these TLRs are also expressed on conventional DCs in mice, making pigs a likely more accurate model of innate immune responses to pathogen-associated molecular patterns (PAMPs) and vaccine adjuvants (Summerfield and McCullough, 2009). In models of sepsis, mice are extremely resistant to endotoxin-induced shock, whereas pigs and humans are both quite sensitive to endotoxin (Fairbairn et al., 2011). Swine are now more tractable models for immunologic study, due to the publication of comprehensive catalogs of swine leukocyte antigens (Piriou-Guzylack and Salmon, 2008), the increasing commercial availability of pig-specific ELISAs and antibodies (Meurens et al., 2012), and the discovery of antibodies that cross-react between human and swine antigens (Faldyna et al., 2007).

1.4. Comparing the immune systems of humans and pigs: a primer on porcine lymphocyte development.

In preparation for constructing a SCID pig and subsequently, a humanized pig, there are some differences to note between the porcine and human immune systems. Pigs express species-specific antimicrobial host defense peptides while lacking α-defensins (Sang et al., 2009). Porcine lymph nodes have an unusual inverted structure which lacks a typical medulla, and is instead composed of a cortical layer surrounded by a paracortex (Rothkötter, 2009). In addition to the typical discrete Peyer's patches seen in the jejunum, pigs also have a continuous ileal Peyer's patch similar to ruminant animals, including sheep and cattle (Barman et al., 1997). The porcine ileal Peyer's patch exists for only a short time in the early postnatal period, and its function in lymphocyte development remains unclear. In humans, passive immunity is conveyed by the mother to her fetus transplacentally in the form of IgG, and after birth, via breast milk containing IgA which coats the mucosal surfaces of the infant's GI tract. In contrast, fetal pigs do not receive maternal antibodies via the placenta; rather, they take up maternal antibodies from the milk or colostrum during neonatal suckling via a specialized mechanism in their gut mucosa whereby enterocytes non-selectively transport macromolecules from the gut lumen into the bloodstream of the newborn piglet (Kömüves and Heath, 1992). This non-specific macromolecule uptake ceases within 24 to 48 hours after birth during a period known as "gut closure" (Leary and Lecce, 1978). Interestingly, there is even evidence that antigen-specific lymphocytes can be taken up by the neonatal gastrointestinal tract and function in the piglet prior to gut closure (Nechvatalova et

al., 2011), highlighting the importance of passively transferred, maternal cell-mediated and humoral immunity in the early neonatal period.

Porcine lymphocyte development is overall quite similar to humans, with a few notable exceptions. Hematopoietic development begins in the porcine yolk sac, and lasts from day of gestation (DG) 16 to DG27, however only a relatively small amount of hematopoietic progenitors are produced during this period (Sinkora and Butler, 2009). B cells are the first of the lymphocyte lineages to appear at DG20 and are the dominant lymphocyte lineage during early gestation. Hematopoietic production is taken over by the fetal liver at DG30 and the first B cells expressing surface IgM appear around DG40. The first T cell progenitors appear on DG38, and have a surface phenotype of CD3- CD4- CD8-. Shortly thereafter on DG40, T cells are first seen in the thymus and almost universally express T cell receptors (TCRs) composed of TCRγδ heterodimers. Unlike humans, γδ T cells compose the majority of T cells during fetal life and the early postnatal period (Gerner et al., 2009). In contrast to T cells bearing a standard TCRαβ heterodimer, γδ T cells participate in MHC-independent responses to non-peptide antigens via cytolytic activity and can serve as memory T cells and professional antigen presenting cells (pAPCs) to stimulate αβ T cells. V(D)J rearrangement and cell surface expression of TCRγδ takes less than 3 days, leading to the appearance of γδ T cells in the peripheral blood around DG45. In contrast, TCRαβ expression requires 15 to 20 days, such that the first αβ T cells do not appear in the thymus until DG55, and are first seen in the periphery on DG58.

DG45 marks a turning point when the bone marrow takes over from the fetal liver as the primary hematopoietic center, with liver hematopoiesis decreasing until cessation at birth.

Peripheral B cells expand rapidly during this period, and B cells remain the dominant lymphoid cell until DG55, when they are overtaken by γδ T cells, which rapidly expand at the end of gestation. Natural killer (NK) cells also make their first appearance on DG45 in the umbilical cord and spleen. NK cell numbers increase and stabilize by DG70 into postnatal life. Lymphopoiesis peaks between DG60 and DG80, during which the majority of peripheral T and B cells are produced. In the thymus, γδ T cells predominate from DG40 to DG60, at which point they are overtaken by conventional CD4+ CD8+ double positive (DP) αβ T cells, which then (similarly to humans) differentiate to either CD4+ or CD8+ single positive (SP) T cells by GD70 (Charerntantanakul and Roth, 2007).

Fetal B cells in the pig exhibit two notable unique features compared to humans. (1) Class switch recombination occurs *in utero* independently of environmental antigens, with the production of low levels of IgM, IgG, and IgA throughout the second half of gestation. (2) B cells expressing all antibody isotypes are present in the thymus through the early postnatal period, though the role of the thymus in porcine B cell development remains unclear (Butler et al., 2009).

There are also several notable differences in postnatal lymphocyte biology between humans and pigs. Among porcine T cell subpopulations, γδ T cells are present in a 2:1 ratio relative to αβ T cells at 4 months after birth, however this ratio is reversed by 12 months of age (Charerntantanakul and Roth, 2007). More CD8+ SP T cells than CD4+ SP T cells are seen in pigs, which is the opposite of the pattern seen in humans and mice (Charerntantanakul and Roth, 2007). As pigs age, the relative numbers of CD4+ SP T cells in the peripheral blood decrease while there is an increase in CD4+ CD8+ DP T cells. Double

positive T cells are not typically observed in humans, however they are common in pigs, and represent memory T cells whose progenitors were CD4+ SP T cells that acquired CD8 expression as part of the transition to the memory phenotype (Gerner et al., 2009; Stepanova et al., 2007).

Understanding the similarities and differences between the pig and human immune systems helps to contextualize the results from the allogeneic transplantation experiments described in Chapter 3 and the xenogeneic transplantation experiments with human donor cells outlined in Chapter 4. In the next sections, I will review the techniques I employed to produce targeted genomic mutations in swine and the use of somatic cell nuclear transfer (SCNT) for the rapid generation of genetically modified pigs.

1.5. Transcription activator-like effector nucleases (TALENs): a method for targeted genomic modification in swine.

The development of targetable nucleases for genomic engineering has revolutionized our ability to rapidly and efficiently produce genetically modified animal models of human disease (Carroll, 2014). This breakthrough resulted from the confluence of several lines of research: (1) the discovery that double strand breaks in chromosomal DNA stimulate the endogenous DNA repair machinery for homologous recombination (HR) or non-homologous end joining (NHEJ), (2) the discovery of zinc fingers as modular DNA recognition domains, and (3) characterization of the *FokI* endonuclease. Three major classes of targetable nucleases have been developed: zinc finger nucleases, transcription activator-like effector nucleases (TALENs), and CRISPR/Cas RNA-guided nucleases. This section will focus on

the biology and applications of TALENs, which were utilized in the present work to generate SCID pigs.

Mammalian cells contain multiple mechanisms to repair genomic double strand breaks (DSBs). Homologous recombination is one such mechanism, which uses an unbroken sister chromatid or homologous chromosome as a template in an attempt to accurately reproduce the DNA sequence lost at the DSB. HR can be appropriated for gene targeting by introducing exogenous DNA sequences flanked by regions homologous to the desired insertion site, allowing for precisely targeted gene "knock-ins" or "knockouts." Alternatively, most cells also have the machinery for non-homologous end joining, which responds to DSBs by rejoining broken chromosomal ends without regard for sequence homology, a process which often introduces short stretches of inserted or deleted sequence that produce frameshift mutations. The introduction of targeted DSBs can thereby exploit NHEJ-mediated mutagenesis to introduce mutations into genomic DNA sequences of interest.

Transcription activator-like effector (TALE) proteins are derived from plant-tropic infectious bacteria and contain sequence-specific DNA binding modules that act as transcriptional activators to promote infection (Bogdanove and Voytas, 2011). The TALE DNA-binding domain is composed of a tandem repeat of ~34 amino acids, with residues in positions 12 and 13 called repeat variable diresidues (RVDs) that correspond to base pairs in the target DNA sequence (Boch et al., 2009; Moscou and Bogdanove, 2009). TALEs bind DNA in the forward orientation, with the N-terminus of the repeat binding the 5'-most base pair. The correspondence between sets of RVDs and their DNA base pair specificity has been decoded, with numerous publicly available methods for the modular generation of TALE

domains that will bind nearly any DNA sequence of interest with high specificity (Joung and Sander, 2013).

In 1992, it was discovered that the type II restriction endonuclease, *FokI*, possessed different domains for target recognition and DNA cleavage that could be separated by proteolysis (Li et al., 1992). This finding was extended by demonstrating that fusion of the *FokI* endonuclease domain to different DNA-binding domains changed the DNA sequence specificity of the nuclease activity (Kim and Chandrasegaran, 1994; Kim et al., 1996). Transcription-activator like effector nucleases (TALENs), then, are fusion proteins that join the sequence specificity of the TALE domain to the endonuclease activity of *FokI*. For each cleavage target, two TALEN binding sites must be chosen to facilitate dimerization of the *FokI* domain, which is necessary for nuclease activity. The binding sites are separated by an intervening spacer, where the DSB is introduced. TALEN expression can be achieved in cultured mammalian cells by the standard methods of transduction or viral transduction. TALENs are less toxic and appear to be more specific than their predecessors, the zinc finger nucleases (ZFNs) (Carroll, 2014).

Both ZFNs and TALENs have been used to introduce targeted genomic modifications into swine. ZFNs were first successfully used in swine to generate pigs with a biallelic knockout of porcine α 1,3-galactosyltransferase (GGTA1) (Hauschild et al., 2011). Messenger RNA encoding ZFNs targeting IL2RG was introduced into fetal fibroblasts and combined with SCNT to produce $IL2RG^{-/Y}$ pigs that were similar in phenotype to human X-linked SCID patients (Watanabe et al., 2013). TALENs targeting the DAZL and APC genes were used to construct pig models of infertility and colon cancer, respectively (Tan et al.,

2013). One group documented monoallelic and biallelic modification rates of 54% and 17%, respectively, following TALEN delivery into porcine fibroblasts (Carlson et al., 2012). These TALENs targeted the LDL receptor gene to produce a pig model of familial hypercholesterolemia. Many of the resultant fibroblast colonies contained large chromosomal deletions (10%) or inversions (4%). More recently, TALENs have been used in swine to produce single gene biallelic knockouts of RAG1 and RAG2 within the founding generation; these studies are discussed in more detail in a later section (Huang et al., 2014; Lee et al., 2014). Overall, these studies demonstrate that swine are amenable to precise TALEN-mediated genomic modification, which has been successful in inactivating genes that regulate a wide variety of biological functions.

1.6. Somatic cell nuclear transfer for the rapid generation of genetically modified swine.

A key advance for the pig as a large animal model was the combination of TALEN technology with somatic cell nuclear transfer (SCNT), known colloquially as cloning. Successful production of cloned pigs from an adult somatic cell donor was first reported in 2000 (Polejaeva et al., 2000), and several successful SCNT protocols exist for swine (Betthauser et al., 2000; Onishi et al., 2000). The SCNT procedure proceeds as follows. Genetically modified cells are selected and maintained in culture. Oocytes in metaphase II are recovered and enucleated. Donor nuclear transfer is accomplished by electrofusion with the enucleated oocyte or piezo-actuated microinjection (less commonly used) and activation. The reconstructed embryos are then cultured *in vitro* and later transferred to synchronized recipient sows for pregnancy with the cloned fetus.

Numerous factors influence the efficiency of pig SCNT, with published estimates ranging from 0.5% to 5% of SCNT-transferred embryos resulting in viable offspring (Aigner et al., 2010). The overall poor efficiency of pig SCNT is attributed to failures in epigenetic reprogramming (Shi et al., 2003). Some of these factors include preventing simultaneous fusion and activation by reducing or removing calcium from the media, use of homogenous media to prevent stress when cells are transferred between different pools of media, and the use of naturally cycling gilts as recipients (Walker et al., 2002). To identify factors that influence the efficiency of SCNT, a multifactorial analysis was recently performed on a data set of 18,649 embryos transferred into 193 recipients comprising 274 SCNT experiments (Kurome et al., 2013). Factors that positively influenced SCNT efficiency included use of mesenchymal stem cells as a donor, *in vitro* embryonic development to the 2- to 4-cell stage, while multiple rounds of cloning worsened outcomes. The authors of that study caution that their results are unlikely to apply to other pig SCNT centers, but that the approach of multifactorial analysis can be applied to improve outcomes within a particular center.

1.7. Human T cell development in the fetal porcine thymus: heralds of the humanized pig?

Despite the relatively recent development of genetic SCID pig models (discussed in the next section), several lines of evidence spanning nearly two decades suggest that the pig can support the development of a human immune system. An early proof-of-principle experiment demonstrated that intravenous transplantation of pigs with crude human bone marrow shortly after birth resulted in engraftment with human cells that remained detectable by PCR on postnatal day 340 (Starzl and Demetris, 1997). Tolerance to human donor cells

was conveyed during transplantation, because human donor-specific suppression of the mixed lymphocyte reaction was seen only in transplanted pigs, and this suppression increased in magnitude over time.

With increasing interest in xenotransplantation and the development of human T cell-based immunotherapies, several groups sought to determine whether porcine thymic tissue can support human T cell development. One particularly well-characterized model involves placement of a fetal pig thymus graft into an immunodeficient pig, followed by transplantation with human hematopoietic precursor cells. Multiple studies with this model demonstrate that porcine thymic tissue supports the development of a diverse human T cell repertoire that is tolerant to antigens from the pig donor (MHC-matched), human donor, and mouse, but is reactive against non-donor human and pig antigens (Habiro et al., 2009; Lan et al., 2004; Nikolic et al., 1999) and is effective with or without co-engraftment with porcine hematopoietic cells (Lan et al., 2004). When comparing T cell development in SCID mice with implanted pig thymic tissue versus human thymic tissue, no difference was seen in TCR Vβ gene segment usage or TCR repertoire (Shimizu et al., 2008). The swine thymus can generate all human T cell subsets, including T regulatory cells (Tregs) (Kalscheuer et al., 2014).

It has been proposed that mechanisms of both central and peripheral tolerance regulate the antigen-response profile of human T cells educated in the implanted pig thymus. The findings above imply that, for central tolerance, human TCRs can undergo positive selection on pig MHC molecules, known as swine leukocyte antigens (SLAs), such that the similarity between HLA and SLA molecules makes a productive human TCR-SLA

interaction possible (Chardon et al., 2001; Gustafsson et al., 1990a, 1990b; Ho et al., 2010; Renard et al., 2001). In contrast, negative selection likely occurs on a variety of human, porcine, and murine antigens (Nikolic et al., 1999). Peripheral tolerance is proposed to be mediated by human Tregs that develop in the pig thymus (Kalscheuer et al., 2014). Education in the implanted pig thymus of SCID mice is, however, associated with some defects in human T cell function, including decreased CD8+ SP T cells in the peripheral blood, suppression of homeostatic T cell proliferation in response to lymphopenia, reduced conversion to the memory phenotype, accelerated decay of memory cells, and reduced responses to protein antigens (Kalscheuer et al., 2014). Why pig thymus-educated human T cells have these functional deficits remains unclear. Despite these limitations, this series of experiments suggests that the pig thymus has the capacity to productively educate and select developing human T cells.

1.8. *In utero* transplantation of human hematopoietic cells and hepatocytes into pigs.

An alternative approach to human immune cell engraftment in the pig is to introduce human cells *in utero* prior to or during porcine lymphopoiesis. The reasoning behind this approach is that the presence of human antigens during T and B cell development will tolerize the pig to the engraftment of human tissues later in life. Fujiki and colleagues delivered human cord blood *in utero* into the intraperitoneal space of fetal pigs, ranging from DG31 to DG78 (Fujiki et al., 2003). Transplanted pigs showed low levels of engraftment by flow cytometry for all leukocyte lineages, including T cells, B cells, NK cells, CD34+ progenitor cells, and myeloid cells. Most animals showed PCR-detectable engraftment until postnatal day 80 to 110, with one animal having detectable human cells until day 315. In

another study, intraperitoneal transplantation of T cell depleted human bone marrow resulted in the presence of rare human T cells in the pig thymus, as detected by IHC and RT-PCR (Ogle et al., 2009). These T cells derived from *de novo* lymphopoiesis, as they showed increased T cell receptor excision circles (TRECs), increased TCR diversity, and new responses to vaccination that were absent in untransplanted, donor human bone marrow cells. The human T cells also showed donor-specific tolerance, but proliferated in response to non-HLA matched allogeneic human cells and non-SLA matched porcine cells, suggesting that human T cells had undergone productive education in the pig thymus.

In utero transplantation has also been suggested to tolerize pigs to postnatal engraftment with non-hematopoietic cells. Fisher and colleagues performed intrahepatic injection of human hepatocytes on DG40, followed by a second intrahepatic transplantation of human hepatocytes around postnatal day 7 (Fisher et al., 2013). Human liver cells were shown to be successfully engrafted by PCR, IHC, and FISH; human albumin was detected in the serum of transplanted pigs as late as postnatal week 6, indicating that the engrafted human hepatocytes were functional.

These studies suggest that *in utero* transplantation can be employed to engraft human T cells and hepatocytes into immunocompetent pigs, presumably due to tolerization of the fetal porcine immune system to exogenously introduced human antigens. It is reasonable to assume, then, that *in utero* transplantation with human hematopoietic progenitors (particularly into the hematopoietically active fetal liver) would be quite effective for repopulating SCID pigs with human lymphocytes to generate humanized pigs.

1.9. Current pig models of severe combined immunodeficiency.

Several SCID pig models have been reported thus far, nearly all of which are based on well-established gene knockouts from SCID mice. The first SCID pigs arose spontaneously, although the genetic basis for their SCID phenotype remains unknown (Basel et al., 2012; Ozuna et al., 2013). These naturally occurring SCID pigs can accept xenografted human tumors and are highly susceptible to pneumonia. They had no thymus and had diminished secondary lymphoid tissues containing only sparse to absent T and B cells.

Two SCID pig models have been generated by targeting the *IL2RG* gene, one of which utilized conventional gene targeting (Suzuki et al., 2012) while the other used an *IL2RG*-specific zinc finger nuclease (Watanabe et al., 2013). *IL2RG* $^{-/Y}$ SCID pigs have an immune deficiency limited to T and NK cells while retaining B cell expression, which mimics human X-linked SCID disease more accurately than the *IL2RG* $^{-/Y}$ mouse model, in which all mature lymphocyte lineages are absent. The remaining B cells are poorly functional, likely due to the absence of T cell help, producing decreased serum levels of IgM, IgG, and IgA. Allogeneic bone marrow transplantation (BMT) of *IL2RG* $^{-/Y}$ SCID pigs led to partial rescue of the lymphocyte populations as well as partial restoration of serum IgM, IgG, and IgA levels (Suzuki et al., 2012).

The remaining SCID pig models are based on biallelic inactivation of either the *RAG1* or *RAG2* gene using TALENs (Huang et al., 2014; Lee et al., 2014). These pigs also had no thymus, lost splenic red/white pulp differentiation, and showed loss of T and B cells with persistence of NK cells. Their TCR and IgH genes remain in the germline configuration due to the absence of V(D)J recombination (Huang et al., 2014). Injection of human induced

pluripotent stem cells into *RAG2*$^{-/-}$ pigs led to the development of mature teratomas containing human tissues derived from all three germ layers (Lee et al., 2014).

A limitation of the current SCID pig models is that none of them can support repopulation with a functional human immune system, due to the inability of a single gene knockout to completely ablate all three lymphocyte lineages. The *IL2RG*$^{-/Y}$ knockout SCID pigs are deficient in T and NK cells, however the B cell population persists. *IL2RG* $^{-/Y}$ SCID pigs require pre-conditioning with cytotoxic drugs to eliminate progenitor cells and allow engraftment of pig hematopoietic stem cells, requiring up to 8 weeks for the detection of donor T cells (Suzuki et al., 2012). The *RAG1*$^{-/-}$ and *RAG2*$^{-/-}$ SCID pig models show loss of T and B cells, however the NK cell population is unchanged, which is problematic because NK cells have been shown to impair stem cell engraftment (Mombaerts et al., 1992; Shinkai et al., 1992). Based on these single knockout models, a double knockout of the *IL2RG* and *RAG1* genes (similar to *IL2RG*$^{-/-}$ *RAG2*$^{-/-}$ mice) would be predicted to cause complete loss of the lymphocyte lineages and produce SCID pigs with no functional T, B, or NK cells.

1.10. Chapter Summary.

In this chapter, I reviewed the development of humanized mice with a focus on the biology of RAG1, RAG2, and IL2RG, and how knockouts of these genes can be used to produce SCID mice that can be repopulated with human immune cells. I then highlighted the pitfalls of using mice as models of human immunology, and outlined how pigs provide several advantages as an animal model that more closely mirrors human physiology and immune function. After comparing and contrasting human and porcine immune development, I discussed how combining TALENs and SCNT can be utilized to rapidly produce

genetically modified swine. I then reviewed multiple studies which indicate that the pig thymus can support development of functional human T cells, and that *in utero* transplantation of human cells into pigs can lead to the successful engraftment of human hematopoietic cells and functional human hepatocytes. Finally, I highlighted the salient features and shortcomings of current SCID pig models, the majority of which were generated using genome-targeted sequence-specific nucleases.

In the following chapters, I describe the production of novel double knockout SCID pigs with inactivating mutations of both the *IL2RG* and *RAG1* loci, thereby eliminating functional T, B, and NK cells. In subsequent chapters, I describe the results of experiments for both allogeneic transplantation and transplantation with human hematopoietic cells to generate humanized pigs reconstituted with a human immune system. I compare several transplantation protocols to find the optimal balance between toxicity of the conditioning regimen and efficacy of repopulation with human lymphocytes.

CHAPTER 2: GENERATION OF *IL2RG*$^{-/Y}$ *RAG1*$^{-/-}$ PIGS WITH SEVERE COMBINED IMMUNODEFICIENCY

2.1. Overview.

There is considerable interest in generating a genetically modified pig with severe combined immunodeficiency (SCID), due to the similarities between human and porcine physiology and the numerous potential biomedical applications of a large animal SCID model. Current SCID pig models rely on genetic disruption of *IL2RG* (Suzuki et al., 2012) or either *RAG1* or *RAG2* (Huang et al., 2014; Lee et al., 2014). IL2RG $^{-/Y}$ pigs lack T and NK cells; in contrast, knockout of RAG1 or RAG2 generates pigs that are defective in T cells and functional B cells, because they are the lymphoid lineages that require RAG activity for development. It would be desirable to generate a pig in which all three lymphoid lineages – T, B, and NK cells – are eliminated or functionally inactivated. This would improve engraftment with donor hematopoietic stem cells, potentially without the need for preconditioning regimens that deplete the bone marrow, but are also toxic to other organs, thereby increasing the costs of maintaining such animals. In this chapter, I report the generation of pigs with combined knockouts of the *IL2RG* and *RAG1* loci to eliminate functional T, B, and NK cells. To overcome the technical challenges of generating a double knockout (DKO) pig within a reasonable time frame, I used transcription activator-like effector nucleases (TALENs) to mutate the *IL2RG* and *RAG1* genes and generated viable mutant pigs via somatic cell nuclear transfer (SCNT). The presence and distribution of lymphoid cells were evaluated by flow cytometry and immunohistochemistry, while plasma Ig levels were measured by ELISA.

2.2. TALEN-mediated genomic modification of *IL2RG*.

To mutate the *IL2RG* locus, a primary porcine male fibroblast (PPMF) cell line was transfected with TALENs targeting the junction between the signal peptide and the extracellular region of the *IL2RG* gene (Fig. 1A). The TALENs were co-transfected with an indicator plasmid (GFP-pSSA) which expresses functional GFP in the presence of sequence-specific TALEN activity. GFP-positive cells were enriched by fluorescence-activated cell sorting and expanded from single cell colonies. The spacer region between the TALEN recognition sites contains an *AvaII* restriction site (Fig. 1B) which is eliminated by TALEN-mediated mutation of the *IL2RG* locus. Genomic DNA (gDNA) was isolated from each clonal cell line and subjected to *AvaII* restriction screening, which demonstrated mutation of *IL2RG* in 3 of the 35 PPMF colonies (8.5%). Genomic DNA sequencing from the 3 modified colonies confirmed that the *IL2RG* gene was mutated in the targeted region.

One of these colonies (*IL2RG* $^{\Delta 79\text{-}83/Y}$) had 5 bases deleted from the targeted region in exon 1 (Fig. 1D), resulting in the loss of 2 amino acids and the generation of a downstream premature stop codon (PSC) adjacent to the 3' end of exon 1 and several additional downstream PSCs in the coding region. Somatic cell nuclear transfer (SCNT) was used to generate 127 embryos from the *IL2RG* $^{\Delta 79\text{-}83/Y}$ fibroblasts. Transfer of these embryos into a gilt generated 6 fetuses (Fig. 1C), all of which were collected at day 42 of gestation to generate six *IL2RG* $^{\Delta 79\text{-}83/Y}$ PPMF cell lines. PCR and restriction screening of *IL2RG* $^{\Delta 79\text{-}83/Y}$ fetal tissues demonstrated the expected loss of the *AvaII* restriction site from the *IL2RG* targeted region (data not shown). Heart tissue genomic DNA from all 6 fetuses was isolated and sequenced to verify the presence of the *IL2RG* $^{\Delta 79\text{-}83/Y}$ deletion. Western blot analysis of

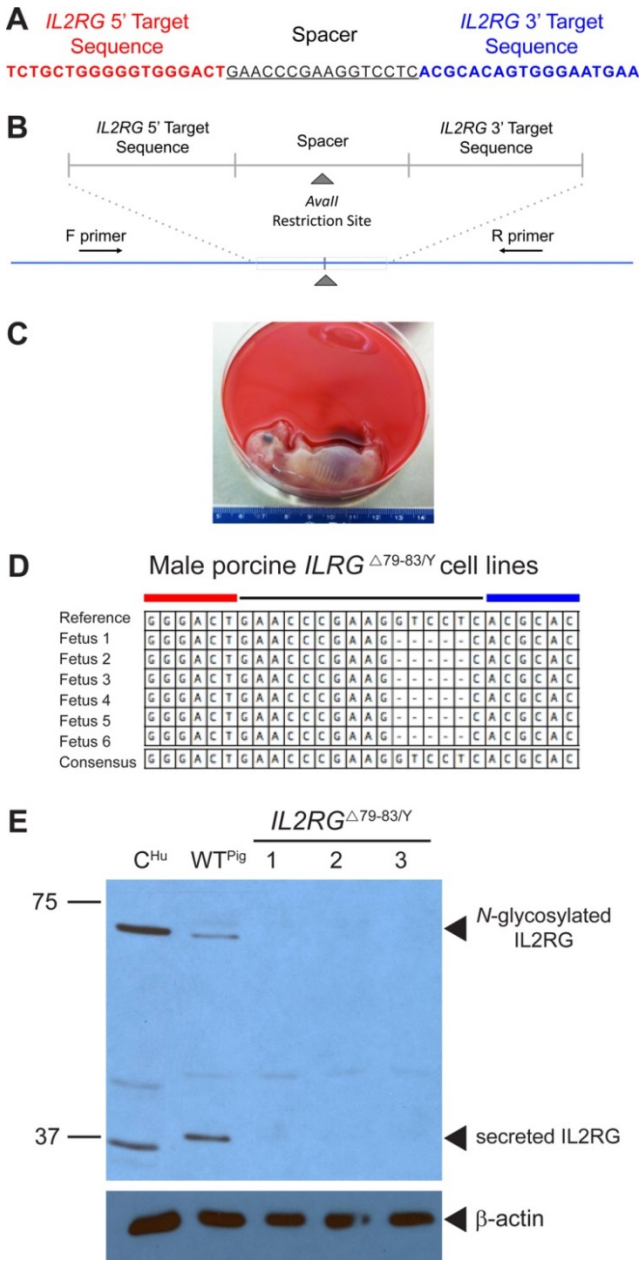

Fig. 1. Generation of *IL2RG*$^{-/Y}$ pigs by TALENs.
(*A*) *IL2RG* 5' and 3' target sequences and the intervening spacer where the TALEN-mediated double strand break is made. (*B*) Locations of the *IL2RG* PCR primer binding sites and *AvaII* restriction site for genotype screening. A total of thirty-five individual colonies were screened. Three positive *IL2RG*$^{-/Y}$ mutants were confirmed. (*C*) *IL2RG*$^{-/Y}$ fetus at 42 days gestation. A total of 6 fetuses were generated from an individual pregnancy and used to generate six primary *IL2RG*$^{-/Y}$ porcine cell lines. (*D*) *IL2RG* sequence alignment showing the TALEN-induced 5 bp deletion. (*E*) IL2RG Western blot from WT and mutant pig cardiomyocyte lysates. Results are representative of three independent experiments.

cellular extracts from the *IL2RG* $^{\Delta 79\text{-}83/Y}$ fibroblasts demonstrated the loss of IL2RG protein expression (Fig. 1E).

2.3. Generation of *IL2RG*$^{-/Y}$ *RAG1*$^{-/-}$ double knockout piglets using TALENs.

To produce SCID piglets containing a double knockout of both *IL2RG* and *RAG1*, we designed TALENs that bind the *RAG1* promoter region and a region just downstream of the translational start site (Fig. 2A). The spacer region between the *RAG1* TALEN recognition sites contains a *NlaIII* restriction site, which is eliminated by TALEN-mediated mutagenesis (Fig. 2B). *IL2RG* $^{\Delta 79\text{-}83/Y}$ fibroblasts were transfected with plasmids encoding the *RAG1* TALENs and GFP-pSSA indicator containing the RAG1 TALEN target site, followed by FACS to enrich for GFP-expressing cells and expansion of single cells into clonal cell lines, as before. Genomic DNA was isolated from these clones, followed by PCR and restriction screening with *NlaIII*. From a total of 103 colonies, the RAG1 TALEN produced eleven *IL2RG* $^{\Delta 79\text{-}83/Y}$ *RAG1*$^{-/+}$ heterozygous colonies (11.7%) and three *IL2RG* $^{\Delta 79\text{-}83/Y}$ *RAG1*$^{-/-}$ homozygous (2.9%) colonies (Fig. 2C).

Sequence analysis of a *RAG1* heterozygote, *IL2RG*$^{\Delta 79\text{-}83/}$ *RAG1*$^{-/+}$ colony 42, revealed a monoallelic deletion of 20 nucleotides resulting in a PSC (Fig. 2D). A series of mutant *RAG1* homozygotes, *IL2RG*$^{\Delta 79\text{-}83/Y}$ *RAG1*$^{-/-}$ colonies 16, 31 and 103, all showed different deletion mutations resulting in frame shifts containing PSCs, with one example shown in Fig. 2D. A total of nine embryo transfers generated seven pregnancies, resulting in the live birth of 18 piglets (Fig. 2E). Two *IL2RG*$^{\Delta 79\text{-}83/Y}$ *RAG1*$^{+/+}$ piglets, eight *IL2RG*$^{\Delta 79\text{-}83/Y}$ *RAG1*$^{-/+}$ piglets, and eight *IL2RG*$^{\Delta 79\text{-}83/Y}$ *RAG1*$^{-/-}$ piglets were born. Peripheral blood mononuclear cells (PBMCs) were collected on postnatal day 1 or 2 from *IL2RG*$^{\Delta 79\text{-}83/Y}$ *RAG1*$^{-/+}$ and *IL2RG*$^{\Delta 79\text{-}}$

Fig. 2. Generation of *IL2RG*$^{-/Y}$ *RAG1*$^{-/-}$ pigs by TALENs.
(*A*) *RAG1* 5' and 3' target sequences and the intervening spacer where the TALEN-mediated double strand break is made. (*B*) Locations of the *RAG1* PCR primer binding sites and *NlaIII* restriction site for genotype screening. (*C*) Restriction screening of fibroblast colonies for mutations in *RAG1*. Genomic DNA from fibroblast colonies was PCR amplified using the primers above and digested with *NlaIII*. Of the 103 *IL2RG*$^{-/Y}$ individual colonies screened, 11 were *IL2RG*$^{-/Y}$ *RAG1*$^{-/+}$ (red arrow) and 3 were *IL2RG*$^{-/Y}$ *RAG1*$^{-/-}$ (yellow arrow). *IL2RG*$^{-/Y}$ *RAG1*$^{-/-}$ colonies were TOPO cloned and sequenced to verify mutations in both alleles. (*D*) Sequence alignment of the *RAG1* gene from *RAG1* heterozygous and homozygous pigs. All *IL2RG*$^{-/Y}$ *RAG1*$^{-/+}$ litters were generated from the same colony. The results are representative of two *IL2RG*$^{-/Y}$ *RAG1*$^{-/+}$ litters. *IL2RG*$^{-/Y}$ *RAG1*$^{-/-}$ litters were generated from the three *IL2RG*$^{-/Y}$ *RAG1*$^{-/-}$ colonies and the results are representative of nine litters. (*E*) Litter of *IL2RG*$^{-/Y}$ *RAG1*$^{-/-}$ pigs. (*F*) Restriction screening of *IL2RG*$^{-/Y}$ *RAG1*$^{-/+}$ and *IL2RG*$^{-/Y}$ *RAG1*$^{-/-}$ pigs. Genomic DNA from PBMCs was PCR amplified and digested with *NlaIII*. Results are representative of experiments from 18 individual piglets.

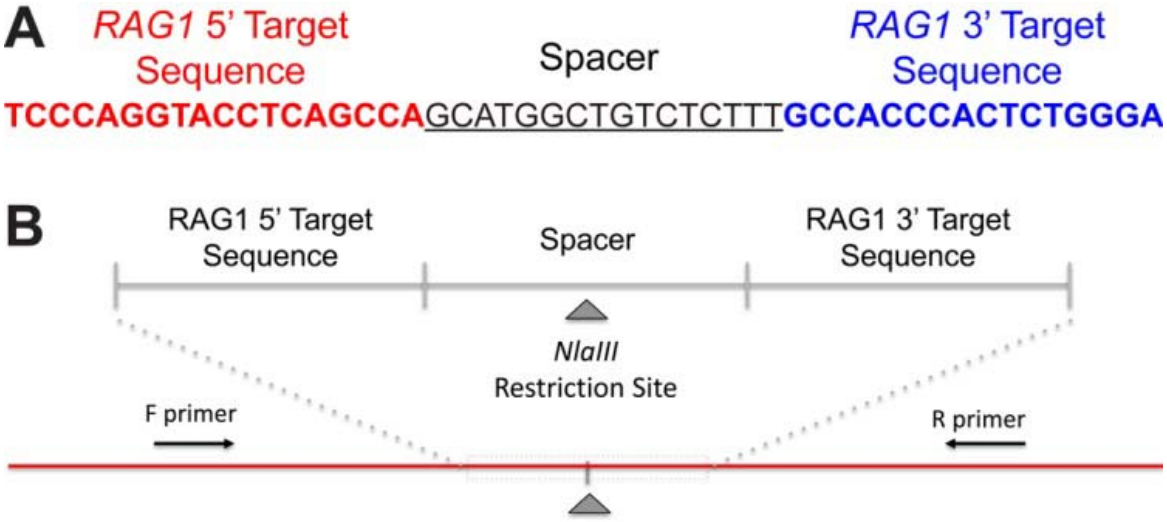
A
RAG1 5' Target Sequence
Spacer
RAG1 3' Target Sequence
TCCCAGGTACCTCAGCCAGCATGGCTGTCTCTTTGCCACCCACTCTGGGA
B
RAG1 5' Target Sequence
Spacer
RAG1 3' Target Sequence
NlaIII Restriction Site
F primer
R primer
C
M
1
2
3
4
KO
WT
D
IL2RG △79-83/Y RAG1△(-)26-11/+
Reference
Allele 1
Allele 2
Consensus
IL2RG △79-83/Y RAG1△(-)69-11/△(-)7-11
Reference
Allele 1
Allele 2
Consensus

E

IL2RG $^{\triangle 79\text{-}83/Y}$ *RAG1* $^{\triangle(-)69\text{-}11/\triangle(-)7\text{-}11}$ Litter

F

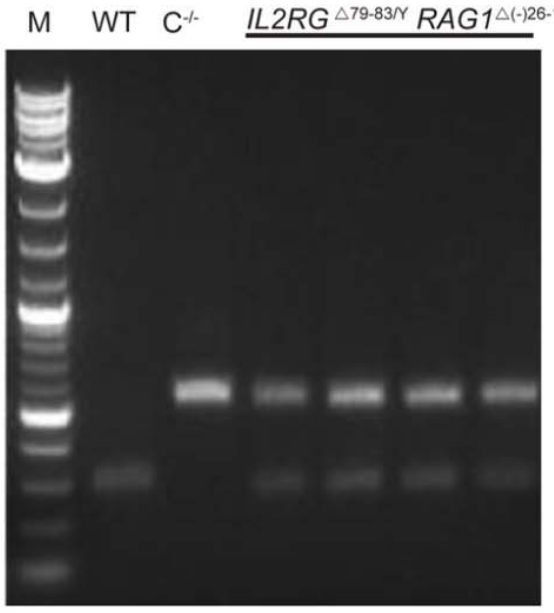

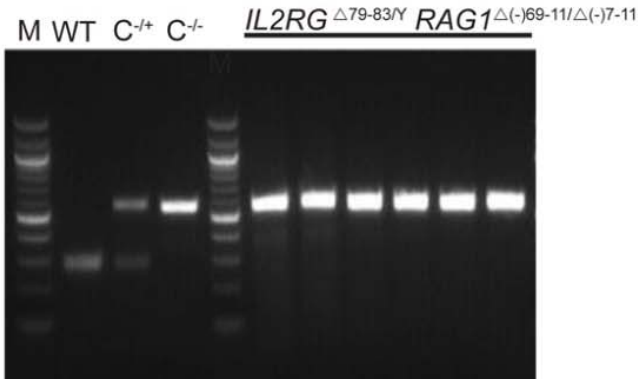

$^{83/Y}$ *RAG1*$^{-/-}$ piglets as well as age-matched WT controls. Genomic DNA was isolated from PBMCs, followed by PCR and restriction screening with *NlaIII* (Fig. 2F). *RAG1* heterozygous animals (*upper panel*) showed the presence of both the WT allele with preservation of the *NlaIII* site (lower band) and a mutant allele (upper band) where the *NlaIII* site has been eliminated. In contrast, *RAG1* homozygous animals (*lower panel*) bear only the mutant allele (upper band only). These data demonstrate the successful construction of both *IL2RG*$^{-/Y}$ *RAG1*$^{-/+}$ heterozygous and *IL2RG*$^{-/Y}$ *RAG1*$^{-/-}$ double knockout (DKO) piglets.

2.4. Survival, gross pathology, and histology of *IL2RG*$^{-/Y}$ *RAG1*$^{-/-}$ piglets.

The Kaplan-Meier survival curves for the *IL2RG*$^{-/Y}$ *RAG1*$^{-/+}$ and *IL2RG*$^{-/Y}$ *RAG1*$^{-/-}$ piglets are plotted in Figure 3. Nearly 40% of both *IL2RG*$^{-/Y}$ *RAG1*$^{-/+}$ and *IL2RG*$^{-/Y}$ *RAG1*$^{-/-}$ piglets died on postnatal day 1, predominantly from failure to thrive. Survival declined steadily until all piglets had died by day 34, with no significant difference in survival between *IL2RG*$^{-/Y}$ *RAG1*$^{-/+}$ and *IL2RG*$^{-/Y}$ *RAG1*$^{-/-}$ animals. These later deaths were due to overwhelming sepsis, with necropsies showing numerous abscesses across multiple organs (discussed below).

Gross pathology revealed that *IL2RG*$^{-/Y}$ *RAG1*$^{-/+}$ and *IL2RG*$^{-/Y}$ *RAG1*$^{-/-}$ piglets had lower body weights compared to age-matched WT piglets. On postnatal day 1, WT piglets had grossly normal thymus glands that were readily visible at the thoracic inlet. In contrast, *IL2RG*$^{-/Y}$ *RAG1*$^{-/+}$ and *IL2RG*$^{-/Y}$ *RAG1*$^{-/-}$ piglets only had a 0.3 mm thymic remnant (Figs. 4A and 5C). Lymph nodes were similarly absent in *IL2RG*$^{-/Y}$ *RAG1*$^{-/+}$ and *IL2RG*$^{-/Y}$ *RAG1*$^{-/-}$ piglets (Fig. 5D). The gross appearance of the liver and spleen was similar between WT, *IL2RG*$^{-/Y}$ *RAG1*$^{-/+}$, and *IL2RG*$^{-/Y}$ *RAG1*$^{-/-}$ piglets (Figs. 5A and 5B). The organ weights of the

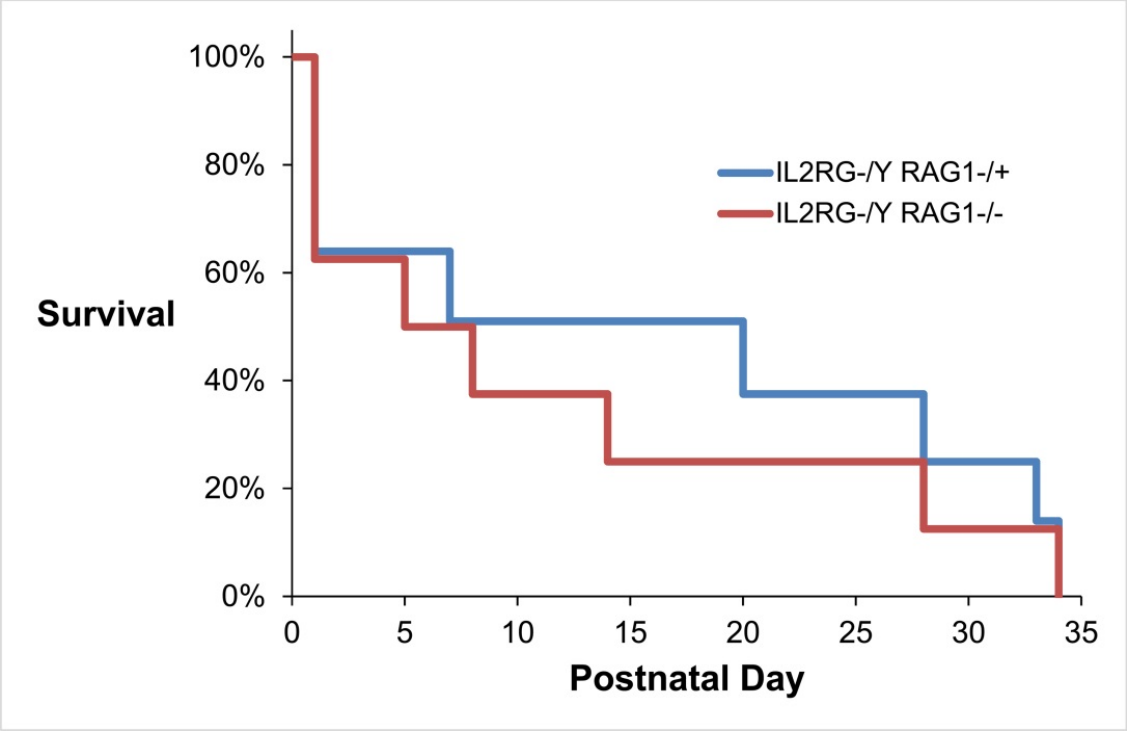

Fig. 3. Kaplan-Meier survival curve for *IL2RG*$^{-/Y}$ *RAG1*$^{-/+}$ and *IL2RG*$^{-/Y}$ *RAG1*$^{-/-}$ pigs.
IL2RG-/Y RAG1-/+ and IL2RG-/Y RAG1-/- piglet survival was tracked from postnatal day 1 to death, with eight animals per experimental group at the beginning of the study.

liver and spleen were lower in the *IL2RG*$^{-/Y}$ *RAG1*$^{-/+}$ and *IL2RG*$^{-/Y}$ *RAG1*$^{-/-}$ piglets compared to WT, however the lower organ weights were in proportion to the lower body weights of the mutant animals (Table 1).

Hemtoxylin and eosin (H&E) staining of the thymus from WT pigs revealed normal lobular architecture with distinct cortical and medullary areas and normal cellularity. In contrast, the thymic remnant of *IL2RG*$^{-/Y}$ *RAG1*$^{-/-}$ piglets was composed almost exclusively of epithelial cell elements arranged in well-defined anastomosing nests with rare lymphocytic infiltrates supported by a collagen stroma, consistent with severe thymic atrophy or complete involution (Fig. 4B). H&E staining of the spleen from both the *IL2RG*$^{-/Y}$ *RAG1*$^{-/+}$ and *IL2RG*$^{-}$

Table 1. Organ and total body weights of the *IL2RG*$^{-/Y}$ *RAG1*$^{-/+}$ and *IL2RG*$^{-/Y}$ *RAG1*$^{-/-}$ pigs.
(A) Thymus. (B) Spleen. (C) Total body weight. All pigs are *IL2RG*$^{-/Y}$. Indicated genotype is for *RAG1*.

A

RAG1 Genotype	Age	Thymus Weight (g)
Heterozygous	1	0.01
Heterozygous	1	0.01
Heterozygous	1	0.00
Heterozygous	7	0.03
Heterozygous	20	0.08
Heterozygous	22	0.99
Heterozygous	33	0.32
Heterozygous	35	0.74
Homozygous	1	0.14
Homozygous	1	0.06
Homozygous	1	0.06
Homozygous	5	0.15
Homozygous	8	0.20
Homozygous	14	0.31
Homozygous	28	0.05
Homozygous	34	0.16

B

RAG1 Genotype	Age	Spleen Weight (g)
Heterozygous	1	1.16
Heterozygous	1	0.34
Heterozygous	1	0.26
Heterozygous	7	1.28
Heterozygous	20	12.64
Heterozygous	22	10.77
Heterozygous	33	3.76
Heterozygous	35	4.81
Homozygous	1	0.53
Homozygous	1	0.94
Homozygous	1	1.30
Homozygous	5	1.52
Homozygous	8	3.44
Homozygous	14	6.37
Homozygous	28	12.64
Homozygous	34	12.30

C

RAG1 Genotype	Age	Total Body Weight (g)
Heterozygous	1	1109
Heterozygous	1	1256
Heterozygous	1	1385
Heterozygous	7	1543
Heterozygous	20	3100
Heterozygous	22	2890
Heterozygous	33	2584
Heterozygous	35	3705
Homozygous	1	1134
Homozygous	1	1348
Homozygous	1	1275
Homozygous	5	1295
Homozygous	8	1453
Homozygous	14	1865
Homozygous	28	2354
Homozygous	34	2875

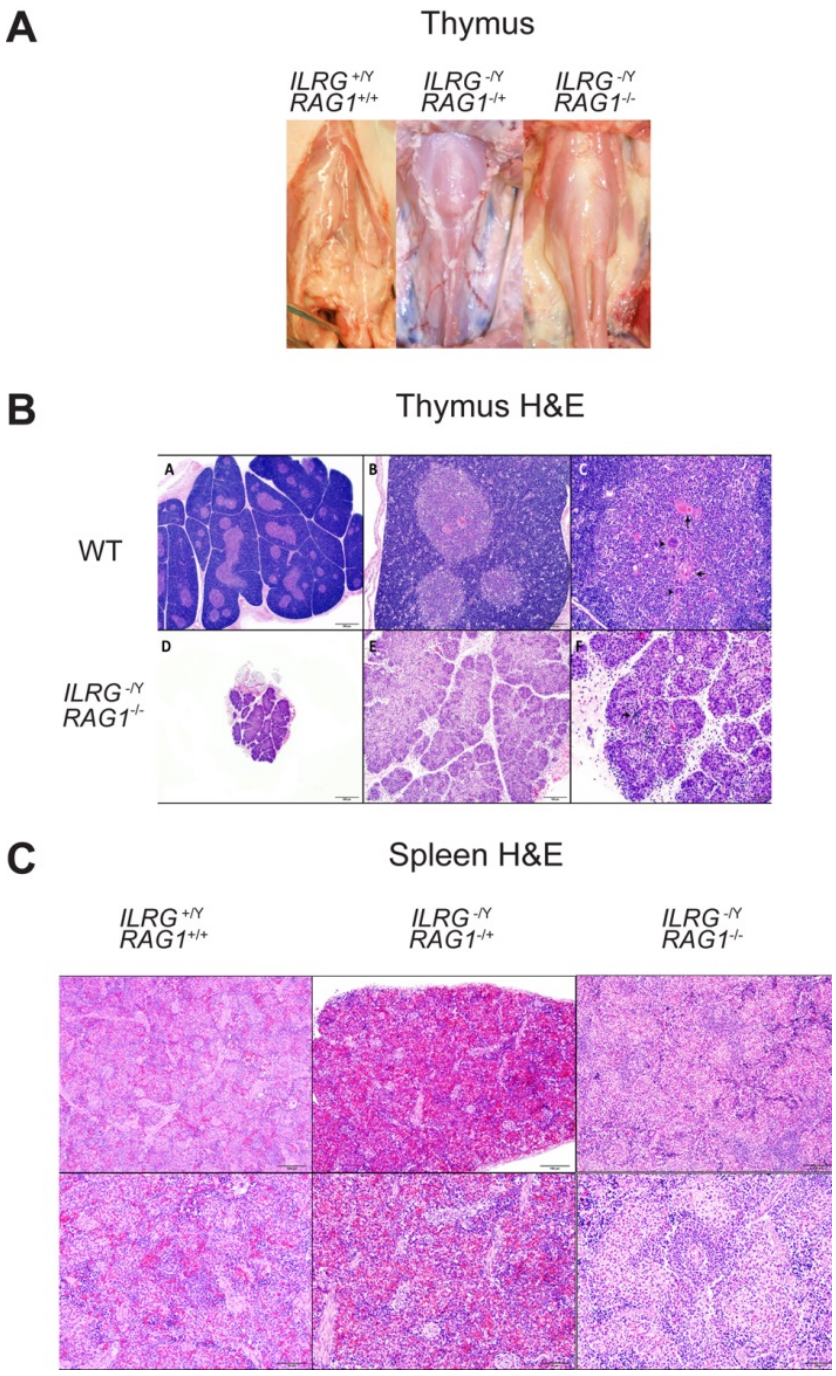

Fig. 4. Gross pathology and histology of *IL2RG*$^{-/Y}$ *RAG1*$^{-/-}$ pigs.
(*A*) Gross pathology of the thymus or thymic remnant on postnatal day 1. Results are representative of three *IL2RG*$^{-/Y}$ *RAG1*$^{-/+}$ and 6 *IL2RG*$^{-/Y}$ *RAG1*$^{-/-}$ piglets. (*B*) H&E stain of thymus sections on postnatal day 1. (*C*) H&E stain of spleen sections from around postnatal day 30. Results are representative of results from the following number of animals in parentheses: *IL2RG*$^{-/Y}$ *RAG1*$^{-/+}$ (2) and *IL2RG*$^{-/Y}$ *RAG1*$^{-/-}$ (2) piglets. Scale bar = 100 μm.

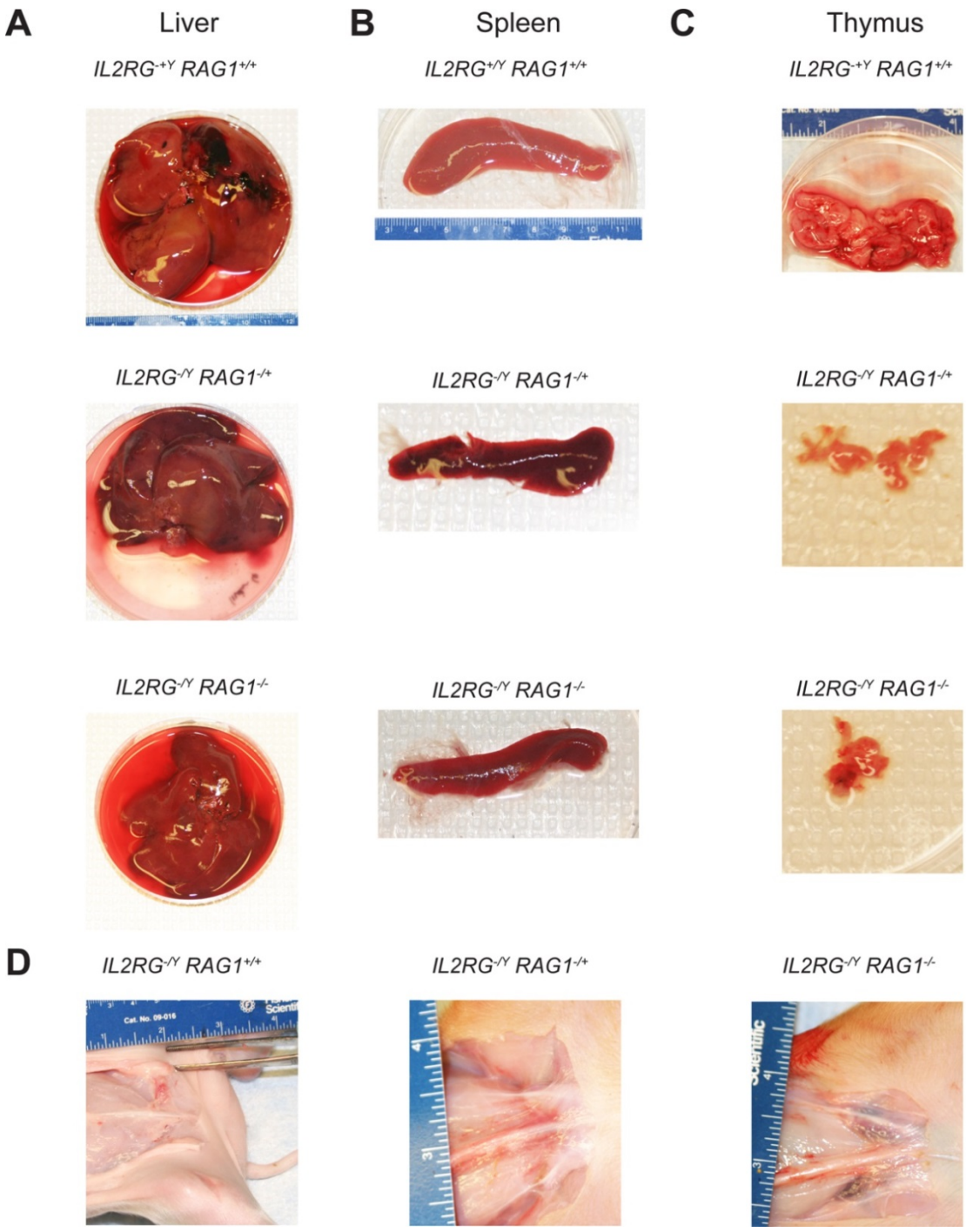

Fig. 5. Gross organ pathology of *IL2RG*$^{-/Y}$ *RAG1*$^{-/-}$ pigs.
(*A*) Liver, (*B*) spleen, (*C*) thymus, and (*D*) lymph nodes were collected or examined on postnatal day 1 and compared to organs from age-matched *IL2RG*$^{+/Y}$ *RAG1*$^{+/+}$ controls. Gross organ pathology is representative of results from the following number of animals in parentheses: *IL2RG*$^{+/Y}$ *RAG1*$^{+/+}$ (3), *IL2RG*$^{-/Y}$ *RAG1*$^{-/+}$ (3), and *IL2RG*$^{-/Y}$ *RAG1*$^{-/-}$ (6) piglets.

$^{/Y}$ *RAG1*$^{-/-}$ pigs showed a hypoplastic white pulp with no germinal centers and no red/white pulp differentiation (Fig. 4C). There were no obvious differences in hepatic architecture between the mutant and WT pigs by H&E staining (data not shown). These data show that the combined mutation of *IL2RG* and *RAG1* in pigs results in thymic atrophy, absent lymph node development, and severe aberrations in splenic architecture.

A total of 10 piglets died within the first week after being farrowed – two *IL2RG*$^{\Delta 79\text{-}83/Y}$ *RAG1*$^{+/+}$, three *IL2RG*$^{\Delta 79\text{-}83/Y}$ *RAG1*$^{-/+}$, and five *IL2RG*$^{\Delta 79\text{-}83/Y}$ *RAG1*$^{-/-}$ piglets. The remaining eight piglets – five *IL2RG*$^{\Delta 79\text{-}83/Y}$ *RAG1*$^{-/+}$ and three *IL2RG*$^{\Delta 79\text{-}83/Y}$ *RAG1*$^{-/-}$ – all succumbed to opportunistic bacterial infections between 8 and 35 days old. Necropsies from several *IL2RG*$^{-/Y}$ *RAG1*$^{-/-}$ DKO pigs were notable for signs of severe exudative epidermitis (greasy pig disease) due to infection with *Staphylococcus hyicus*, which is a normal component of the commensal porcine skin flora (L'Ecuyer, 1966; L'Ecuyer and Jericho, 1966; Tanabe et al., 1996). These pigs had oily skin and hairs, crusting lesions over the eyes and ears, and skin lesions over their abdomen and legs, with some black-tinged lesions due to skin necrosis (Fig. 6A). No pigs with a *IL2RG*$^{-/Y}$ *RAG1*$^{-/+}$ genotype developed exudative epidermitis. The observation that a commensal organism caused severe systemic infection in *IL2RG*$^{-/Y}$ *RAG1*$^{-/-}$ pigs suggests that these animals are severely immunocompromised. In addition to greasy pig disease, multiple organs showed diffuse, pale inflammatory infiltrates, including the lungs (Fig. 6B) and liver (Fig. 6C). Gross abscesses were also visible in the lung, liver, kidney (Figs. 6B-D), leg, and peritoneal wall (Fig. 6E). Culture data from these animals prior to euthanasia demonstrated polymicrobial bacterial infection (data not shown), consistent with severe immunocompromise.

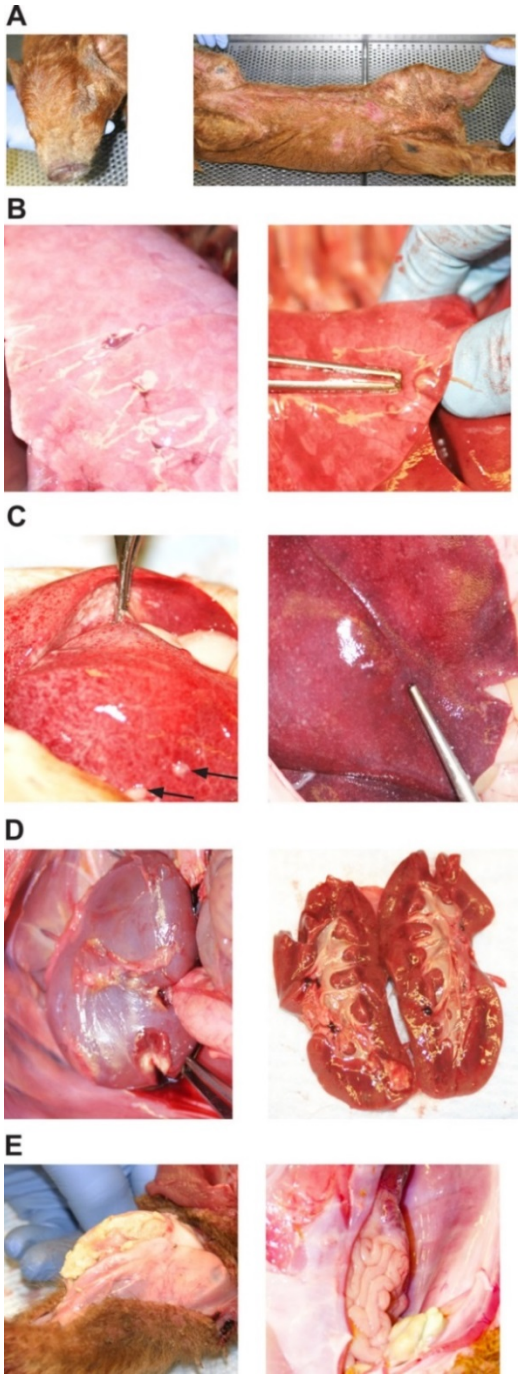

Fig. 6. Gross pathology of diseased organs from *IL2RG*$^{-/Y}$ *RAG1*$^{-/-}$ pigs.
(*A*) Exudative epidermitis (greasy pig disease) present at postnatal day 26. Findings are representative of six piglets. (*B*) Lungs with diffuse pulmonary inflammatory infiltrates and abscesses. Findings are representative of eight piglets. (*C*) Liver with diffuse hepatic inflammatory infiltrates and abscesses (*arrows*). (*D*) Kidney with renal abscess. *(E*) Abscesses in the leg and on the peritoneum. Findings in *C-E* are representative of results from two *IL2RG*$^{-/Y}$ *RAG1*$^{-/-}$ piglets.

2.5. Immunophenotyping of *IL2RG*$^{-/Y}$ *RAG1*$^{-/-}$ piglets by flow cytometry.

To investigate the effects of mutating the *IL2RG* and *RAG1* loci on lymphocyte populations, peripheral blood mononuclear cells (PBMCs) were collected at different time points from both *IL2RG*$^{-/Y}$ *RAG1*$^{-/+}$ and *IL2RG*$^{-/Y}$ *RAG1*$^{-/-}$ piglets and were analyzed via flow cytometry for the presence of T, B, and NK cells. The porcine T cell population is defined by positive staining with CD3, with additional T cell subsets defined by coexpression of CD4 and/or CD8 (Piriou-Guzylack and Salmon, 2008). On postnatal day 1 (Fig. 7A) and day 28 (Fig. 8A), only a trace population of CD3+ T cells was detected in both *IL2RG*$^{-/Y}$ *RAG1*$^{-/+}$ and *IL2RG*$^{-/Y}$ *RAG1*$^{-/-}$ piglets compared to WT. Staining for CD3+ CD4+ T helper cells or CD3+ CD8+ cytotoxic T lymphocytes (CTLs) showed loss of both of these populations in *IL2RG*$^{-/Y}$ *RAG1*$^{-/+}$ and *IL2RG*$^{-/Y}$ *RAG1*$^{-/-}$ piglets (Figs. 7B and 8B).

Porcine NK cells are defined by negative staining for the myeloid marker, 74-22-15 (also known as SWC3), and positive staining with CD16 (Piriou-Guzylack and Salmon, 2008). Both *IL2RG*$^{-/Y}$ *RAG1*$^{-/+}$ and *IL2RG*$^{-/Y}$ *RAG1*$^{-/-}$ piglets showed near absence of the NK cell population in the peripheral blood on postnatal day 1 (Fig. 7C) and day 28 (Fig. 8C) relative to WT controls.

The porcine B cell population is defined by negative staining for 74-22-15 and CD3 and positive staining for CD45RA (Piriou-Guzylack and Salmon, 2008). On postnatal day 1, the B cell population in the peripheral blood was decreased, but not absent in the mutant piglets relative to WT (Fig. 9, *left column*). In WT piglets, B cells composed 12.7% of PBMCs; this decreased to 3.63% in *IL2RG*$^{-/Y}$ *RAG1*$^{-/+}$ piglets (28.5% of WT levels) and to 3.45% in *IL2RG*$^{-/Y}$ *RAG1*$^{-/-}$ DKO piglets (27.2.2% of WT levels). On postnatal days 14 and

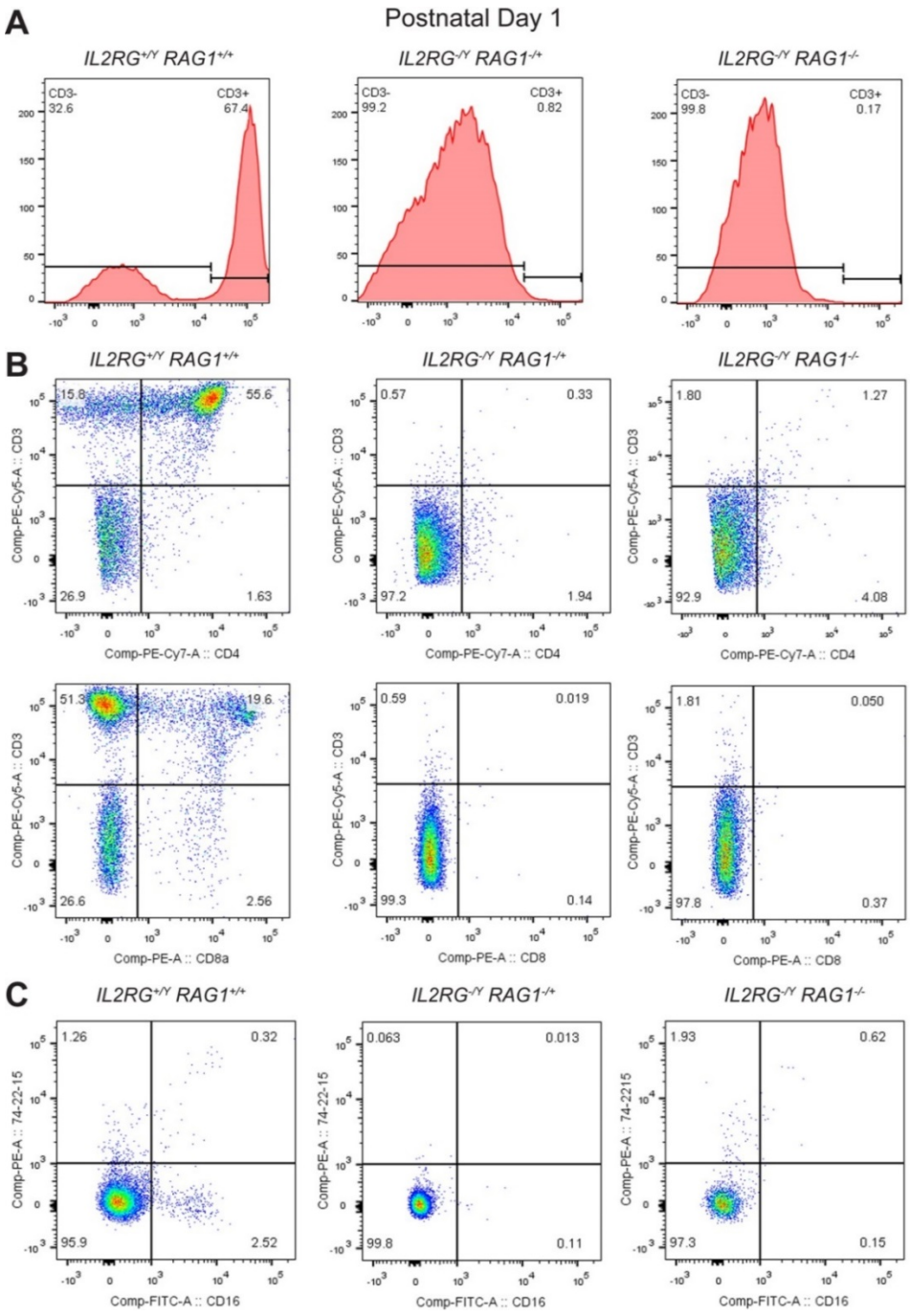

Fig. 7. Peripheral blood T cells and NK cells in newborn *IL2RG*$^{-/Y}$ *RAG1*$^{-/-}$ pigs.
PBMCs were collected on postnatal day 1 and stained for (*A*) CD3, (*B*), CD4, and CD8 to identify the T cell lineage and (*C*) 74-22-15(-) CD16(+) to identify the NK cell lineage. $P < 0.01$ for the differences in T and NK cell percentages, WT vs *IL2RG*$^{-/Y}$ *RAG1*$^{-/+}$, and WT vs *IL2RG*$^{-/Y}$ *RAG1*$^{-/-}$. Flow cytometry data are representative of results from the following number of animals in parentheses: *IL2RG*$^{+/Y}$ *RAG1*$^{+/+}$ (3), *IL2RG*$^{-/Y}$ *RAG1*$^{-/+}$ (8), and *IL2RG*$^{-/Y}$ *RAG1*$^{-/-}$ (8) piglets.

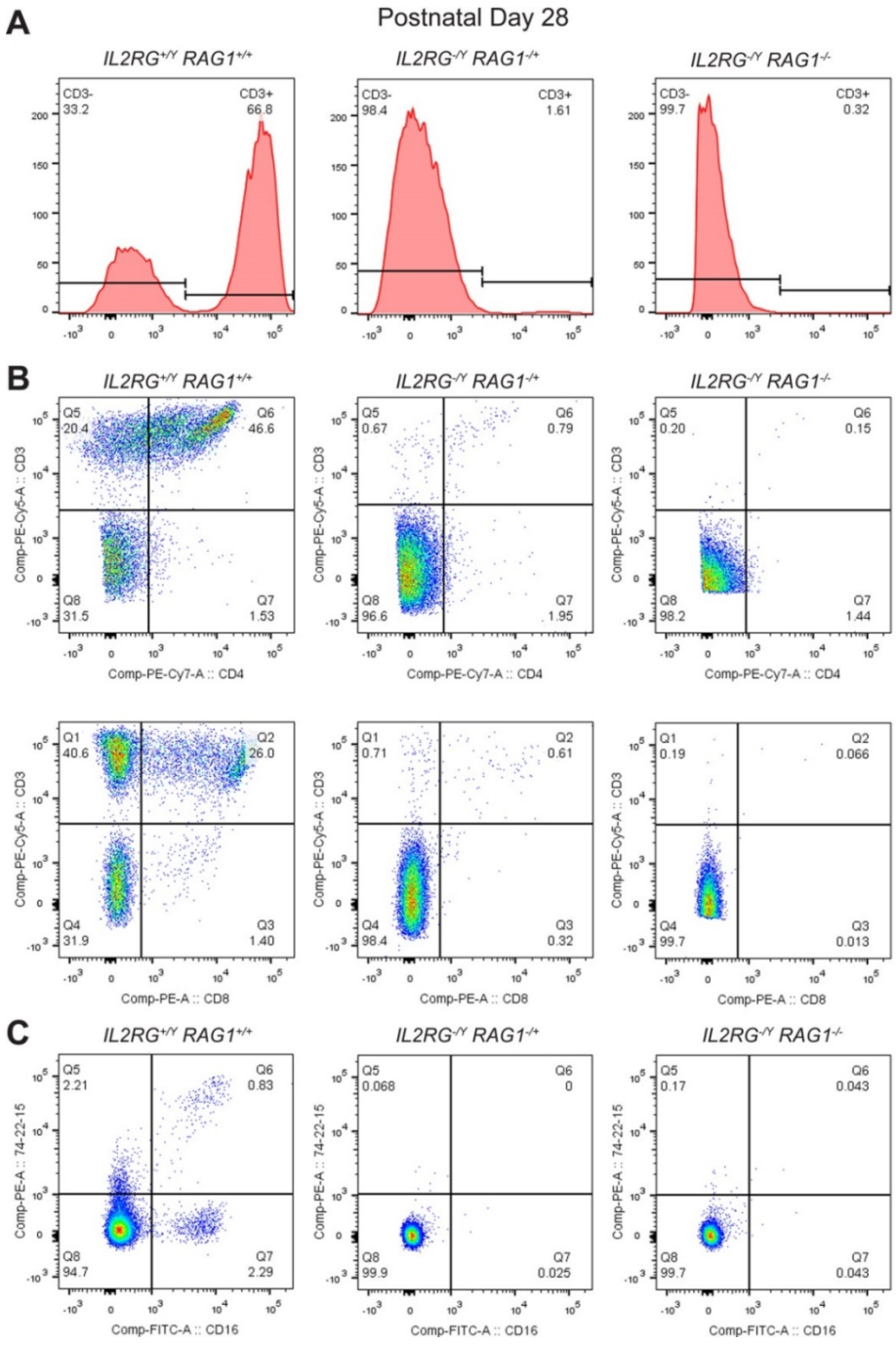

Fig. 8. Peripheral blood T cells and NK cells from *IL2RG*$^{-/Y}$ *RAG1*$^{-/-}$ pigs on postnatal day 28. PBMCs were collected and stained for (*A*) CD3, (*B*), CD4, and CD8 to identify the T cell lineage and (*C*) 74-22-15(-) CD16(+) to identify the NK cell lineage. $P < 0.01$ for the differences in T cell percentages, WT vs *IL2RG*$^{-/Y}$ *RAG1*$^{-/+}$, and WT vs *IL2RG*$^{-/Y}$ *RAG1*$^{-/-}$. $P = 0.239$ for the differences in NK cell percentages. Flow cytometry data are representative of results from the following number of animals in parentheses: *IL2RG*$^{+/Y}$ *RAG1*$^{+/+}$ (3), *IL2RG*$^{-/Y}$ *RAG1*$^{-/+}$ (2), and *IL2RG*$^{-/Y}$ *RAG1*$^{-/-}$ (2) piglets.

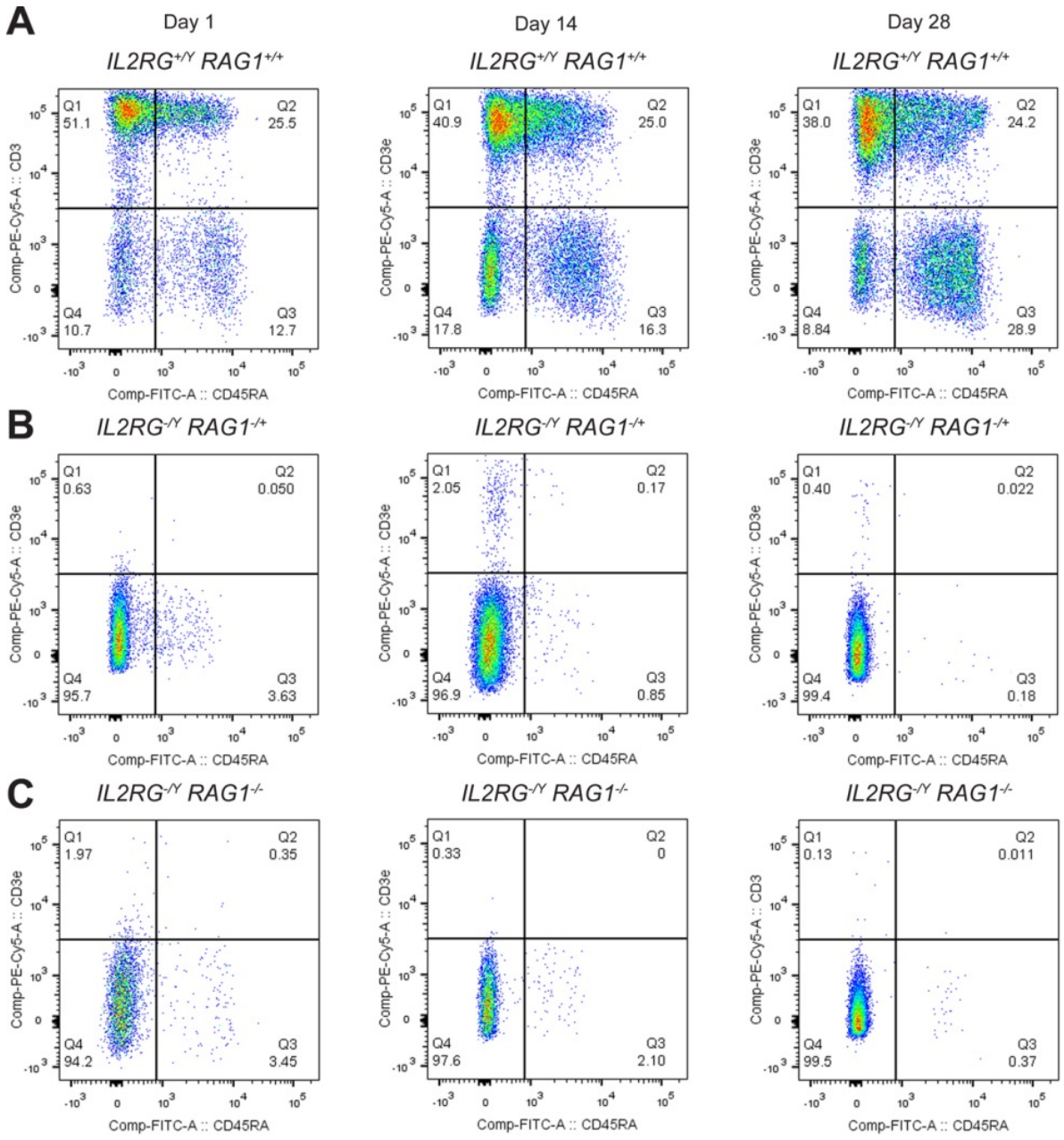

Fig. 9. Peripheral blood B cells from *IL2RG*$^{-/Y}$ *RAG1*$^{-/-}$ pigs.
PBMCs were collected on postnatal days 1, 14, and 28, and the B cell population was identified as 74-22-15(-) CD3(-) CD45RA(+). (*A*) WT, (*B*) *IL2RG*$^{-/Y}$ *RAG1*$^{-/+}$, and (*C*) *IL2RG*$^{-/Y}$ *RAG1*$^{-/-}$ pigs. $P < 0.01$ for the differences in B cell percentages, WT vs *IL2RG*$^{-/Y}$ *RAG1*$^{-/+}$, and WT vs *IL2RG*$^{-/Y}$ *RAG1*$^{-/-}$. Flow cytometry data are representative of results from the following number of animals, given in parentheses, day 1: *IL2RG*$^{+/Y}$ *RAG1*$^{+/+}$ (3), *IL2RG*$^{-/Y}$ *RAG1*$^{-/+}$ (8), and *IL2RG*$^{-/Y}$ *RAG1*$^{-/-}$ (8) piglets. Day 14: *IL2RG*$^{+/Y}$ *RAG1*$^{+/+}$ (3), *IL2RG*$^{-/Y}$ *RAG1*$^{-/+}$ (4), and *IL2RG*$^{-/Y}$ *RAG1*$^{-/-}$ (3) piglets. Day 28: *IL2RG*$^{+/Y}$ *RAG1*$^{+/+}$ (3), *IL2RG*$^{-/Y}$ *RAG1*$^{-/+}$ (3), and *IL2RG*$^{-/Y}$ *RAG1*$^{-/-}$ (2) piglets.

28, the B cell population steadily increased in WT piglets (Fig. 9A), while it decreased to nearly absent in both *IL2RG*$^{-/Y}$ *RAG1*$^{-/+}$ (Fig. 9B) and *IL2RG*$^{-/Y}$ *RAG1*$^{-/-}$ piglets (Fig. 9C). In summary, these flow cytometry studies demonstrate that combined mutation of the *IL2RG* and *RAG1* genes in pigs leads to loss of all the lymphoid lineages in the peripheral blood – T, B, and NK cells.

To evaluate the effects of the combined *IL2RG* and *RAG1* mutations on lymphoid populations in the bone marrow and spleen, cell suspensions were generated from each anatomic site using WT and mutant pigs sacrificed around postnatal day 30. Cells were then analyzed via flow cytometry for T, B, and NK cells using the cell surface markers described above. The bone marrow and spleen of *IL2RG*$^{-/Y}$ *RAG1*$^{-/+}$ and *IL2RG*$^{-/Y}$ *RAG1*$^{-/-}$ piglets showed near total loss of the T cell population relative to WT (Fig. 10, *first and second columns*). A markedly reduced but detectable population of splenic B cells was present in both the *IL2RG*$^{-/Y}$ *RAG1*$^{-/+}$ and *IL2RG*$^{-/Y}$ *RAG1*$^{-/-}$ piglets (Fig. 10, *third column*); B cells made up 18.5% of splenic cells in WT, 10.1% in *IL2RG*$^{-/Y}$ *RAG1*$^{-/+}$ (54.6% of WT levels), and 8.88% in the *IL2RG*$^{-/Y}$ *RAG1*$^{-/-}$ DKO (48% of WT levels). The splenic NK cell population was markedly reduced to nearly absent in both *IL2RG*$^{-/Y}$ *RAG1*$^{-/+}$ and *IL2RG*$^{-/Y}$ *RAG1*$^{-/-}$ animals (Fig. 10, *final column*). There was insufficient thymic tissue in either the *IL2RG*$^{-/Y}$ *RAG1*$^{-/+}$ or *IL2RG*$^{-/Y}$ *RAG1*$^{-/-}$ animals to perform flow cytometry. These experiments demonstrate that combined mutation of the *IL2RG* and *RAG1* genes leads to loss of T cells in the bone marrow and loss of T and NK cells in the spleen. A small population of putative splenic B cells persists in mutant piglets.

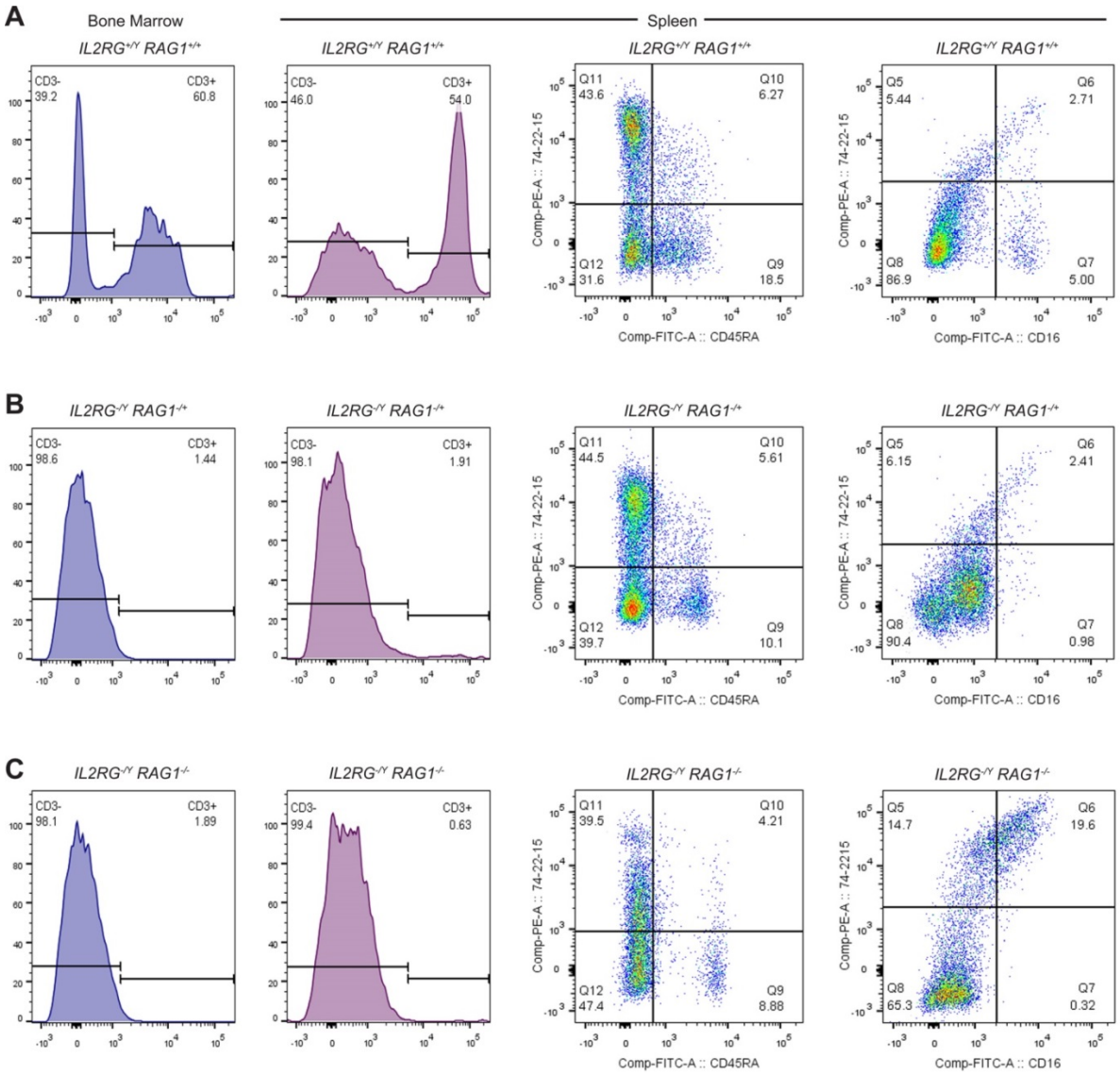

Fig. 10. Immunophenotype of bone marrow and spleen cells from *IL2RG$^{-/Y}$ RAG1$^{-/-}$* pigs.
(*A) IL2RG$^{+/Y}$ RAG1$^{+/+}$*, *(B) IL2RG$^{-/Y}$ RAG1$^{-/+}$*, and *(C) IL2RG$^{-/Y}$ RAG1$^{-/-}$*. Bone marrow and spleen cells were collected from animals sacrificed around postnatal day 30 and used to generate single cell suspensions. Bone marrow was collected from the right and left femur, and right tibia, and stained for CD3. Cell suspensions from the spleen were stained for 74-22-15, CD3, CD45RA, and CD16. CD3 identified the T cells, the B cells are 74-22-15(-) CD3(-) CD45RA(+), and the NK cells are 74-22-15(-) CD3(-) CD16(+). The last two columns (staining for B and NK cells, respectively) are gated on CD3(-) cells. $P < 0.01$ for the differences in T or B cell percentages, WT vs *IL2RG$^{-/Y}$ RAG1$^{-/+}$*, and WT vs *IL2RG$^{-/Y}$ RAG1$^{-/-}$* except for B cells in column 3 ($p = 0.0185$). Flow cytometry data are representative of results from the following number of animals in parentheses: *IL2RG$^{+/Y}$ RAG1$^{+/+}$* (3), *IL2RG$^{-/Y}$ RAG1$^{-/+}$* (2), and *IL2RG$^{-/Y}$ RAG1$^{-/-}$* (2) piglets.

2.6. Immunohistochemistry of *IL2RG*$^{-/Y}$ *RAG1*$^{-/-}$ piglets.

Thymic and splenic tissues from WT and mutant piglets were subjected to immunohistochemistry (IHC) to determine the amounts and tissue distribution patterns of T cells and B cells. Cytokeratin staining of the thymic remnant from *IL2RG*$^{-/Y}$ *RAG1*$^{-/-}$ piglets confirmed loss of distinct cortical and medullary zones with only cytokeratin-positive epithelial cell nests remaining (Fig. 11A). While CD3+ T cells localized predominantly to the thymic medulla in WT animals, the thymic remnant in *IL2RG*$^{-/Y}$ *RAG1*$^{-/-}$ animals contained only rare infiltrating CD3+ T cells. Neither WT nor *IL2RG*$^{-/Y}$ *RAG1*$^{-/-}$ piglets showed significant thymic expression of the B cell marker, CD79a (Piriou-Guzylack and Salmon, 2008).

In the spleen from WT piglets, CD3+ T cells displayed a characteristic staining pattern within the periarteriolar lymphoid sheath (PALS), while only rare CD3+ T cells were seen in the spleens from *IL2RG*$^{-/Y}$ *RAG1*$^{-/+}$ and *IL2RG*$^{-/Y}$ *RAG1*$^{-/-}$ piglets (Fig. 11B, *upper panel*). Splenic CD79a+ B cells were present in *IL2RG*$^{-/Y}$ *RAG1*$^{-/+}$ animals, but were largely absent from *IL2RG*$^{-/Y}$ *RAG1*$^{-/-}$ DKO animals (Fig. 11B, *lower panel*) despite detection of a distinct population of putative splenic B cells by flow cytometry (Fig. 10).

2.7. ELISA measurement of plasma immunoglobulins from *IL2RG*$^{-/Y}$ *RAG1*$^{-/-}$ piglets.

Humoral immunity was assessed via ELISA by measuring the concentrations of IgM, IgG, and IgA in plasma collected from *IL2RG*$^{-/Y}$ *RAG1*$^{-/+}$ and *IL2RG*$^{-/Y}$ *RAG1*$^{-/-}$ animals. *IL2RG*$^{-/Y}$ *RAG1*$^{-/+}$ piglets showed markedly decreased serum IgM expression compared to wild type (Fig. 12A). Furthermore, serum IgG was detected at lower levels but began to recover by day 20 compared to wild type (Fig. 12B). However, IgA was undetectable in the

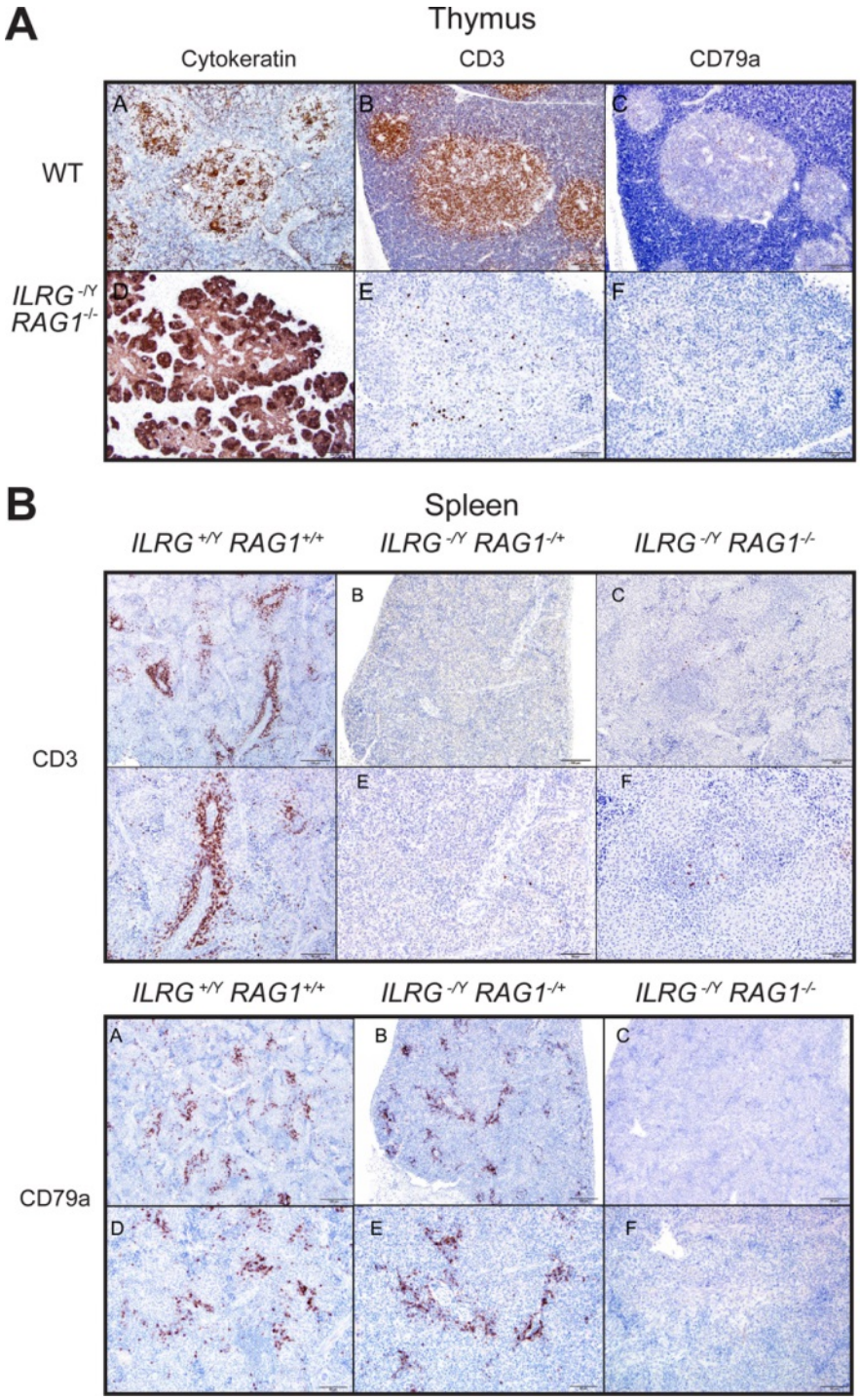

Fig. 11. Immunohistochemistry of immune organs from *IL2RG*$^{-/Y}$ *RAG1*$^{-/-}$ pigs.
(*A*) Thymus sections from postnatal day 1 stained for cytokeratin, CD3, and CD79a. (*B*) Spleen sections from approximately postnatal day 30 stained for CD3 and CD79a. IHC results are representative of two *IL2RG*$^{-/Y}$ *RAG1*$^{-/+}$ piglets and two *IL2RG*$^{-/Y}$ *RAG1*$^{-/-}$ piglets.

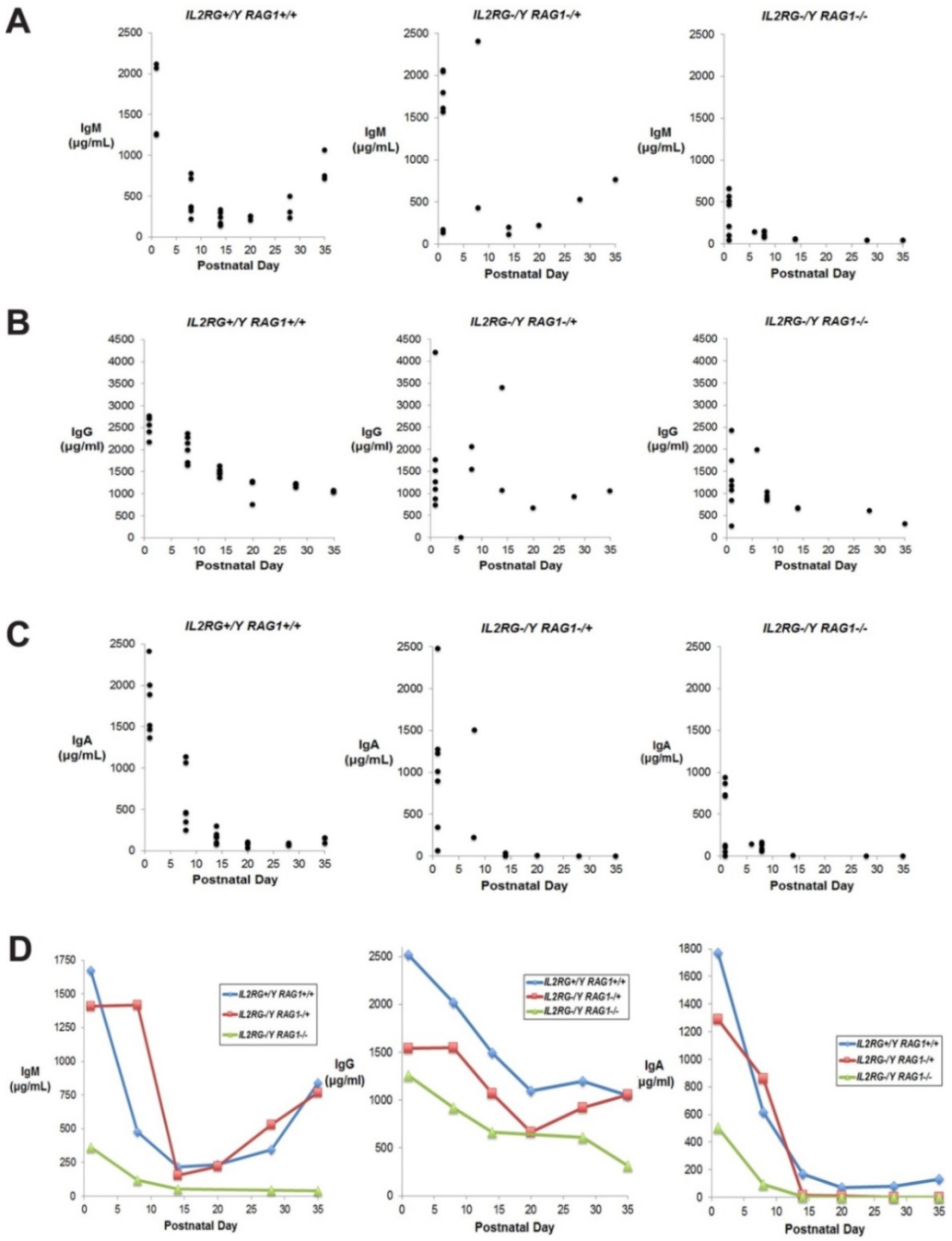

Fig. 12. Plasma immunoglobulin levels in SCID pigs.
Number of animals for each experimental group indicated in parentheses. Plasma was collected from individual WT (5) and SCID (*IL2RG*$^{-/Y}$ *RAG1*$^{-/+}$ (7), *IL2RG*$^{-/Y}$ *RAG1*$^{-/-}$ (8)) piglets at the time points indicated and subjected to ELISA to measure levels of (*A*) IgM, (*B*) IgG, and (*C*) IgA. (*D*) Mean Ig titers in the surviving pigs. Experiments were performed in triplicate for each time point and animal shown.

IL2RG$^{-/Y}$ *RAG1*$^{-/+}$ piglets (Fig. 12C). In contrast, *IL2RG*$^{-/Y}$ *RAG1*$^{-/-}$ piglets showed an even more severe phenotype, with only trace plasma levels of IgM, IgG, or IgA detected after the first week of life, similar to prior observations in *IL2RG*$^{-/Y}$ pigs (Suzuki et al., 2012). The low levels of plasma IgM, IgG, and IgA detected during postnatal week one likely reflect maternal transfer of antibodies via the colostrum (Nechvatalova et al., 2011). The observed deficits in humoral immunity are consistent with the *RAG1* mutation causing the loss of functional T helper cells, which are necessary for B cell-mediated antibody production.

2.8. Chapter Summary.

The experiments in this chapter demonstrate the first successful production of *IL2RG*$^{-/Y}$ *RAG1*$^{-/-}$ double knockout pigs. TALEN-mediated knockout of the *IL2RG* and *RAG1* loci, combined with somatic cell nuclear transfer (SCNT), facilitated the rapid production of *IL2RG*$^{-/Y}$ *RAG1*$^{-/-}$ DKO pigs within two reproductive generations. *IL2RG*$^{-/Y}$ *RAG1*$^{-/-}$ DKO pigs have an atrophic thymic remnant, absent lymph nodes, and markedly distorted splenic architecture. Table 2 summarizes the lymphocyte profiles from *IL2RG*$^{-/Y}$ *RAG1*$^{-/+}$ and *IL2RG*$^{-/Y}$ *RAG1*$^{-/-}$ pigs. Knockout of both the *IL2RG* and *RAG1* genes produces pigs that have severely reduced to absent numbers of: (1) all lymphocytes cells in the peripheral blood, (2) T cells in the thymus, and (3) T and NK cells in the spleen. A small population of putative splenic B cells was observed by flow cytometry in both *IL2RG*$^{-/Y}$ *RAG1*$^{-/+}$ and *IL2RG*$^{-/Y}$ *RAG1*$^{-/-}$ pigs. While this splenic B cell population was seen by IHC in *IL2RG*$^{-/Y}$ *RAG1*$^{-/+}$ pigs, it was not detected by IHC staining for CD79a in DKO pigs. In the absence of T cell help, the few remaining B cells are likely to be functionally defective, similar to human X-linked SCID (Noguchi et al., 1993; Puck et al., 1993), and as evidenced by nearly undetectable

Table 2. Summary of lymphocyte profiles from *IL2RG*$^{-/Y}$ *RAG1*$^{-/+}$ and *IL2RG*$^{-/Y}$ *RAG1*$^{-/-}$ pigs.
Values shown for T and NK cells are percent of total leukocytes. Values shown for B cells are percent of non-myeloid leukocytes. Values shown are the highest measured across all trials and time points.

SCID PIG CHARACTERIZATION

IL2RG+/Y RAG1+/+

Organ/Tissue	total	activated	naïve	T cells DN	DP	CD4 SP	CD8 SP	B cells	NK cells	*n*
blood	70.90	51.10	25.50	54.80	13.20	39.50	29.60	28.90	11.00	3
spleen	54.00	38.40	14.70	13.40	12.60	46.60	27.40	18.50	5.00	3
bone marrow	60.80									3

IL2RG-/Y RAG1-/+

Organ/Tissue	total	activated	naïve	T cells DN	DP	CD4 SP	CD8 SP	B cells	NK cells	*n*
blood	2.10	0.17				0.79	0.61	3.63	0.11	8
spleen	1.91							10.10	0.98	8
bone marrow	1.44	0.00								8

IL2RG-/Y RAG1-/-

Organ/Tissue	total	activated	naïve	T cells DN	DP	CD4 SP	CD8 SP	B cells	NK cells	*n*
blood	0.59					0.15	0.07	3.45	0.15	8
spleen	0.63							8.88	0.32	8
bone marrow	1.89									8

plasma levels of IgM, IgG, and IgA in DKO pigs. In total, the *IL2RG*$^{-/Y}$ *RAG1*$^{-/-}$ DKO pigs display the hallmarks of severe combined immunodeficiency and are the first pig model generated that lacks T and NK cells as well as functional B cells. In the next chapter, I describe proof-of-principle experiments for allogeneic bone marrow transplantation of these novel SCID pigs.

CHAPTER 3: ALLOGENEIC BONE MARROW TRANSPLANTATION OF SCID PIGS

3.1. Overview.

In the previous chapter, I reported the generation of *IL2RG*$^{-/Y}$ *RAG1*$^{-/-}$ SCID pigs which lack T and NK cells and functional B cells. SCID animal models are powerful tools for the study of hematopoietic development, stem cell biology, and bone marrow transplantation (BMT). A major technical challenge is the development of BMT protocols that facilitate optimal engraftment and production of donor-derived lymphoid cells while minimizing toxicity to the animal, as many bone marrow-ablative protocols cause severe, and potentially lethal toxicity. In this chapter, I describe proof-of-principle allogeneic transplantation experiments conducted in both *IL2RG*$^{-/Y}$ *RAG1*$^{-/+}$ and *IL2RG*$^{-/Y}$ *RAG1*$^{-/-}$ DKO SCID pigs. I compare several different BMT protocols for their efficacy in reconstituting lymphocytes in the SCID pigs.

3.2. Survival and analysis of peripheral blood lymphocytes after allogeneic transplantation by flow cytometry.

Figure 13 compares the Kaplan-Meier survival curves of SCID pigs after undergoing different protocols for allogeneic BMT. Regardless of the protocol used, the majority of pigs died between postnatal day 20 and day 54 of overwhelming sepsis. One of the pigs that was irradiated and underwent intraosseous BMT survived until day 79, however this pig was persistently ill and required broad spectrum antibiotics to keep alive before also succumbing to sepsis. One pig that underwent intraosseous BMT without irradiation survived until day 97

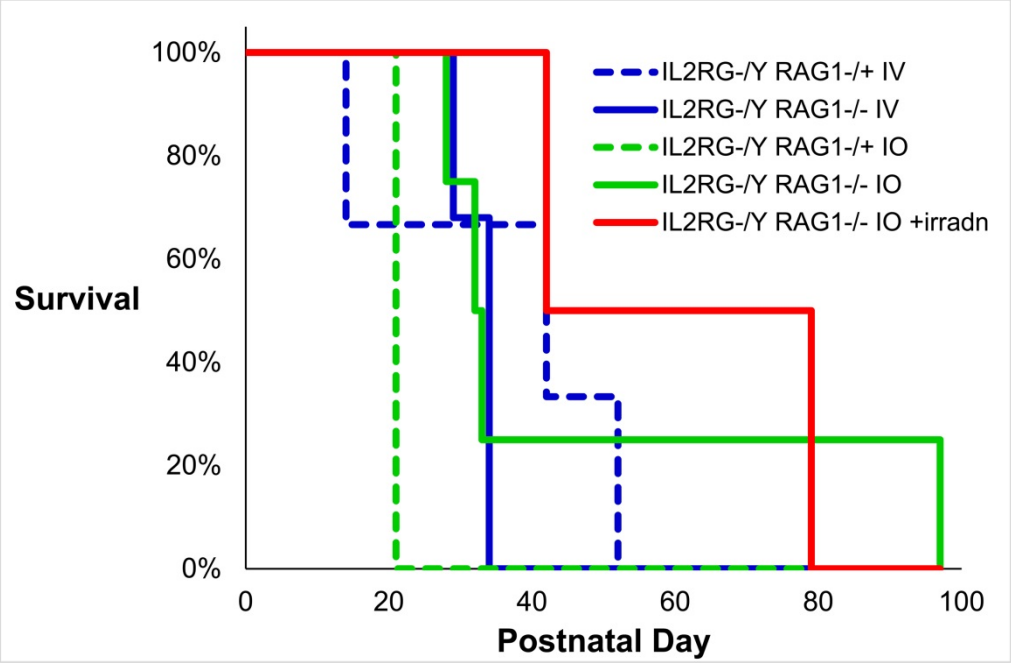

Fig. 13. Kaplan-Meier survival curve for SCID pigs after allogeneic transplant. *IL2RG*$^{-/Y}$ *RAG1*$^{-/+}$ or *IL2RG*$^{-/Y}$ *RAG1*$^{-/-}$ piglets were transplanted with allogeneic T cell depleted pig bone marrow on postnatal day 1 or 2, with their survival tracked over time. The starting number of animals in each experimental group was as follows: a total of five *IL2RG*$^{-/Y}$ *RAG1*$^{-/+}$ piglets were transplanted – three via IV route and two via IO route. A total of nine *IL2RG*$^{-/Y}$ *RAG1*$^{-/-}$ piglets were transplanted – three via IV route, four via IO route without irradiation, and two via IO route with irradiation (+irradn).

and died of severe anemia without evidence of infection. Notably, this pig showed the highest levels of reconstitution across all lymphocyte lineages (reviewed in detail below).

I next tested the efficacy of allogeneic BMT in SCID pig reconstitution with T, B, and NK cells in the peripheral blood. On postnatal day 1 or 2, *IL2RG*$^{-/Y}$ *RAG1*$^{-/+}$ and *IL2RG*$^{-/Y}$ *RAG1*$^{-/-}$ SCID pigs were transplanted via intravenous or intraosseous injection with T cell-depleted bone marrow (BM) leukocytes from an allogeneic donor pig. A total of $2x10^7$ donor BM cells were used per animal for intravenous transplant and $4x10^7$ cells for intraosseous transplant. The donor pigs expressed a transgenic marker (either Cre or H2B-GFP) which

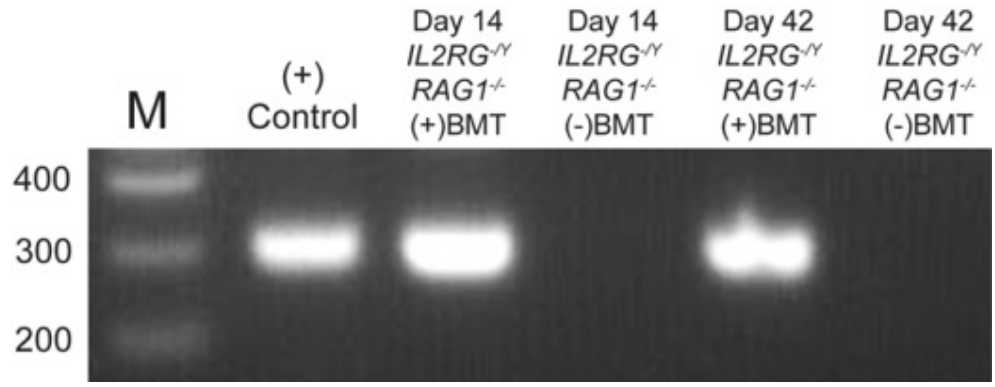

Fig. 14. Detection of donor-specific transgene in SCID pigs after allogeneic transplant.
PBMCs were harvested from the indicated animals +/- allogeneic transplant on postnatal days 14 and 42. PCR was performed on gDNA isolated from the PBMCs to detect a Cre transgene present only in donor-derived cells. Results are representative of four independent experiments.

was used to distinguish donor-derived and recipient-derived cells. On the day of transplant, two pigs were additionally treated with 1.6 Gy of total body irradiation to determine whether irradiation improves donor cell engraftment. Non-irradiated pigs (n = 5) that underwent allogeneic BMT lived for an average of 47.2 days.

To verify that peripheral blood mononuclear cells (PBMCs) in BMT recipients were donor-derived, endpoint PCR targeting the donor Cre transgene was performed on genomic DNA from the PBMCs of intraosseously transplanted and non-transplanted SCID pigs (Fig. 14). Only transplanted pigs showed the presence of the donor transgene on postnatal days 14 and 42.

Flow cytometry was used to compare the efficacy of intravenous versus intraosseous reconstitution of peripheral blood lymphocytes after allogeneic BMT. WT pigs showed a large, stable population of CD3+ T cells (Fig. 15A). Intravenous BMT of *IL2RG*$^{-/Y}$ *RAG1*$^{-/+}$ pigs led to a transient increase in peripheral blood T cells that peaked by postnatal day 28 and

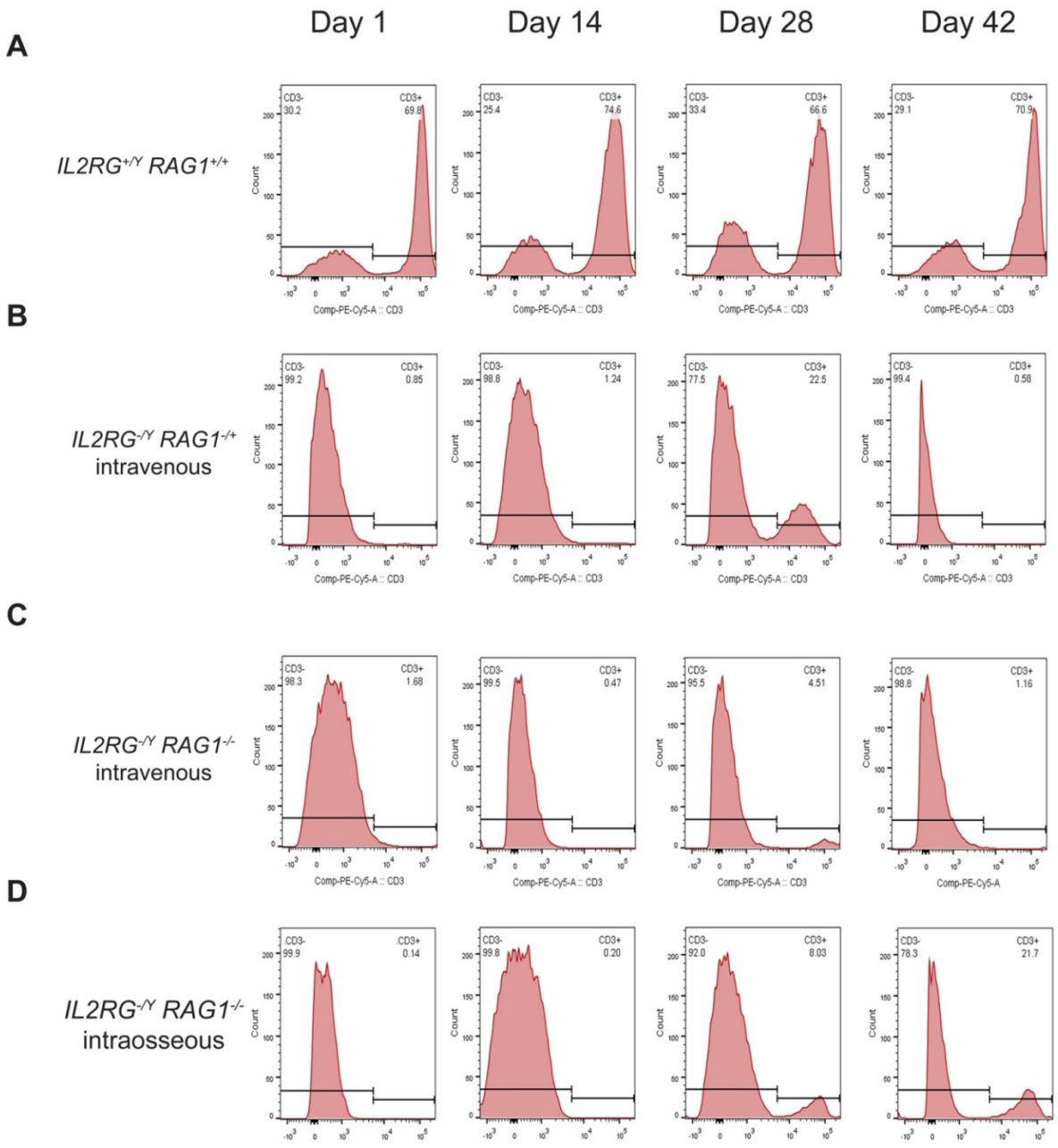

Fig. 15. Peripheral blood T cell reconstitution after intravenous or intraosseous allogeneic bone marrow transplantation in SCID pigs.
IL2RG$^{-/Y}$ *RAG1*$^{-/+}$ and *IL2RG*$^{-/Y}$ *RAG1*$^{-/-}$ piglets were transplanted intravenously or intraosseously with allogeneic pig bone marrow (allogeneic BMT) on postnatal day 1. PBMCs were collected on the days indicated (except *C, last column*, which was collected on day 34) and stained with CD3 for flow cytometry. Flow cytometry data are representative results from the following number of animals in parentheses: (*A*) WT (3), (*B*) *IL2RG*$^{-/Y}$ *RAG1*$^{-/+}$ IV (3), (*C*) *IL2RG*$^{-/Y}$ *RAG1*$^{-/-}$ IV (3), and (*D*) *IL2RG*$^{-/Y}$ *RAG1*$^{-/-}$ IO (3). $P < 0.01$ for the difference in T cell percentage between *IL2RG*$^{-/Y}$ *RAG1*$^{-/-}$ IV on day 34 and *IL2RG*$^{-/Y}$ *RAG1*$^{-/-}$ IO on day 42.

disappeared by day 42 (Fig. 15B). A similar time course was seen after BMT of *IL2RG*$^{-/Y}$ *RAG1*$^{-/-}$ pigs, however the magnitude of the increase on day 28 was only 20% of the level seen for *IL2RG*$^{-/Y}$ *RAG1*$^{-/+}$ animals (Fig. 15C). In contrast, intraosseous BMT led to a slower but sustained rise in peripheral blood T cells (Fig. 15D). Examination of the T cell subsets showed that in WT pigs, there is a rise and then fall in CD4– CD8– double negative (DN) T cells, consistent with production then differentiation of the DN cells. Over time, the proportion of CD4+ CD8+ double positive (DP) and CD8+ single positive (SP) T cells increases, while the proportion of CD4+ SP T cells decreases (Fig. 16A). In *IL2RG*$^{-/Y}$ *RAG1*$^{-/+}$ pigs after intravenous BM, on day 28 the transient T cell population seen is composed largely of CD8+ SP T cells, with much smaller populations of DN, followed by DP T cells, and almost no CD4+ SP T cells (Fig. 16C). Intraosseous BMT led to the accumulation of largely CD8 SP cells on day 28, but then mostly DP cells by day 42 with only a small CD4 SP T cell population (Fig. 16F).

Expression of CD45RA is a marker of naïve T cells, while loss of CD45RA expression on T cells is a marker of activation or a memory phenotype (Mackall et al., 1993; Piriou-Guzylack and Salmon, 2008). WT pigs had large numbers of both naïve and activated T cells, with a slightly higher number of activated T cells in early postnatal life (Fig. 17A). In contrast, regardless of BMT method used, reconstituted T cells were overwhelming activated/memory cells, at levels 6- to 10-fold higher than naïve T cells (Fig. 17C-F). Only intraosseous BMT produced a small population of naïve T cells. Similarly, while intravenous BMT led to minimal rescue of B cells (74-22-15–, CD3–, CD45RA+) (Fig. 17C and Fig. 17E) and NK cells (74-22-15–, CD3–, CD16+) (Fig. 18C and Fig. 18E), intraosseous BMT

Fig. 16. Peripheral blood T cell subsets after intravenous or intraosseous allogeneic bone marrow transplantation in SCID pigs.

Allogeneic BMT was conducted as described in Fig. 15. PBMCs were collected on the days indicated, gated on CD3(+) cells, and stained for CD4 and CD8 for flow cytometry. Flow cytometry data are representative results from the following number of animals in parentheses: (*A*) WT (3), (*B*) *IL2RG*$^{-/Y}$ *RAG1*$^{-/+}$ non-transplanted (4), (*C*) *IL2RG*$^{-/Y}$ *RAG1*$^{-/+}$ IV BMT (3), (D) *IL2RG*$^{-/Y}$ *RAG1*$^{-/-}$ non-transplanted (2), (*E*) *IL2RG*$^{-/Y}$ *RAG1*$^{-/-}$ IV BMT (3), and (*F*) *IL2RG*$^{-/Y}$ *RAG1*$^{-/-}$ IO BMT (4) piglets. $P <$ 0.01 for the percentage of double positive T cells in IO BMT versus non-transplanted pigs on postnatal days 28 and 42.

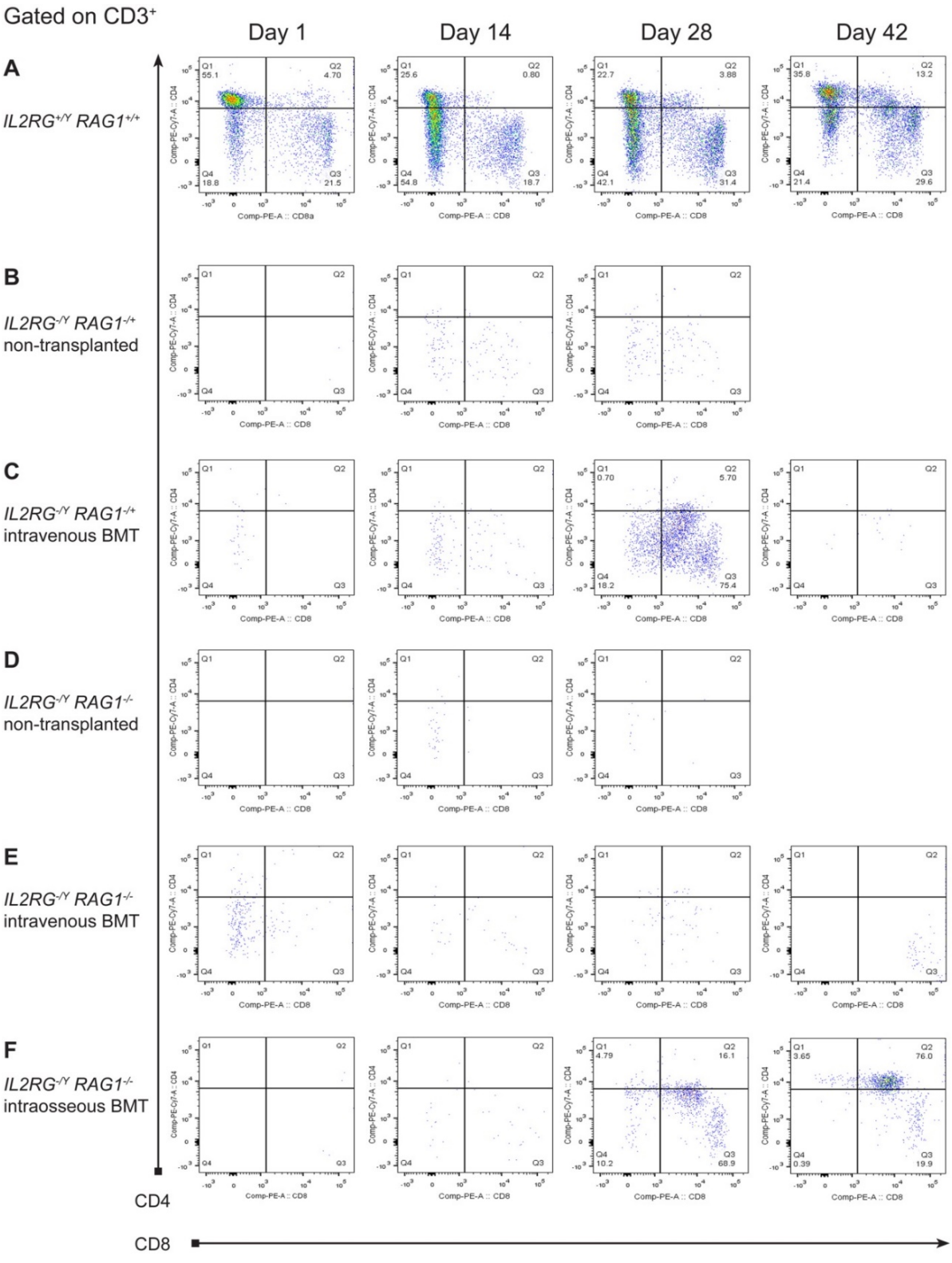
Gated on CD3+
Day 1
Day 14
Day 28
Day 42
A
IL2RG+/Y RAG1+/+
B
IL2RG-/Y RAG1-/+
non-transplanted
C
IL2RG-/Y RAG1-/+
intravenous BMT
D
IL2RG-/Y RAG1-/-
non-transplanted
E
IL2RG-/Y RAG1-/-
intravenous BMT
F
IL2RG-/Y RAG1-/-
intraosseous BMT
CD4
CD8
Comp-PE-Cy7-A :: CD4
Comp-PE-A :: CD8a
Comp-PE-A :: CD8
Q1 55.1
Q2 4.70
Q4 18.8
Q3 21.5
Q1 25.6
Q2 0.80
Q4 54.8
Q3 18.7
Q1 22.7
Q2 3.88
Q4 42.1
Q3 31.4
Q1 35.8
Q2 13.2
Q4 21.4
Q3 29.6
Q1 0.70
Q2 5.70
Q4 18.2
Q3 75.4
Q1 4.79
Q2 16.1
Q4 10.2
Q3 68.9
Q1 3.65
Q2 76.0
Q4 0.39
Q3 19.9

Fig. 17. Naïve T and B cells in the peripheral blood after intravenous or intraosseous allogeneic bone marrow transplantation in SCID pigs.
Allogeneic BMT was conducted as described in Fig. 15. PBMCs were collected on the days indicated, gated on 74-22-15 (-), and stained for CD3 and CD45RA for flow cytometry. Naïve T cells are CD3(+)CD45RA(+); activated or memory T cells are CD3(+) CD45RA (-); B cells are 74-22-15(-) CD3(-) CD45RA(+). Flow cytometry data are representative results from the following number of animals in parentheses: (*A*) WT (3), (*B*) *IL2RG*$^{-/Y}$ *RAG1*$^{-/+}$ non-transplanted (4), (*C*) *IL2RG*$^{-/Y}$ *RAG1*$^{-/+}$ IV BMT (3), (D) *IL2RG*$^{-/Y}$ *RAG1*$^{-/-}$ non-transplanted (2), (*E*) *IL2RG*$^{-/Y}$ *RAG1*$^{-/-}$ IV BMT (3), and (*F*) *IL2RG*$^{-/Y}$ *RAG1*$^{-/-}$ IO BMT (4) piglets. $P < 0.01$ for the difference in B cell percentage between *IL2RG*$^{-/Y}$ *RAG1*$^{-/-}$ intraosseous BMT and *IL2RG*$^{-/Y}$ *RAG1*$^{-/-}$ intravenous BMT.

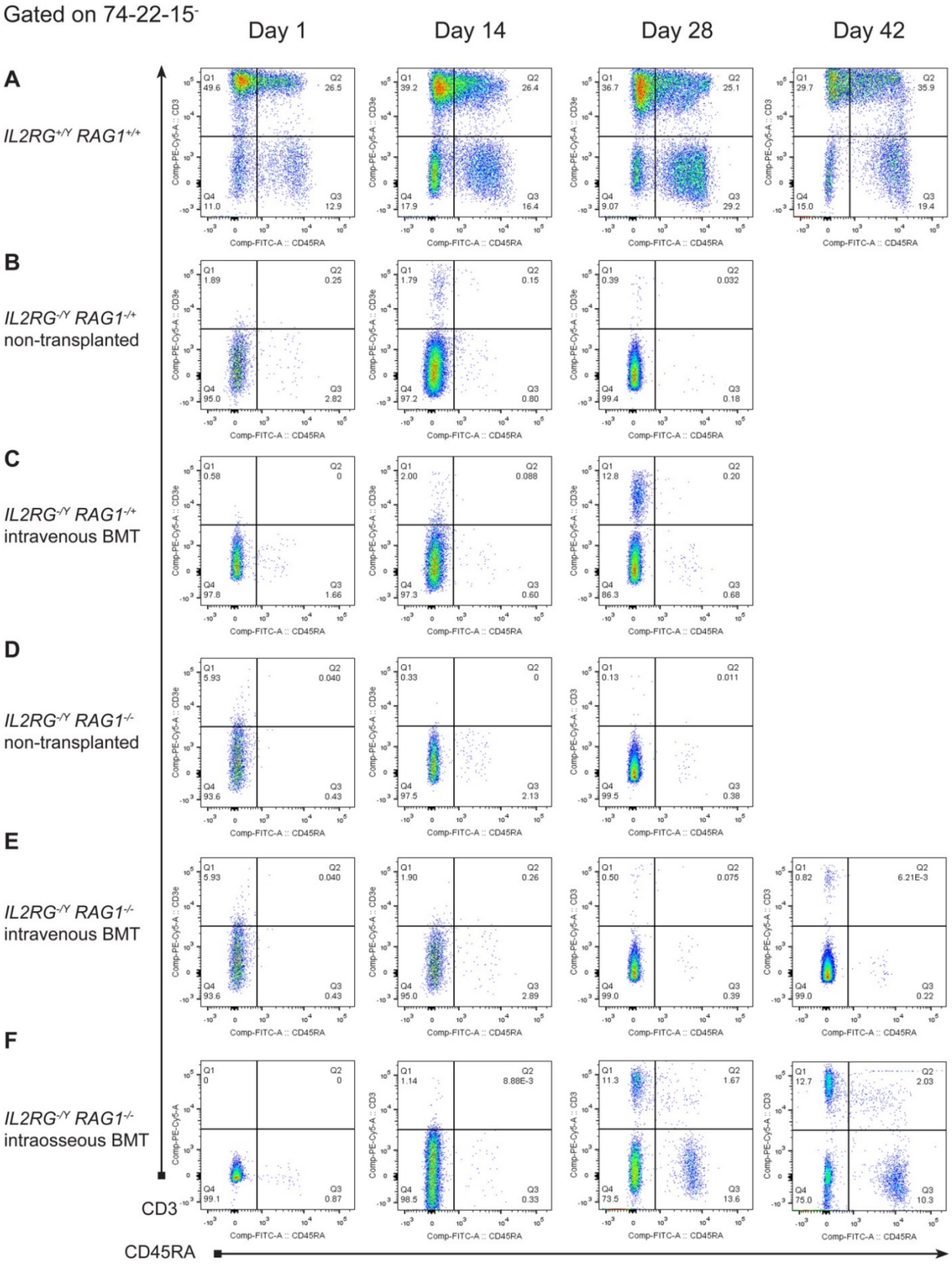
Gated on 74-22-15-
Day 1
Day 14
Day 28
Day 42
A
IL2RG+/Y RAG1+/+
B
IL2RG-/Y RAG1-/+
non-transplanted
C
IL2RG-/Y RAG1-/+
intravenous BMT
D
IL2RG-/Y RAG1-/-
non-transplanted
E
IL2RG-/Y RAG1-/-
intravenous BMT
F
IL2RG-/Y RAG1-/-
intraosseous BMT
CD3
CD45RA

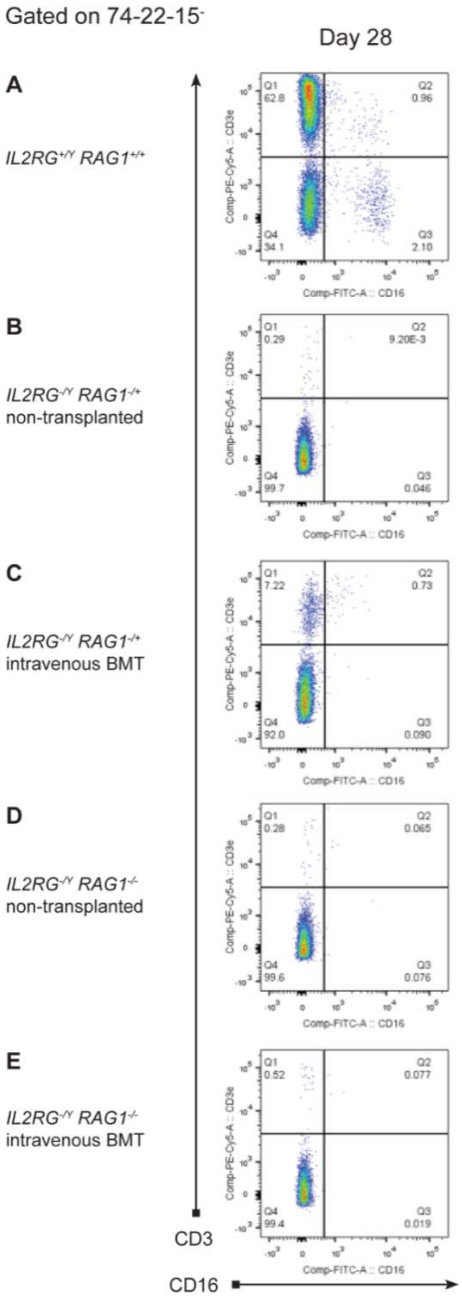

Fig. 18. Peripheral blood NK cells after intravenous or intraosseous allogeneic bone marrow transplantation in SCID pigs.

Allogeneic BMT was conducted as described in Fig. 15. PBMCs were collected on the days indicated, gated on 74-22-15(-), and stained for CD3 and CD16 for flow cytometry. NK cells are 74-22-15(-), CD3(-), CD16(+). Flow cytometry data are representative results from the following number of animals in parentheses: (*A*) WT (3), (*B*) *IL2RG*$^{-/Y}$ *RAG1*$^{-/+}$ non-transplanted (4), (*C*) *IL2RG*$^{-/Y}$ *RAG1*$^{-/+}$ IV BMT (3), (D) *IL2RG*$^{-/Y}$ *RAG1*$^{-/-}$ non-transplanted (2), and (*E*) *IL2RG*$^{-/Y}$ *RAG1*$^{-/-}$ IV BMT (3) piglets.

yielded significant, sustained reconstitution of B cells (Fig. 17F) and NK cells (Fig. 21C and 21D). Together, these data demonstrate that intraosseous BMT is superior to intravenous BMT for the reconstitution of peripheral blood lymphocytes. Intraosseous transplantation was therefore used for the remaining allogeneic BMT experiments described in this chapter.

Peripheral blood was harvested after allogeneic intraosseous BMT on postnatal days 1, 14, 28, and 42, with the levels of T, B, and NK cells measured by flow cytometry. As before, WT pigs showed a large, stable population of peripheral blood CD3+ T cells (Fig. 19A) composed of CD4– CD8– double negative cells, CD4+ CD8+ double positive (DP) cells, CD4+ CD8– single positive (SP) T helper (T_H) cells , and CD4– CD8+ SP cells (Fig. 19B). Within both the DN and CD8+ SP cells is a significant population of γδ T cells, which express a T cell receptor (TCR) heterodimer composed of the γ and δ TCR subunits (Gerner et al., 2009; Sinkora and Butler, 2009). The γδ T cells are the major T cell subpopulation in early postnatal life, but as pigs age, their repertoire shifts towards T cells that express the more typical TCRαβ heterodimer (Charerntantanakul and Roth, 2007). Our data showed a time-dependent rise and fall in both the DN and CD8+ SP populations, consistent with the previously described dynamics of γδ T cells in pigs. From postnatal day 14 to 42, there was an increase in CD4+ CD8+ DP cells; unlike humans and mice, these DP cells are commonly found in the peripheral blood and represent a memory T cell population (Gerner et al., 2009). There is also a decrease in CD4+ SP cells with age (the higher proportion on day 42 is due to the relative decrease in the DN population), consistent with prior observations that the CD4/CD8 ratio in SP T cells shifts from CD4-dominant to CD8-dominant as pigs age (Stepanova et al., 2007).

Fig. 19. Immunophenotype of peripheral blood T cells from SCID pigs after allogeneic transplant.
IL2RG$^{-/Y}$ *RAG1*$^{-/-}$ piglets were transplanted intraosseously with allogeneic pig bone marrow (allogeneic BMT) on postnatal day 1; irradiated pigs were transplanted 6 hours post irradiation. PBMCs were collected on the days indicated and stained for flow cytometry. (*A*) CD3, (*B*) Gated on CD3(+) cells, stained for CD8 (*x-axis*) and CD4 (*y-axis*). $P < 0.01$ for the difference in the percentage of CD3(+) T cells and DP T cells between non-irradiated and irradiated BMT pigs on postnatal day 42. Flow cytometry data are representative results from the following number of animals in parentheses: WT (3), *IL2RG*$^{-/Y}$ *RAG1*$^{-/-}$ non-transplanted (2), *IL2RG*$^{-/Y}$ *RAG1*$^{-/-}$ IO BMT (4), and *IL2RG*$^{-/Y}$ *RAG1*$^{-/-}$ IO irradiated BMT (2) piglets.

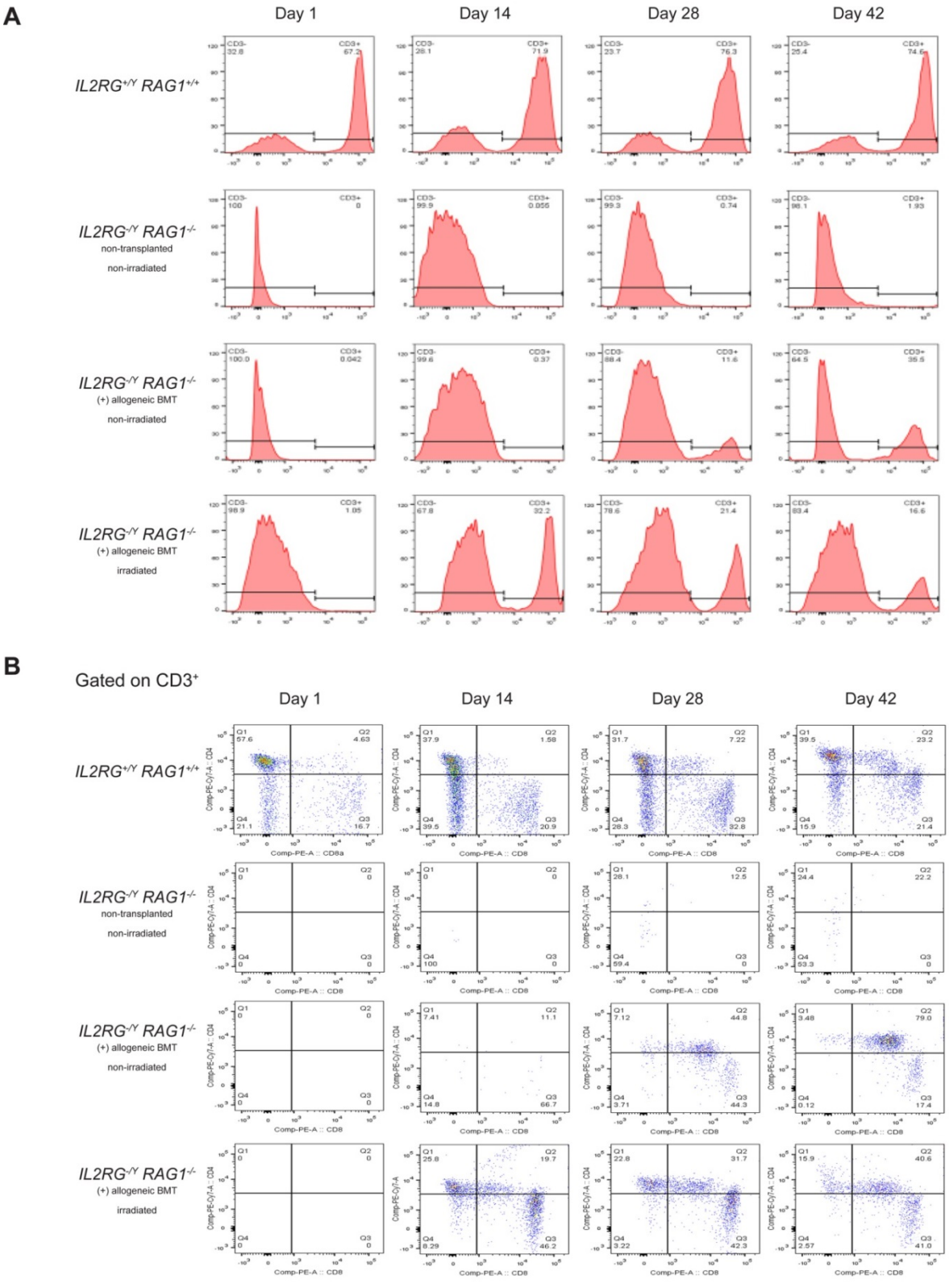
A
Day 1
Day 14
Day 28
Day 42
IL2RG+/Y RAG1+/+
IL2RG-/Y RAG1-/-
non-transplanted
non-irradiated
IL2RG-/Y RAG1-/-
(+) allogeneic BMT
non-irradiated
IL2RG-/Y RAG1-/-
(+) allogeneic BMT
irradiated
B
Gated on CD3+
Day 1
Day 14
Day 28
Day 42
IL2RG+/Y RAG1+/+
IL2RG-/Y RAG1-/-
non-transplanted
non-irradiated
IL2RG-/Y RAG1-/-
(+) allogeneic BMT
non-irradiated
IL2RG-/Y RAG1-/-
(+) allogeneic BMT
irradiated
Comp-PE-A :: CD8a
Comp-PE-A :: CD8
Comp-PE-Cy7-A :: CD4

Non-transplanted SCID pigs showed rare to absent CD3+ T cells in the peripheral blood at all time points tested (Fig. 19A). In non-irradiated SCID pigs receiving allogeneic BMT, CD3+ T cells first appeared in the peripheral blood on postnatal day 28 and continued to increase through day 42. The T cells observed on day 28 in these animals were an approximately equal mix of CD8+ SP cells and CD4+ CD8+ DP T cells, while only a small population of CD4+ SP T cells was seen (Fig. 19B). By day 42, there was a relative increase in the size of the DP cell population while the numbers of CD4+ and CD8+ SP T cells remained largely unchanged. These data show that allogeneic BMT of non-irradiated SCID pigs partially reconstitutes peripheral blood T cells. There were more CD8+ SP cells than CD4+ SP cells, consistent with the CD8+ SP-biased developmental program of the DP to SP T cell transition seen with aging (Charerntantanakul and Roth, 2007; Stepanova et al., 2007). The increase in DP cells represents either a growing population of DP progenitors or an increasing pool of DP memory T cells in the periphery. The latter possibility is the more likely identity of these DP cells, however given the thymic atrophy seen in SCID animals, it is possible that DP progenitors may be seen in increased numbers in the peripheral blood as they search for alternative lymphoid organs to complete T cell differentiation.

SCID pigs that underwent both irradiation and allogeneic BMT showed faster reconstitution of peripheral blood T cells than non-irradiated animals, with a large CD3+ population present by postnatal day 14 (Fig. 19A). The largest proportion of these cells was CD8+ T cells (46.2%), with smaller but substantial numbers of CD4+ T cells (25.8%) and DP T cells (19.7%) (Fig. 19B). Subsequent time points, however, showed progressive decreases in the proportion of CD3+ cells in irradiated BMT pigs, dropping below the level

seen in non-irradiated BMT pigs by day 42. Irradiated pigs also showed a relative shift from CD4+ T cells towards DPT cells, while the CD8+ T cell population was largely unchanged, consistent with the CD8 bias of the CD4/CD8 SP ratio discussed previously. This could also reflect conversion of a subset of CD4+ SP cells to DP memory T cells. These data show that allogeneic BMT of irradiated SCID pigs leads to the rapid reconstitution and expansion of peripheral blood T cells, but that this T cell population is not sustained over time.

There are several possible explanations for the T cell dynamics seen in irradiated BMT pigs. First, radiation-induced ablation of the bone marrow could create a more favorable early niche for the engraftment of hematopoietic progenitors. Second, T cell expansion may have initially occurred in response to occult viral infection or radiation-induced tissue inflammation, as irradiated animals were persistently very ill. The post-expansion decrease in T cell numbers is likely multifactorial, including normal contraction of the T cell population after completion of the acute response, disruption of T cell survival signals due to the poor health of the animals, and impaired lymphopoiesis due to side effects from the antibiotics.

As discussed above, the peripheral blood population of DN T cells in WT animals likely represents γδ T cells. Notably, both non-irradiated and irradiated pigs that underwent BMT had low to absent DN T cell populations in the peripheral blood (Fig. 19B). This suggests that donor-derived T cell progenitors are largely directed to differentiate into T cells expressing TCRαβ which predominate in the later postnatal period, rather than γδ T cells which compose the majority of T cells during fetal and early postnatal life. Alternatively, the

paucity of DN cells in BMT pigs may reflect the effects of a compensatory increase in signals to stimulate T cell development, due to the low numbers of T cells in SCID animals.

To investigate the activation state of T cells observed in transplanted pigs, CD3+ cells were co-stained with CD45RA+, a marker of naïve T cells which is lost with activation (Piriou-Guzylack and Salmon, 2008). WT pigs had robust populations of both naïve CD45RA+ T cells and activated CD45RA– T cells (Fig. 20A), while both populations were minimal to absent in non-transplanted *IL2RG*$^{-/Y}$ *RAG1*$^{-/-}$ SCID pigs (Fig. 20B). Non-irradiated pigs that underwent allogeneic BMT showed time-dependent accumulation of a larger population of CD45RA– T cells with a smaller CD45RA+ T cell population (Fig. 20C). Irradiated BMT pigs showed early accumulation of CD45RA– T cells by day 14 which had decreased rapidly by 28, while CD45RA+ T cells formed a small, stable population comparable in proportion to non-irradiated counterparts (Fig. 20D). These data show that the majority of T cells in transplanted pigs are activated, suggesting that they are rapidly activated in response to environmental antigens after completing development. In irradiated pigs, the rapid expansion and decrease in the activated CD45RA– T cell population with the stability of the naïve CD45RA+ pool is consistent with contraction of activated T cells at the completion of an acute immune response.

The B cell population in the peripheral blood of transplanted pigs was measured by staining for 74-22-15 (myeloid lineage) negative, CD3–, CD45RA+ cells. WT pigs had a large B cell population that increased in size over time (Fig. 20A), while only a trace population was retained in non-transplanted *IL2RG*$^{-/Y}$ *RAG1*$^{-/-}$ SCID pigs that was lost by day 28 (Fig. 20B). Non-irradiated BMT pigs had a large peripheral blood B cell population by

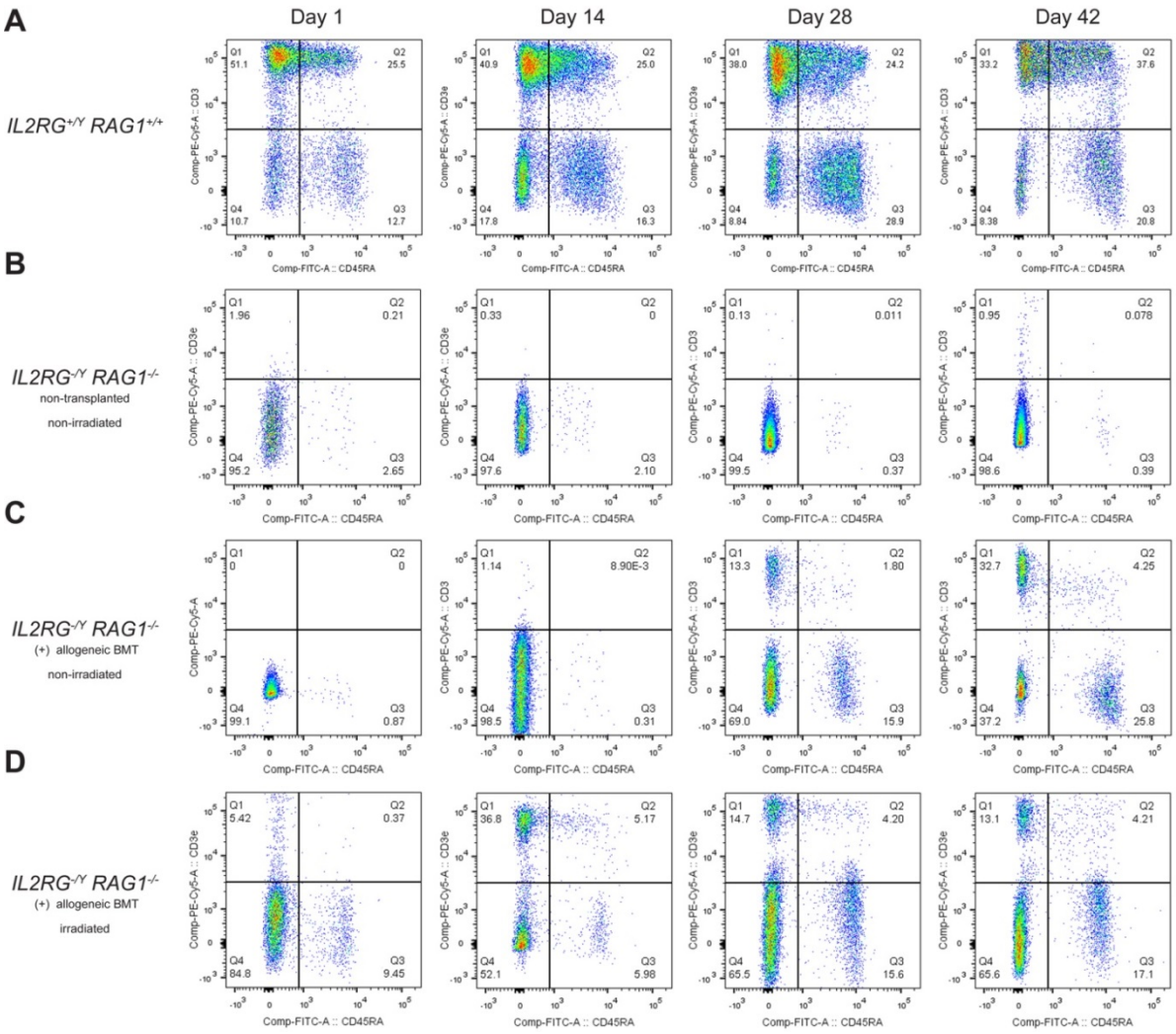

Fig. 20. Naïve T and B cells in peripheral blood from SCID pigs after allogeneic transplant. *IL2RG*$^{-/Y}$ *RAG1*$^{-/-}$ piglets were transplanted intraosseously with allogeneic pig bone marrow (allogeneic BMT) as in Fig. 19. PBMCs were collected on the days indicated and stained for flow cytometry. PBMCs from (*A*) WT, (*B*) non-transplanted/non-irradiated, (*C*) allogeneic BMT/non-irradiated and (*D*) allogeneic BMT/irradiated piglets were gated 74-22-15(-) to detect non-myeloid cells and stained with CD3 and CD45RA. CD45RA is a marker of naïve T cells, while loss of CD45RA is a marker of T cell activation. CD3(-) CD45RA(+) cells in these flow plots are B cells. Flow cytometry data are representative results from the following number of animals in parentheses: WT (3), *IL2RG*$^{-/Y}$ *RAG1*$^{-/-}$ non-transplanted (2), *IL2RG*$^{-/Y}$ *RAG1*$^{-/-}$ IO BMT (4), and *IL2RG*$^{-/Y}$ *RAG1*$^{-/-}$ IO irradiated BMT (2) piglets.

day 28 which continued to increase by day 42 (Fig. 20C). Irradiated BMT pigs showed earlier production of peripheral blood B cells by day 14, however there was no significant difference between irradiated and non-irradiated pigs in the B cell percentage on postnatal day 42 (Fig. 20D). These studies show that allogeneic transplant of SCID pigs successfully repopulates B cells in the peripheral blood.

WT pigs showed a small population of NK cells (74-22-15– CD16+) which increased on day 42 (Fig. 21A), while this population was absent in non-transplanted *IL2RG*$^{-/Y}$ *RAG1*$^{-/-}$ SCID pigs (Fig. 21B). Allogeneic BMT in either non-irradiated (Fig. 21C) or irradiated (Fig. 21D) SCID pigs led to partial NK cell reconstitution, seen minimally on day 28 and increasing by day 42. Also noted is a 74-22-15+ CD16+ population in the peripheral blood which represents dendritic cells (DCs) (Piriou-Guzylack and Salmon, 2008). In WT pigs peripheral blood DCs first appeared on day 28 and had increased in number by day 42 (Fig. 21A). The appearance of DCs is delayed in non-transplanted SCID pigs, however a substantial population is seen by day 42 (Fig. 21B), indicating that DCs are relatively insensitive to mutations in *IL2RG* and *RAG1*, as predicted. Peripheral blood DCs appear in non-irradiated BMT pigs on day 28, similar to WT (Fig. 21C), while they appear even earlier in irradiated pigs on day 14 (Fig. 21D), however both non-irradiated and irradiated BMT pigs have substantial peripheral blood DC populations by day 42.

3.3. Analysis of lymphocytes in the spleen and thymus after allogeneic transplantation.

Lymphocyte populations in the spleen were measured from SCID pigs that underwent allogeneic BMT without total body irradiation. Over half of splenic cells in WT pigs were CD3+ (Fig. 22A), localized predominantly to the periarteriolar lymphoid sheath (PALS) by

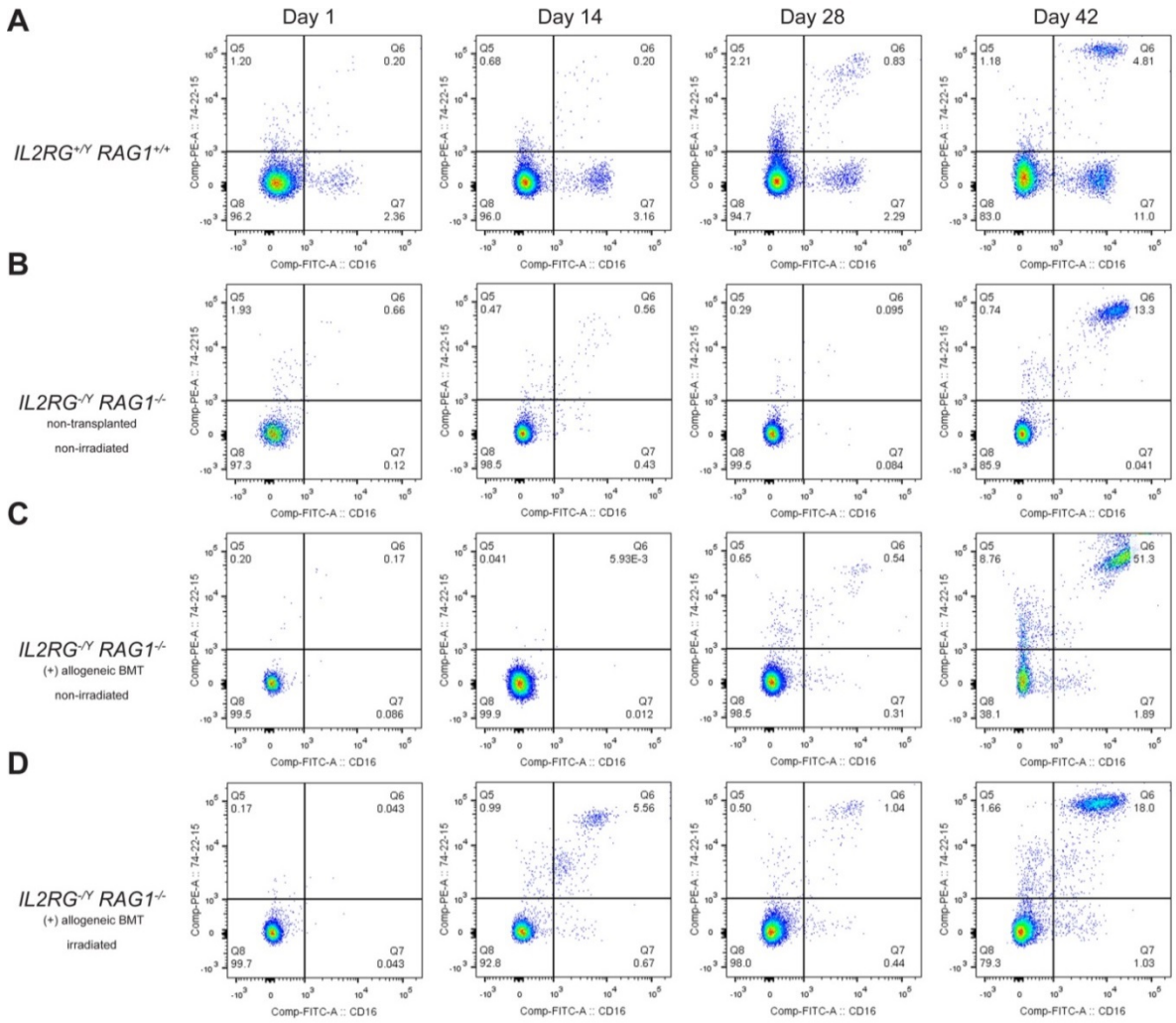

Fig. 21. NK cells in peripheral blood from SCID pigs after allogeneic transplant.
IL2RG$^{-/Y}$ *RAG1*$^{-/-}$ piglets were transplanted intraosseously with allogeneic pig bone marrow (allogeneic BMT) as in Fig. 19. PBMCs were collected on the days indicated and stained for flow cytometry with 74-22-15 and CD16 to identify NK cells, defined as 74-22-15(-) CD16(+). Flow cytometry data are representative results from the following number of animals in parentheses: WT (3), *IL2RG*$^{-/Y}$ *RAG1*$^{-/-}$ non-transplanted (2), *IL2RG*$^{-/Y}$ *RAG1*$^{-/-}$ IO BMT (4), and *IL2RG*$^{-/Y}$ *RAG1*$^{-/-}$ IO irradiated BMT (2) piglets.

Fig. 22. Rescue of splenic T cells in SCID pigs after allogeneic transplant.
Splenic cell suspensions were generated from (*A*) WT (postnatal day 80 or d80), (*B*) *IL2RG*$^{-/Y}$ *RAG1*$^{-/+}$, (non-transplanted d32, IV allogeneic BMT d52, IO allogeneic BMT d21) and (*C*) *IL2RG*$^{-/Y}$ *RAG1*$^{-/-}$ (non-transplanted d28, IO allogeneic BMT d97) animals. The efficacy of allogeneic transplant via intravenous versus intraosseous routes was compared (*B*, $p < 0.01$). Flow cytometry data are representative results from the following number of animals in parentheses: WT (3), *IL2RG*$^{-/Y}$ *RAG1*$^{-/+}$ non-transplanted (4), *IL2RG*$^{-/Y}$ *RAG1*$^{-/+}$ IV BMT (3), *IL2RG*$^{-/Y}$ *RAG1*$^{-/+}$ IV BMT (2), *IL2RG*$^{-/Y}$ *RAG1*$^{-/-}$ non-transplanted (2), *IL2RG*$^{-/Y}$ *RAG1*$^{-/-}$ IV BMT (3), and *IL2RG*$^{-/Y}$ *RAG1*$^{-/-}$ IO BMT (4) piglets.

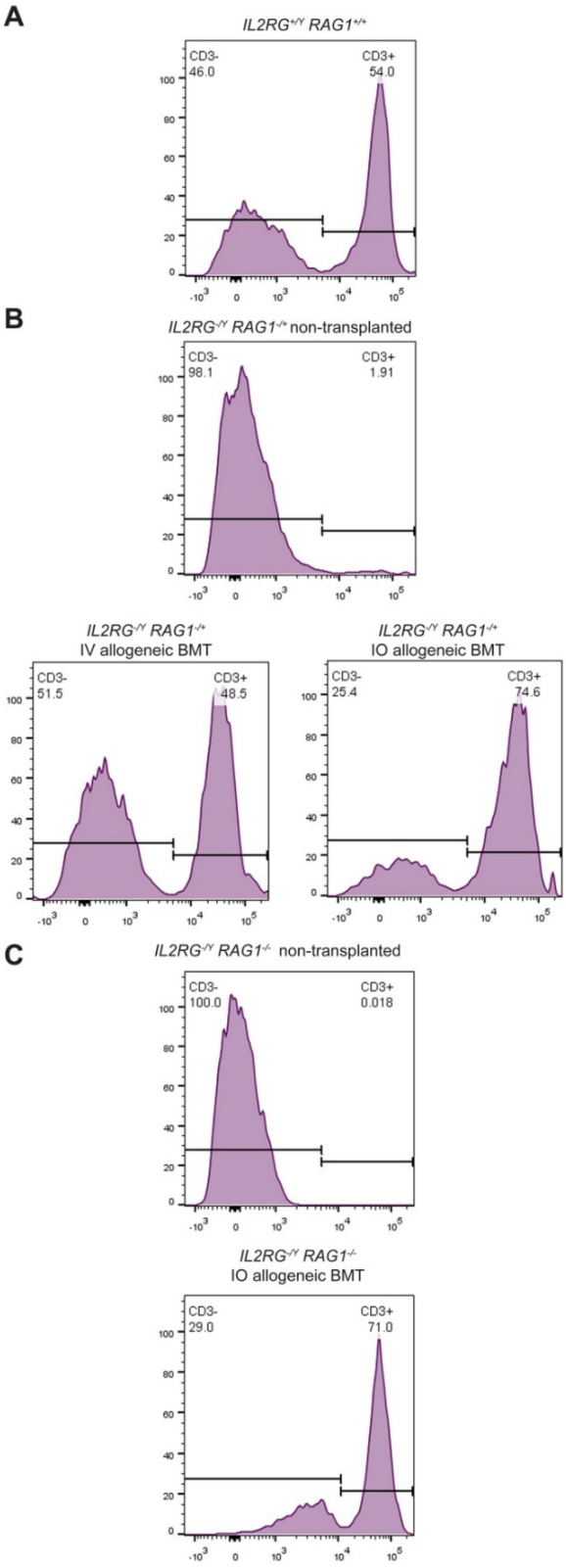
A
IL2RG+/Y RAG1+/+
CD3-
46.0
CD3+
54.0
B
IL2RG-/Y RAG1-/+ non-transplanted
CD3-
98.1
CD3+
1.91
IL2RG-/Y RAG1-/+
IV allogeneic BMT
CD3-
51.5
CD3+
48.5
IL2RG-/Y RAG1-/+
IO allogeneic BMT
CD3-
25.4
CD3+
74.6
C
IL2RG-/Y RAG1-/- non-transplanted
CD3-
100.0
CD3+
0.018
IL2RG-/Y RAG1-/-
IO allogeneic BMT
CD3-
29.0
CD3+
71.0

IHC (Fig. 23A). The largest T cell subset was CD4+ SP cells, consistent with their role in providing T cell help to splenic B cells (Fig. 24A). A smaller population of CD8+ SP T cells was present, with even smaller populations of DN and DP cells, with the latter population likely representing a subset of DP memory T cells. Only a trace CD3+ population remained in *IL2RG*$^{-/Y}$ *RAG1*$^{-/+}$ pigs (Figs. 22B and 23B) which was lost in *IL2RG*$^{-/Y}$ *RAG1*$^{-/-}$ DKO pigs (Fig. 22C and 24B). Intraosseous BMT was more effective in reconstituting splenic T cells than intravenous BMT (Fig. 22B). Intraosseous allogeneic BMT of DKO pigs led to complete rescue of the T cell population (Fig. 22C), with the CD3+ fraction higher than that seen in WT, possibly due to thymic atrophy in SCID pigs leading to redirection of T cells to other lymphoid organs, including the spleen. Similar to the peripheral blood, the splenic T cell population after allogeneic BMT was mostly DP (memory) cells with a small population of CD8+ SP cells (Fig. 24C). Irradiated allogeneic BMT pigs showed reduced numbers of T cells, which were mostly DP cells with a slightly smaller population of CD8+ SP cells (Fig. 24D). The reconstituted T cell population in *IL2RG*$^{-/Y}$ *RAG1*$^{-/+}$ pigs localized to the PALS, similar to the IHC pattern observed for WT (Fig. 23C). In WT pigs, splenic T cells were composed of both naïve (CD45RA+) and activated (CD45RA–) subpopulations in an approximately 1:2.6 ratio (Fig. 25A). In transplanted non-irradiated animals, the ratio is even more markedly skewed towards activated T cells in a greater than 1:8 CD45RA+/CD45RA– ratio (Fig. 25C), consistent with the large numbers of activated T cells seen in the peripheral blood (Fig. 20). Splenic B cells in non-transplanted *IL2RG*$^{-/Y}$ *RAG1*$^{-/-}$ DKO pigs were reduced to less than half of the levels seen in WT pigs but not absent (Fig. 25A and 18B), as described in the previous chapter. Allogeneic BMT without irradiation failed to reconstitute

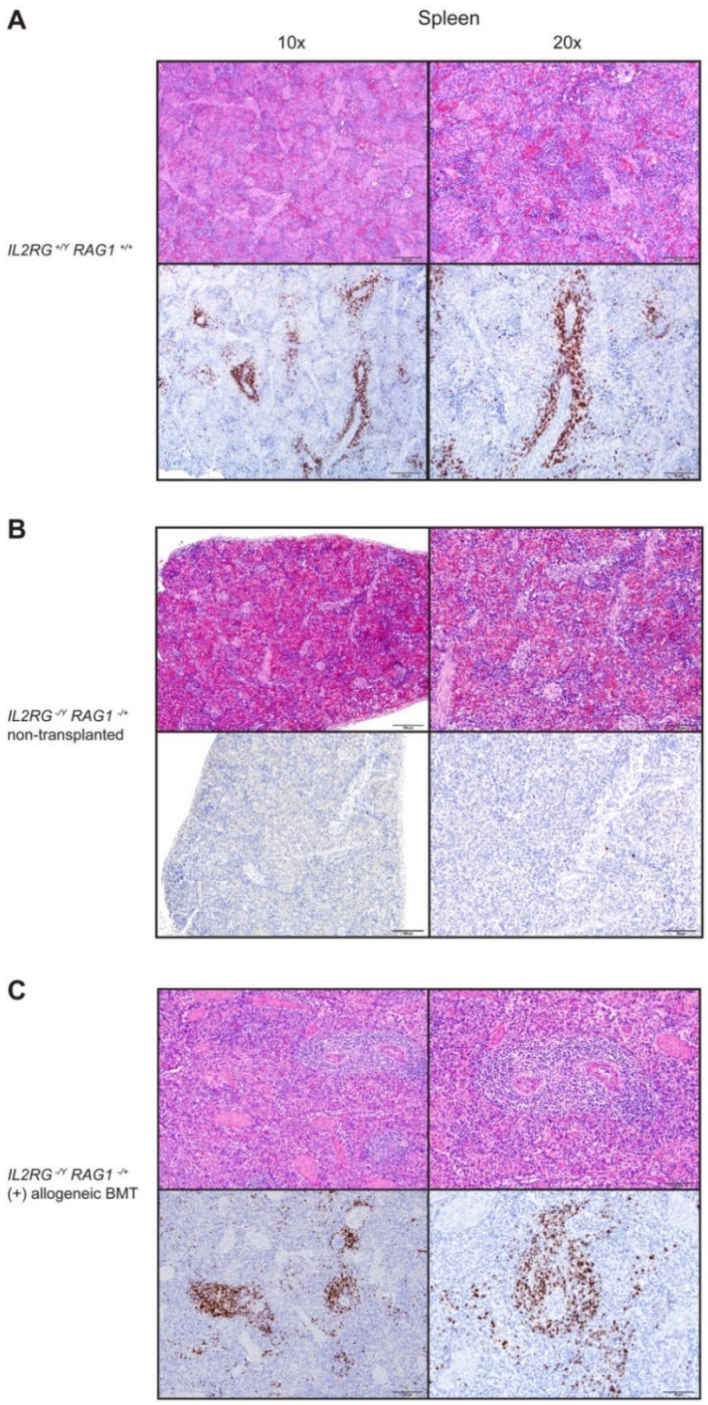

Fig. 23. Histology and immunohistochemistry of allogeneic T cell repopulation of the spleen in transplanted SCID pigs.
Spleen sections from (*A*) WT postnatal d42, (*B*) non-transplanted d32, and (*C*) transplanted d54 were stained with hematoxylin and eosin (*upper panels*) or CD3 (*lower panels*). Representative results shown are from two independent experiments.

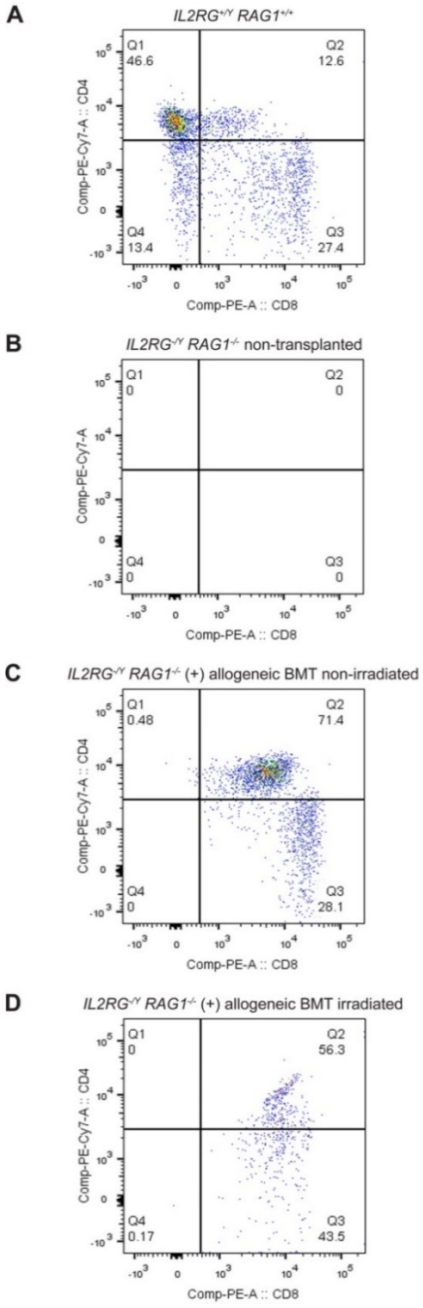

Fig. 24. Splenic T cell subtypes in *IL2RG*$^{-/Y}$ *RAG1*$^{-/-}$ pigs after allogeneic transplant.
Splenic cells from (*A*) WT postnatal d80, (*B*) non-transplanted d28, (C) allogeneic BMT/non-irradiated d97, and (D) allogeneic BMT/irradiated piglets d79 were gated for CD3+ cells and stained with CD4 and CD8. $P < 0.01$ for DP T cells in transplanted pigs versus non-transplanted. Flow cytometry data are representative results from the following number of animals in parentheses: WT (3), *IL2RG*$^{-/Y}$ *RAG1*$^{-/-}$ non-transplanted (2), *IL2RG*$^{-/Y}$ *RAG1*$^{-/-}$ IO BMT (4) and *IL2RG*$^{-/Y}$ *RAG1*$^{-/-}$ IO irradiated BMT (2) piglets.

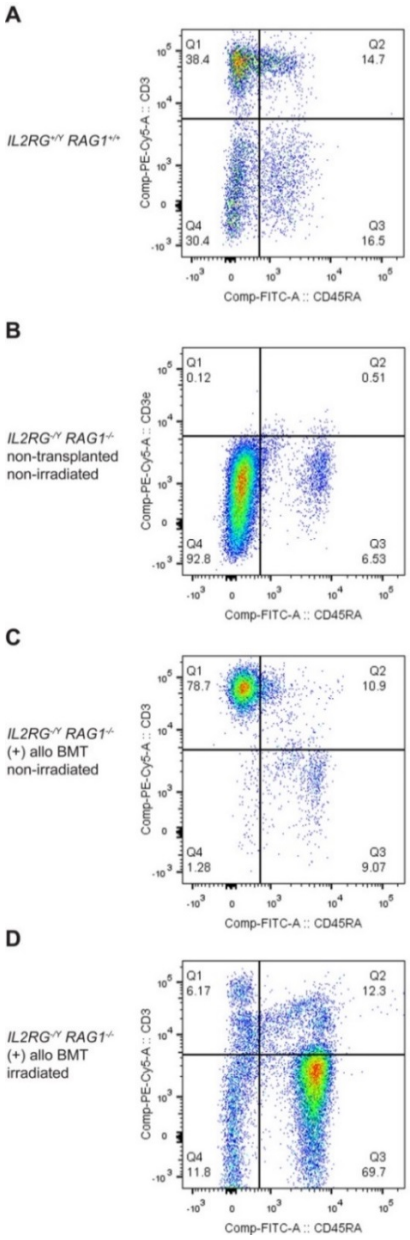

Fig. 25. Splenic naïve T and B cells in *IL2RG*$^{-/Y}$ *RAG1*$^{-/-}$ pigs after allogeneic transplant.
Splenic cells from (*A*) WT postnatal d80, (*B*) non-transplanted d28, (C) allogeneic BMT/non-irradiated d97, and (D) allogeneic BMT/irradiated d79 piglets were gated on 74-22-15(-) cells and stained with CD3 and CD45RA to identify naïve T cells, defined here as CD3(+) CD45RA(+), and B cells, defined here as CD3(-) CD45RA(+). Allogeneic BMT/non-irradiated generated a significantly higher naïve T cell population than WT ($p < 0.01$) while allogeneic BMT/irradiation produced a significantly higher B cell population compared to WT ($p < 0.01$). Flow cytometry data are representative results from the following number of animals in parentheses: WT (3), *IL2RG*$^{-/Y}$ *RAG1*$^{-/-}$ non-transplanted (2), *IL2RG*$^{-/Y}$ *RAG1*$^{-/-}$ IO BMT (4), and *IL2RG*$^{-/Y}$ *RAG1*$^{-/-}$ IO irradiated BMT (2) piglets.

splenic B cells in the SCID pigs (Fig. 25C), however there was substantial rescue of splenic B cells in irradiated animals (Fig. 25D). Splenic NK cells were partially reconstituted by allogeneic transplant (Fig. 26). Gross pathology of thymic tissue from non-transplanted *IL2RG*$^{-/Y}$ *RAG1*$^{-/-}$ DKO pigs showed only a small thymic remnant (Fig. 27, *middle panel*). DKO pigs that underwent allogeneic transplant showed an increase in the amount of thymic tissue, but not to the amount seen in WT pigs (Fig. 27, *top and lower panels*). IHC was performed with staining for CD3 in tissue sections from the thymus or thymic remnant from WT, non-transplanted SCID, and allogeneic BMT pigs (Fig. 28). Allogeneic transplant led to scattered, partial reconstitution of CD3+ T cells in the thymic tissue, however the abnormal tissue architecture persisted, composed of epithelial cell nests without a cortex or medulla, similar to non-transplanted controls. Flow cytometry performed on thymic cell suspensions showed that allogeneic transplant resulted in the reconstitution of the thymus with large numbers of both CD3– and CD3+ T cells relative to non-transplanted pigs, which showed only a small thymic population of CD3– cells (Fig. 29A). Similar to peripheral blood T cells, the majority of thymic T cells were CD45RA–, suggesting they are activated, with only a small population of CD45RA+ naïve T cells (Fig. 29B). Staining for T cell subsets showed the majority of thymic T cells were SPs in roughly equal amounts between CD4+ and CD8+ SP cells, with smaller populations of DP and DN cells (Fig. 29C). These studies demonstrate that allogeneic BMT repopulates the thymus of SCID pigs with T cells, however BMT does not rescue thymic architecture and the majority of thymic T cells show an activated, differentiated SP phenotype.

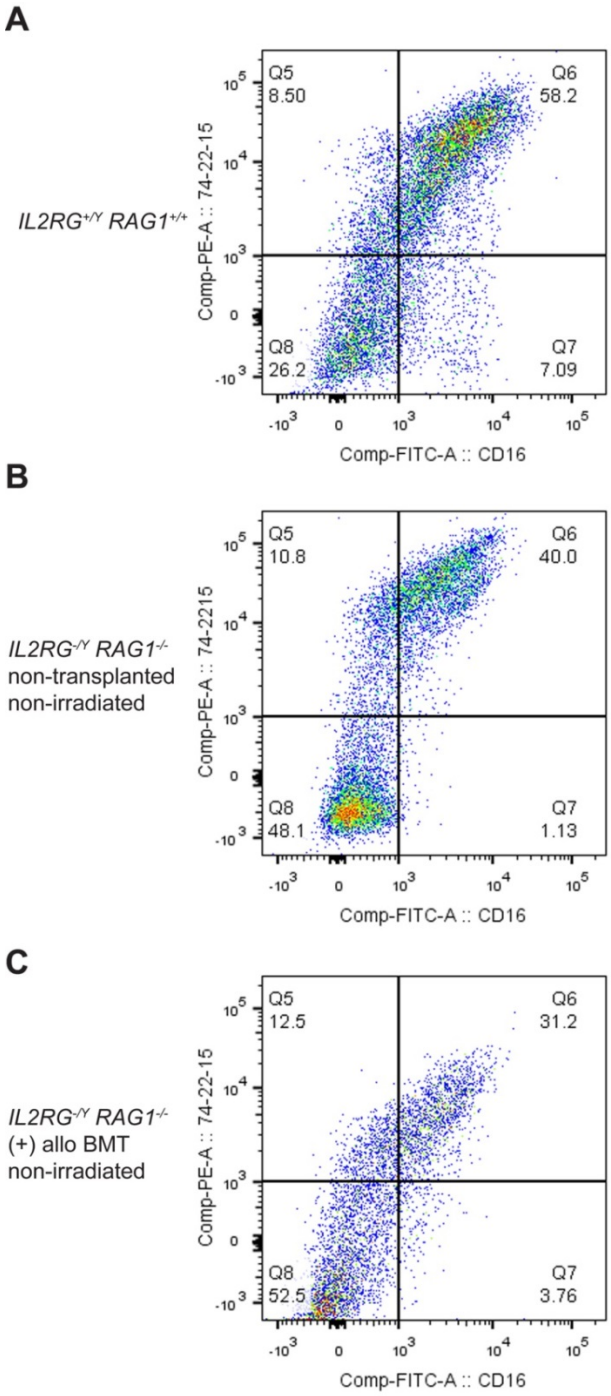

Fig. 26. Splenic NK cells in *IL2RG*$^{-/Y}$ *RAG1*$^{-/-}$ pigs after allogeneic transplant.
Splenic cells from (*A*) WT postnatal d80, (*B*) non-transplanted d28, and (C) allogeneic BMT/non-irradiated d97 piglets were stained to identify NK cells, defined as CD16(+) 74-22-15(-). Flow cytometry data are representative results from the following number of animals in parentheses: WT (3), *IL2RG*$^{-/Y}$ *RAG1*$^{-/-}$ non-transplanted (2), and *IL2RG*$^{-/Y}$ *RAG1*$^{-/-}$ IO BMT (4) piglets.

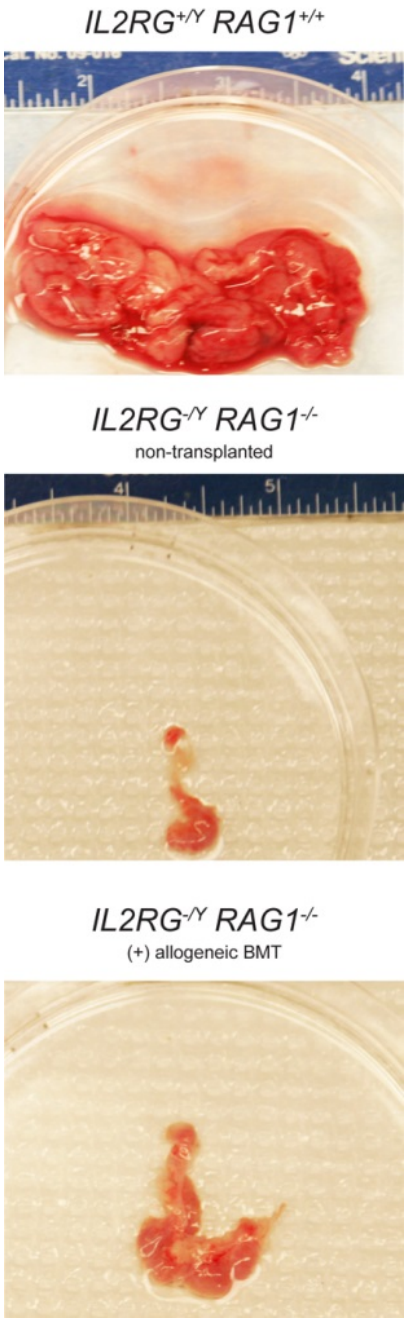

Fig. 27. Gross pathology of thymic remnant from *IL2RG*$^{-/Y}$ *RAG1*$^{-/-}$ pigs after allogeneic transplant.

The thymus was harvested on postnatal d1 from WT pigs and on d28 from non-transplanted and allogeneic BMT pigs. Gross pathology specimens shown are representative results from the following number of animals in parentheses: WT (2), *IL2RG*$^{-/Y}$ *RAG1*$^{-/-}$ non-transplanted (2), *IL2RG*$^{-/Y}$ *RAG1*$^{-/-}$ IO BMT (4) piglets.

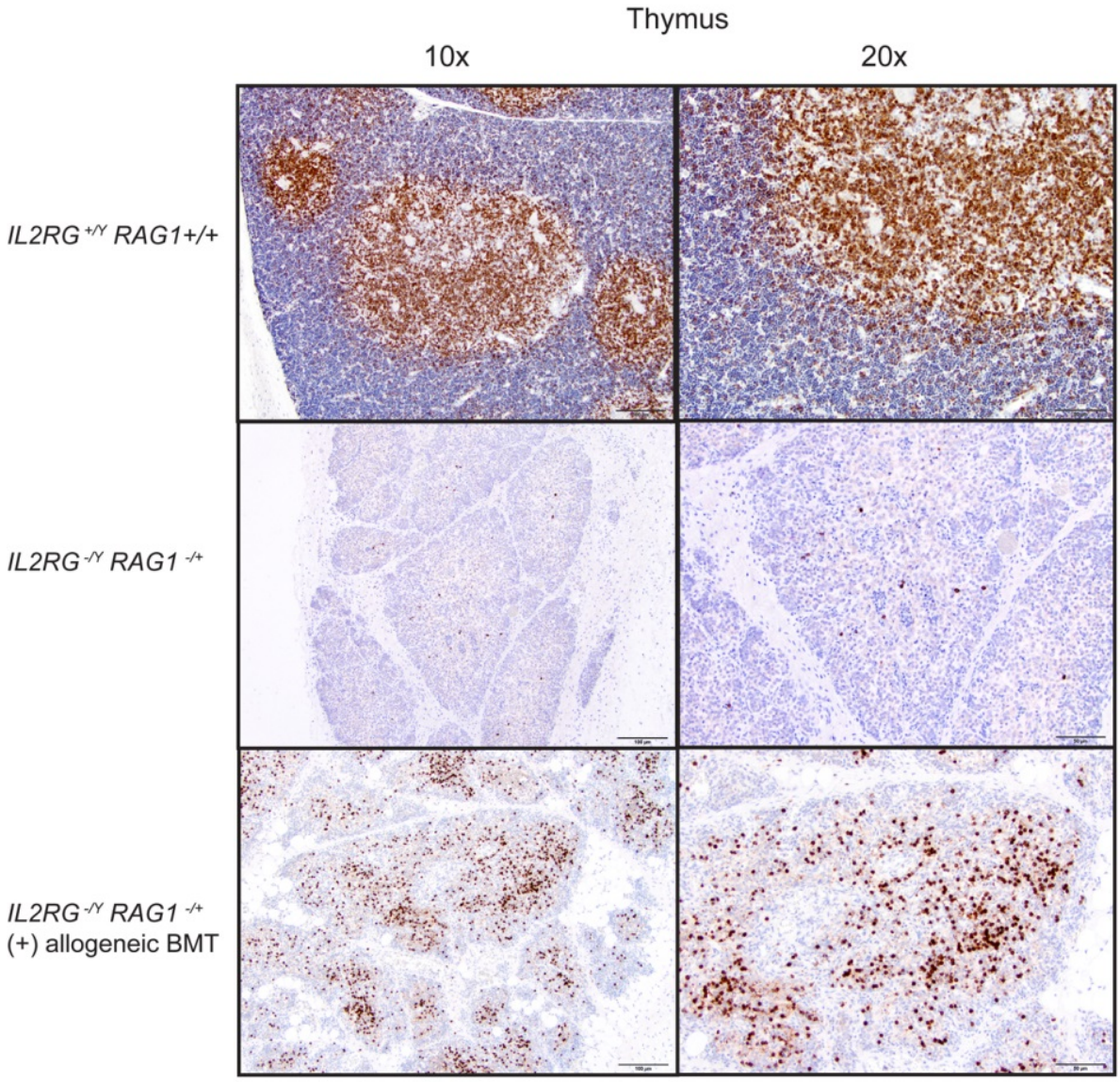

Fig. 28. Repopulation of thymic remnant with T cells in SCID pigs after allogeneic transplant. Thymic tissue sections were generated from the animals indicated on postnatal day 14 (except for the non-transplanted *IL2RG*$^{-/Y}$ *RAG1*$^{-/+}$ sample, which is from day 22). Tissues were stained for CD3 by immunohistochemistry. Results are representative of two independent experiments.

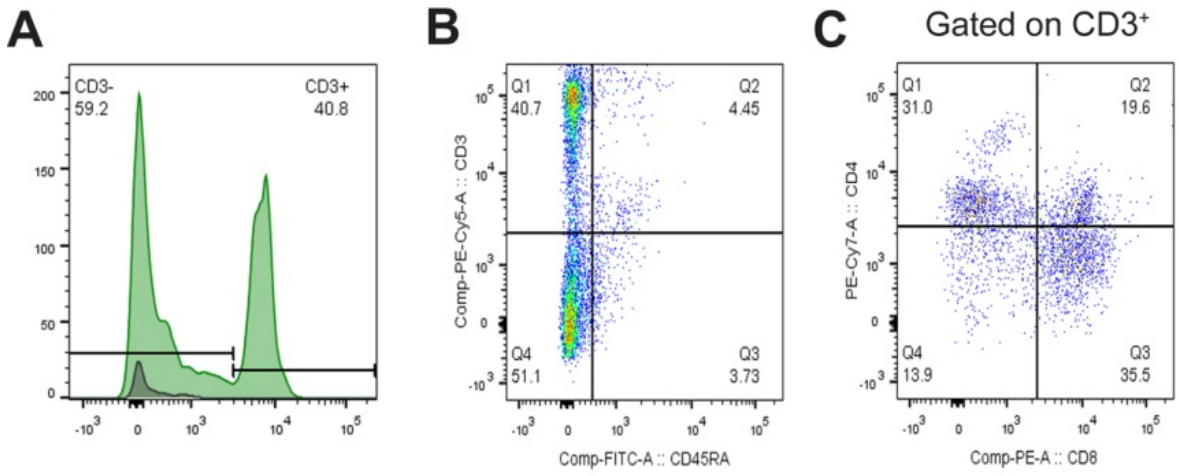

Fig. 29. T cell subsets in the thymic remnant of SCID pigs after allogeneic transplant.
Thymic tissue was harvested on d28 from non-transplanted and d97 from allogeneic BMT piglets. Thymic cell suspensions were stained with (*A-C*) CD3, (*B*) CD45RA, (*C*) CD4, and CD8. Repopulation of thymic T cells was significantly higher in allogeneic BMT compared to non-transplanted pigs ($p < 0.01$). Flow cytometry data are representative of results from the following number of animals in parentheses: *IL2RG*$^{-/Y}$ *RAG1*$^{-/-}$ non-transplanted (2) and *IL2RG*$^{-/Y}$ *RAG1*$^{-/-}$ IO BMT (4) piglets.

3.4. Analysis of bone marrow lymphocytes after allogeneic transplantation.

The effects of allogeneic BMT on the repopulation of recipient SCID pig bone marrow were examined by flow cytometry. In irradiated pigs, the bone marrow was composed mostly of dead cells or cell fragments, and did not yield usable samples for flow cytometry (data not shown). SCID pigs that underwent allogeneic BMT without irradiation had a population of bone marrow T cells that showed signs of differentiation into DP and CD4+ SP populations (Fig. 30). (There is also likely a separate CD8+ SP population that stains brighter than the DP population in this experiment but due to voltage settings during flow cytometry, the cells shown stain spuriously positive for CD4.) The majority of these T cells had an activated CD45RA– phenotype, however a smaller population of naïve CD45RA+ T cells was also present in transplanted pigs (Fig. 31). For B and NK cells, only

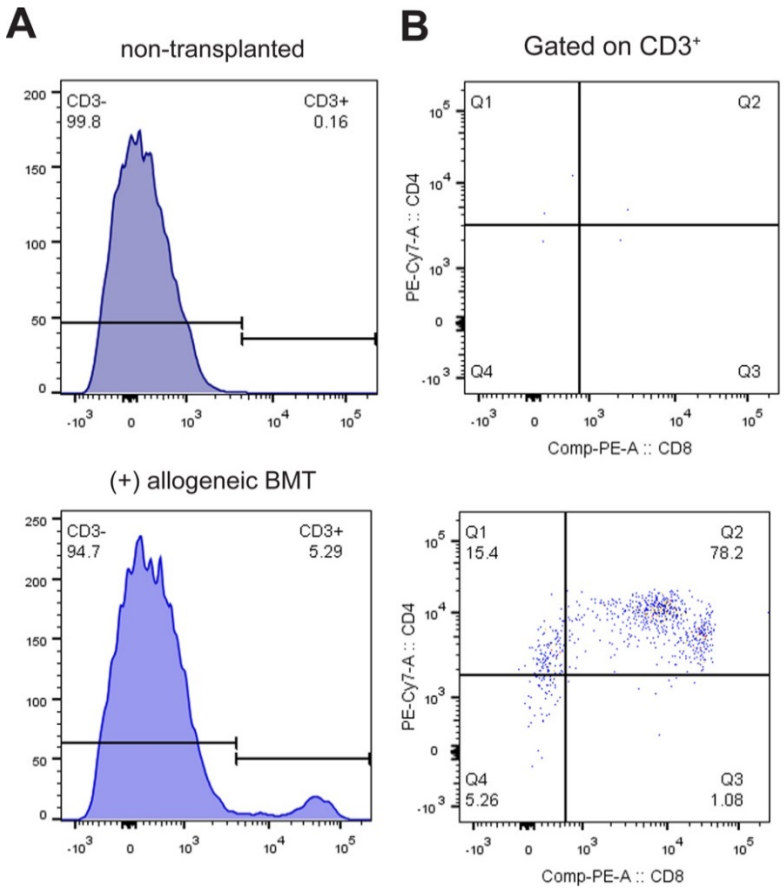

Fig. 30. Bone marrow T cells in SCID pigs after allogeneic transplant.
Bone marrow was harvested from sacrificed pigs on d39 from non-transplanted and d97 from allogeneic BMT pigs. Bone marrow cell suspensions were stained for CD3 (*A*) and gated on CD3+ cells with staining of CD8 and CD4 (*B*). Flow cytometry data are representative results from the following number of animals in parentheses: *IL2RG*$^{-/Y}$ *RAG1*$^{-/-}$ non-transplanted (2), and *IL2RG*$^{-/Y}$ *RAG1*$^{-/-}$ IO BMT (4) piglets.

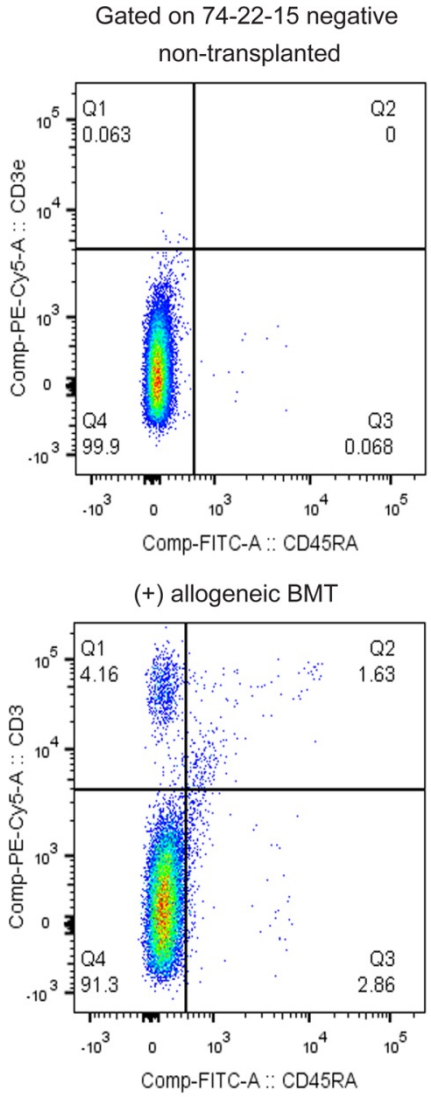

Fig. 31. Naïve T and B cells in the bone marrow of SCID pigs after allogeneic transplant.
Bone marrow suspensions were generated as described in Fig. 30, gated on 74-22-15(-) to exclude myeloid cells, and stained with CD3 and CD45RA. Flow cytometry data are representative results from the following number of animals in parentheses: *IL2RG*$^{-/Y}$ *RAG1*$^{-/-}$ non-transplanted (2), and *IL2RG*$^{-/Y}$ *RAG1*$^{-/-}$ IO BMT (4) piglets.

small populations slightly above non-transplanted controls were seen in the bone marrow after allogeneic BMT (Figs. 31 and 32). These data show allogeneic BMT of SCID pigs leads to bone marrow reconstitution with predominantly activated T cells, and only low level reconstitution with B and NK cells.

3.5. Effects of allogeneic transplant on plasma immunoglobulins in SCID pigs.

To measure the effects of allogeneic transplantation on immunoglobulin production, I conducted ELISAs to measure plasma levels of pig IgM, IgG, and IgA at various time points (Fig. 33 and Fig. 34). In WT pigs, IgM levels decreased from postnatal day 1 until day 14, reflecting the loss of IgM initially transferred from the colostrum (Fig. 33A and Fig. 34A), similar to prior data on perinatal porcine Ig kinetics (Suzuki et al., 2012). IgM levels then increased from day 14 to day 84 as IgM production from the newborn pigs' B cells is upregulated. In contrast, in *IL2RG*$^{-/Y}$ *RAG1*$^{-/-}$ pigs, IgM levels do not recover after the initial decline from day 1 to day 14 (Fig. 33A and Fig. 34A). Analysis of the aggregate data suggested that allogeneic BMT did not rescue IgM production, with or without irradiation (Fig. 34A), however analysis of individual piglets with high levels of reconstitution with peripheral blood B cells (Fig. 35) revealed a transient increase in IgM production up to WT levels on day 28 after intraosseous BMT without irradiation, however by day 42, IgM levels in this pig again became undetectable (Fig. 35C). In contrast, no such increase was seen in irradiated SCID pigs that underwent intraosseous BMT.

The initial decline in IgG titer is slower than IgM because of the longer half-life of IgG (Fig. 33B and Fig. 34B). Again, allogeneic BMT did not appear to durably rescue IgG levels in the aggregate analysis (Fig. 34B), however pigs that underwent intraosseous BMT

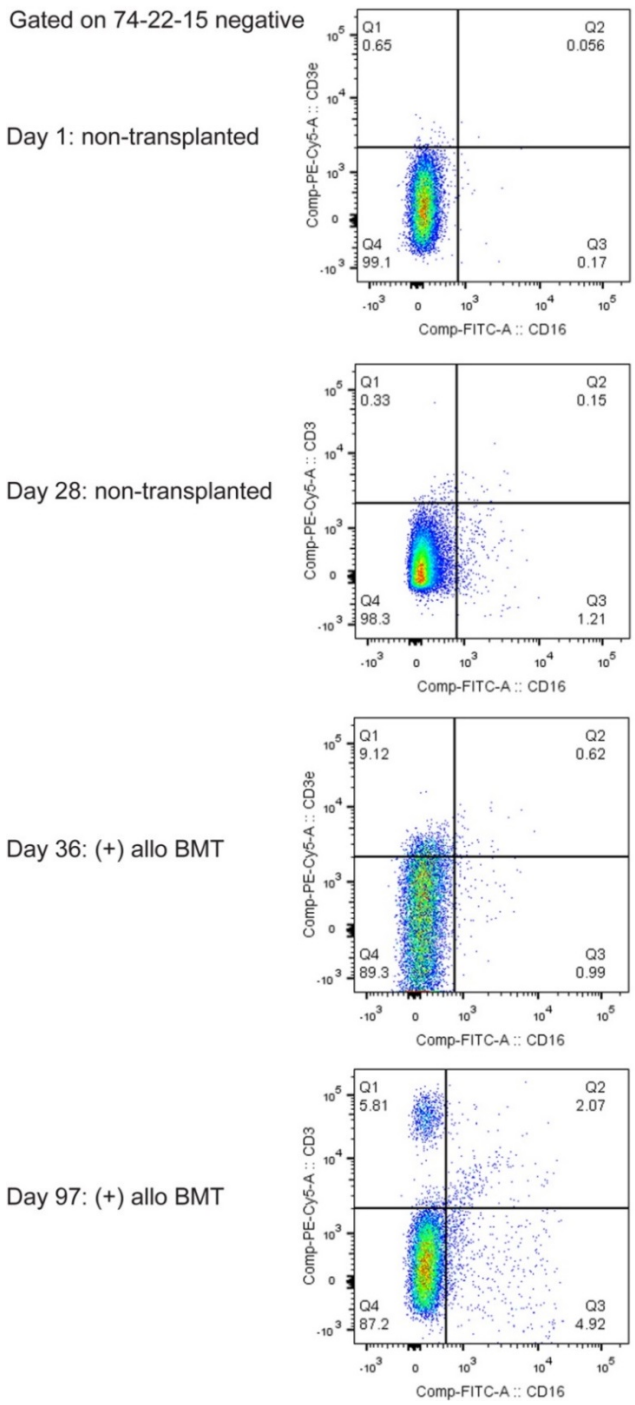

Fig. 32. Bone marrow NK cells in SCID pigs after allogeneic transplant.
Bone marrow suspensions were generated as described in Fig. 30, gated on 74-22-15(-) to exclude myeloid cells, and stained with CD3 and CD16. The NK cell population increased significantly over time ($p < 0.01$). Flow cytometry data are representative results from the following number of animals in parentheses: *IL2RG*$^{-/Y}$ *RAG1*$^{-/-}$ non-transplanted (2) and *IL2RG*$^{-/Y}$ *RAG1*$^{-/-}$ IO BMT (4) piglets.

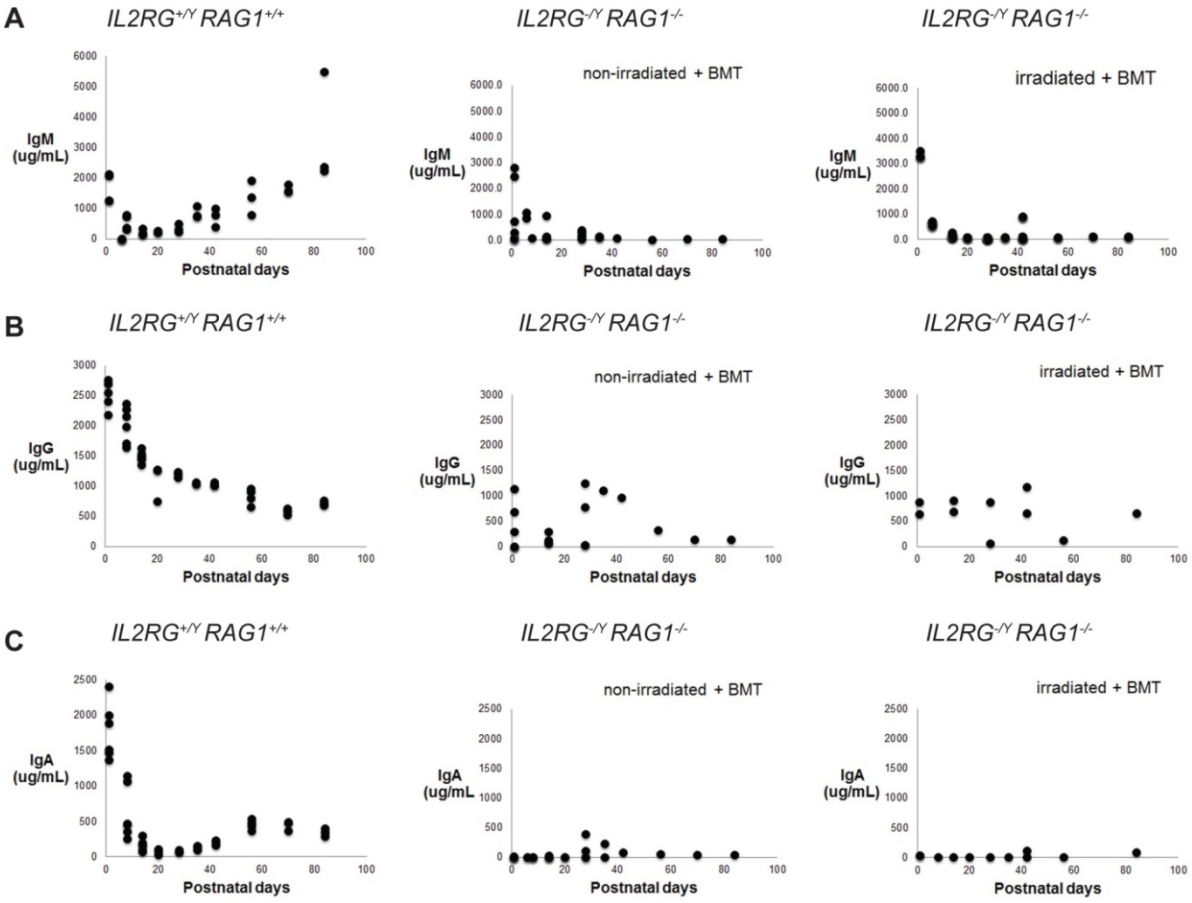

Fig. 33. Plasma immunoglobulin levels in *IL2RG*$^{-/Y}$ *RAG1*$^{-/-}$ pigs after allogeneic transplant.
Bone marrow was intraosseously injected into IL2RG$^{-/Y}$ RAG1$^{-/-}$ pigs on postnatal day 1, with or without total body irradiation on the day of injection. Plasma was collected at various time points from individual WT (5), *IL2RG*$^{-/Y}$ *RAG1*$^{-/-}$ IO BMT (4), and *IL2RG*$^{-/Y}$ *RAG1*$^{-/-}$ IO irradiated BMT (2) piglets. Plasma was tested for titers of (*A*) IgM, (*B*) IgG, and (*C*) IgA, which were measured by ELISA. Results are from at least three independent experiments.

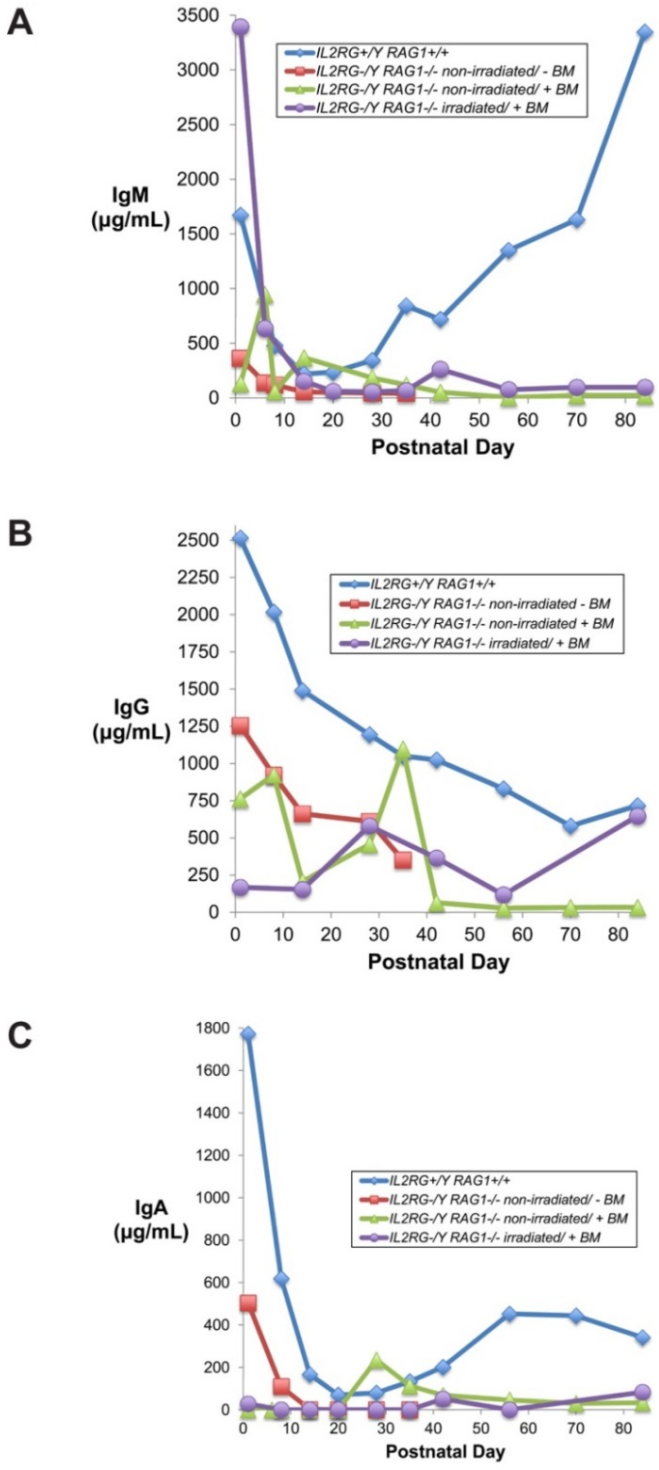

Fig. 34. Plasma immunoglobulin levels in IL2RG-/Y RAG1-/- pigs after allogeneic transplant. Experiments were performed as in Fig. 33 with saline injection (- BM) as a negative control. Results shown are the mean titer from the surviving piglets of at least three independent experiments.

Fig. 35. Comparison of B cell levels and IgM production in SCID pigs after allogeneic transplant.

Flow plots show peripheral blood B cells gated on 74-22-15(-) with CD45RA versus CD3 and the plasma IgM level from each corresponding day plotted below. B cells are defined as the CD45RA(+) CD3(-) population. (*A*) WT, (*B*) non-transplanted *IL2RG*$^{-/Y}$ *RAG1*$^{-/-}$, and (*C*) allogeneic BMT +/- irradiation. Flow cytometry data and plasma IgM ELISA analysis at various time points are from a single piglet. Flow cytometry and ELISA data are representative results from the following number of animals in parentheses: *IL2RG*$^{+/Y}$ *RAG1*$^{+/+}$ (1), *IL2RG*$^{-/Y}$ *RAG1*$^{-/-}$ (1), and *IL2RG*$^{-/Y}$ *RAG1*$^{-/-}$ IO irradiated BMT (1) piglet.

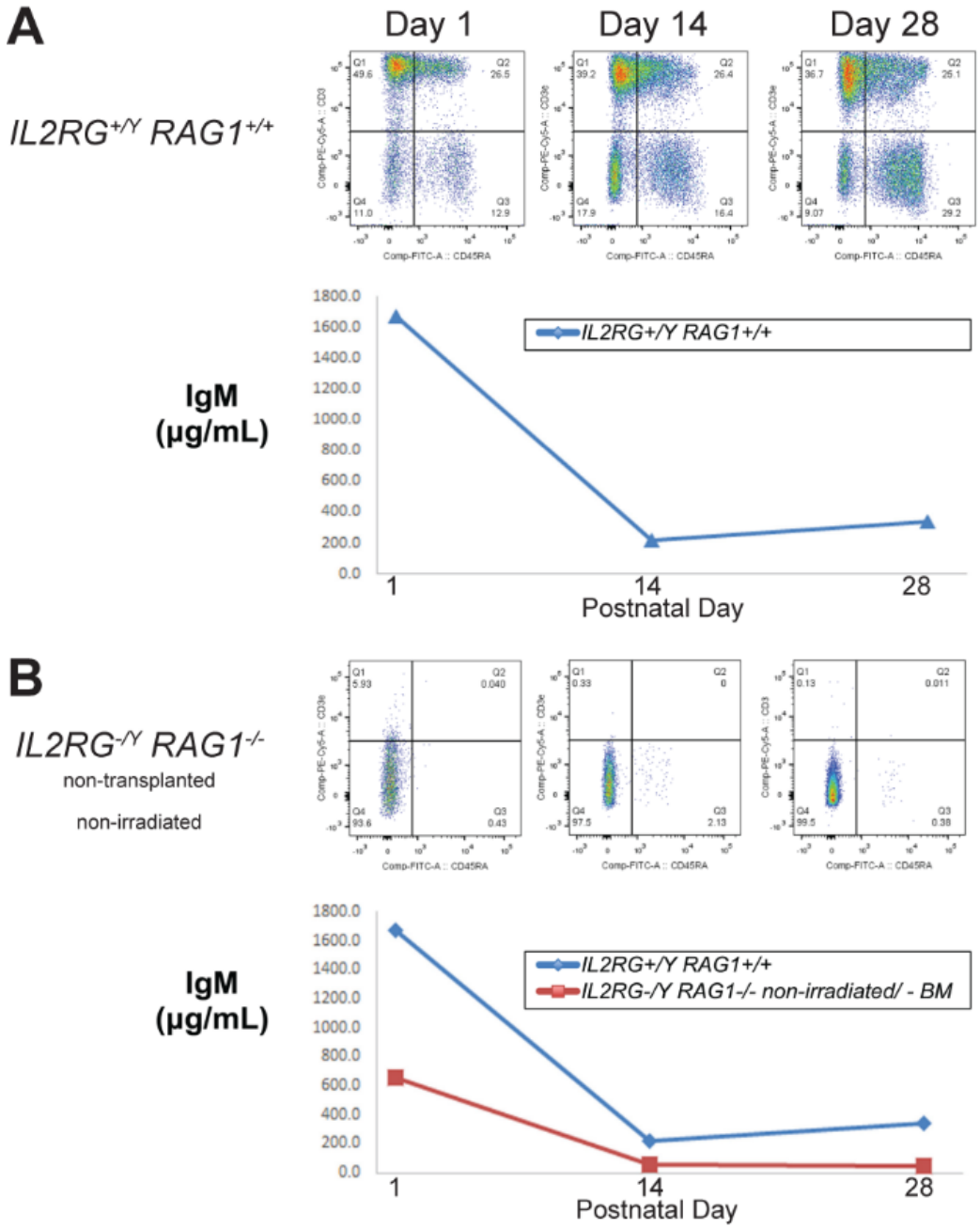
A
Day 1
Day 14
Day 28
IL2RG+/Y RAG1+/+
IgM (µg/mL)
IL2RG+/Y RAG1+/+
Postnatal Day
B
IL2RG-/Y RAG1-/-
non-transplanted
non-irradiated
IgM (µg/mL)
IL2RG+/Y RAG1+/+
IL2RG-/Y RAG1-/- non-irradiated/ - BM
Postnatal Day

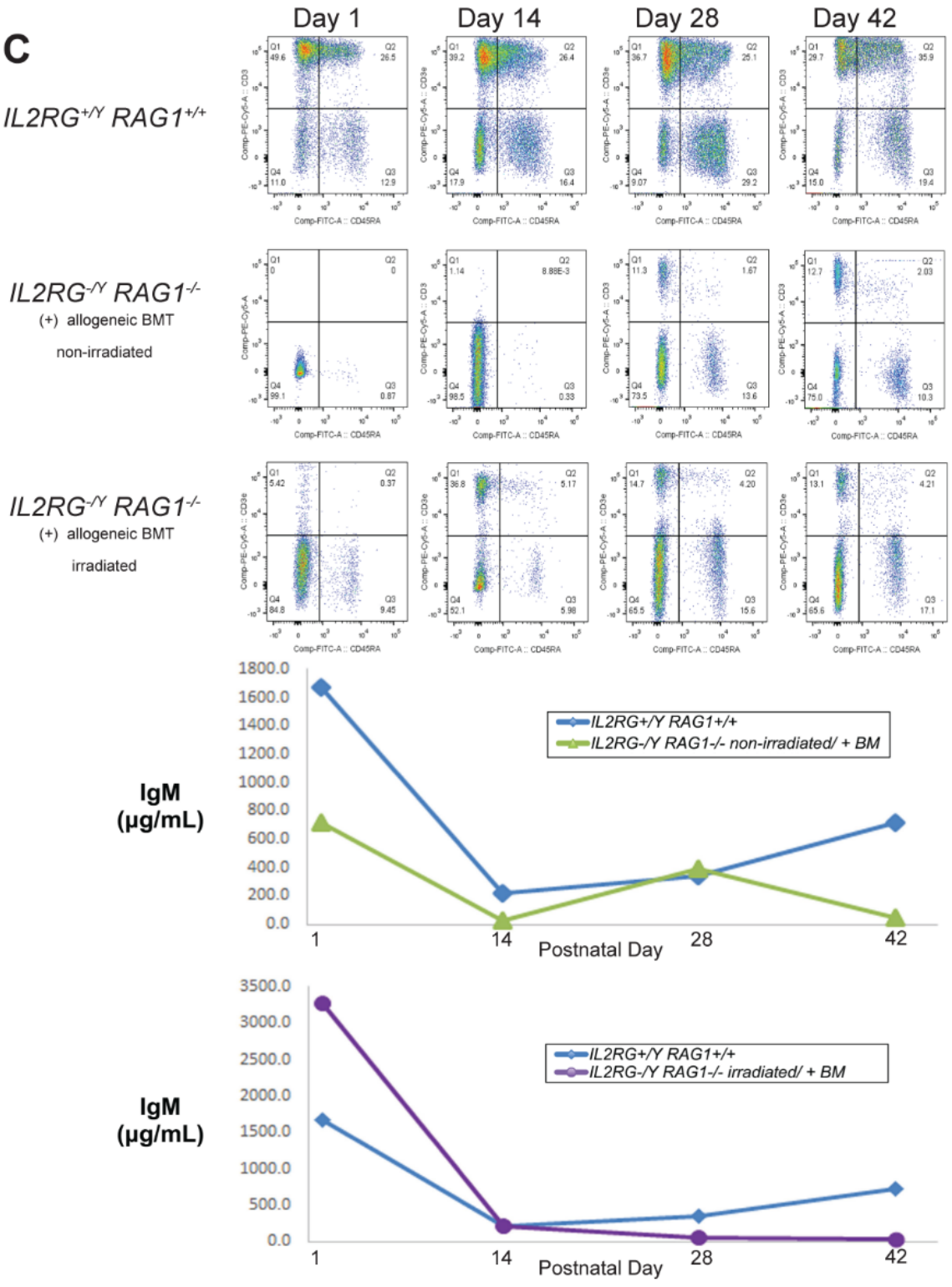
C
Day 1
Day 14
Day 28
Day 42
IL2RG+/Y RAG1+/+
IL2RG-/Y RAG1-/-
(+) allogeneic BMT
non-irradiated
IL2RG-/Y RAG1-/-
(+) allogeneic BMT
irradiated
IgM (µg/mL)
IL2RG+/Y RAG1+/+
IL2RG-/Y RAG1-/- non-irradiated/ + BM
Postnatal Day
IgM (µg/mL)
IL2RG+/Y RAG1+/+
IL2RG-/Y RAG1-/- irradiated/ + BM
Postnatal Day

without irradiation and had strong B cell repopulation showed a steady increase in IgG titers from day 28 to 42 up to WT levels, while this IgG increase was not seen in irradiated animals (Fig. 36C). I speculate that the transient increase in IgM followed by the steady increase in IgG production reflects Ig class switching. In contrast, WT IgA levels declined from postnatal day 1 until day 20, then increased to a plateau on day 56, while allogeneic transplant failed to rescue IgA production (Fig. 33C and Fig. 34C), even in pigs that showed strong B cell repopulation (Fig. 37).

The large variability in Ig titers between experimental groups on postnatal day 1 likely reflects variations in the Ig composition of colostrum between sows, as well as differences in the number of piglets feeding from a given sow. These ELISA studies show that donor-derived B cells produce low to absent levels of IgM, IgG, and IgA following allogeneic BMT into *IL2RG*$^{-/Y}$ *RAG1*$^{-/-}$ pigs.

3.6. Chapter Summary.

This chapter reviewed the results of allogeneic bone marrow transplantation experiments in *IL2RG*$^{-/Y}$ *RAG1*$^{-/-}$ SCID pigs, with the lymphocyte phenotypes summarized in Table 3. PCR of a donor transgenic marker demonstrated that PBMCs in transplanted pigs are of donor origin. While intravenous BMT led to transient reconstitution of only the T cell lineage, intraosseous BMT resulted in sustained reconstitution of T, B, and NK cells, likely due to the direct delivery of donor precursors into a supportive hematopoietic niche. T cells were partially reconstituted in the peripheral blood and thymic remnant and fully reconstituted in the spleen, however the thymus remained devoid of normal tissue architecture. Thymic T cells were predominantly activated, differentiated SP cells. The T cell

Fig. 36. Comparison of B cell levels and IgG production in SCID pigs after allogeneic transplant.

Flow plots show peripheral blood B cells gated on 74-22-15(-) with CD45RA versus CD3 and the plasma IgG level from each corresponding day plotted below. B cells are defined as the CD45RA(+) CD3(-) population. (*A*) WT, (*B*) non-transplanted *IL2RG*$^{-/Y}$ *RAG1*$^{-/-}$, and (*C*) allogeneic BMT +/- irradiation. Flow cytometry data and plasma IgG ELISA analysis at various time points are from the same piglet as in Fig. 35. Flow cytometry and ELISA data are representative results from the following number of animals in parentheses: *IL2RG*$^{+/Y}$ *RAG1*$^{+/+}$ (1), *IL2RG*$^{-/Y}$ *RAG1*$^{-/-}$ (1), and *IL2RG*$^{-/Y}$ *RAG1*$^{-/-}$ IO irradiated BMT (1) piglet.

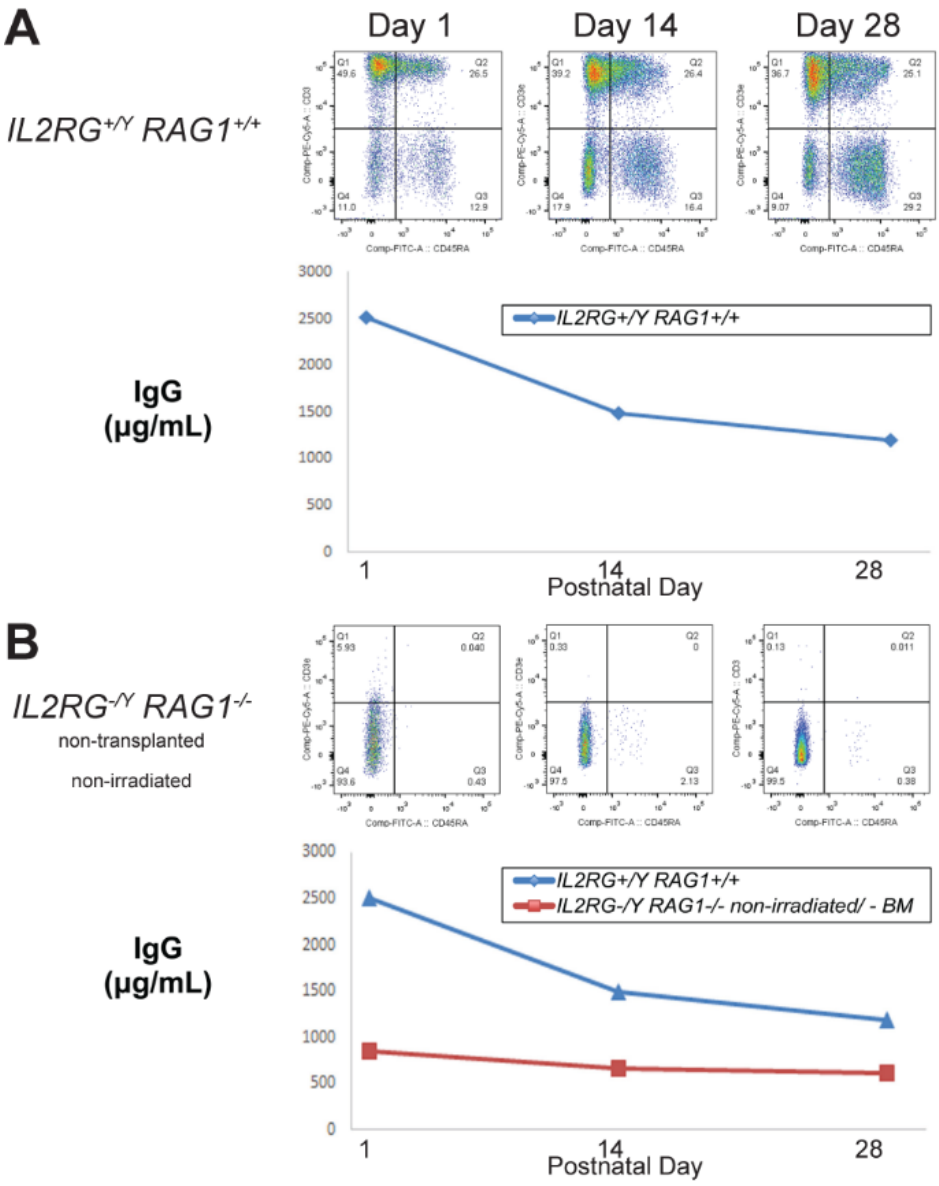
A
Day 1
Day 14
Day 28
IL2RG+/Y RAG1+/+
IgG (µg/mL)
IL2RG+/Y RAG1+/+
Postnatal Day
B
IL2RG-/Y RAG1-/-
non-transplanted
non-irradiated
IgG (µg/mL)
IL2RG+/Y RAG1+/+
IL2RG-/Y RAG1-/- non-irradiated/ - BM
Postnatal Day

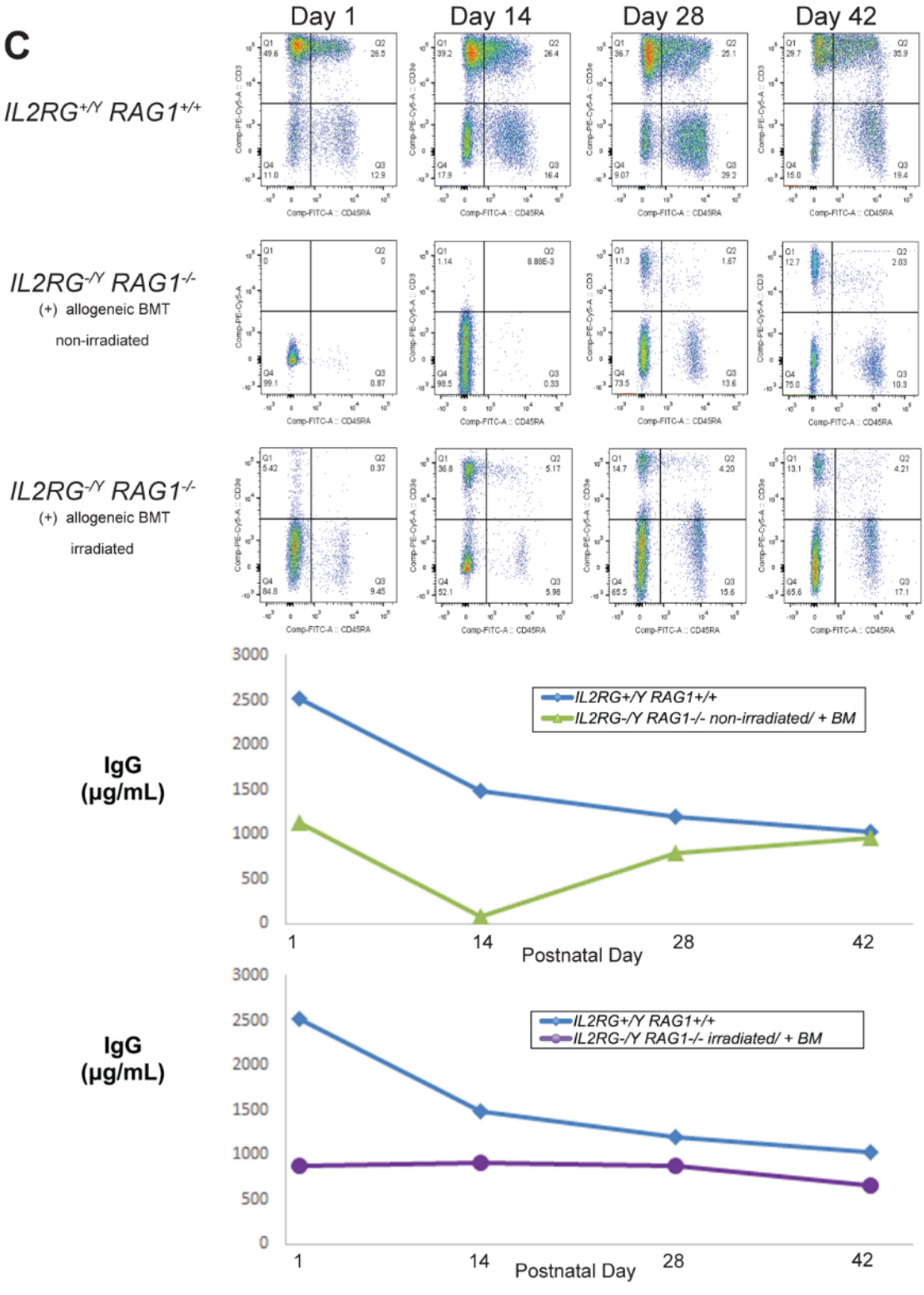
C
Day 1
Day 14
Day 28
Day 42
IL2RG+/Y RAG1+/+
IL2RG-/Y RAG1-/-
(+) allogeneic BMT
non-irradiated
IL2RG-/Y RAG1-/-
(+) allogeneic BMT
irradiated
IgG (µg/mL)
IL2RG+/Y RAG1+/+
IL2RG-/Y RAG1-/- non-irradiated/ + BM
Postnatal Day
IgG (µg/mL)
IL2RG+/Y RAG1+/+
IL2RG-/Y RAG1-/- irradiated/ + BM
Postnatal Day

Fig. 37. Comparison of B cell levels and IgA production in SCID pigs after allogeneic transplant.

Flow plots show peripheral blood B cells gated on 74-22-15(-) with CD45RA versus CD3 and the plasma IgA level from each corresponding day plotted below. B cells are defined as the CD45RA(+) CD3(-) population. (*A*) WT, (*B*) non-transplanted *IL2RG*$^{-/Y}$ *RAG1*$^{-/-}$, and (*C*) allogeneic BMT +/- irradiation. Flow cytometry data and plasma IgA ELISA analysis at various time points from the same piglet as in Fig. 35-36. Flow cytometry and ELISA data are representative results from the following number of animals in parentheses: *IL2RG*$^{+/Y}$ *RAG1*$^{+/+}$ (1), *IL2RG*$^{-/Y}$ *RAG1*$^{-/-}$ (1), and *IL2RG*$^{-/Y}$ *RAG1*$^{-/-}$ IO irradiated BMT (1) piglet.

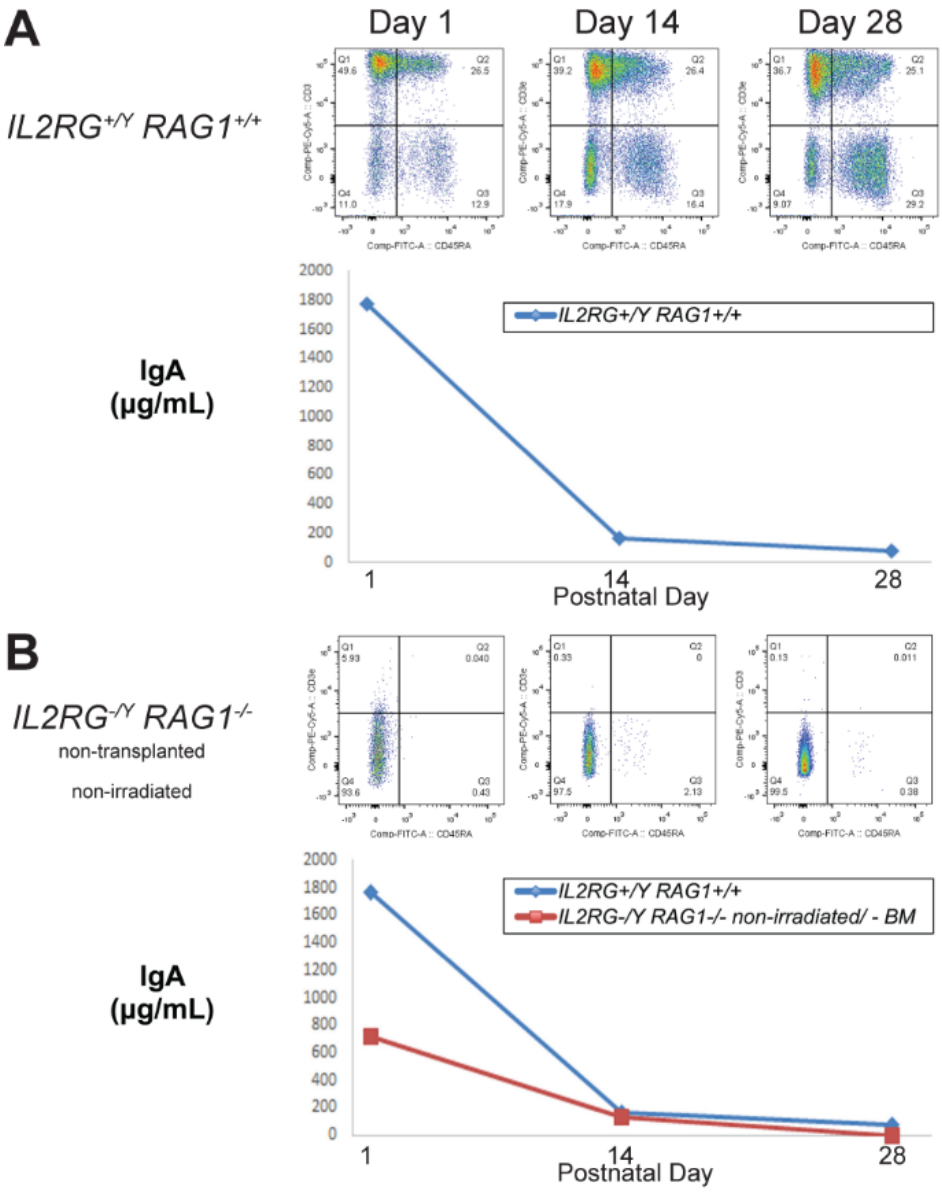
A
Day 1
Day 14
Day 28
IL2RG+/Y RAG1+/+
IgA (µg/mL)
IL2RG+/Y RAG1+/+
Postnatal Day
B
IL2RG-/Y RAG1-/-
non-transplanted
non-irradiated
IgA (µg/mL)
IL2RG+/Y RAG1+/+
IL2RG-/Y RAG1-/- non-irradiated/ - BM
Postnatal Day

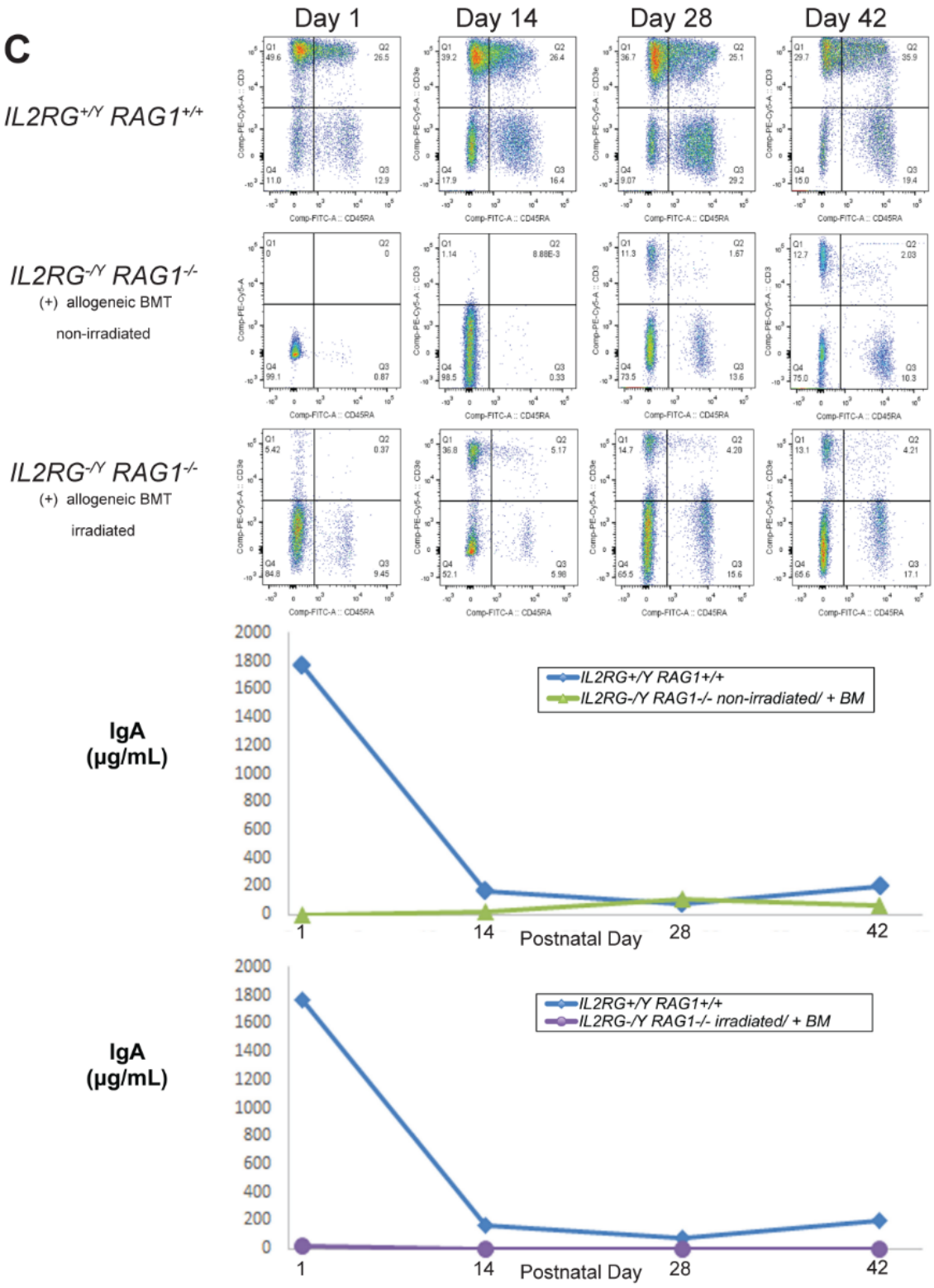
C
Day 1
Day 14
Day 28
Day 42
IL2RG+/Y RAG1+/+
IL2RG-/Y RAG1-/-
(+) allogeneic BMT
non-irradiated
IL2RG-/Y RAG1-/-
(+) allogeneic BMT
irradiated
IgA (µg/mL)
IL2RG+/Y RAG1+/+
IL2RG-/Y RAG1-/- non-irradiated/ + BM
Postnatal Day
IgA (µg/mL)
IL2RG+/Y RAG1+/+
IL2RG-/Y RAG1-/- irradiated/ + BM
Postnatal Day

Table 3. Summary of lymphocyte profiles from SCID pigs after allogeneic BMT.
Values shown for total, activated, and naïve T cells and NK cells are percent of total leukocytes. Values shown for DN, DP, CD4 SP, and CD8 SP cells are percent of total T cells. Values shown for B cells are percent of non-myeloid leukocytes. Bone marrow from irradiated pigs contained dead or necrotic cells and could not be analyzed. Values shown are the highest measured across all trials and time points.

ALLOGENEIC TRANSPLANTATION

non-irradiated *IL2RG-/Y RAG1-/-*

Organ/Tissue	T cells total	activated	naïve	DN	DP	CD4 SP	CD8 SP	B cells	NK cells	*n*
blood	35.50	32.70	4.25	0.12	79.00	3.48	17.40	25.80	1.89	4
spleen	78.70	78.70	10.90	0.00	71.40	0.48	28.10	9.07	1.13	4
thymic remnant	40.80	40.70	4.45	13.90	19.60	31.00	35.50			4
bone marrow	5.29		1.63					2.86	4.92	4

irradiated *IL2RG-/Y RAG1-/-*

Organ/Tissue	T cells total	activated	naïve	DN	DP	CD4 SP	CD8 SP	B cells	NK cells	*n*
blood	16.60	13.10	4.21	2.57	40.60	15.90	41.00	17.10	1.03	2
spleen	6.17	6.17	12.30	0.17	56.30	0.00	43.50	69.70	3.76	2
thymic remnant	10.20	8.52	2.03	4.56	3.56	5.45	8.43			2

staining characteristics from the peripheral blood of transplanted animals suggested these were largely TCRαβ-expressing T cells with almost no expression of DN γδ T cells and a larger population of CD8+ SP relative to CD4+ SP cells, all of which is consistent with a late postnatal T cell development program in pigs (Gerner et al., 2009; Sinkora and Butler, 2009; Stepanova et al., 2007). T cells from transplanted animals showed a time-dependent increase in CD4+ CD8+ DP cells, reflecting an increase in either T cell progenitors or memory T cells. T cells were also predominantly activated (CD45RA–), particularly splenic T cells, with only a small, stable population of naïve CD45RA+ T cells. Allogeneic BMT led to B cell reconstitution in the blood, at low levels in the bone marrow, and in the spleen only in irradiated animals. Pigs that underwent intraosseous BMT without irradiation and showed strong B cell reconstitution also expressed IgM and IgG up to WT titers, however this was

not seen for IgA. Partial NK cell repopulation was observed in the peripheral blood, spleen, and bone marrow following allogeneic BMT.

Total body irradiation led to the earlier appearance of lymphoid cells, particularly activated T cells, however this population contracted rapidly and by postnatal day 42, was smaller than the amount of T cells seen in non-irradiated age-matched BMT pigs. Irradiation did promote splenic repopulation with B cells, which was not observed in non-irradiated pigs receiving allogeneic BMT. Irradiated animals that underwent intraosseous BMT showed no rescue of plasma IgM, IgG, or IgA expression. Irradiated animals were very ill, had lots of dead cells in their bone marrow, were unresponsive to broad-spectrum antibiotics, and required significant time and resources to maintain.

Overall, the studies in this chapter demonstrate that intraosseous allogeneic BMT of SCID pigs leads to the reconstitution of T, B, and NK cells. In the next chapter, I explore the possibility of generating a “humanized” pig by using xenogeneic transplantation with human bone marrow to repopulate SCID pigs with human lymphocytes.

CHAPTER 4: TRANSPLANTATION OF SCID PIGS WITH HUMAN HEMATOPOIETIC CELLS

4.1. Overview.

In Chapter 2, I characterized the *IL2RG*$^{-/Y}$ *RAG1*$^{-/-}$ SCID pigs and determined that they lack mature T, B, and NK cells. In Chapter 3, I demonstrated that allogeneic bone marrow transplantation of *IL2RG*$^{-/Y}$ *RAG1*$^{-/-}$ SCID pigs leads to repopulation with lymphocytes from all three lymphoid lineages. A primary motivation for pursuing the porcine SCID model is to develop a "humanized" pig – a SCID pig repopulated with human lymphocytes, analogous to humanized mouse models. In this chapter, I describe the results of experiments comparing the efficacy of different methods of human bone marrow (BM) transplantation into *IL2RG-/Y RAG1-/-* SCID pigs.

4.2. Intraosseous transplantation of human bone marrow or CD34^{+} cells into SCID pigs.

Based on the success of intraosseous BMT for allogeneic transplantation, I applied the intraosseous approach for transplanting human bone marrow into SCID pigs. Two formulations of human donor cells were tested – one with T cell-depleted human bone marrow (similar to the allogeneic BMT experiments), and the other with hematopoietic progenitor cells purified from human mobilized peripheral blood using the cell surface marker CD34 (Payne and Crooks, 2002). On postnatal day 1 or 2, recipient SCID pigs were injected intraosseously with 2.48 x 10^7 cells human donor cells. A subset of pigs was treated with 1.6 Gy of total body irradiation to determine whether irradiation improved reconstitution with human lymphocytes.

As a preliminary test of human cell engraftment and repopulation, peripheral blood was collected on postnatal day 42 and stained for human CD45, a broadly reactive cell surface marker of lymphoid and myeloid cells (Hermiston et al., 2003). None of the human BMT protocols tested led to the appearance of human CD45+ cells in the peripheral blood (Fig. 38). Bone marrow was collected to determine the efficacy of human cell engraftment in the bone marrow (Fig. 39); marrow was collected both from the site of intraosseous injection ((+) injected bone) and from a bone which was not directly injected ((-) injected bone) to determine whether human donor cells were able to traffic away from the local injection site and engraft bone marrow in other locations. Transplantation of T cell-depleted human BM was ineffective for both *IL2RG*$^{-/Y}$ *RAG1*$^{-/+}$ and *IL2RG*$^{-/Y}$ *RAG1*$^{-/-}$ pigs (Fig. 39, *first and second columns*). Transplantation with CD34-selected human cell resulted in minimal engraftment of human CD45+ cells in the marrow of non-irradiated recipient pigs (Fig. 39, *third column*). In contrast, irradiated pigs showed a small but definite population of human CD45+ cells in the bone marrow, both at the site of injection and in a non-injected bone (Fig. 39, *final column*). These CD45+ cells were not T cells, as they were negative for human CD3. These experiments were repeated with staining for HLA-DR, a human major histocompatibility complex (MHC) class II receptor expressed on several immune cell types, particularly professional antigen presenting cells (pAPCs). None of the transplantation methods tested led to reconstitution with HLA-DR+ cells in either the peripheral blood (Fig. 40A) or the bone marrow (Fig. 40B). Additional treatment with the human granulocyte colony-stimulating factor analogue, filgrastim (Neupogen) had no effect on human cell engraftment (data not shown). These initial studies demonstrated limited reconstitution

Fig. 38. Absent repopulation of peripheral blood with CD45+ human cells after intraosseous transplantation of human bone marrow or mobilized CD34+ cells in SCID pigs.
Human bone marrow was either T cell depleted or enriched for CD34 stem cells, then intraosseously transplanted on postnatal day 1 into the bone marrow of the indicated SCID pigs using the described conditioning regimens. On postnatal day 42, peripheral blood was collected from each of the recipient animals (except for *IL2RG*$^{-/Y}$ *RAG1*$^{-/-}$ T cell depleted/non-irradiated, which was collected on day 32 due to euthanasia). PBMCs were stained for human CD45, a general leukocyte marker. Flow cytometry data are representative results from the following number of animals in parentheses: *IL2RG*$^{-/Y}$ *RAG1*$^{-/+}$ (2) non-transplanted, *IL2RG*$^{-/Y}$ *RAG1*$^{-/+}$ T cell depleted IO BMT (3), *IL2RG*$^{-/Y}$ *RAG1*$^{-/-}$ non-transplanted (2), *IL2RG*$^{-/Y}$ *RAG1*$^{-/-}$ non-transplanted irradiated (1), *IL2RG*$^{-/Y}$ *RAG1*$^{-/-}$ T cell depleted IO BMT (2), *IL2RG*$^{-/Y}$ *RAG1*$^{-/-}$ CD34 cell selected IO BMT (7), and *IL2RG*$^{-/Y}$ *RAG1*$^{-/-}$ CD34 cell selected IO BMT irradiated (7) piglets.

Human

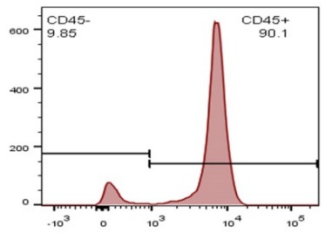

IL2RG$^{-/Y}$ *RAG1*$^{-/+}$
non-transplanted
non-irradiated

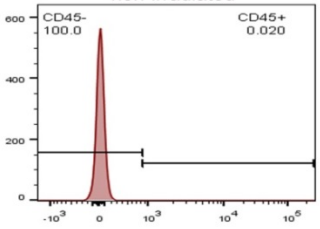

IL2RG$^{-/Y}$ *RAG1*$^{-/+}$
intraosseous T cell depleted
non-irradiated

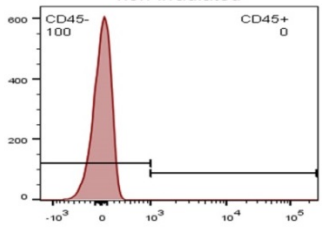

IL2RG$^{-/Y}$ *RAG1*$^{-/-}$
non-transplanted
non-irradiated

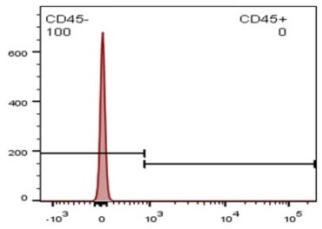

IL2RG$^{-/Y}$ *RAG1*$^{-/-}$
intraosseous T cell depleted
non-irradiated

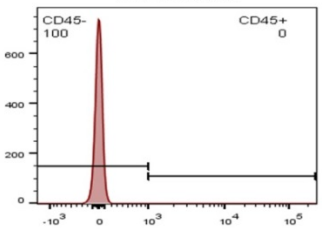

IL2RG$^{-/Y}$ *RAG1*$^{-/-}$
non-transplanted
non-irradiated

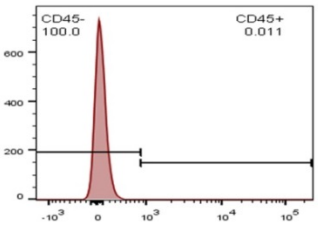

IL2RG$^{-/Y}$ *RAG1*$^{-/-}$
intraosseous CD34 selected
non-irradiated

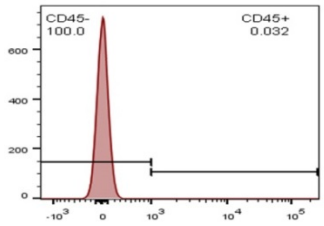

IL2RG$^{-/Y}$ *RAG1*$^{-/-}$
non-transplanted
irradiated

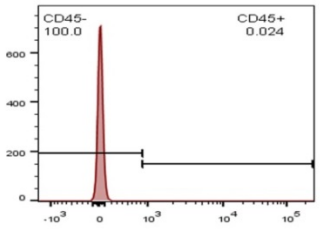

IL2RG$^{-/Y}$ *RAG1*$^{-/-}$
intraosseous CD34 selected
irradiated

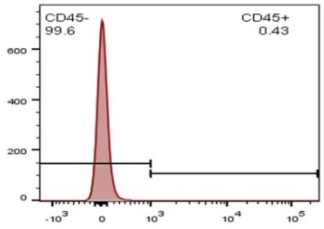

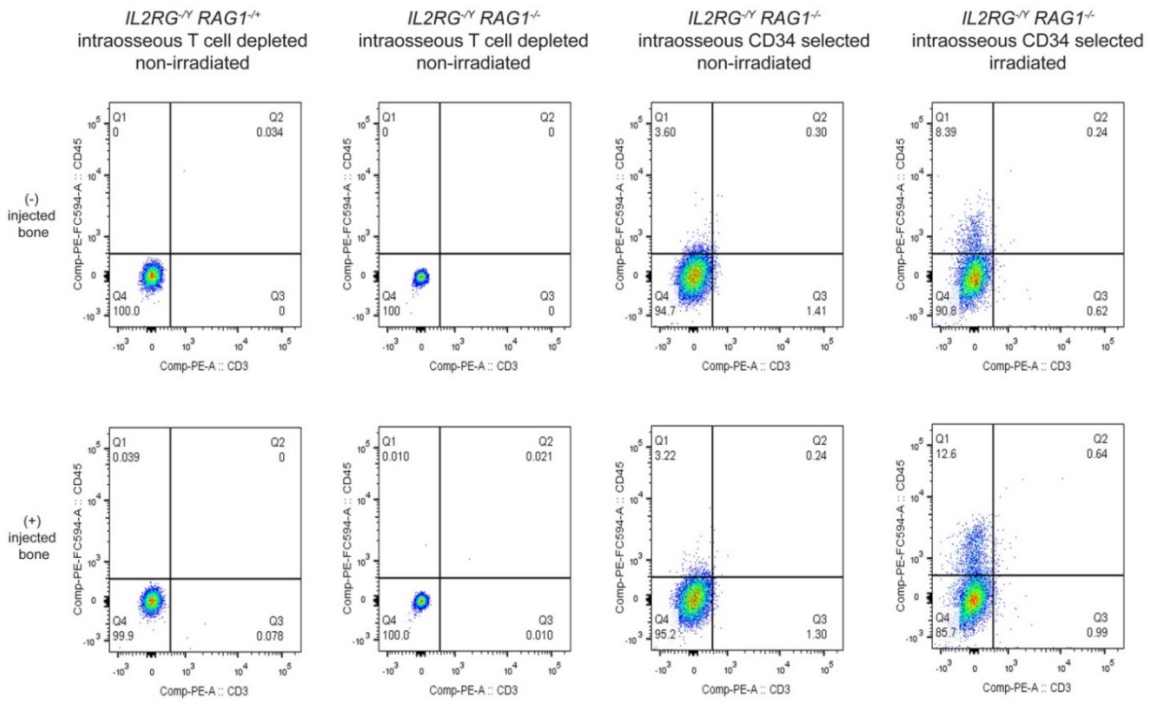

Fig. 39. Low level repopulation of bone marrow with human cells after intraosseous transplantation of human bone marrow or mobilized CD34+ cells in SCID pigs.
Human bone marrow or human $CD34^+$ selected cells was intraosseously transplanted into the bone marrow of the indicated SCID pigs using the described conditioning regimens. Bone marrow was harvested either from a bone that was injected during intraosseous transplantation ((+) injected bone) or a non-injected bone ((-) injected bone). Bone marrow was harvested from the following sacrificed animals: on postnatal day 42 (*IL2RG*$^{-/Y}$ *RAG1*$^{-/+}$ T cell depleted/non-irradiated), d32 (*IL2RG*$^{-/Y}$ *RAG1*$^{-/-}$ T cell depleted/ non-irradiated), d79 (*IL2RG*$^{-/Y}$ *RAG1*$^{-/-}$ CD34 selected/non-irradiated), and d82 (*IL2RG*$^{-/Y}$ *RAG1*$^{-/-}$ CD34 selected/irradiated). Bone marrow cell suspensions were stained for human CD45 and human CD3. The detected human CD45+ population was significantly different between transplanted and non-transplanted animals ($p < .00154$). Flow cytometry data are representative results from the following number of animals in parentheses: *IL2RG*$^{-/Y}$ *RAG1*$^{-/+}$ T cell depleted IO BMT (3), *IL2RG*$^{-/Y}$ *RAG1*$^{-/-}$ T cell depleted IO BMT (2), *IL2RG*$^{-/Y}$ *RAG1*$^{-/-}$ CD34 cell selected IO BMT (7), and *IL2RG*$^{-/Y}$ *RAG1*$^{-/-}$ CD34 cell selected IO BMT irradiated (7) piglets.

Fig. 40. Absent repopulation of peripheral blood and bone marrow with HLA-DR+ human cells after intraosseous transplantation of human bone marrow or mobilized CD34+ cells in SCID pigs.

Human bone marrow or human $CD34^+$ selected cells was intraosseously transplanted into the bone marrow of the indicated SCID pigs using the described conditioning regimens. (*A*) On postnatal day 14 and 42 blood was collected from all piglets, except for *IL2RG*$^{-/Y}$ *RAG1*$^{-/-}$ T cell depleted/non-irradiated, which was collected on d32 due to euthanasia. (*B*) Bone marrow was harvested from sacrificed animals on postnatal day 42 (*IL2RG*$^{-/Y}$ *RAG1*$^{-/+}$ T cell depleted/non-irradiated), d32 (*IL2RG*$^{-/Y}$ *RAG1*$^{-/-}$ T cell depleted/non-irradiated), d79 (*IL2RG*$^{-/Y}$ *RAG1*$^{-/-}$ CD34 selected/non-irradiated), and d82 (*IL2RG*$^{-/Y}$ *RAG1*$^{-/-}$ CD34 selected/irradiated). Bone marrow was collected from the recipient animals at the site of transplantation ((+) injected bone) and from a bone that was not injected for transplantation ((-) injected bone). Cells were stained for human HLA-DR, a broadly specific marker for professional antigen presenting cells. Flow cytometry data are representative results from the following number of animals in parentheses: *IL2RG*$^{-/Y}$ *RAG1*$^{-/+}$ T cell depleted IO BMT (3), *IL2RG*$^{-/Y}$ *RAG1*$^{-/-}$ T cell depleted IO BMT (2), *IL2RG*$^{-/Y}$ *RAG1*$^{-/-}$ CD34 cell selected IO BMT (7), and *IL2RG*$^{-/Y}$ *RAG1*$^{-/-}$ CD34 cell selected IO BMT irradiated (7) piglets.

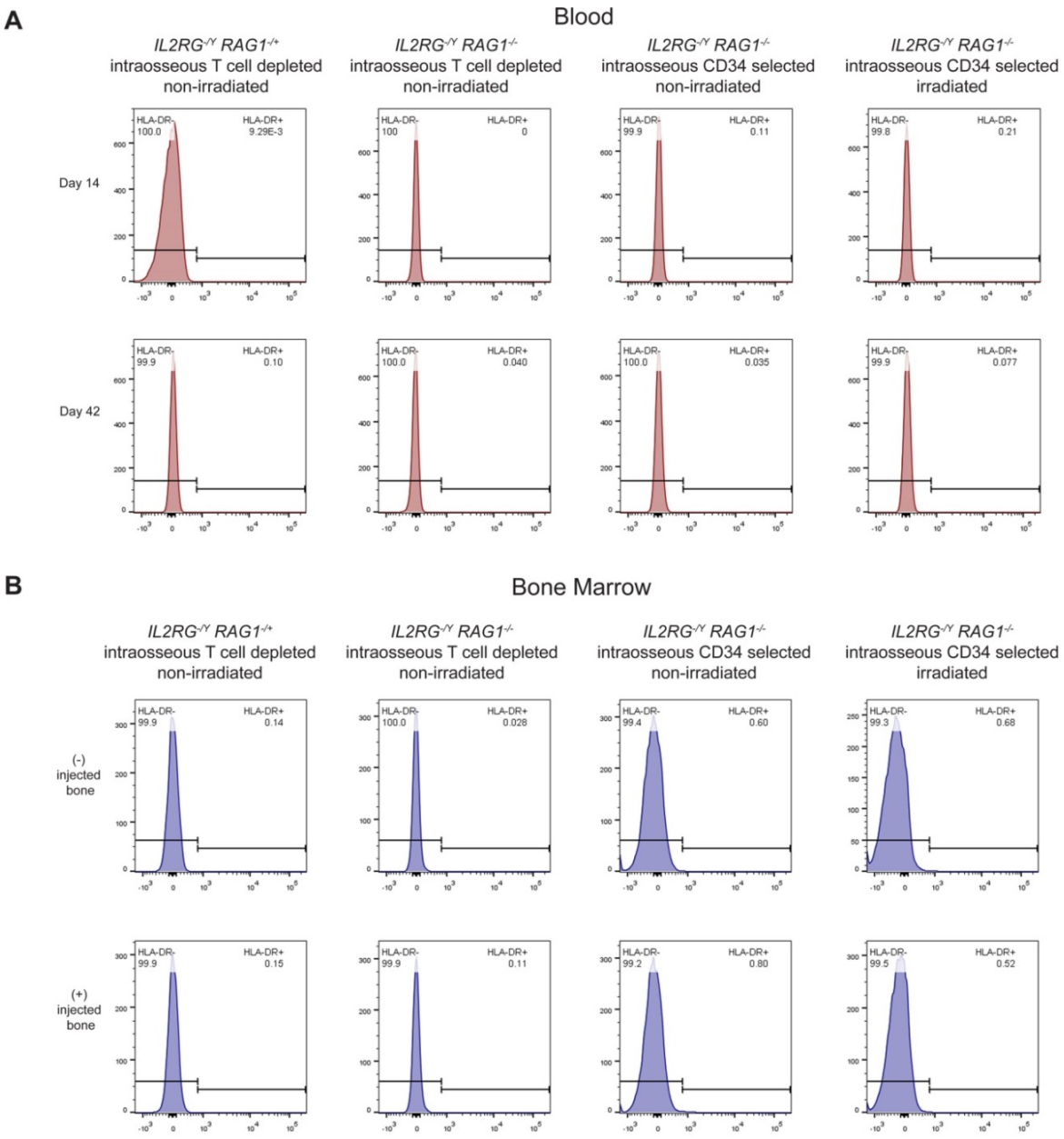
A
Blood
IL2RG-/Y RAG1-/+
intraosseous T cell depleted
non-irradiated
IL2RG-/Y RAG1-/-
intraosseous T cell depleted
non-irradiated
IL2RG-/Y RAG1-/-
intraosseous CD34 selected
non-irradiated
IL2RG-/Y RAG1-/-
intraosseous CD34 selected
irradiated
Day 14
HLA-DR- 100.0
HLA-DR+ 9.29E-3
HLA-DR- 100
HLA-DR+ 0
HLA-DR- 99.9
HLA-DR+ 0.11
HLA-DR- 99.8
HLA-DR+ 0.21
Day 42
HLA-DR- 99.9
HLA-DR+ 0.10
HLA-DR- 100.0
HLA-DR+ 0.040
HLA-DR- 100.0
HLA-DR+ 0.035
HLA-DR- 99.9
HLA-DR+ 0.077
B
Bone Marrow
IL2RG-/Y RAG1-/+
intraosseous T cell depleted
non-irradiated
IL2RG-/Y RAG1-/-
intraosseous T cell depleted
non-irradiated
IL2RG-/Y RAG1-/-
intraosseous CD34 selected
non-irradiated
IL2RG-/Y RAG1-/-
intraosseous CD34 selected
irradiated
(-) injected bone
HLA-DR- 99.9
HLA-DR+ 0.14
HLA-DR- 100.0
HLA-DR+ 0.028
HLA-DR- 99.4
HLA-DR+ 0.60
HLA-DR- 99.3
HLA-DR+ 0.68
(+) injected bone
HLA-DR- 99.9
HLA-DR+ 0.15
HLA-DR- 99.9
HLA-DR+ 0.11
HLA-DR- 99.2
HLA-DR+ 0.80
HLA-DR- 99.5
HLA-DR+ 0.52

following transplantation of CD34-selected human cells into irradiated DKO SCID pigs, however the resources and costs involved in maintaining the chronically ill irradiated pigs made continued use of this approach unfeasible.

4.3. Human CD34+ cell transplantation via *in utero* injection into the fetal liver of SCID pigs.

Due to the poor engraftment efficiency of human donor cells into SCID pigs and the need for irradiation to promote engraftment, alternative transplantation methods were explored for the delivery of CD34-selected human cells. A previous study demonstrated low-level multilineage engraftment of human cord blood transplanted into pig fetuses *in utero* (Fujiki et al., 2003). *In utero* transplantation of sheep with human hematopoietic stem cells has been shown to promote long-term multilineage expression of human hematopoietic cells (Zanjani et al., 1992, 1994). A more recent study demonstrated that *in utero* injection of the fetal pig liver on DG40 with human hepatocytes facilitated later engraftment with human hepatocytes when they were re-injected intrahepatically on postnatal day 7 (Fisher et al., 2013). A transplantation protocol was therefore developed for *in utero* intrahepatic injection of fetal SCID pigs with human CD34 selected cells.

Gestational day 42 was selected for transplantation, since this is when the fetal liver is both the dominant site of lymphopoiesis (Sinkora and Butler, 2009) and physically large enough to be injected accurately. Pregnant sows underwent surgery under sterile conditions to expose the gravid uterus. Human CD34 selected cells were then delivered via transuterine injection into the fetal liver under live ultrasound guidance.

The Kaplan-Meier survival curves for SCID pigs transplanted via different protocols with human cells are summarized in Figure 41. Regardless of the transplant method used, the majority of pigs died between postnatal day 20 and day 50. All deaths were due to overwhelming sepsis. Nearly 40% of pigs transplanted *in utero* were stillborn for unclear reasons. One SCID pig transplanted intraosseously survived to day 81, while another survived to day 80 after irradiation and intraosseous transplant with human CD34+ cells. I speculate that these pigs survived longer

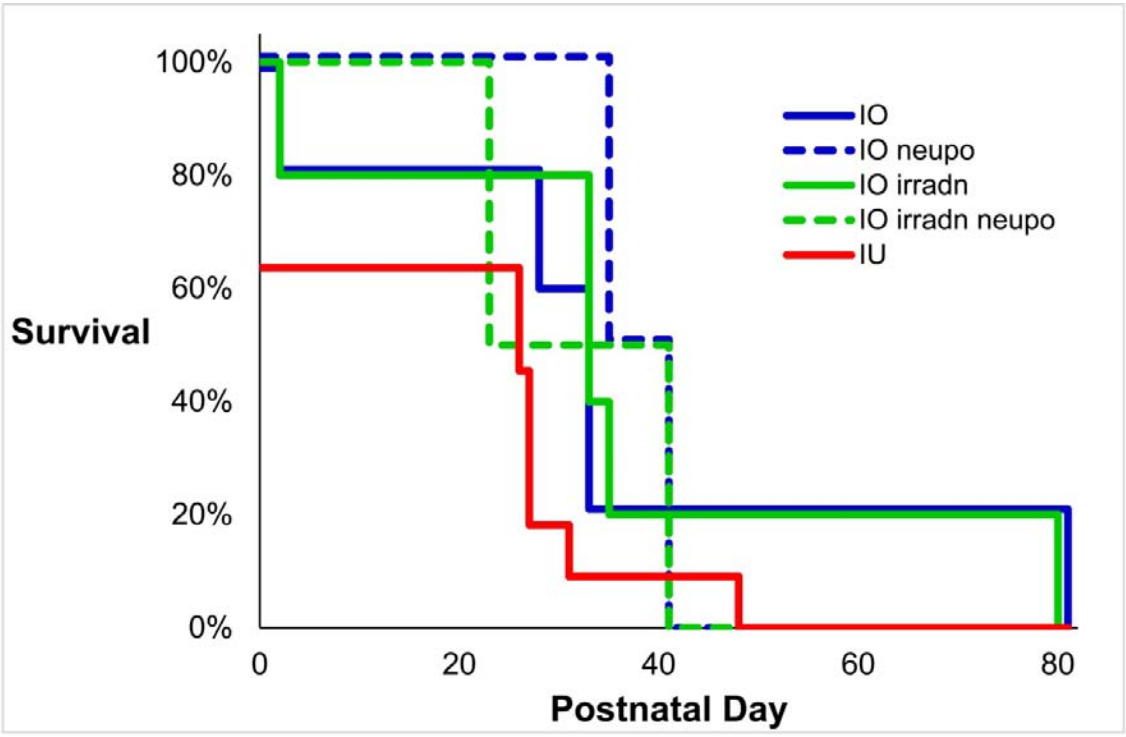

Fig. 41. Kaplan-Meier survival curve for SCID pigs after transplant with human hematopoietic cells.
IL2RG-/Y RAG1-/- piglets were transplanted intraosseously (IO) with human CD34 selected mobilized stem cells on postnatal day 1 or 2, or *in utero* (IU) on gestational day 42. Neupo indicates pigs treated with Neupogen (filgrastim). A total of 25 *IL2RG-/Y RAG1-/-* piglets were used for transplantation: five IO, two IO with Neupogen, seven IO with irradiation, two IO with irradiation and Neupogen, and eleven IU.

because they were separated from their mother on day 30 and thereby exposed to fewer infectious pathogens.

In SCID pigs transplanted *in utero* with human CD34+ cells, gross pathology revealed a thymus substantially larger than the thymic remnant seen in non-transplanted controls (Fig. 42). Tissue sections from the thymus and spleen were taken from transplanted animals and stained via IHC for human CD45 (Fig. 43). Intraosseous injection did not repopulate the thymus with human cells, while the spleen showed low levels of human CD45+ cells (Fig. 43B, *see inset*). In contrast, both the thymus and spleen showed robust repopulation with CD45+ human hematopoietic cells after *in utero* transplantation (Fig. 43, *final column*).

To determine the effects of *in utero* human CD34+ cell transplantation on peripheral T cell repopulation, PBMCs were collected and stained for human CD45, CD3, CD45RA, CD4, and CD8. Non-transplanted *IL2RG*$^{-/Y}$ *RAG1*$^{-/-}$ DKO pigs showed no appreciable staining with any human cell surface markers used (Figs. 44 and 45). Similarly, *in utero* transplantation of *IL2RG*$^{-/Y}$ *RAG1*$^{-/+}$ pigs yielded minimal to absent staining for human cells in the peripheral blood (Fig. 44, *second row*). However, *in utero* transplantation of *IL2RG*$^{-/Y}$ *RAG1*$^{-/-}$ DKO pigs led to repopulation with human CD45+ PBMCs by postnatal day 3 (Fig. 44A, *bottom row*) which were nearly all CD3+ T cells (Fig. 44B, *bottom row*). Staining for human T cell subsets showed that the CD3+ cells were CD45RA+ (Fig. 45A) and predominantly CD4+ CD8+ DP cells with small populations of CD8+ SP and CD4+ SP cells (Fig. 44C, *bottom row* and 45B). Notably, the CD3+ population disappeared by day 14 and remained absent on day 27 (Fig. 45A and 45B). Additionally, a substantial human CD19+ B

Fig. 42. Thymic expansion after *in utero* transplantation with CD34+ human cells in SCID pigs. Thymus was collected from a non-transplanted (*middle panel*) and transplanted (*lower panel*) SCID piglet on d27 and a WT piglet on d1.

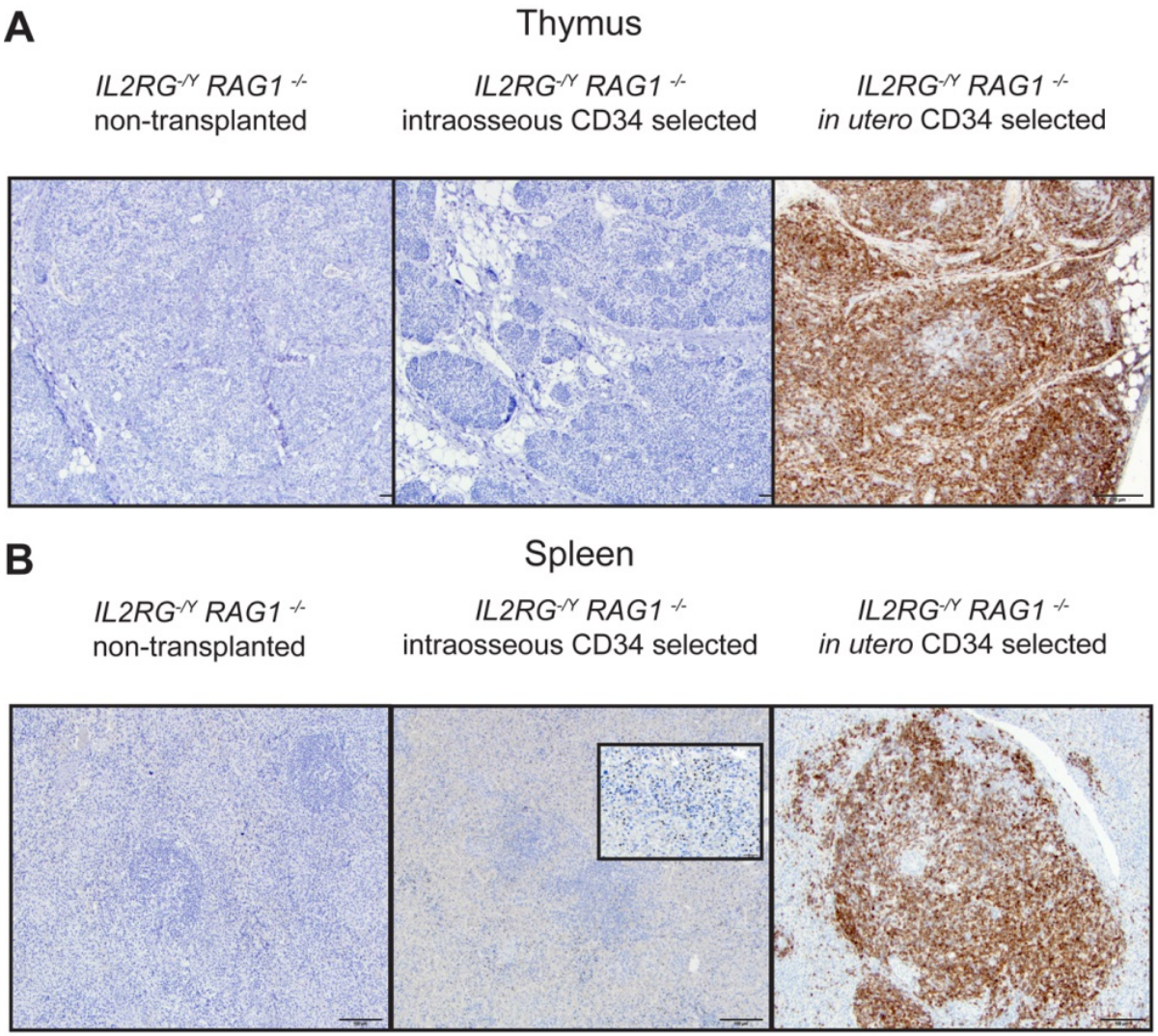

Fig. 43. *In utero* transplantation is more effective than intraosseous transplantation for repopulation of the thymus and spleen of SCID pigs with human hematopoietic cells.
Tissue sections of (*A*) thymus and (*B*) spleen were generated on postnatal day 26 from sacrificed *IL2RG*$^{-/Y}$ *RAG1*$^{-/-}$ pigs transplanted with CD34+ human cells via the protocols indicated. All tissues were stained for human CD45 by IHC.

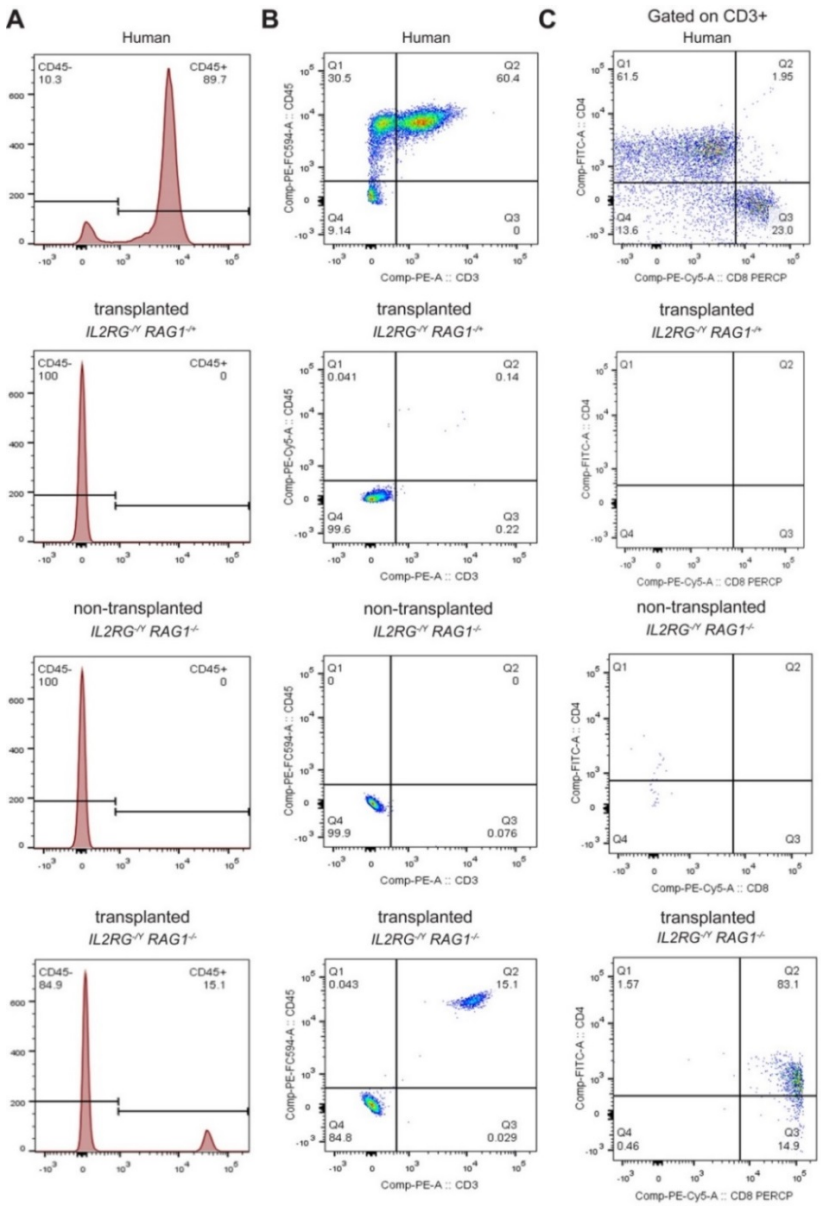

Fig. 44. Effects of *in utero* transplantation with CD34+ human cells on peripheral blood human T cells.

PBMCs were harvested on postnatal day 3 and stained for the following human cell surface markers: (*A*) CD45, a general leukocyte marker (*B*) CD45 and CD3, (*C*) gated on CD3+ cells, staining for CD4 and CD8. The top row shows human PBMCs as a positive control, second row is *in utero* transplanted *IL2RG*$^{-/Y}$ *RAG1*$^{-/+}$ pigs, third row is non-transplanted *IL2RG*$^{-/Y}$ *RAG1*$^{-/-}$ pigs, and bottom row is *in utero* transplanted *IL2RG*$^{-/Y}$ *RAG1*$^{-/-}$ pigs. $P < 0.01$ for *in utero* transplantation of *IL2RG*$^{-/Y}$ *RAG1*$^{-/-}$ pigs versus *in utero* transplanted *IL2RG*$^{-/Y}$ *RAG1*$^{-/+}$and non-transplanted *IL2RG*$^{-/Y}$ *RAG1*$^{-/-}$ pigs. Flow cytometry data are representative results from the following number of animals in parentheses: *IL2RG*$^{-/Y}$ *RAG1*$^{-/+}$ IU BMT (1), *IL2RG*$^{-/Y}$ *RAG1*$^{-/-}$ IU non-transplanted (7), and *IL2RG*$^{-/Y}$ *RAG1*$^{-/-}$ IU BMT (1) piglet.

Fig. 45. Dynamics of human peripheral blood T cell subpopulations after *in utero* transplantation of SCID pigs.
Peripheral blood was collected on postnatal day 3, 14, and 27 from the piglets described in Fig. 44 and stained for human (*A*) CD3 and CD45RA, and (*B*) CD3, CD4, and CD8; last column is gated on CD3(+) cells. On day 3, there were significantly higher T cell and DP T cell populations in transplanted pigs versus non-transplanted or WT ($p < 0.01$). Human PBMCs are shown as a positive control. Flow cytometry data are representative results from the following number of animals in parentheses: *IL2RG*$^{-/Y}$ *RAG1*$^{-/-}$ IU BMT (1) piglet.

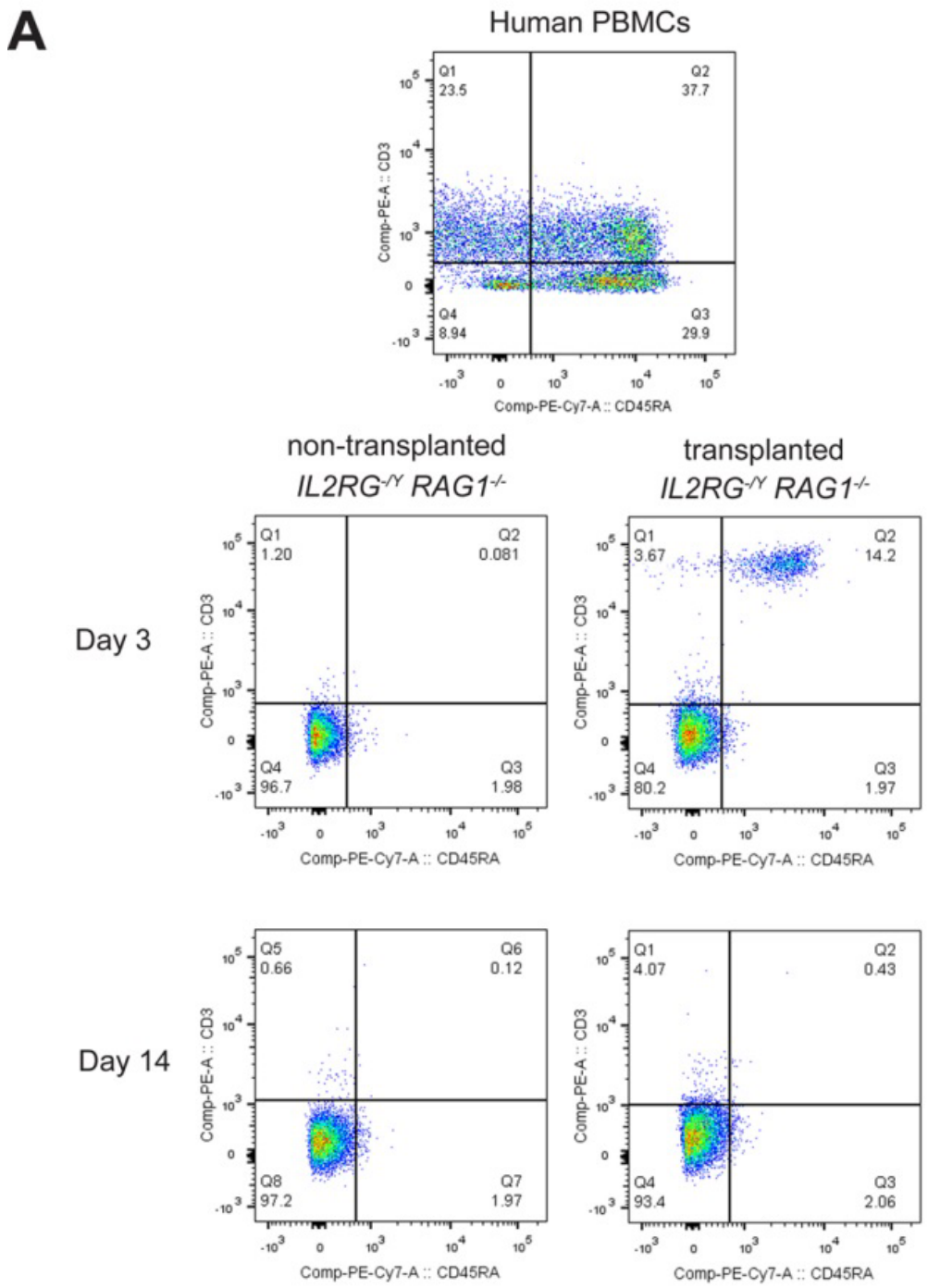
A
Human PBMCs
Q1
23.5
Q2
37.7
Q4
8.94
Q3
29.9
Comp-PE-A :: CD3
Comp-PE-Cy7-A :: CD45RA
non-transplanted
IL2RG-/Y RAG1-/-
transplanted
IL2RG-/Y RAG1-/-
Day 3
Q1
1.20
Q2
0.081
Q4
96.7
Q3
1.98
Q1
3.67
Q2
14.2
Q4
80.2
Q3
1.97
Day 14
Q5
0.66
Q6
0.12
Q8
97.2
Q7
1.97
Q1
4.07
Q2
0.43
Q4
93.4
Q3
2.06

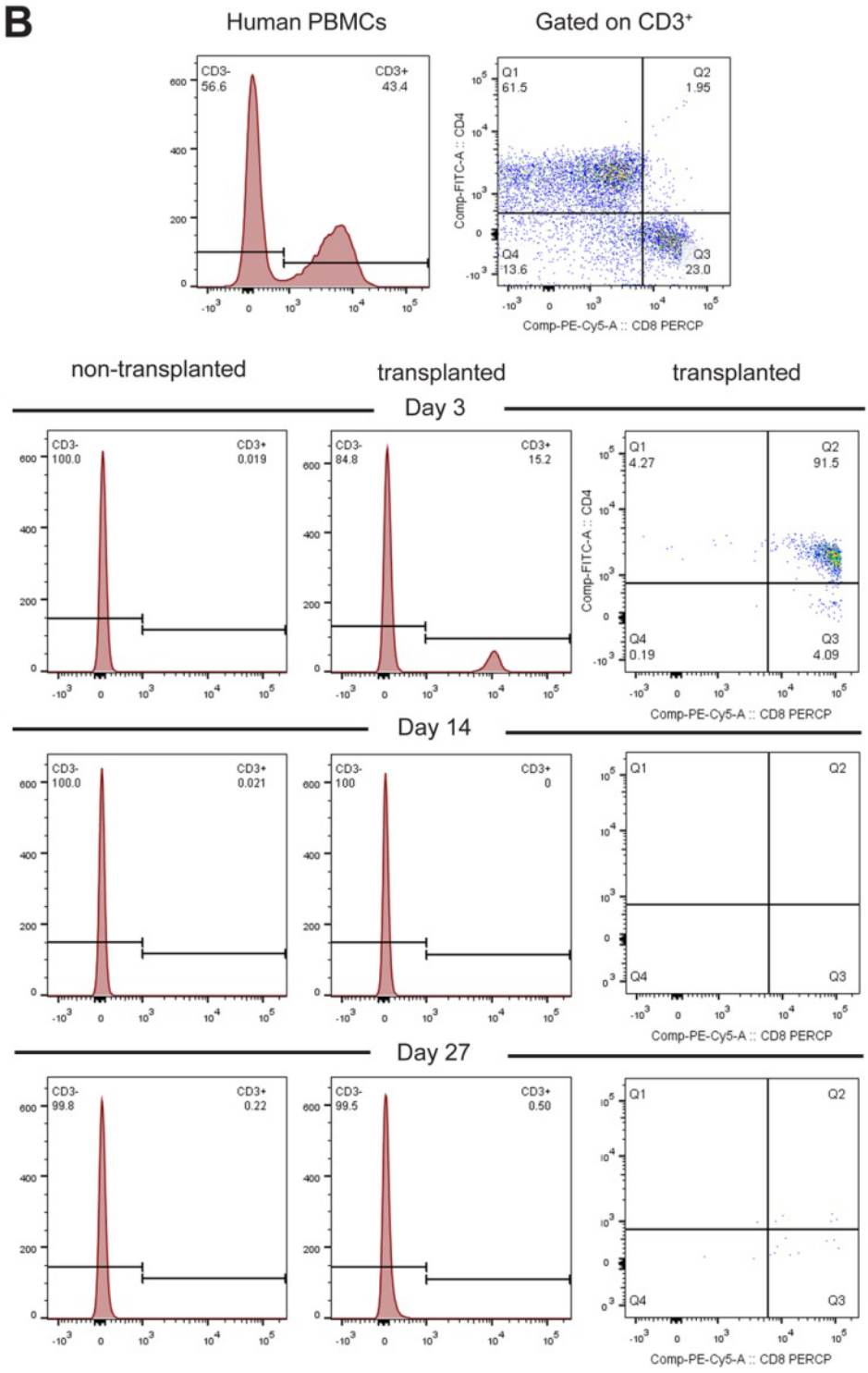
B
Human PBMCs
Gated on CD3+
CD3-
56.6
CD3+
43.4
Q1
61.5
Q2
1.95
Q4
13.6
Q3
23.0
Comp-FITC-A :: CD4
Comp-PE-Cy5-A :: CD8 PERCP
non-transplanted
transplanted
transplanted
Day 3
CD3-
100.0
CD3+
0.019
CD3-
84.8
CD3+
15.2
Q1
4.27
Q2
91.5
Q4
0.19
Q3
4.09
Day 14
CD3-
100.0
CD3+
0.021
CD3-
100
CD3+
0
Day 27
CD3-
99.8
CD3+
0.22
CD3-
99.5
CD3+
0.50

cell population was present in the peripheral blood after *in utero* transplantation on postnatal day 3, however this population disappeared by day 14, similar to T cells (Fig. 46).

Human hematopoietic cell repopulation of solid organs was tested by performing flow cytometry on single cell suspensions generated from the liver, spleen, and thymus of pigs (Fig. 47). *In utero* transplantation of *IL2RG*$^{-/Y}$ *RAG1*$^{-/+}$ pigs yielded no appreciable repopulation with human CD45+ cells over non-transplanted DKO controls. In *IL2RG*$^{-/Y}$ *RAG1*$^{-/-}$ DKO pigs that underwent transplant, a small population of human CD45+ cells was found in the liver (Fig. 47A), while the spleen and thymus (Fig. 47B and 47C) showed substantial numbers of human CD45+ cells. A significant population of human CD19+ B cells was present in the spleen from *in utero* transplanted SCID pigs on day 27 (Fig. 48). The experiments above were repeated with staining for HLA-DR in PBMCs, the spleen, and thymus (Fig. 49). *In utero* transplantation of *IL2RG*$^{-/Y}$ *RAG1*$^{-/+}$ pigs resulted in a small but appreciable increase in HLA-DR+ cells over non-transplanted DKO controls. *In utero* transplantation of *IL2RG*$^{-/Y}$ *RAG1*$^{-/-}$ DKO pigs again showed substantial repopulation with human HLA-DR+ cells in all compartments tested. In total, these data demonstrate that *in utero* intrahepatic transplantation with CD34+ human cells results in successful repopulation with human hematopoietic cells in the peripheral blood, liver, spleen, and thymus.

To determine the efficacy and characteristics of human T cell repopulation in the thymus and spleen, single cell suspensions were generated from these organs, stained for CD3, CD4, and CD8, and evaluated by flow cytometry (Fig. 50). *IL2RG*$^{-/Y}$ *RAG1*$^{-/+}$ pigs that underwent transplant showed no clear increase in human CD3 staining compared to non-transplanted DKO controls. *In utero* transplanted *IL2RG*$^{-/Y}$ *RAG1*$^{-/-}$ DKO pigs showed

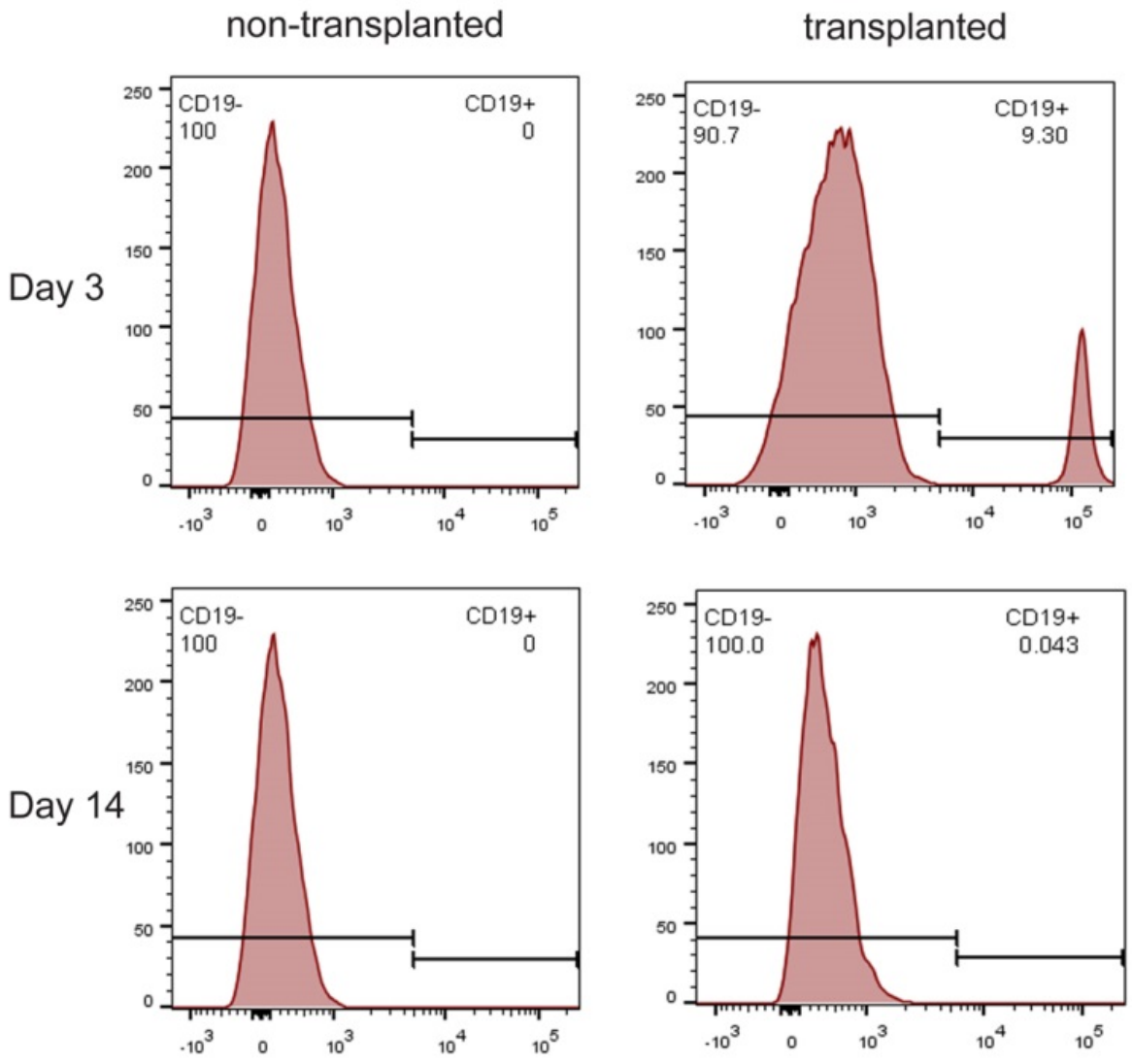

Fig. 46. Repopulation of peripheral blood with human B cells after *in utero* transplantation of SCID pigs with CD34+ human cells.

Peripheral blood was collected on postnatal days 3 and 14 then stained for human CD19, a B cell marker. $P < 0.01$ for transplanted versus non-transplanted. Flow cytometry data are representative results from the following number of animals in parentheses: *IL2RG*$^{-/Y}$ *RAG1*$^{-/-}$ IU non-transplanted (7), and *IL2RG*$^{-/Y}$ *RAG1*$^{-/-}$ IU BMT (1) piglets.

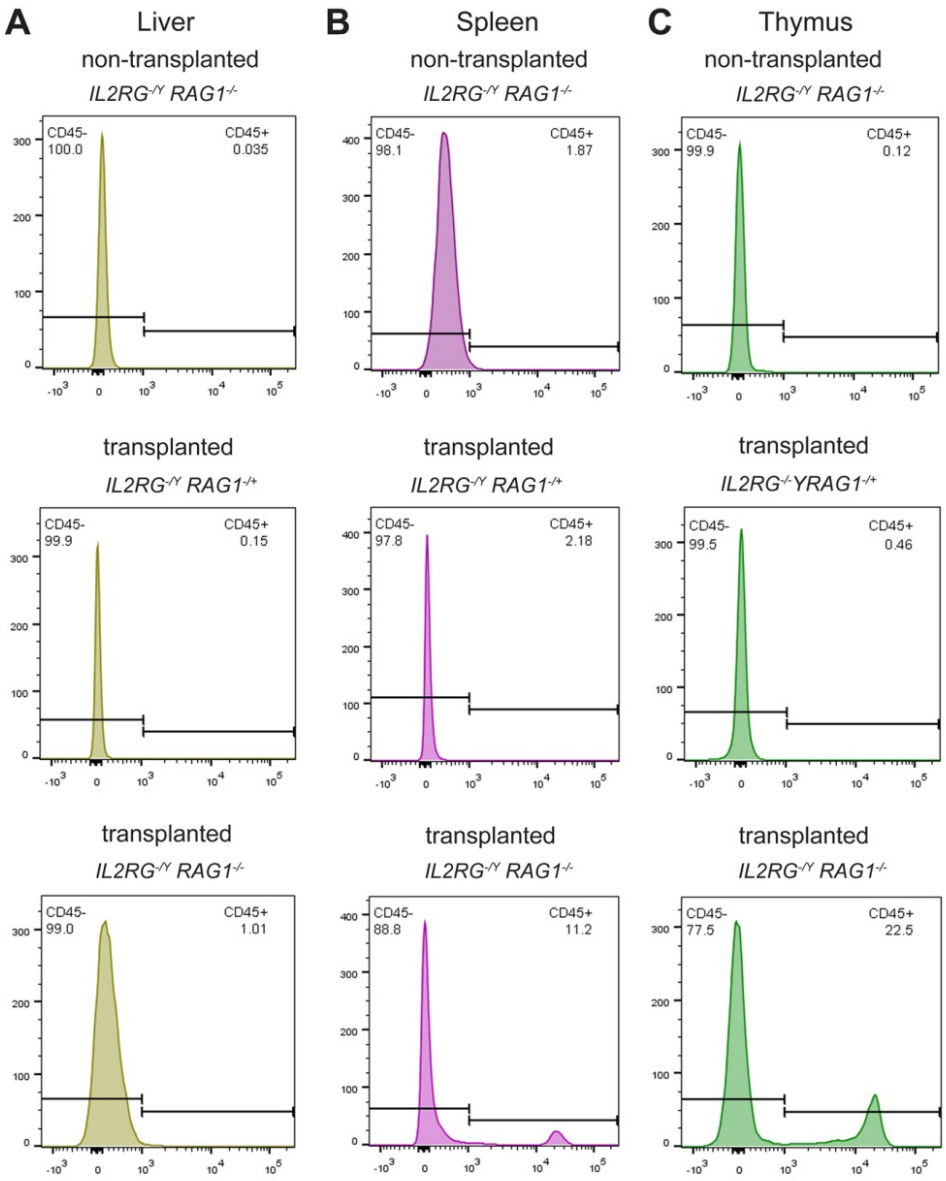

Fig. 47. Human leukocyte populations in solid organs after *in utero* transplant of CD34+ human cells into SCID pigs.

Cell suspensions from the (*A*) liver, (*B*) spleen, and (*C*) thymus were obtained from SCID pigs at the following times: non-transplanted *IL2RG*$^{-/Y}$ *RAG1*$^{-/-}$ on postnatal day 26, transplanted *IL2RG*$^{-/Y}$ *RAG1*$^{-/+}$ on day 27, transplanted *IL2RG*$^{-/Y}$ *RAG1*$^{-/-}$ liver on day 48, and transplanted *IL2RG*$^{-/Y}$ *RAG1*$^{-/-}$ spleen and thymus on day 27. Cells were stained with CD45 and assayed by flow cytometry. Among the *in utero* transplanted pigs, there was a significantly larger splenic human CD45+ population ($p = 0.018$) and thymic human CD45+ population ($p < 0.01$) in *IL2RG*$^{-/Y}$ *RAG1*$^{-/-}$ compared to non-transplanted and transplanted *IL2RG*$^{-/Y}$ *RAG1*$^{-/+}$pigs. Flow cytometry data are representative results from the following number of animals in parentheses: *IL2RG*$^{-/Y}$ *RAG1*$^{-/+}$ IU BMT (1), *IL2RG*$^{-/Y}$ *RAG1*$^{-/-}$ IU non-transplanted (7), and *IL2RG*$^{-/Y}$ *RAG1*$^{-/-}$ IU BMT (4) piglets.

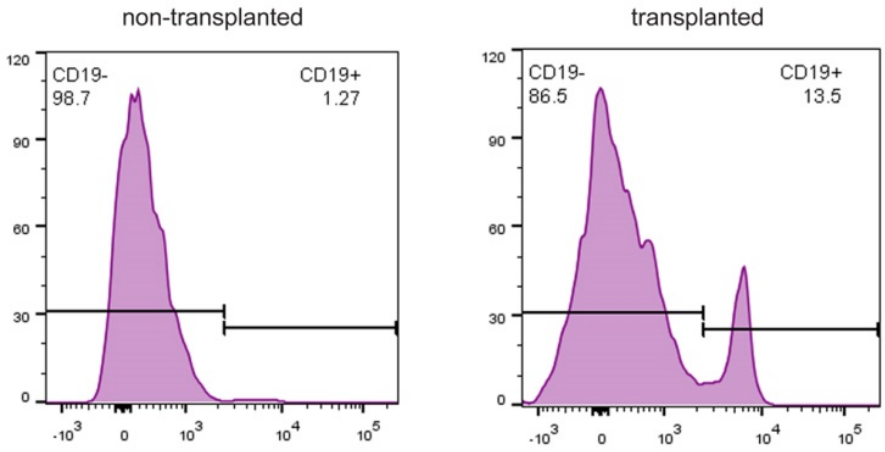

Fig. 48. Splenic repopulation with human B cells after *in utero* transplant of CD34+ human cells into SCID pigs.
Cell suspensions from the spleen were obtained on postnatal day 27 from non-transplanted (left panel) and *in utero* transplanted (right panel) *IL2RG*$^{-/Y}$ *RAG1*$^{-/-}$ piglets and stained for human CD19 (B cells). $P < 0.01$ transplanted versus non-transplanted. Flow cytometry data are representative results from the following number of animals in parentheses: *IL2RG*$^{-/Y}$ *RAG1*$^{-/-}$ IU non-transplanted (7), and *IL2RG*$^{-/Y}$ *RAG1*$^{-/-}$ IU BMT (2) piglets.

substantial populations of human T cells in both the thymus (Fig. 50, *lower row*) and spleen (Fig. 51). In the thymus, these were almost all CD4+ CD8+ DP T cells (Fig. 50C), with the majority staining CD45RA+ (Fig. 50B), suggestive that these are naïve T cells. In contrast, splenic T cells were largely SPs, with a slightly higher number of CD4+ SPs versus CD8+ SPs (Fig. 51C); the splenic T cells also predominantly stained CD45RA+ (Fig. 51B). These results are consistent with human T cells undergoing development and selection within the pig thymus, where predominantly DP cells are seen (Spits et al., 1995). (DN human T cells are not detected in the thymus by this gating strategy because they are largely CD3 negative.) The findings also suggest that after the DP to SP transition, naïve SP human T cells exit the thymus to the periphery, as observed in the spleens of transplanted animals.

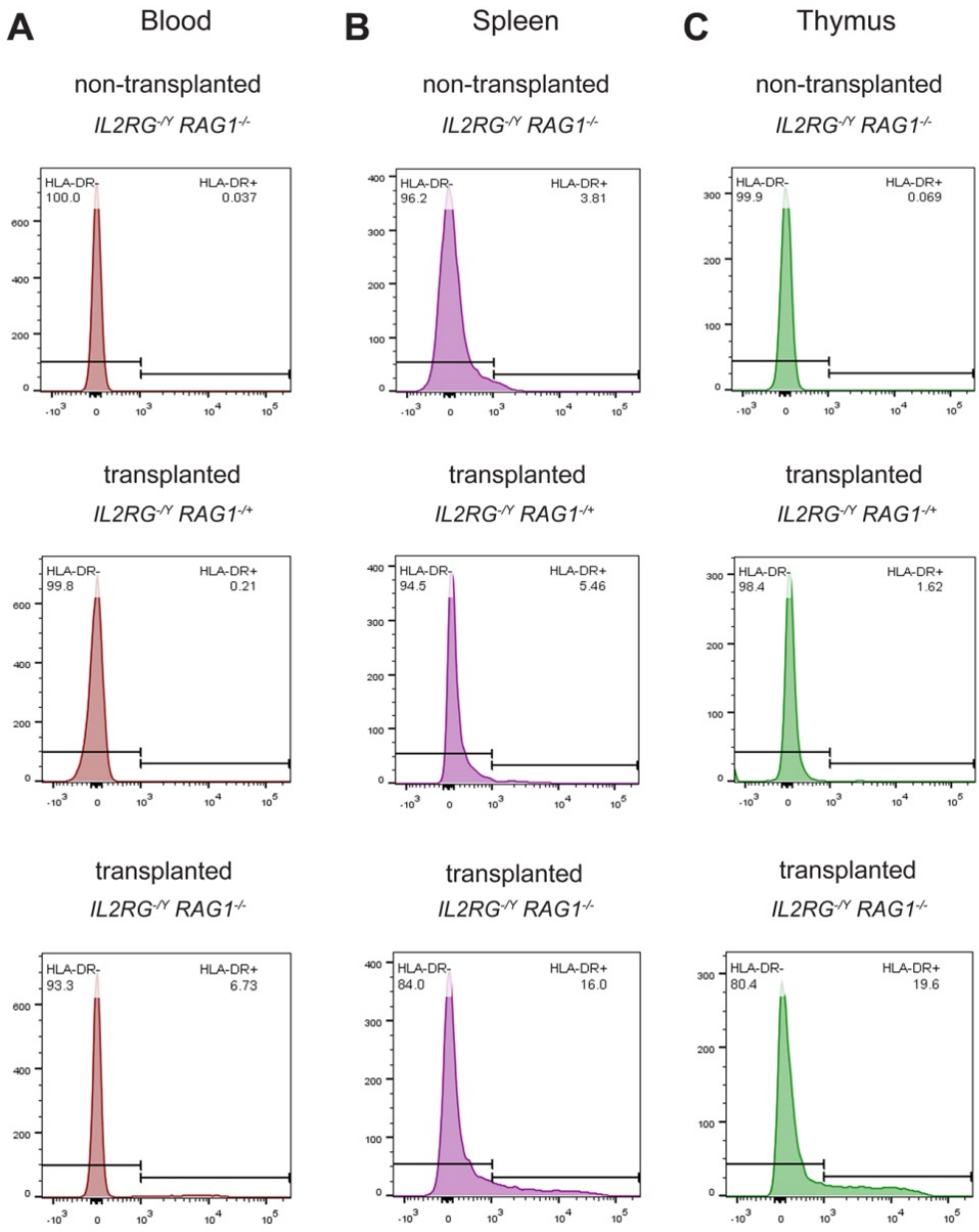

Fig. 49. Human HLA-DR+ cell populations in blood and solid organs after *in utero* transplant of CD34+ human cells into SCID pigs.

(*A*) Peripheral blood was obtained on postnatal day 3 and cell suspensions from the (*B*) spleen and (*C*) thymus were obtained on d1 from a *IL2RG*$^{-/Y}$ *RAG1*$^{-/+}$ pig and d26 from a *IL2RG*$^{-/Y}$ *RAG1*$^{-/-}$ pig after both pigs were transplanted *in utero*. Cells were stained for HLA-DR and evaluated by flow cytometry. For transplanted *IL2RG*$^{-/Y}$ *RAG1*$^{-/-}$ versus non-transplanted or transplanted *IL2RG*$^{-/Y}$ *RAG1*$^{-/+}$, $p = 0.29$ for the peripheral blood, $p = 0.19$ for the spleen, and $p < 0.01$ for the thymus. Flow cytometry data are representative results from the following number of animals in parentheses: *IL2RG*$^{-/Y}$ *RAG1*$^{-/+}$ IU BMT (1), and *IL2RG*$^{-/Y}$ *RAG1*$^{-/-}$ IU non-transplanted (7), and *IL2RG*$^{-/Y}$ *RAG1*$^{-/-}$ IU BMT (4) piglets.

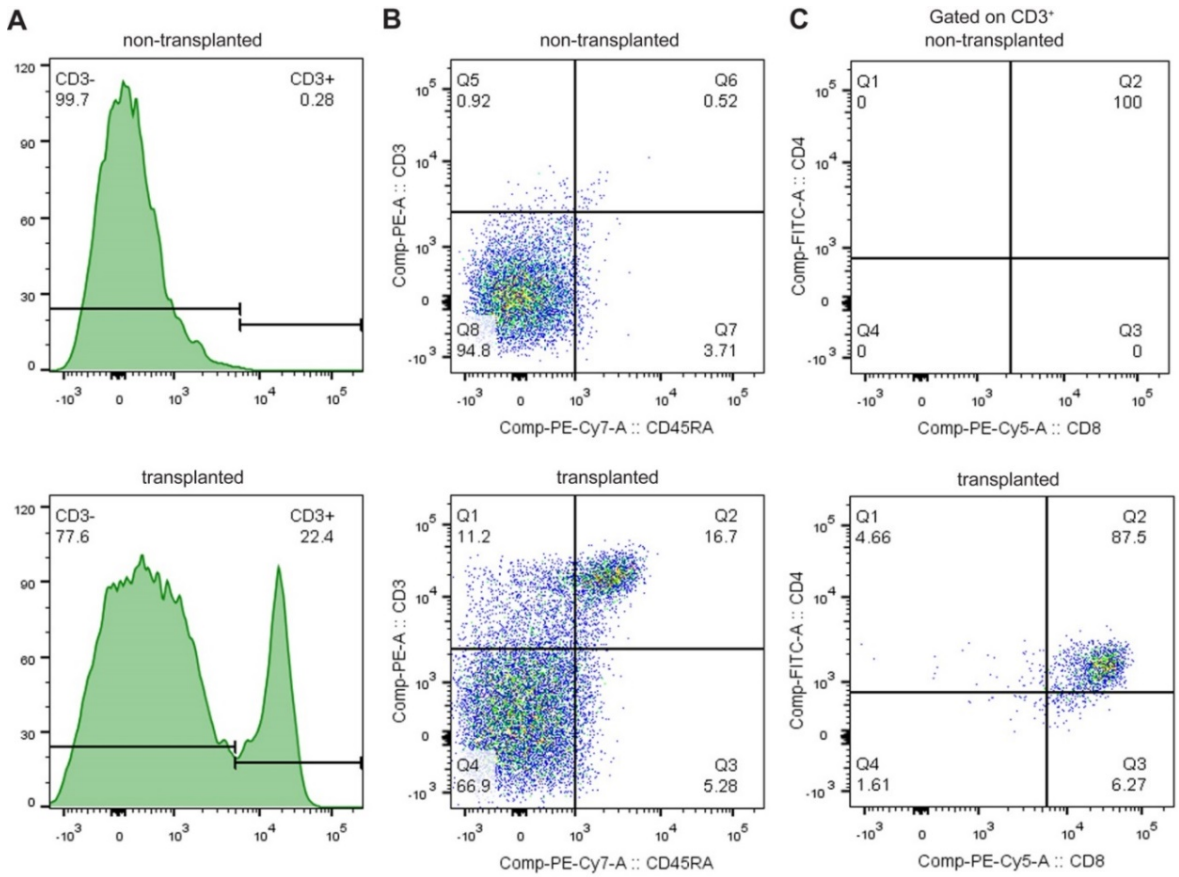

Fig. 50. Thymic repopulation with human T cells after *in utero* transplant of CD34+ human cells into SCID pigs.

Cell suspensions from the thymus were obtained on postnatal day 27 from non-transplanted *IL2RG*$^{-/Y}$ *RAG1*$^{-/-}$ and *in utero* transplanted *IL2RG*$^{-/Y}$ *RAG1*$^{-/-}$ piglets. Cells were stained for the following human markers: (*A*) CD3, (*B*) CD3 and CD45RA, and (*C*) Gated on CD3+ cells, staining for CD4 and CD8. $P < 0.01$ for transplanted versus non-transplanted piglets. Flow cytometry data are representative results from the following number of animals in parentheses: *IL2RG*$^{-/Y}$ *RAG1*$^{-/-}$ IU non-transplanted (7), and *IL2RG*$^{-/Y}$ *RAG1*$^{-/-}$ IU BMT (4) piglets.

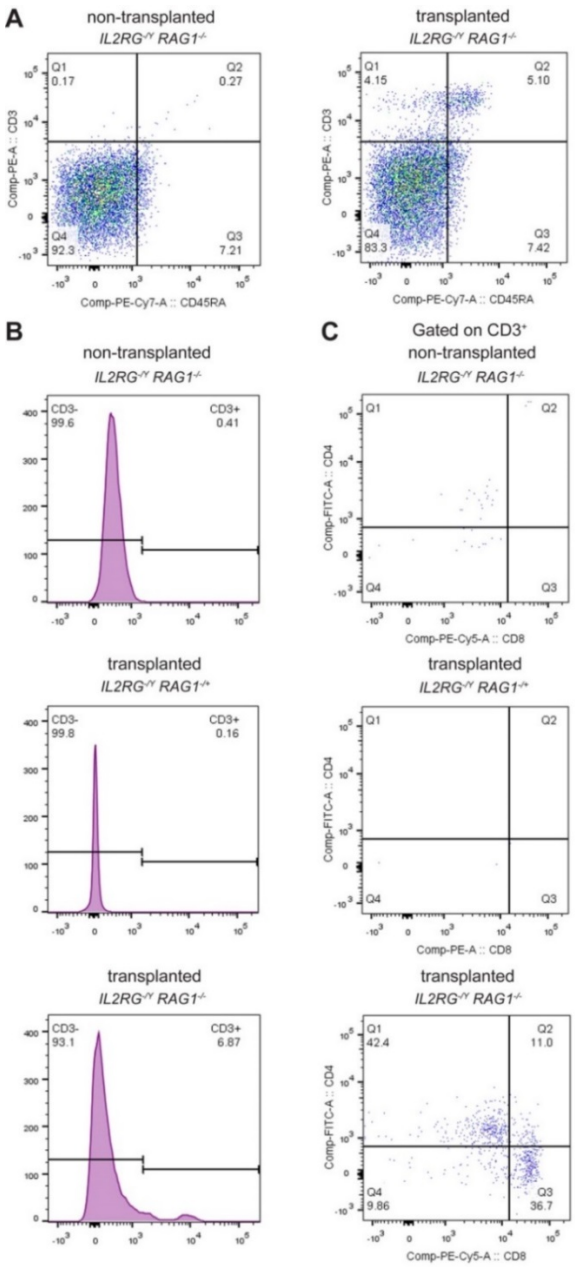

Fig. 51. Splenic repopulation with human T cells after *in utero* transplant of CD34+ human cells into SCID pigs.

Cell suspensions from the spleen were obtained as described in Fig. 50. Cells were stained for the following human markers: (*A*) CD3 and CD45RA, (*B*) CD3, and (*C*) Gated on CD3+, staining for CD4 and CD8. For transplanted versus non-transplanted, $p = 0.029$ for the difference in total CD3+ cells, while $p < 0.01$ for the difference in CD3+ CD45RA+ naïve T cells, CD3+ CD4+ SP T cells, or CD3+ CD8+ SP T cells. Flow cytometry data are representative results from the following number of animals in parentheses: *IL2RG*$^{-/Y}$ *RAG1*$^{-/+}$ IU BMT (1), *IL2RG*$^{-/Y}$ *RAG1*$^{-/-}$ IU non-transplanted (7), and *IL2RG*$^{-/Y}$ *RAG1*$^{-/-}$ IU BMT (4) piglets.

Flow cytometry was performed on cell suspensions generated from the bone marrow of SCID pigs transplanted *in utero* to determine the efficacy of marrow repopulation by human lymphocytes. Transplanted pigs showed a time-dependent accumulation of human CD45+ hematopoietic cells in the marrow (Fig. 52A). The majority of these were T cells, which on day 1 and day 31 showed a nearly equal balance between activated CD45RA– T cells and naïve CD45RA+ T cells (Fig. 52B). By day 48, the proportion of activated CD45RA– T cells had increased substantially. The majority of human T cells in the human bone marrow was DP, with a small population of CD4+ SP cells and essentially absent populations of DN or CD8+ SP cells (Fig. 52C). These studies demonstrate successful bone marrow repopulation with T cells following *in utero* transplantation, with rapidly increasing numbers of activated T cells associated with aging and impaired differentiation to the CD8+ SP T cell fate.

4.4. Human antibody production after *in utero* transplantation of human CD34+ cells into SCID pigs.

To measure antibody production from human B cells, anti-human IgM ELISAs were performed on plasma collected from *IL2RG*$^{-/Y}$ *RAG1*$^{-/-}$ pigs that had been transplanted with human bone marrow (Fig. 53). Prior to postnatal day 14 there was significant variability in measured IgM levels due to cross-reactivity between the anti-human IgM antibody and maternal porcine IgM transferred via the colostrum (data not shown). Neither irradiation nor Neupogen treatment with intraosseous human BMT led to sustained increases in IgM titers during the first 40 days of life. Irradiation and neupogen treatment with intraosseous human BMT led to a rise in human IgM levels in a single animal on day 42. In contrast, *in utero* injection of human CD34+ cells led to a steady increase in human IgM titers from day 27 to

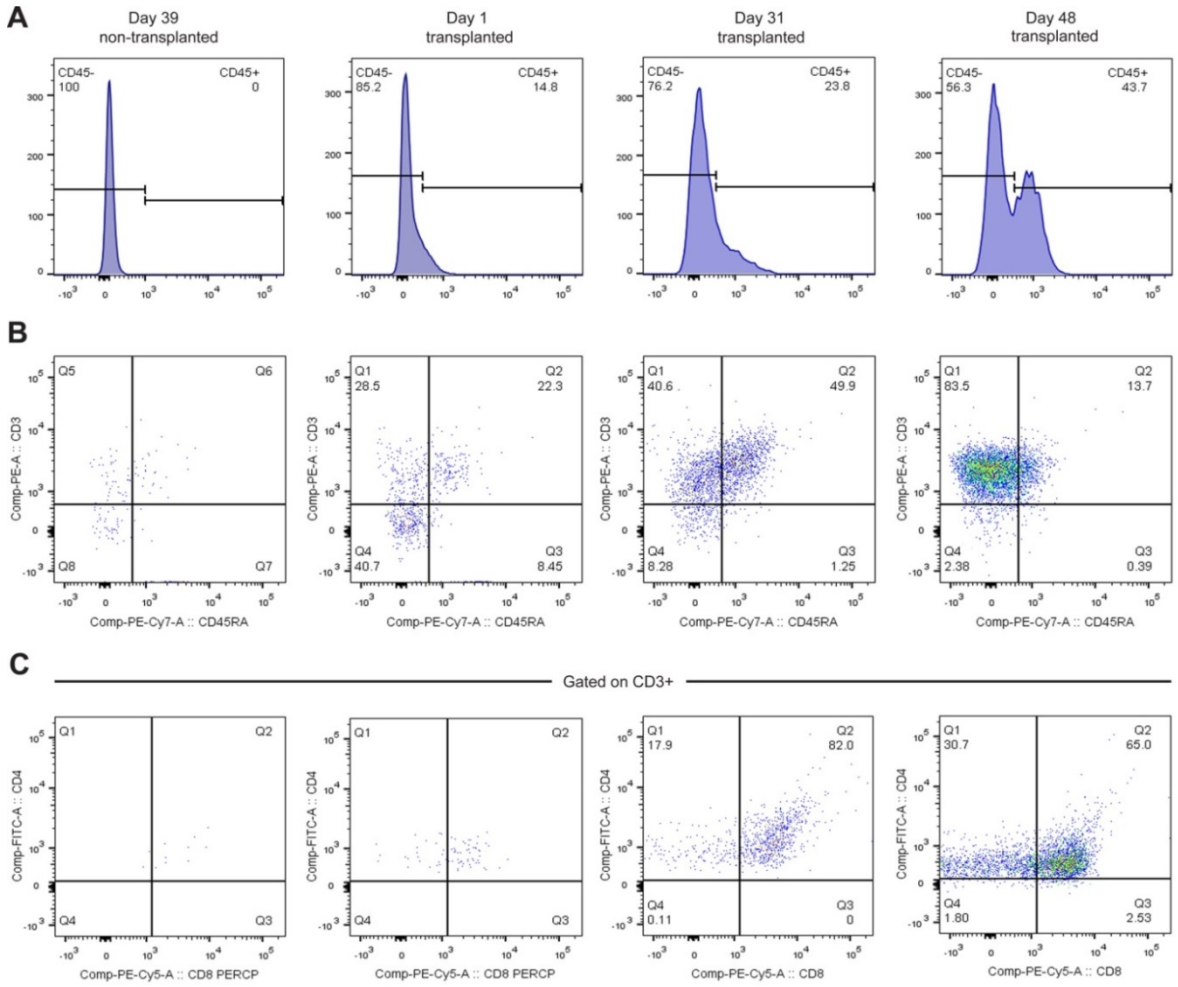

Fig. 52. Bone marrow reconstitution with human T cells after *in utero* transplant of CD34+ human cells into SCID pigs.

Bone marrow was collected on postnatal day 1, 31, and 48 from sacrificed piglets transplanted *in utero* and on day 39 from the non-transplanted control. The bone marrow cells were then stained for human (A) CD45, (B) CD3 and CD45RA, or (C) gated on CD3+, staining for CD4 and CD8. $P < 0.01$ for transplanted versus non-transplanted pigs on all days tested. Flow cytometry data are representative results from the following number of animals in parentheses: *IL2RG*$^{-/Y}$ *RAG1*$^{-/-}$ IU non-transplanted (7) and *IL2RG*$^{-/Y}$ *RAG1*$^{-/-}$ IU BMT (3) piglets.

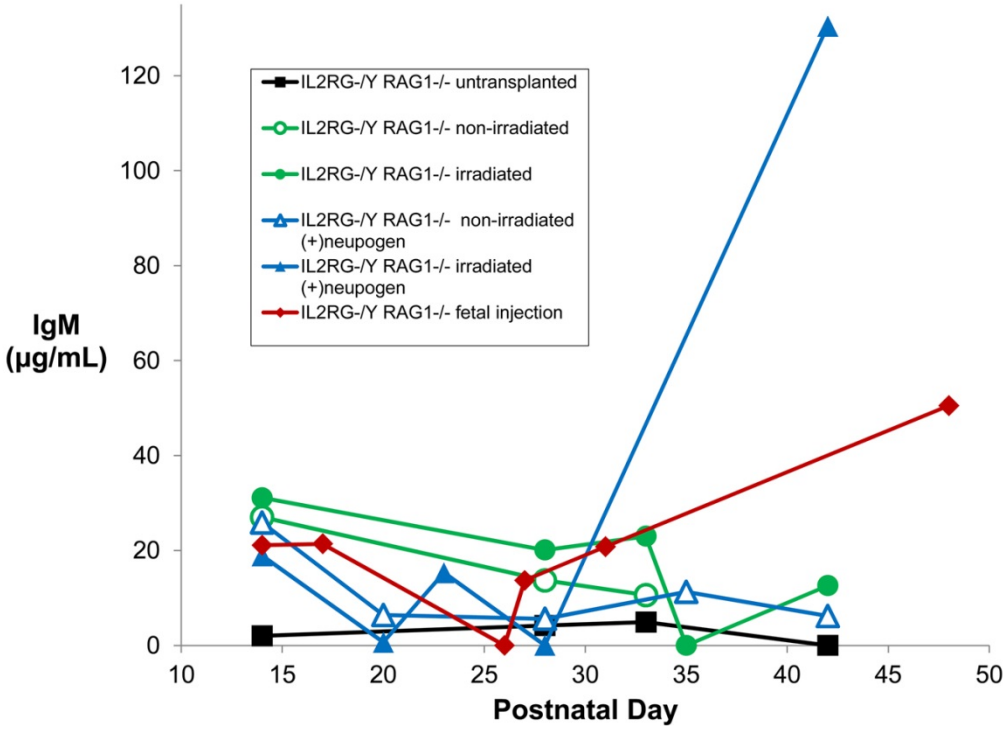

Fig. 53. Plasma immunoglobulin levels in *IL2RG*$^{-/Y}$ *RAG1*$^{-/-}$ pigs after transplantation with CD34+ human cells.
IL2RG$^{-/Y}$ *RAG1*$^{-/-}$ pigs were intraosseously administered either saline (*non-transplanted*) or CD34-enriched human cells +/- total body irradiation on postnatal day 2 and +/- Neupogen treatment on d14. Another group of *IL2RG*$^{-/Y}$ *RAG1*$^{-/-}$ pigs was transplanted with human bone marrow *in utero* (*fetal injection*) on DG42. Plasma was collected at the indicated times and used to measure human IgM levels by ELISA. ELISA data are representative results from the following number of animals in parentheses: *IL2RG*$^{-/Y}$ *RAG1*$^{-/-}$ non-transplanted (2), *IL2RG*$^{-/Y}$ *RAG1*$^{-/-}$ IO BMT (5), *IL2RG*$^{-/Y}$ *RAG1*$^{-/-}$ IO irradiated BMT (5), *IL2RG*$^{-/Y}$ *RAG1*$^{-/-}$ IO BMT plus Neupogen (2), *IL2RG*$^{-/Y}$ *RAG1*$^{-/-}$ IO irradiated BMT plus Neupogen (2), and *IL2RG*$^{-/Y}$ *RAG1*$^{-/-}$ fetal injection IU (4) pigs. Plasma was tested for titers of (*A*) IgM, (*B*) IgG, and (*C*) IgA as measured by ELISA. Results shown are the mean titer from the surviving piglets (see Fig. 41 for number of surviving piglets at each time point). ELISA was performed in triplicate for each animal at each time point.

day 48. These ELISA results suggest that *in utero* intrahepatic transplantation of human CD34+ cells leads to the generation of antibody-secreting human B cells in SCID pigs.

4.5. Chapter Summary.

In this chapter, I demonstrated successful xenogeneic transplantation of human CD34+ cells into *IL2RG*$^{-/Y}$ *RAG1*$^{-/-}$ SCID pigs and repopulation with human T and B cells.

Table 4. Summary of lymphocyte profiles from SCID pigs after transplantation with human HSCs.

Values shown for CD45+, total T cells, and B cells are percent of total leukocytes. Values shown for activated, naïve, DN, DP, CD4, and CD8 cells are percent of total T cells. Values shown are the highest measured across all trials and time points.

HUMAN TO PIG

IL2RG-/Y RAG1-/-

Organ/Tissue	CD45+	T Cells total	activated	naïve	DN	DP	CD4	CD8	B cells	*n*
blood	15.10	15.10	79.46	20.54	0.46	91.50	4.27	4.10	9.30	4
spleen	11.20	6.87	55.14	44.86	9.86	11.00	42.40	36.70	13.50	4
thymus	22.50	24.30	59.86	40.14	1.61	87.50	4.66	6.27		4
bone marrow	43.70	38.20	83.50	13.70	1.80	82.00	30.70	2.53		4

The leukocyte profile from SCID pigs transplanted *in utero* with human CD34+ cells is summarized in Table 4. *In utero* intrahepatic transplantation of CD34 selected human cells was clearly superior to intraosseous transplantation. SCID pigs transplanted intraosseously showed no improvement in engraftment with irradiation or G-CSF treatment. *In utero* transplant resulted in increased thymic size, and thymic repopulation with predominantly naïve human DP T cells, prior to the DP to SP transition. The peripheral blood was transiently repopulated with predominantly naïve human DP T cells, with smaller populations of CD4+ and CD8+ SP T cells, however T cells were absent from the peripheral blood by postnatal day 14. The spleen contained largely naïve human CD4+ and CD8+ SP T cells. The bone marrow had a shift from naïve to activated human T cells with increasing age; these bone marrow T cells were mostly DP, with a smaller population of CD4+ SP cells and no CD8+ SP cells. There was also strong repopulation of the peripheral blood and spleen with human B cells, at least some of which are functional and secrete human IgM. These results demonstrate, to my knowledge, the first successful construction of a human hemato-lymphoid system "humanized" pig.

CHAPTER 5: DISCUSSION

5.1. Summary of primary findings.

In Chapter 2, I reported the use transcription-activator like effector nucleases (TALENs) to generate *IL2RG*$^{-/Y}$ *RAG1*$^{-/-}$ double knockout pigs that lack functional T, B, and NK cells. *IL2RG*$^{-/Y}$ *RAG1*$^{-/-}$ pigs have an atrophied thymic remnant, absent lymph nodes, and loss of splenic red/white pulp differentiation. Flow cytometry and IHC studies demonstrated the loss of T, B, and NK cells in the peripheral blood, thymus, and spleen, with the exception of a small population of 74-22-15– CD3– CD45RA+ cells in the spleen, putatively identified as B cells. *IL2RG*$^{-/Y}$ *RAG1*$^{-/-}$ pigs had only trace levels of plasma IgM, IgG, and IgA, consistent with a severe defect in humoral immunity. These studies demonstrated that *IL2RG*$^{-/Y}$ *RAG1*$^{-/-}$ pigs have severe combined immunodeficiency (SCID) and are the first immunodeficient pig model with functional loss of all mature lymphocyte lineages.

In Chapter 3, I compared the efficacy of several protocols for allogeneic bone marrow transplantation (BMT) in *IL2RG*$^{-/Y}$ *RAG1*$^{-/-}$ pigs. PCR amplification of a transgenic marker was used to verify the donor origin of PBMCs in transplanted animals. The most effective BMT protocol for sustained repopulation with donor lymphocytes was intraosseous transplantation of T cell depleted porcine bone marrow into non-irradiated *IL2RG*$^{-/Y}$ *RAG1*$^{-/-}$ pigs. Intravenous BMT led to transient reconstitution of only the T cell lineage in the peripheral blood. Intraosseous BMT of irradiated pigs led to earlier repopulation with T and B cells, however the T cell population contracted after initial expansion and neither T nor B cells in irradiated pigs achieved the levels seen in age-matched non-irradiated controls at later time points. Allogeneic BMT resulted in repopulation with predominantly CD45RA–

activated T cells in all compartments tested, with only a small population of CD45RA+ naïve T cells. In the blood and spleen, the majority of T cells were CD4+ CD8+ DP cells, while CD4+ and CD8+ SP cells were more prominent in the thymus with a smaller DP population. While B cells strongly repopulated the peripheral blood, no B cell repopulation was seen in the spleen. Allogeneic BMT led to weak but detectable NK cell reconstitution. The bone marrow was reconstituted with low levels of all lymphocyte lineages after allogeneic BMT. SCID pigs that underwent intraosseous BMT without irradiation and showed strong B cell reconstitution also displayed rescue of IgM and IgG expression, but not IgA. Rescue of antibody production was absent in irradiated allogeneic BMT recipients.

In Chapter 4, I performed xenogeneic transplantation of human CD34+ bone marrow cells into *IL2RG*$^{-/Y}$ *RAG1*$^{-/-}$ pigs to repopulate the SCID pig with human lymphocytes. *In utero* intrahepatic transplantation of CD34+ human bone marrow cells was substantially more effective in promoting human cell engraftment than intraosseous postnatal transplantation. Conditioning with total body irradiation or filgrastim (Neupogen) treatment did not improve engraftment. Transplanted animals showed an increase in thymic size. Human T cells showed clear engraftment in all compartments tested, with a predominance of naïve CD45RA+ T cells. While only DP T cells were seen in the thymus, a mixture of DP, CD4+ SP and CD8+ SP was seen in the peripheral blood, and only SPs were seen in the spleen. There was also strong repopulation with human B cells in the peripheral blood and spleen, at least some of which are functional and secrete human IgM. These studies demonstrate that *in utero* intrahepatic transplantation with CD34+ human bone marrow cells into *IL2RG*$^{-/Y}$ *RAG1*$^{-/-}$ pigs leads to repopulation with human T cells and B cells. Overall, this

body of work represents the first (to my knowledge) successful construction of a humanized pig.

5.2. TALENs and SCNT for the rapid production of genetically modified swine.

This study highlights the power of combining TALEN technology with SCNT as a rapid and efficient method to generate genetically modified pigs, particularly when mutations in multiple genes are desired. The combined TALEN/SCNT strategy allowed for the generation of DKO *IL2RG*$^{-/Y}$ *RAG1*$^{-/-}$ pigs in only 10 months with a pregnancy rate of greater than 50% and at least 4 live births per litter. All the piglets born contained the predicted mutations. To generate a double knockout SCID pig, we used TALENs followed by SCNT to generate *IL2RG*$^{-/Y}$ fetuses, from which several *IL2RG* knockout cell lines were directly produced. This approach offers both flexibility and speed by creating a genetically modified cell line on which nearly any additional desired mutations can be introduced (via a different TALEN set – in our study, targeting *RAG1*) without requiring a full reproductive generation (*i.e.*, growing an adult animal). Not only does this strategy speed up the process of producing large animals containing mutations in multiple genes, but it also circumvents the problem of keeping animals alive through reproductive age and pregnancy, particularly when they bear deleterious mutations. Furthermore, TALENs allowed the production of a biallelic knockout (of *RAG1*) pig in a single generation, similar to prior studies (Huang et al., 2014; Lee et al., 2014).

5.3. Comparison of *IL2RG*$^{-/Y}$ *RAG1*$^{-/-}$ pigs to existing SCID mouse and pig models and humanized mice.

The *IL2RG*$^{-/Y}$ *RAG1*$^{-/-}$ SCID pigs share several gross pathological and histological features consistent with previously reported SCID models and human SCID disease. *IL2RG*$^{-/Y}$ *RAG1*$^{-/-}$ SCID pigs are a phenocopy of mice bearing inactivating mutations at the same loci (Pearson et al., 2008), which is summarized in Table 5. The double knockout SCID pigs were

Table 5. Phenotype comparison between mouse and pig models of the *IL2RG RAG1* double knockout.
Mouse data from (Pearson et al., 2008).

Lymphocyte Profile

	Mouse NOD-*Rag1*^{null} *IL2rγ*^{null}	Pig *IL2RG*$^{-/Y}$ *RAG1*$^{-/-}$
CD3$^+$ CD4$^+$ T cells	Absent	Absent
CD3$^+$ CD8$^+$ T cells	Absent	Absent
B cells (splenic)	Absent	Absent
NK cells	Absent	Absent

Lymphoid Organ Profile

	Mouse NOD-*Rag1*^{null} *IL2rγ*^{null}	Pig IL2RG$^{-/Y}$ RAG1$^{-/-}$
Thymus cortex and medulla	Absent	Absent
Spleen follicles and germinal centers	Absent	Absent
Lymph Nodes	Absent	Absent

underweight, consistent with neonatal failure to thrive seen in SCID pigs with spontaneous primary immunodeficiency (Basel et al., 2012; Ozuna et al., 2013), *RAG1*$^{-/-}$ and *RAG2*$^{-/-}$ pigs (Huang et al., 2014; Lee et al., 2014), and human SCID patients (Leonard, 1995). Similar to all the previously described SCID pig models, the *IL2RG*$^{-/Y}$ *RAG1*$^{-/-}$ SCID pigs lack a thymus or possess only a small thymic remnant, and show a markedly decreased spleen size with hypoplastic white pulp, absence of germinal centers, and disorganization of splenic tissue architecture. While spontaneously generated SCID pigs have small lymph nodes and Peyer's patches with abnormal architecture (Ozuna et al., 2013), in *IL2RG*$^{-/Y}$ *RAG1*$^{-/-}$ SCID pigs these secondary lymphoid structures are completely absent, highlighting the severity of the double knockout SCID phenotype.

The previously reported single knockout SCID pig models each have one preserved lymphocyte lineage that develops to maturity. B cells are preserved in *IL2RG*$^{-/Y}$ pigs, although they do not produce antibodies, presumably due to the absence of T cell help (Suzuki et al., 2012; Watanabe et al., 2013). NK cells are preserved in *RAG2*$^{-/-}$ pigs (Lee et al., 2014). The *IL2RG*$^{-/Y}$ *RAG1*$^{-/-}$ SCID pigs successfully combine these characteristics to generate a large animal model deficient in functional lymphocytes from all three lineages. Like *IL2RG*$^{-/Y}$ pigs, *IL2RG*$^{-/Y}$ *RAG1*$^{-/-}$ pigs only show low-level expression of IgM, IgG, and IgA (Suzuki et al., 2012).

The antibodies that are detected in the double knockout animals are likely derived from colostrum prior to gut "closure," since the piglets were allowed to continue suckling from the sow for the duration of their lifespan (Nechvatalova et al., 2011). To prevent confounding from variable, sow-dependent maternal transfer of colostrum antibodies, high

levels of glucose can be fed to the newborn piglets to promote early gut closure and inhibit antibody transfer through the wall of the neonatal GI tract. Piglets can also be fed from birth on formula which contains predetermined concentrations of the different Ig isotypes.

The only notably persistent lymphocytes in *IL2RG*$^{-/Y}$ *RAG1*$^{-/-}$ SCID pigs is a small population of 74-22-15– CD3– CD45RA+ cells in the spleen (Fig. 10C); although these were putatively identified as B cells, IHC of the spleen from *IL2RG*$^{-/Y}$ *RAG1*$^{-/-}$ SCID pigs showed no staining with CD79a (Fig. 11B), a marker of the earliest stages of B cell commitment which even precedes rearrangement of the IgH locus (Chu and Arber, 2001). Furthermore, expression of IgM, IgG, and IgA is nearly absent in the *IL2RG*$^{-/Y}$ *RAG1*$^{-/-}$ SCID pigs (Fig. 12), indicating the absence of functional B cells. Based on these data, it is highly unlikely that the 74-22-15– CD3– CD45RA+ CD79a– population in the spleen represents B cells. An alternative explanation is that these cells are common lymphoid progenitors (CLPs), which stain negative for myeloid markers (Piriou-Guzylack and Salmon, 2008) but do express CD45RA (Blom and Spits, 2006). The persistence of CLPs is consistent with *RAG1* inactivation, as hematopoietic progenitors would be arrested at a developmental stage prior to RAG activation (and T versus B lineage commitment). It is unclear why CLPs would traffic to the spleen; in the absence of a functional thymus or lymph nodes in *IL2RG*$^{-/Y}$ *RAG1*$^{-/-}$ SCID pigs, it is possible that the spleen, as the only remnant secondary lymphoid organ, provides the primary source of lymphoid chemoattractant signals in these animals.

Table 6. Comparison of lymphocyte profiles from humanized mouse and pig models.
Humanized mouse data are summarized from Pearson et al. 2008, in which *NOD-Rag1^{null} IL2rγ^{null}* SCID mice were irradiated with 550 cGy prior to transplantation with 3 x 10^4 CD34+ human HSCs via lateral tail vein injection. Flow cytometry was then used to determine the percentage of lymphocytes in the peripheral blood and organs of transplanted *NOD-Rag1^{null} IL2rγ^{null}* SCID mice 90 days post transplantation. *IL2RG$^{-/Y}$ RAG1$^{-/-}$* pigs were injected with 7 x 10^6 CD34+ human HSCs *in utero* on gestational day 42 and assessed 72 days post-transplantation. Values shown for CD45+, total T cells, and B cells are percent of total leukocytes. Values shown for activated, naïve, DN, DP, CD4, and CD8 cells are percent of total T cells. Values shown from the humanized pig are the highest measured across all trials and time points.

XENOGENEIC TRANSPLANTATION

HUMAN TO MOUSE

NOD-*Rag1^{null} IL2rγ^{null}*

Organ/Tissue	CD45+	T Cells							B cells
		total	activated	naïve	DN	DP	CD4	CD8	
blood	9.50	5.40		85.20					58.70
spleen	37.70	2.90					65.10	46.20	60.60
thymus	18.50					58.90	5.30	5.70	
bone marrow	48.10								5.50

HUMAN TO PIG

IL2RG-/Y RAG1-/-

Organ/Tissue	CD45+	T Cells							B cells	*n*
		total	activated	naïve	DN	DP	CD4	CD8		
blood	15.10	15.10	79.46	20.54	0.46	91.50	4.27	4.10	9.30	4
spleen	11.20	6.87	55.14	44.86	9.86	11.00	42.40	36.70	13.50	4
thymus	22.50	24.30	59.86	40.14	1.61	87.50	4.66	6.27		4
bone marrow	43.70	38.20	83.50	13.70	1.80	82.00	30.70	2.53		4

Table 6 compares the lymphocyte profile of humanized *IL2RG$^{-/Y}$ RAG1$^{-/-}$* pigs generated by *in utero* transplantation to the profile from humanized NOD-*Rag1^{null} IL2rγ^{null}* mice generated by lateral tail vein injection (Pearson et al., 2008). In humanized *IL2RG$^{-/Y}$ RAG1$^{-/-}$* pigs, 15.1% of leukocytes were positive for the human pan-leukocyte marker, CD45, on postnatal day 72. This efficacy of repopulation with human leukocytes is comparable or slightly better than humanized NOD-*Rag1^{null} IL2rγ^{null}* mice, which contain 9.5% human CD45+ cells at 90 days post-transplant. Furthermore, humanized pigs were generated without

irradiation, while comparable humanized mice required preconditioning with 550 cGy of irradiation for engraftment.

The peripheral blood of humanized NOD-*Rag1*^{null} *IL2rγ*^{null} mice showed 5.4% human T cells, compared to 15.1% in humanized *IL2RG*$^{-/Y}$ *RAG1*$^{-/-}$ pigs. In humanized mice, 85.2% of the peripheral blood T cells are naïve, compared to 20.54% in humanized pigs. While Pearson et al. did not measure CD4+ and CD8+ T cell subsets in the peripheral blood of humanized mice, humanized *IL2RG*$^{-/Y}$ *RAG1*$^{-/-}$ pigs had detectable naïve, double positive, CD4+, and CD8+ peripheral blood T cells.

The spleens of NOD-*Rag1*^{null} *IL2rγ*^{null} mice showed a higher percentage of human CD45+ cells at 37.7% compared to the *IL2RG*$^{-/Y}$ *RAG1*$^{-/-}$ pigs, which had only 11.2%. However, only 2.9% of the human leukocytes were CD3+ positive in the humanized mice compared to 6.87% in the humanized pigs. In addition, the spleens of humanized *IL2RG*$^{-/Y}$ *RAG1*$^{-/-}$ pigs showed the development of double positive, double negative, and single positive human T cells, while these subsets were not fully evaluated in the humanized mouse model. Similar to the peripheral blood, in the spleen there was a larger population of human B cells in the NOD-*Rag1*^{null} *IL2rγ*^{null} mice at 60.6%, compared to 13.5% in the *IL2RG*$^{-/Y}$ *RAG1*$^{-/-}$ pigs. Engraftment in the bone marrow with human CD45+ cells was similar at 48.1% in NOD-*Rag1*^{null} *IL2rγ*^{null} mice and 43.7% in the *IL2RG*$^{-/Y}$ *RAG1*$^{-/-}$ pigs.

Overall, comparison of the T cell data between humanized mice and pigs is consistent with impaired maturation of human T cells in the mouse thymic remnant, while human T cells from humanized pigs show a more normal developmental progression, possibly because HSCs were transplanted *in utero*. Although irradiated NOD-*Rag1*^{null} *IL2rγ*^{null} mice showed

high levels of repopulation with human B cells in the peripheral blood, spleen, and bone marrow, the ability of these B cells to produce antibodies was not assessed. In contrast, my studies showed that human IgM is detectable in the plasma of humanized pigs, demonstrating that the human B cells in *IL2RG*$^{-/Y}$ *RAG1*$^{-/-}$ pigs are functional.

5.4. Predominance of activated T cells with a memory phenotype in SCID pigs after allogeneic transplantation and associated B cell dysfunction.

The most prominent result from the allogeneic transplantation experiments was the reconstitution of *IL2RG*$^{-/Y}$ *RAG1*$^{-/-}$ pigs with mostly CD45RA– CD4+ CD8+ T cells, indicative of an activated memory phenotype (Sinkora and Butler, 2009). Of note, while SCID pigs receiving allogeneic BMT showed a modest increase in thymic size (Fig. 27) and repopulation with CD3+ cells by IHC (Fig. 28), thymic architecture remained highly abnormal and is likely unable to support normal thymic T cell development. These findings are consistent with both human and mouse studies of T cell development following transplantation with hematopoietic cells. These studies describe the existence of an extrathymic development pathway for transplanted peripheral T cell precursors which rapidly differentiate to an activated, memory phenotype (Mackall et al., 1993; Williams et al., 2007). In the absence of an functional thymus, donor hematopoietic progenitors are activated upon peripheral encounter with antigen (Dulude et al., 1997). A comparison between athymic and thymic patients receiving BMT demonstrated that the thymus is necessary for the reconstitution of CD45RA+ naïve T helper cells (Heitger et al., 1997). In the 6 months after BMT in humans, preconditioning leads to severely impaired thymic function. During this 6 month window, the reconstituted T cells predominantly express a memory and effector

phenotype, with delayed recovery of CD45RA+ T cell expression until 6 months post-transplant (Dumont-Girard et al., 1998) (Fallen et al., 2003) (Sarzotti et al., 2003). Due to age-related decreases in thymic function for older patients receiving BMT, recovery of CD45RA+ T cells is substantially delayed with an increase in effector and memory T cells (Fallen et al., 2003; Roux et al., 2000). The extrathymic and classical intrathymic T cell differentiation pathways compete with one another due to limited supplies of growth factors (Mackall et al., 2001). The site of extrathymic T cell differentiation remains unclear; the liver has been identified as one of these sites in mice (Sato et al., 1995), with hepatically-matured, transplanted T cells bearing a high proportion of autoreactive clones, due to the absence of normal thymic stroma for negative selection.

Based on these studies from humans and mice, the large populations of activated, memory T cells seen in SCID pigs after allogeneic BMT most likely represent the products of extrathymic differentiation of T cell precursors due to the absence of a functional thymus. Evaluation of this model can be pursued by comparing T cell reconstitution in SCID pigs with and without transplanted porcine thymic tissue. This model would predict that implantation of porcine thymic tissue into SCID pigs would rescue production of CD45RA+ naïve T cells and outcompete the extrathymic development pathway.

Despite strong reconstitution of peripheral blood B cells after allogeneic BMT in non-irradiated animals, the B cells fail to traffic to the spleen (Fig. 25C), indicative of B cell dysfunction. Splenic B cells do repopulate after allogeneic BMT in irradiated animals (Fig. 25D), possibly in response to radiation-induced inflammation, however irradiated pigs showed no rescue of plasma immunoglobulins. A major reason for the observed B cell

dysfunction is the dependence of normal B cell function on T cell help (Allen et al., 2007; Garside, 1998; Okada et al., 2005), which is absent due to lack of normal thymic T cell development as described above. I also speculate that the encounter of transplanted B cells with alloantigens in the absence of costimulatory signals from T cell help renders them anergic and prevents normal trafficking to the spleen.

NK cell repopulation was relatively poor in all tissues examined (Figs. 21, 22, 32), however this is consistent with other studies showing limited human NK cell repopulation after (albeit, xenogeneic) BMT in SCID mice (André et al., 2010; Strowig et al., 2010), which has been attributed to the absence of IL-15 signaling due to mutation of *IL2RG*. Expression of IL-15/IL-15Rα complexes or exogenous IL-15 has been shown to improve NK cell reconstitution, and a similar approach would likely also work in the SCID pig model (Huntington et al., 2009; Pek et al., 2011).

It is not apparent why allogeneic BMT results in relatively low levels of lymphocyte reconstitution in the SCID pig bone marrow. The dominance of extrathymic T cell differentiation may divert T cells from bone marrow to peripheral sites. The putative B cell dysfunction posited above may also prevent normal B cell trafficking into the bone marrow. One caveat is that my study did not directly examine the engraftment of porcine hematopoietic stem cells in the bone marrow. This could be accomplished by staining bone marrow aspirates from transplanted SCID pigs for porcine hematopoietic progenitor cell surface markers, particularly CD34 (Le Guern et al., 2003; Heinz et al., 2002; Layton et al., 2007).

5.5. Comparison of transplantation methods.

Multiple factors were evaluated when comparing transplantation protocols, particularly the efficacy of lymphocyte repopulation, toxicity of the conditioning regimen, morbidity of the transplantation procedure, and costs/resources necessary to maintain the transplanted animals. Intraosseous transplantation was superior to intravenous delivery (Fig. 16F) (Fig. 22B), likely due to the direct delivery of donor progenitor cells into the appropriate microenvironmental niche in the bone marrow to support hematopoiesis. For allogeneic transplantation, irradiation led to earlier repopulation with T and B cells, possibly due to the radioablative effect on the bone marrow to make more "niches" available for hematopoietic progenitor cell engraftment. An additional explanation is that the early expansion of T and B cells (and B cell trafficking to the spleen) was a transient response to radiation-induced tissue inflammation. This is supported by the eventual contraction of the activated CD45RA– T cell population, which is consistent with resolution of an acute immune response. By postnatal day 42, however, T and B cell reconstitution in the peripheral blood of irradiated SCID piglets was inferior to age-matched littermates who were not irradiated (Figs. 19 and 20). This was potentially due to the toxicity of total body irradiation, as these animals had almost no viable cells in their bone marrow, were persistently sick and refractory to antibiotics, and required significant amounts of care and resources to maintain. Based on the lower efficacy of sustained lymphocyte reconstitution and the toxicity of the protocol, irradiation is not recommended to condition SCID pigs for transplantation.

The experiments in Chapter 4 clearly demonstrated that *in utero* intrahepatic transplantation was superior to postnatal intraosseous transplantation for the engraftment of

human cells in SCID pigs (Fig. 43). The likely primary reason for this is that *in utero* intrahepatic injection on DG40 directly delivers human CD34+ progenitor cells to the primary site of hematopoiesis, the fetal liver (Sinkora and Butler, 2009), thereby increasing the chance that the human HSCs will engraft in a favorable microenvironment. Prior studies of *in utero* BMT in immunocompetent pigs demonstrated successful, low level engraftment of human hematopoietic cells (Fujiki et al., 2003). The limitations of *in utero* transplantation include the requirements for a large animal surgical suite with general anesthesia capability, veterinary personnel with the technical expertise to perform ultrasound-guided *in utero* injections, and the need for two surgeries separated by only 42 days, allowing minimal intervening time for healing – the first for delivery of the SCNT embryos, and the second for *in utero* intrahepatic transplantation. Despite these limitations, *in utero* transplantation is, at present, the only effective method to generate humanized pigs.

5.6. Characterization and future investigations of human lymphocytes in humanized pigs.

The experiments in Chapter 4 are consistent with human T cell development in the thymus of SCID pigs transplanted *in utero* with CD34+ human bone marrow cells. The human T cells are predominantly CD45RA+, suggesting that they have undergone normal thymic development. In support of this, only DP T cells are found in the periphery while SP T cells are found in the blood and spleen, supporting a model where completion of the DP to SP T cell transition leads to egress of SP human T cells from the thymus into the periphery. These findings are in accord with studies that show (relatively) normal human T cell development is supported by fetal pig thymus tissue implanted into SCID mice (Kalscheuer

et al., 2014). The ability of the pig thymus to support human T cell development has been attributed to the similarity between the structure of human HLA and porcine SLA molecules, such that human TCRs can bind productively to swine SLAs in the pig thymus for positive and negative selection (Shimizu et al., 2008).

The DP T cells present in the peripheral blood likely represent human T cells that have not yet undergone the DP to SP transition. Their continued circulation in the periphery may represent the absence of available space in the SCID pig thymus, which is diminished relative to WT animals. Alternatively, there may be inadequate cross-talk between porcine chemokines and human chemokine receptors to fully recruit all the DP human T cells from the peripheral blood to their appropriate home in the thymus. Interestingly, in the bone marrow of humanized pigs there is a large population of DP human T cells, a smaller population of CD4+ SP cells, and a nearly even mixture of CD45RA– and CD45RA+ cells. I speculate that the DP T cells in the marrow represent developing T cells awaiting entry into the thymus for maturation to SP cells, similar to the DP T cell population in the peripheral blood. The reason for the selective presence of CD4+ SP T cells in the marrow is unclear, however it is possible the bone marrow provides a favorable site for the provision of T cell help. Over time, the CD45RA+ T cell population in the marrow decreases while the CD45RA– population increases, consistent with depletion and maturation of the developing DP T cell progenitor pool and the accumulation of activated T cells, possibly performing T helper functions in this compartment.

For *in utero* transplanted SCID pigs, human T cells in the peripheral blood were lost after postnatal day 3 and were not subsequently detected. This is consistent with observations

of T cell dynamics in humanized mice, where there is an initial transient burst of T cell production and thymic maturation, then disappearance from the peripheral blood as the mature T cells traffic to secondary lymphoid organs. The T cells in humanized mice do not reappear until the 6th week of postnatal life (Rongvaux et al., 2013). Maintaining humanized pigs for longer periods with serial evaluation of PBMCs will be necessary to evaluate whether human T cell dynamics follow a similar course in the SCID pig.

Several characteristics of the engrafted human T cell repertoire in humanized pigs remain to be characterized. The accumulation of T cell receptor excision circles (TRECs) in the peripheral blood can be used as a surrogate marker of the development of naïve T cells as they under TCR gene rearrangement (Ogle et al., 2009). TCR diversity can be assessed by evaluating the usage frequency of V gene segments in conjunction with sequencing of the recombined TCR gene repertoire (Shimizu et al., 2008). In SCID mice, the human T cells that develop in the implanted fetal pig thymus can develop into all major T cell subsets, including T regulatory (Treg) cells, and exhibit donor-specific tolerance for both human donor (HLA-matched) and swine donor (SLA-matched) antigens (Kalscheuer et al., 2012). Evaluating the balance of human Th1 and Th2 cells, as well as for the presence and function of human Treg cells will help elucidate how accurately the humanized pig recapitulates human immune function. Human T cells in humanized pigs would be predicted to be tolerant of cells derived from the human bone marrow donor and the recipient pig, and reactive against non-donor human cells and allogeneic pig cells. The tolerance profile can be evaluated by use of a mixed lymphocyte reaction or CFSE dilution/proliferation assay, and potentially provide support for the normal functionality of the engrafted human T cells.

I speculate that the development of the human T cell repertoire in SCID pigs was made possible by partial restoration of thymic function from *in utero* human HSC transplantation during lymphopoiesis. It follows that the failure of significant human cell engraftment after intraosseous transplantation may largely be due to the absence of a functional thymus. Evidence from my allogeneic transplantation experiments as well as data from human and mouse BMT experiments (Williams et al., 2007) suggests that the presence of functional thymic tissue can rescue normal thymic T cell development. Implantation of SCID pigs with human fetal thymic tissue may be sufficient to rescue human T cell development following intraosseous transplantation, and would likely bolster reconstitution following *in utero* transplantation as well. A provocative extension of those experiments would be to compare how implantation of SCID pigs with either a pig thymus or a human thymus affects the development of the human T cell repertoire. If the T cell repertoires are similar in phenotype and function, as has been observed in SCID mice bearing pig thymus tissue (Kalscheuer et al., 2014; Shimizu et al., 2008), implanted fetal pig thymus (which is more readily available than human tissue) may be sufficient to support human T cell development.

My studies of B cells in the humanized pig indicate robust repopulation of the peripheral blood and spleen (Figs. 46 and 48). The presence of human IgM in the plasma of humanized pigs implies that at least a subset of these B cells are functional and, in turn, that they are likely engaging in productive interactions with human T helper cells (Fig. 53). These findings are similar to humanized mice, where human B cells are detected at high frequency (Rongvaux et al., 2013), however they exhibit abnormal characteristics and function,

including impaired class switch recombination, low levels of IgG with only IgM responses to vaccination (Ishikawa et al., 2005; Traggiai et al., 2004), a broad BCR repertoire but no somatic hypermutation, and a high frequency of autoreactive B cells (Becker et al., 2010; Chang et al., 2012). These defects are attributable, in part, to the absence of human MHC II molecules, and can be partially rescued by implantation of human fetal thymic and liver tissue DCs (Kalscheuer et al., 2012; Lan et al., 2006; Melkus et al., 2006) or transgenic expression of human MHC II molecules (Danner et al., 2011). Immediate future experiments to address B cell function in humanized pigs would include ELISAs for other human Ig isotypes, studies of BCR gene sequence diversity, and assessment of responses to vaccines for which there are commercially available kits to measure serum antibody responses, such as measles.

Further characterization of the humanized pig would include evaluation of human NK cell and myeloid cell engraftment. NK cell engraftment is historically poor in humanized mice with knockout of *IL2RG* due to the loss of IL-15 signaling (André et al., 2010; Strowig et al., 2010). Finally, direct assessment of human CD34+ hematopoietic progenitor cells by bone marrow aspirate and biopsy will assist with evaluating the efficacy of human cell engraftment.

5.7. Strategies for improving human cell engraftment in SCID pigs.

A multitude of approaches has been explored to improve human cell engraftment in SCID mice, and with the availability of tools for rapid production of genetically modified swine, many of the same approaches can be applied to improve the fidelity of the humanized pig model. These include the following:

(1) Implantation of human fetal liver or thymic tissue into SCID pigs. In SCID mice, this approach is known as the BLT model, and successfully supports the development of human T cells, B cells, monocytes, macrophages, and dendritic cells (Kalscheuer et al., 2012; Lan et al., 2006; Melkus et al., 2006). However, for the reasons discussed above, implantation of fetal pig thymus may be sufficient to accomplish the same effect using a more readily available tissue source. Alternatively, lymphoid tissue inducer (LTi) cells can be transplanted from WT pigs to SCID pigs to support the development of lymphoid organs (especially the thymus, lymph nodes, and Peyer's patches) and thereby promote the development and expansion of transplanted lymphocytes.

(2) Exogenous administration or transgenic expression of human cytokines (Chen et al., 2009). Ideally, this would be accomplished via knock-in replacement of the pig cytokine with the human cytokine at the endogenous locus (Willinger et al., 2011). This has proven effective in humanized mice which transgenically express thrombopoietin, which is important for the maintenance of the human hematopoietic stem cell niche (Fox et al., 2002; Qian et al., 2007). The complement of this approach would be to produce non-lethal knockouts of genes encoding porcine growth factors.

(3) Suppress host innate immunity. Porcine recipient macrophages, dendritic cells, and granulocytes can impair engraftment. Ablation of this lineages can be accomplished (a) pharmacologically, using drugs like clodronate, (b) by depletion via lineage-specific monoclonal antibodies, or (c) genetically by inducible or tissue-specific promoters that regulate the production of a toxic protein, such as diphtheria toxin (Shultz et al., 2007).

(4) Inhibit phagocytosis by innate immune cells. In humanized mice, donor human T and NK cell engraftment is impaired because both cell populations are susceptible to phagocytosis. Furthermore, interaction with recipient phagocytes leads to spurious T cell activation (Strowig et al., 2011). These effects were mediated by SIRPα on recipient phagocytes (Strowig et al., 2011), and were inhibited by expressing mouse CD47 in transplanted human HSCs.

(5) Implant synthetic lymphoid-like organoids to replace absent lymph nodes and Peyer's patches (Suematsu and Watanabe, 2004).

(6) Improve the hematopoietic niche by implanting a human marrow-containing bone fragment in which the human CD34+ donor cells can engraft (Rongvaux et al., 2013).

(7) Humanize the swine MHC I and MHC II loci by knock-in replacement with HLAs (Danner et al., 2011).

5.8. Experimental challenges and limitations in working with SCID pigs.

Some limitations of the studies with SCID pigs relate to practical challenges in maintaining and experimenting with immunodeficient large animals. Wild type controls were age-matched, rather than litter-matched due to constraints with breeding and the need to optimize the chances of bringing the SCID pig pregnancies to term. Maintaining a germ-free environment to raise pigs is practically very challenging and resource-intensive. The IL2RG-/Y RAG1-/- pigs in this study were housed in a non-sterile environment, and succumbed to bacterial sepsis within 4 weeks, including severe infection with the commensal organism, Staphylococcus hyicus. These infections limited the ability to perform long-term studies on non-transplanted SCID pigs. To optimally support the nutrition of the piglets, they were fed

on colostrum for the duration of their lifespan. This partially limits the ability to ascribe differences in serum Ig levels solely to differences in B cell-mediated production, as it is not possible to formally eliminate differences in the feeding fitness of WT, IL2RG$^{-/Y}$ RAG1$^{+/-}$, and IL2RG$^{-/Y}$ RAG1$^{-/-}$ pigs and increased access to colostrum following the death of littermates as possible contributing factors.

5.9. Biomedical applications of humanized pigs, with a focus on human liver transplantation.

The potential biomedical applications of humanized pigs are numerous. With the similarities in size and physiology to humans, and now with the engraftment of a human immune system, humanized pigs offer a power predictive model to study human disease and novel therapeutics. They offer the opportunity to evaluate the human immune responses to infections that have tropism for both species (Ramer et al., 2011), and the durability of human immunity to vaccines, due to their long lifespan. The mechanisms of autoimmune diseases can be studied *in vivo* by adoptive transfer of PBMCs from patients with these conditions, as has been done in humanized mice for systemic lupus erythematosus (Andrade et al., 2011) and type 1 diabetes (Unger et al., 2012). SCID pigs can be used to study the development of xenografted human solid and liquid tumors, with humanized pigs as a model to study anti-tumor immune responses (Aspord et al., 2007; Hope et al., 2004). Humanized pigs also offer a potential source of hematopoietic cells that can be used for autologous transplantation and adoptive T cell based immunotherapy (Ogle et al., 2009), and have even been proposed as a means to tolerize human patients for xenotransplantation (Lan et al., 2004; Starzl and Demetris, 1997).

The Piedrahita Laboratory has a special interest in utilizing humanized pigs to support the growth of human livers for transplantation. SCID mice can bearing "humanized" liver recapitulate human-type metabolic responses to drugs, have global gene expression profiles similar to mature human hepatocytes, and maintained high metabolic activity for up to 8 months (Sanoh et al., 2012; Suemizu et al., 2008; Tateno et al., 2004). The proposed approach in humanized pigs relies on the engrafted human immune system facilitating tolerance of the pig to intrahepatic transplantation with human hepatocytes. Endogenous porcine liver tissue can be gradually removed by inducible, liver-specific expression of a transgene that induces apoptosis. Human hepatocytes would be harvested from the patient awaiting transplant, then engrafted into humanized pigs where the human hepatocytes would regenerate to fill the vacated space, producing a chimeric pig-human liver. Once the human component of the graft is large enough, it can be harvested for transplantation into a human patient. The pig offers clear advantages for human transplantation, as the size of the pig liver closely approximates that of a human. There is promising data from a recent study showing successful human hepatocyte engraftment and synthetic function from an immunocompetent pig (Fisher et al., 2013). Engraftment should be even more robust in a humanized or SCID pig.

There is as urgent need for bringing this research to fruition; as of this writing, nearly 16,000 people in the USA are awaiting a liver transplant, while only 6,000 liver transplants occur per year, with 1,500 people dying annually waiting for a donor liver (ALF, 2013). My hope is that the generation of the humanized pig described in this thesis will lay the groundwork for closing, and someday erasing, that organ shortage.

REFERENCES

Aigner, B., Renner, S., Kessler, B., Klymiuk, N., Kurome, M., Wünsch, A., and Wolf, E. (2010). Transgenic pigs as models for translational biomedical research. J. Mol. Med. *88*, 653–664.

ALF, A.L.F. (2013). More About Organ Donation.

Allen, C.D.C., Okada, T., and Cyster, J.G. (2007). Germinal-center organization and cellular dynamics. Immunity *27*, 190–202.

Andrade, D., Redecha, P.B., Vukelic, M., Qing, X., Perino, G., Salmon, J.E., and Koo, G.C. (2011). Engraftment of peripheral blood mononuclear cells from systemic lupus erythematosus and antiphospholipid syndrome patient donors into BALB-RAG-2 -/-IL-2R??-/- mice: A promising model for studying human disease. Arthritis Rheum. *63*, 2764–2773.

André, M.C., Erbacher, A., Gille, C., Schmauke, V., Goecke, B., Hohberger, A., Mang, P., Wilhelm, A., Mueller, I., Herr, W., et al. (2010). Long-term human CD34+ stem cell-engrafted nonobese diabetic/SCID/IL-2R gamma(null) mice show impaired CD8+ T cell maintenance and a functional arrest of immature NK cells. J. Immunol. *185*, 2710–2720.

Aspord, C., Pedroza-Gonzalez, A., Gallegos, M., Tindle, S., Burton, E.C., Su, D., Marches, F., Banchereau, J., and Palucka, A.K. (2007). Breast cancer instructs dendritic cells to prime interleukin 13-secreting CD4+ T cells that facilitate tumor development. J. Exp. Med. *204*, 1037–1047.

Barman, N.N., Bianchi, A.T.J., Zwart, R.J., Pabst, R., and Rothkötter, H.J. (1997). Jejunal and ileal Peyer's patches in pigs differ in their postnatal development. Anat. Embryol. (Berl). *195*, 41–50.

Basel, M.T., Balivada, S., Beck, A.P., Kerrigan, M. a, Pyle, M.M., Dekkers, J.C.M., Wyatt, C.R., Rowland, R.R.R., Anderson, D.E., Bossmann, S.H., et al. (2012). Human xenografts are not rejected in a naturally occurring immunodeficient porcine line: a human tumor model in pigs. Biores. Open Access *1*, 63–68.

Bassing, C.H., Swat, W., and Alt, F.W. (2002). The mechanism and regulation of chromosomal V(D)J recombination. Cell *109*.

Becker, P.D., Legrand, N., van Geelen, C.M.M., Noerder, M., Huntington, N.D., Lim, A., Yasuda, E., Diehl, S.A., Scheeren, F.A., Ott, M., et al. (2010). Generation of human antigen-specific monoclonal IgM antibodies using vaccinated "human immune system" mice. PLoS One *5*.

Betthauser, J., Forsberg, E., Augenstein, M., Childs, L., Eilertsen, K., Enos, J., Forsythe, T., Golueke, P., Jurgella, G., Koppang, R., et al. (2000). Production of cloned pigs from in vitro systems. Nat. Biotechnol. *18*, 1055–1059.

Blom, B., and Spits, H. (2006). Development of human lymphoid cells. Annu. Rev. Immunol. *24*, 287–320.

Boch, J., Scholze, H., Schornack, S., Landgraf, A., Hahn, S., Kay, S., Lahaye, T., Nickstadt, A., and Bonas, U. (2009). Breaking the code of DNA binding specificity of TAL-type III effectors. Science *326*, 1509–1512.

Bogdanove, A.J., and Voytas, D.F. (2011). TAL Effectors: Customizable Proteins for DNA Targeting. Science (80-.). *333*, 1843–1846.

Bosma, G.C., Custer, R.P., and Bosma, M.J. (1983). A severe combined immunodeficiency mutation in the mouse. Nature *301*, 527–530.

Butler, J.E., Lager, K.M., Splichal, I., Francis, D., Kacskovics, I., Sinkora, M., Wertz, N., Sun, J., Zhao, Y., Brown, W.R., et al. (2009). The piglet as a model for B cell and immune system development. Vet. Immunol. Immunopathol. *128*, 147–170.

Cao, X., Shores, E.W., Hu-Li, J., Anver, M.R., Kelsall, B.L., Russell, S.M., Drago, J., Noguchi, M., Grinberg, A., and Bloom, E.T. (1995). Defective lymphoid development in mice lacking expression of the common cytokine receptor gamma chain. Immunity *2*, 223–238.

Carlson, D.F., Tan, W., Lillico, S.G., Stverakova, D., Proudfoot, C., Christian, M., Voytas, D.F., Long, C.R., Whitelaw, C.B. a, and Fahrenkrug, S.C. (2012). Efficient TALEN-mediated gene knockout in livestock. Proc. Natl. Acad. Sci. U. S. A. *109*, 17382–17387.

Carroll, D. (2014). Genome engineering with targetable nucleases. Annu. Rev. Biochem. *83*, 409–439.

Chang, H., Biswas, S., Tallarico, A.S., Sarkis, P.T.N., Geng, S., Panditrao, M.M., Zhu, Q., and Marasco, W.A. (2012). Human B-cell ontogeny in humanized NOD/SCID γcnull mice generates a diverse yet auto/poly- and HIV-1-reactive antibody repertoire. Genes Immun. *13*, 399–410.

Chardon, P., Rogel-Gaillard, C., Cattolico, L., Duprat, S., Vaiman, M., and Renard, C. (2001). Sequence of the swine major histocompatibility complex region containing all non-classical class I genes. Tissue Antigens *57*, 55–65.

Charerntantanakul, W., and Roth, J. a (2007). Biology of porcine T lymphocytes. Anim. Health Res. Rev. *7*, 81–96.

Chen, Q., Khoury, M., and Chen, J. (2009). Expression of human cytokines dramatically improves reconstitution of specific human-blood lineage cells in humanized mice. Proc. Natl. Acad. Sci. U. S. A. *106*, 21783–21788.

Christianson, S.W., Greiner, D.L., Schweitzer, I.B., Gott, B., Beamer, G.L., Schweitzer, P.A., Hesselton, R.M., and Shultz, L.D. (1996). Role of natural killer cells on engraftment of human lymphoid cells and on metastasis of human T-lymphoblastoid leukemia cells in C57BL/6J-scid mice and in C57BL/6J-scid bg mice. Cell. Immunol. *171*, 186–199.

Chu, P., and Arber, D. (2001). CD79: a review. Appl. Immunohistochem. Mol. … *9*, 97–106.

Danner, R., Chaudhari, S.N., Rosenberger, J., Surls, J., Richie, T.L., Brumeanu, T.D., and Casares, S. (2011). Expression of HLA class II molecules in humanized NOD.Rag1KO.IL2RgcKO mice is critical for development and function of human T and B cells. PLoS One *6*, e19826.

Dawson, H. (2011). A comparative assessment of the pig, mouse, and human genomes: structural and functional analysis of genes involved in immunity and inflammation. In The Minipig in Biomedical Research, P. McNulty, ed. (CRC Press, Taylor & Francis Group), pp. 321–341.

DiSanto, J.P., Müller, W., Guy-Grand, D., Fischer, A., and Rajewsky, K. (1995). Lymphoid development in mice with a targeted deletion of the interleukin 2 receptor gamma chain. Proc. Natl. Acad. Sci. U. S. A. *92*, 377–381.

Dulude, G., Brochu, S., Fontaine, P., Baron, C., Gyger, M., Roy, D.C., and Perreault, C. (1997). Thymic and extrathymic differentiation and expansion of T lymphocytes following bone marrow transplantation in irradiated recipients. Exp. Hematol. *25*, 992–1004.

Dumont-Girard, F., Roux, E., van Lier, R.A., Hale, G., Helg, C., Chapuis, B., Starobinski, M., and Roosnek, E. (1998). Reconstitution of the T-cell compartment after bone marrow transplantation: restoration of the repertoire by thymic emigrants. Blood *92*, 4464–4471.

Fairbairn, L., Kapetanovic, R., Sester, D.P., and Hume, D.A. (2011). The mononuclear phagocyte system of the pig as a model for understanding human innate immunity and disease. J. Leukoc. Biol. *89*, 855–871.

Faldyna, M., Samankova, P., Leva, L., Cerny, J., Oujezdska, J., Rehakova, Z., and Sinkora, J. (2007). Cross-reactive anti-human monoclonal antibodies as a tool for B-cell identification in dogs and pigs. Vet. Immunol. Immunopathol. *119*, 56–62.

Fallen, P.R., McGreavey, L., Madrigal, J.A., Potter, M., Ethell, M., Prentice, H.G., Guimarães, A., and Travers, P.J. (2003). Factors affecting reconstitution of the T cell compartment in allogeneic haematopoietic cell transplant recipients. Bone Marrow Transplant. *32*, 1001–1014.

Fisher, J.E., Lillegard, J.B., McKenzie, T.J., Rodysill, B.R., Wettstein, P.J., and Nyberg, S.L. (2013). In utero transplanted human hepatocytes allow postnatal engraftment of human hepatocytes in pigs. Liver Transpl. *19*, 328–335.

Fox, N., Priestley, G., Papayannopoulou, T., and Kaushansky, K. (2002). Thrombopoietin expands hematopoietic stem cells after transplantation. J. Clin. Invest. *110*, 389–394.

Fujiki, Y., Fukawa, K., Kameyama, K., Kudo, O., Onodera, M., Nakamura, Y., Yagami, K., Shiina, Y., Hamada, H., Shibuya, A., et al. (2003). Successful multilineage engraftment of human cord blood cells in pigs after in utero transplantation. Transplantation *75*, 916–922.

Garside, P. (1998). Visualization of Specific B and T Lymphocyte Interactions in the Lymph Node. Science (80-.). *281*, 96–99.

Gerner, W., Käser, T., and Saalmüller, A. (2009). Porcine T lymphocytes and NK cells--an update. Dev. Comp. Immunol. *33*, 310–320.

Groenen, M. a M., Archibald, A.L., Uenishi, H., Tuggle, C.K., Takeuchi, Y., Rothschild, M.F., Rogel-Gaillard, C., Park, C., Milan, D., Megens, H.-J., et al. (2012). Analyses of pig genomes provide insight into porcine demography and evolution. Nature *491*, 393–398.

Le Guern, A.C., Giovino, M.A., Abe, M., Theodore, P.R., Qi, J., Down, J.D., Sachs, D.H., Sykes, M., and Yang, Y.G. (2003). Stem cell activity of porcine c-kit+ hematopoietic cells. Exp. Hematol. *31*, 833–840.

Gustafsson, K., Germana, S., Hirsch, F., Pratt, K., LeGuern, C., and Sachs, D.H. (1990a). Structure of miniature swine class II DRB genes: conservation of hypervariable amino acid residues between distantly related mammalian species. Proc. Natl. Acad. Sci. U. S. A. *87*, 9798–9802.

Gustafsson, K., LeGuern, C., Hirsch, F., Germana, S., Pratt, K., and Sachs, D.H. (1990b). Class II genes of miniature swine. IV. Characterization and expression of two allelic class II DQB cDNA clones. J. Immunol. *145*, 1946–1951.

Habiro, K., Sykes, M., and Yang, Y.-G. (2009). Induction of human T-cell tolerance to pig xenoantigens via thymus transplantation in mice with an established human immune system. Am. J. Transplant *9*, 1324–1329.

Hao, Y.H., Yong, H.Y., Murphy, C.N., Wax, D., Samuel, M., Rieke, A., Lai, L., Liu, Z., Durtschi, D.C., Welbern, V.R., et al. (2006). Production of endothelial nitric oxide synthase (eNOS) over-expressing piglets. Transgenic Res. *15*, 739–750.

Hart, E.A., Caccamo, M., Harrow, J.L., Humphray, S.J., Gilbert, J.G.R., Trevanion, S., Hubbard, T., Rogers, J., and Rothschild, M.F. (2007). Lessons learned from the initial sequencing of the pig genome: comparative analysis of an 8 Mb region of pig chromosome 17. Genome Biol. *8*, R168.

Hauschild, J., Petersen, B., Santiago, Y., Queisser, A.-L., Carnwath, J.W., Lucas-Hahn, A., Zhang, L., Meng, X., Gregory, P.D., Schwinzer, R., et al. (2011). Efficient generation of a biallelic knockout in pigs using zinc-finger nucleases. Proc. Natl. Acad. Sci. U. S. A. *108*, 12013–12017.

Heinz, M., Huang, C.A., Emery, D.W., Giovino, M.A., LeGuern, A., Kurilla-Mahon, B., Theodore, P., Arn, J.S., Sykes, M., Mulligan, R., et al. (2002). Use of CD9 expression to enrich for porcine hematopoietic progenitors. Exp. Hematol. *30*, 809–815.

Heitger, A., Neu, N., Kern, H., Panzer-Grümayer, E.R., Greinix, H., Nachbaur, D., Niederwieser, D., and Fink, F.M. (1997). Essential role of the thymus to reconstitute naive (CD45RA+) T-helper cells after human allogeneic bone marrow transplantation.

Hermiston, M.L., Xu, Z., and Weiss, A. (2003). CD45: a critical regulator of signaling thresholds in immune cells. Annu. Rev. Immunol. *21*, 107–137.

Hesselton, R.M., Greiner, D.L., Mordes, J.P., Rajan, T. V, Sullivan, J.L., and Shultz, L.D. (1995). High levels of human peripheral blood mononuclear cell engraftment and enhanced susceptibility to human immunodeficiency virus type 1 infection in NOD/LtSz-scid/scid mice. J. Infect. Dis. *172*, 974–982.

Ho, C.S., Lunney, J.K., Lee, J.H., Franzo-Romain, M.H., Martens, G.W., Rowland, R.R.R., and Smith, D.M. (2010). Molecular characterization of swine leucocyte antigen class II genes in outbred pig populations. Anim. Genet. *41*, 428–432.

Hope, K.J., Jin, L., and Dick, J.E. (2004). Acute myeloid leukemia originates from a hierarchy of leukemic stem cell classes that differ in self-renewal capacity. Nat. Immunol. *5*, 738–743.

Huang, J., Guo, X., Fan, N., Song, J., Zhao, B., Ouyang, Z., Liu, Z., Zhao, Y., Yan, Q., Yi, X., et al. (2014). RAG1/2 Knockout Pigs with Severe Combined Immunodeficiency. J. Immunol. *193*, 1496–1503.

Huntington, N.D., Legrand, N., Alves, N.L., Jaron, B., Weijer, K., Plet, A., Corcuff, E., Mortier, E., Jacques, Y., Spits, H., et al. (2009). IL-15 trans-presentation promotes human NK cell development and differentiation in vivo. J. Exp. Med. *206*, 25–34.

Ishikawa, F., Yasukawa, M., Lyons, B., Yoshida, S., Miyamoto, T., Yoshimoto, G., Watanabe, T., Akashi, K., Shultz, L.D., and Harada, M. (2005). Development of functional human blood and immune systems in NOD/SCID/IL2 receptor {gamma} chain(null) mice. Blood *106*, 1565–1573.

Ito, M., Hiramatsu, H., Kobayashi, K., Suzue, K., Kawahata, M., Hioki, K., Ueyama, Y., Koyanagi, Y., Sugamura, K., Tsuji, K., et al. (2002). NOD/SCID/gamma(c)(null) mouse: an excellent recipient mouse model for engraftment of human cells. Blood *100*, 3175–3182.

Jørgensen, F.G., Hobolth, A., Hornshøj, H., Bendixen, C., Fredholm, M., and Schierup, M.H. (2005). Comparative analysis of protein coding sequences from human, mouse and the domesticated pig. BMC Biol. *3*, 2.

Joung, J.K., and Sander, J.D. (2013). TALENs: a widely applicable technology for targeted genome editing. Nat. Rev. Mol. Cell Biol. *14*, 49–55.

Kalscheuer, H., Danzl, N., Onoe, T., Faust, T., Winchester, R., Goland, R., Greenberg, E., Spitzer, T.R., Savage, D.G., Tahara, H., et al. (2012). A model for personalized in vivo analysis of human immune responsiveness. Sci. Transl. Med. *4*, 125ra30.

Kalscheuer, H., Onoe, T., Dahmani, A., Li, H.-W., Hölzl, M., Yamada, K., and Sykes, M. (2014). Xenograft tolerance and immune function of human T cells developing in pig thymus xenografts. J. Immunol. *192*, 3442–3450.

Käser, T., Gerner, W., and Saalmüller, A. (2011). Porcine regulatory T cells: Mechanisms and T-cell targets of suppression. Dev. Comp. Immunol. *35*.

Kim, Y.G., and Chandrasegaran, S. (1994). Chimeric restriction endonuclease. Proc. Natl. Acad. Sci. U. S. A. *91*, 883–887.

Kim, Y.G., Cha, J., and Chandrasegaran, S. (1996). Hybrid restriction enzymes: zinc finger fusions to Fok I cleavage domain. Proc. Natl. Acad. Sci. U. S. A. *93*, 1156–1160.

Kiros, T.G., van Kessel, J., Babiuk, L.A., and Gerdts, V. (2011). Induction, regulation and physiological role of IL-17 secreting helper T-cells isolated from PBMC, thymus, and lung lymphocytes of young pigs. Vet. Immunol. Immunopathol. *144*, 448–454.

Kömüves, L.G., and Heath, J.P. (1992). Uptake of maternal immunoglobulins in the enterocytes of suckling piglets: improved detection with a streptavidin-biotin bridge gold technique. J. Histochem. Cytochem. *40*, 1637–1646.

Kraft, T.W., Allen, D., Petters, R.M., Hao, Y., Peng, Y.-W., and Wong, F. (2005). Altered light responses of single rod photoreceptors in transgenic pigs expressing P347L or P347S rhodopsin. Mol. Vis. *11*, 1246–1256.

Kragh, P.M., Nielsen, A.L., Li, J., du, Y., Lin, L., Schmidt, M., Bøgh, I.B., Holm, I.E., Jakobsen, J.E., Johansen, M.G., et al. (2009). Hemizygous minipigs produced by random gene insertion and handmade cloning express the Alzheimer's disease-causing dominant mutation APPsw. Transgenic Res. *18*, 545–558.

Kurome, M., Geistlinger, L., Kessler, B., Zakhartchenko, V., Klymiuk, N., Wuensch, A., Richter, A., Baehr, A., Kraehe, K., Burkhardt, K., et al. (2013). Factors influencing the efficiency of generating genetically engineered pigs by nuclear transfer: multi-factorial analysis of a large data set. BMC Biotechnol. *13*, 43.

L'Ecuyer, C. (1966). Exudative epidermitis in pigs. Clinical studies and preliminary transmission trials. Can. J. Comp. Med. Vet. Sci. *30*, 9–16.

L'Ecuyer, C., and Jericho, K. (1966). Exudative epidermitis in pigs: etiological studies and pathology. Can. J. Comp. Med. Vet. Sci. *30*, 94–101.

Lan, P., Wang, L., Diouf, B., Eguchi, H., Su, H., Bronson, R., Sachs, D.H., Sykes, M., and Yang, Y.G. (2004). Induction of human T-cell tolerance to porcine xenoantigens through mixed hematopoietic chimerism. Blood *103*, 3964–3969.

Lan, P., Tonomura, N., Shimizu, A., Wang, S., and Yang, Y.-G. (2006). Reconstitution of a functional human immune system in immunodeficient mice through combined human fetal thymus/liver and CD34+ cell transplantation. Blood *108*, 487–492.

Lapidot, T., Pflumio, F., Doedens, M., Murdoch, B., Williams, D.E., and Dick, J.E. (1992). Cytokine stimulation of multilineage hematopoiesis from immature human cells engrafted in SCID mice. Science *255*, 1137–1141.

Layton, D.S., Strom, A.D.G., O'Neil, T.E., Broadway, M.M., Stephenson, G.L., Morris, K.R., Muralitharan, M., Sandrin, M.S., Ierino, F.L., and Bean, A.G.D. (2007). Development of an anti-porcine CD34 monoclonal antibody that identifies hematopoietic stem cells. Exp. Hematol. *35*, 171–178.

Leary, H.L., and Lecce, J.G. (1978). Effect of feeding on the cessation of transport of macromolecules by enterocytes of neonatal piglet intestine. Biol. Neonate *34*, 174–176.

Lee, K., Kwon, D.-N., Ezashi, T., Choi, Y.-J., Park, C., Ericsson, A.C., Brown, A.N., Samuel, M.S., Park, K.-W., Walters, E.M., et al. (2014). Engraftment of human iPS cells and allogeneic porcine cells into pigs with inactivated RAG2 and accompanying severe combined immunodeficiency. Proc. Natl. Acad. Sci. U. S. A. *111*, 7260–7265.

Leonard, W. (1995). The molecular basis of X-linked severe combined immunodeficiency: defective cytokine receptor signaling. Annu. Rev. Med.

Li, L., Wu, L.P., and Chandrasegaran, S. (1992). Functional domains in Fok I restriction endonuclease. Proc. Natl. Acad. Sci. U. S. A. *89*, 4275–4279.

Lowry, P.A., Shultz, L.D., Greiner, D.L., Hesselton, R.M., Kittler, E.L., Tiarks, C.Y., Rao, S.S., Reilly, J., Leif, J.H., Ramshaw, H., et al. (1996). Improved engraftment of human cord blood stem cells in NOD/LtSz-scid/scid mice after irradiation or multiple-day injections into unirradiated recipients. Biol. Blood Marrow Transplant. *2*, 15–23.

Lunney, J.K. (2007). Advances in swine biomedical model genomics. Int. J. Biol. Sci. *3*, 179–184.

Mackall, C.L., Granger, L., Sheard, M.A., Cepeda, R., and Gress, R.E. (1993). T-cell regeneration after bone marrow transplantation: differential CD45 isoform expression on thymic-derived versus thymic-independent progeny. Blood *82*, 2585–2594.

Mackall, C.L., Fry, T.J., Bare, C., Morgan, P., Galbraith, A., and Gress, R.E. (2001). IL-7 increases both thymic-dependent and thymic-independent T-cell regeneration after bone marrow transplantation. Blood *97*, 1491–1497.

Mazurier, F., Doedens, M., Gan, O.I., and Dick, J.E. (2003). Rapid myeloerythroid repopulation after intrafemoral transplantation of NOD-SCID mice reveals a new class of human stem cells. Nat. Med. *9*, 959–963.

McBlane, J.F., van Gent, D.C., Ramsden, D.A., Romeo, C., Cuomo, C.A., Gellert, M., and Oettinger, M.A. (1995). Cleavage at a V(D)J recombination signal requires only RAG1 and RAG2 proteins and occurs in two steps. Cell *83*, 387–395.

McCune, J.M., Namikawa, R., Kaneshima, H., Shultz, L.D., Lieberman, M., and Weissman, I.L. (1988). The SCID-hu mouse: murine model for the analysis of human hematolymphoid differentiation and function. Science *241*, 1632–1639.

Melkus, M.W., Estes, J.D., Padgett-Thomas, A., Gatlin, J., Denton, P.W., Othieno, F.A., Wege, A.K., Haase, A.T., and Garcia, J.V. (2006). Humanized mice mount specific adaptive and innate immune responses to EBV and TSST-1. Nat. Med. *12*, 1316–1322.

Mestas, J., and Hughes, C.C.W. (2004). Of mice and not men: differences between mouse and human immunology. J. Immunol. *172*, 2731–2738.

Meurens, F., Summerfield, A., Nauwynck, H., Saif, L., and Gerdts, V. (2012). The pig: a model for human infectious diseases. Trends Microbiol. *20*, 50–57.

Mombaerts, P., Iacomini, J., Johnson, R.S., Herrup, K., Tonegawa, S., and Papaioannou, V.E. (1992). RAG-1-deficient mice have no mature B and T lymphocytes. Cell *68*, 869–877.

Moscou, M.J., and Bogdanove, A.J. (2009). A simple cipher governs DNA recognition by TAL effectors. Science *326*, 1501.

Mosier, D.E., Gulizia, R.J., Baird, S.M., and Wilson, D.B. (1988). Transfer of a functional human immune system to mice with severe combined immunodeficiency. Nature *335*, 256–259.

Murtaugh, M.P., Johnson, C.R., Xiao, Z., Scamurra, R.W., and Zhou, Y. (2009). Species specialization in cytokine biology: Is interleukin-4 central to the TH1-TH2 paradigm in swine? Dev. Comp. Immunol. *33*, 344–352.

Nechvatalova, K., Kudlackova, H., Leva, L., Babickova, K., and Faldyna, M. (2011). Transfer of humoral and cell-mediated immunity via colostrum in pigs. Vet. Immunol. Immunopathol. *142*, 95–100.

Nikolic, B., Gardner, J.P., Scadden, D.T., Arn, J.S., Sachs, D.H., and Sykes, M. (1999). Normal development in porcine thymus grafts and specific tolerance of human T cells to porcine donor MHC. J. Immunol. *162*, 3402–3407.

Noguchi, M., Yi, H., Rosenblatt, H.M., Filipovich, A.H., Adelstein, S., Modi, W.S., McBride, O.W., and Leonard, W.J. (1993). Interleukin-2 receptor ?? chain mutation results in X-linked severe combined immunodeficiency in humans. Cell *73*, 147–157.

Oettinger, M.A., Schatz, D.G., Gorka, C., and Baltimore, D. (1990). RAG-1 and RAG-2, adjacent genes that synergistically activate V(D)J recombination. Science *248*, 1517–1523.

Ogle, B.M., Knudsen, B.E., Nishitai, R., Ogata, K., and Platt, J.L. (2009). Toward development and production of human T cells in swine for potential use in adoptive T cell immunotherapy. Tissue Eng. Part A *15*, 1031–1040.

Ohbo, K., Suda, T., Hashiyama, M., Mantani, A., Ikebe, M., Miyakawa, K., Moriyama, M., Nakamura, M., Katsuki, M., Takahashi, K., et al. (1996). Modulation of hematopoiesis in mice with a truncated mutant of the interleukin-2 receptor gamma chain. Blood *87*, 956–967.

Okada, T., Miller, M.J., Parker, I., Krummel, M.F., Neighbors, M., Hartley, S.B., O'Garra, A., Cahalan, M.D., and Cyster, J.G. (2005). Antigen-engaged B cells undergo chemotaxis toward the T zone and form motile conjugates with helper T cells. PLoS Biol. *3*, e150.

Onishi, A., Iwamoto, M., Akita, T., Mikawa, S., Takeda, K., Awata, T., Hanada, H., and Perry, A.C. (2000). Pig cloning by microinjection of fetal fibroblast nuclei. Science *289*, 1188–1190.

Ozuna, a G.C., Rowland, R.R.R., Nietfeld, J.C., Kerrigan, M. a, Dekkers, J.C.M., and Wyatt, C.R. (2013). Preliminary findings of a previously unrecognized porcine primary immunodeficiency disorder. Vet. Pathol. *50*, 144–146.

Payne, K.J., and Crooks, G.M. (2002). Human hematopoietic lineage commitment. Immunol. Rev. *187*, 48–64.

Pearson, T., Shultz, L.D., Miller, D., King, M., Laning, J., Fodor, W., Cuthbert, a, Burzenski, L., Gott, B., Lyons, B., et al. (2008). Non-obese diabetic-recombination activating gene-1 (NOD-Rag1 null) interleukin (IL)-2 receptor common gamma chain (IL2r gamma null) null mice: a radioresistant model for human lymphohaematopoietic engraftment. Clin. Exp. Immunol. *154*, 270–284.

Pek, E.A., Chan, T., Reid, S., and Ashkar, A.A. (2011). Characterization and IL-15 dependence of NK cells in humanized mice. Immunobiology *216*, 218–224.

Petters, R.M., Alexander, C.A., Wells, K.D., Collins, E.B., Sommer, J.R., Blanton, M.R., Rojas, G., Hao, Y., Flowers, W.L., Banin, E., et al. (1997). Genetically engineered large animal model for studying cone photoreceptor survival and degeneration in retinitis pigmentosa. Nat. Biotechnol. *15*, 965–970.

Pflumio, F., Izac, B., Katz, A., Shultz, L.D., Vainchenker, W., and Coulombel, L. (1996). Phenotype and function of human hematopoietic cells engrafting immune-deficient CB17-severe combined immunodeficiency mice and nonobese diabetic-severe combined immunodeficiency mice after transplantation of human cord blood mononuclear cells. Blood *88*, 3731–3740.

Piriou-Guzylack, L., and Salmon, H. (2008). Membrane markers of the immune cells in swine: an update. Vet. Res.

Polejaeva, I. a, Chen, S.H., Vaught, T.D., Page, R.L., Mullins, J., Ball, S., Dai, Y., Boone, J., Walker, S., Ayares, D.L., et al. (2000). Cloned pigs produced by nuclear transfer from adult somatic cells. Nature *407*, 86–90.

Puck, J.M., Deschênes, S.M., Porter, J.C., Dutra, A.S., Brown, C.J., Willard, H.F., and Henthorn, P.S. (1993). The interleukin-2 receptor gamma chain maps to Xq13.1 and is mutated in X-linked severe combined immunodeficiency, SCIDX1. Hum. Mol. Genet. *2*, 1099–1104.

Qian, H., Buza-Vidas, N., Hyland, C.D., Jensen, C.T., Antonchuk, J., Månsson, R., Thoren, L.A., Ekblom, M., Alexander, W.S., and Jacobsen, S.E.W. (2007). Critical Role of Thrombopoietin in Maintaining Adult Quiescent Hematopoietic Stem Cells. Cell Stem Cell *1*, 671–684.

Ramer, P.C., Chijioke, O., Meixlsperger, S., Leung, C.S., and Munz, C. (2011). Mice with human immune system components as in vivo models for infections with human pathogens. Immunol. Cell Biol. *89*, 408–416.

Renard, C., Vaiman, M., Chiannilkulchai, N., Cattolico, L., Robert, C., and Chardon, P. (2001). Sequence of the pig major histocompatibility region containing the classical class I genes. Immunogenetics *53*, 490–500.

Renner, S., Fehlings, C., Herbach, N., Hofmann, A., von Waldthausen, D.C., Kessler, B., Ulrichs, K., Chodnevskaja, I., Moskalenko, V., Amselgruber, W., et al. (2010). Glucose intolerance and reduced proliferation of pancreatic beta-cells in transgenic pigs with impaired glucose-dependent insulinotropic polypeptide function. Diabetes *59*, 1228–1238.

Reyon, D., Tsai, S.Q., Khayter, C., Foden, J. a, Sander, J.D., and Joung, J.K. (2012). FLASH assembly of TALENs for high-throughput genome editing. Nat. Biotechnol. *30*, 460–465.

Rogers, C.S., Stoltz, D.A., Meyerholz, D.K., Ostedgaard, L.S., Rokhlina, T., Taft, P.J., Rogan, M.P., Pezzulo, A.A., Karp, P.H., Itani, O.A., et al. (2008a). Disruption of the CFTR gene produces a model of cystic fibrosis in newborn pigs. Science *321*, 1837–1841.

Rogers, C.S., Hao, Y., Rokhlina, T., Samuel, M., Stoltz, D.A., Li, Y., Petroff, E., Vermeer, D.W., Kabel, A.C., Yan, Z., et al. (2008b). Production of CFTR-null and CFTR-DeltaF508 heterozygous pigs by adeno-associated virus-mediated gene targeting and somatic cell nuclear transfer. J. Clin. Invest. *118*, 1571–1577.

Rongvaux, A., Takizawa, H., Strowig, T., Willinger, T., Eynon, E.E., Flavell, R. a, and Manz, M.G. (2013). Human hemato-lymphoid system mice: current use and future potential for medicine.

Rothkötter, H.-J. (2009). Anatomical particularities of the porcine immune system--a physician's view. Dev. Comp. Immunol. *33*, 267–272.

Roux, E., Dumont-Girard, F., Starobinski, M., Siegrist, C.A., Helg, C., Chapuis, B., and Roosnek, E. (2000). Recovery of immune reactivity after T-cell-depleted bone marrow transplantation depends on thymic activity. Blood *96*, 2299–2303.

Russell, S.M., Johnston, J.A., Noguchi, M., Kawamura, M., Bacon, C.M., Friedmann, M., Berg, M., McVicar, D.W., Witthuhn, B.A., and Silvennoinen, O. (1994). Interaction of IL-2R beta and gamma c chains with Jak1 and Jak3: implications for XSCID and XCID. Science *266*, 1042–1045.

Sang, Y., Ruchala, P., Lehrer, R.I., Ross, C.R., Rowland, R.R.R., and Blecha, F. (2009). Antimicrobial host defense peptides in an arteriviral infection: differential peptide expression and virus inactivation. Viral Immunol. *22*, 235–242.

Sanoh, S., Horiguchi, A., and Sugihara, K. (2012). Prediction of in vivo hepatic clearance and half-life of drug candidates in human using chimeric mice with humanized liver. Drug Metab. … *405*, 405–410.

Sarzotti, M., Patel, D.D., Li, X., Ozaki, D.A., Cao, S., Langdon, S., Parrott, R.E., Coyne, K., and Buckley, R.H. (2003). T cell repertoire development in humans with SCID after nonablative allogeneic marrow transplantation. J. Immunol. *170*, 2711–2718.

Sato, K., Ohtsuka, K., Hasegawa, K., Yamagiwa, S., Watanabe, H., Asakura, H., and Abo, T. (1995). Evidence for extrathymic generation of intermediate T cell receptor cells in the liver revealed in thymectomized, irradiated mice subjected to bone marrow transplantation. J. Exp. Med. *182*, 759–767.

Schoeberlein, A., Schatt, S., Troeger, C., Surbek, D., Holzgreve, W., and Hahn, S. (2004). Engraftment kinetics of human cord blood and murine fetal liver stem cells following in utero transplantation into immunodeficient mice. Stem Cells Dev. *13*, 677–684.

Schwarz, K., Gauss, G.H., Ludwig, L., Pannicke, U., Li, Z., Lindner, D., Friedrich, W., Seger, R.A., Hansen-Hagge, T.E., Desiderio, S., et al. (1996). RAG mutations in human B cell-negative SCID. Science *274*, 97–99.

Seok, J., Warren, H.S., Cuenca, A.G., Mindrinos, M.N., Baker, H. V, Xu, W., Richards, D.R., McDonald-Smith, G.P., Gao, H., Hennessy, L., et al. (2013). Genomic responses in mouse models poorly mimic human inflammatory diseases. Proc. Natl. Acad. Sci. U. S. A. *110*, 3507–3512.

Shi, W., Zakhartchenko, V., and Wolf, E. (2003). Epigenetic reprogramming in mammalian nuclear transfer. Differentiation *71*, 91–113.

Shimizu, I., Fudaba, Y., Shimizu, A., Yang, Y.-G., and Sykes, M. (2008). Comparison of human T cell repertoire generated in xenogeneic porcine and human thymus grafts. Transplantation *86*, 601–610.

Shinkai, Y., Rathbun, G., Lam, K.P., Oltz, E.M., Stewart, V., Mendelsohn, M., Charron, J., Datta, M., Young, F., and Stall, A.M. (1992). RAG-2-deficient mice lack mature lymphocytes owing to inability to initiate V(D)J rearrangement. Cell *68*, 855–867.

Shultz, L.D., Schweitzer, P.A., Christianson, S.W., Gott, B., Schweitzer, I.B., Tennent, B., McKenna, S., Mobraaten, L., Rajan, T. V, and Greiner, D.L. (1995). Multiple defects in innate and adaptive immunologic function in NOD/LtSz-scid mice. J. Immunol. *154*, 180–191.

Shultz, L.D., Lyons, B.L., Burzenski, L.M., Gott, B., Chen, X., Chaleff, S., Kotb, M., Gillies, S.D., King, M., Mangada, J., et al. (2005). Human Lymphoid and Myeloid Cell Development in NOD/LtSz-scid IL2R null Mice Engrafted with Mobilized Human Hemopoietic Stem Cells. J. Immunol. *174*, 6477–6489.

Shultz, L.D., Ishikawa, F., and Greiner, D.L. (2007). Humanized mice in translational biomedical research. Nat. Rev. Immunol. *7*, 118–130.

Shultz, L.D., Brehm, M. a, Garcia-Martinez, J.V., and Greiner, D.L. (2012). Humanized mice for immune system investigation: progress, promise and challenges. Nat. Rev. Immunol. *12*, 786–798.

Sinkora, M., and Butler, J.E. (2009). The ontogeny of the porcine immune system. Dev. Comp. Immunol. *33*, 273–283.

Spits, H., Lanier, L.L., and Phillips, J.H. (1995). Development of human T and natural killer cells. Blood *85*, 2654–2670.

Starzl, T., and Demetris, A. (1997). The future of transplantation: with particular reference to chimerism and xenotransplantation. Transplant. … *29*, 19–27.

Stepanova, H., Samankova, P., Leva, L., Sinkora, J., and Faldyna, M. (2007). Early postnatal development of the immune system in piglets: the redistribution of T lymphocyte subsets. Cell. Immunol. *249*, 73–79.

Stoltz, D.A., Rokhlina, T., Ernst, S.E., Pezzulo, A.A., Ostedgaard, L.S., Karp, P.H., Samuel, M.S., Reznikov, L.R., Rector, M. V, Gansemer, N.D., et al. (2013). Intestinal CFTR expression alleviates meconium ileus in cystic fibrosis pigs. J. Clin. Invest. *123*, 2685–2693.

Strowig, T., Chijioke, O., Carrega, P., Arrey, F., Meixlsperger, S., Rämer, P.C., Ferlazzo, G., and Münz, C. (2010). Human NK cells of mice with reconstituted human immune system components require preactivation to acquire functional competence. Blood *116*, 4158–4167.

Strowig, T., Rongvaux, A., Rathinam, C., Takizawa, H., Borsotti, C., Philbrick, W., Eynon, E.E., Manz, M.G., and Flavell, R.A. (2011). Transgenic expression of human signal regulatory protein alpha in Rag2-/- c-/- mice improves engraftment of human hematopoietic cells in humanized mice. Proc. Natl. Acad. Sci. *108*, 13218–13223.

Suematsu, S., and Watanabe, T. (2004). Generation of a synthetic lymphoid tissue-like organoid in mice. Nat. Biotechnol. *22*, 1539–1545.

Suemizu, H., Hasegawa, M., Kawai, K., Taniguchi, K., Monnai, M., Wakui, M., Suematsu, M., Ito, M., Peltz, G., and Nakamura, M. (2008). Establishment of a humanized model of liver using NOD/Shi-scid IL2Rgnull mice. Biochem. Biophys. Res. Commun. *377*, 248–252.

Sugamura, K., Asao, H., Kondo, M., Tanaka, N., Ishii, N., Ohbo, K., Nakamura, M., and Takeshita, T. (1996). The interleukin-2 receptor gamma chain: its role in the multiple cytokine receptor complexes and T cell development in XSCID. Annu Rev Immunol *14*, 179–205.

Summerfield, A., and McCullough, K.C. (2009). The porcine dendritic cell family. Dev. Comp. Immunol. *33*, 299–309.

Sun, H.F., Ernst, C.W., Yerle, M., Pinton, P., Rothschild, M.F., Chardon, P., Rogel-Gaillard, C., and Tuggle, C.K. (1999). Human chromosome 3 and pig chromosome 13 show complete synteny conservation but extensive gene-order differences. Cytogenet. Cell Genet. *85*, 273–278.

Suzuki, S., Iwamoto, M., Saito, Y., Fuchimoto, D., Sembon, S., Suzuki, M., Mikawa, S., Hashimoto, M., Aoki, Y., Najima, Y., et al. (2012). Il2rg gene-targeted severe combined immunodeficiency pigs. Cell Stem Cell *10*, 753–758.

Takao, K., and Miyakawa, T. (2014). Genomic responses in mouse models greatly mimic human inflammatory diseases. Proc. Natl. Acad. Sci. 1–6.

Tan, W., Carlson, D.F., Lancto, C.A., Garbe, J.R., Webster, D.A., Hackett, P.B., and Fahrenkrug, S.C. (2013). Efficient nonmeiotic allele introgression in livestock using custom endonucleases. Proc. Natl. Acad. Sci. U. S. A. *110*, 16526–16531.

Tanabe, T., Sato, H., Watanabe, K., Hirano, M., Hirose, K., Kurokawa, S., Nakano, K., Saito, H., and Maehara, N. (1996). Correlation between occurrence of exudative epidermitis and exfoliative toxin-producing ability of Staphylococcus hyicus. Vet. Microbiol. *48*, 9–17.

Tateno, C., Yoshizane, Y., Saito, N., Kataoka, M., Utoh, R., Yamasaki, C., Tachibana, A., Soeno, Y., Asahina, K., Hino, H., et al. (2004). Near completely humanized liver in mice shows human-type metabolic responses to drugs. Am. J. Pathol. *165*, 901–912.

Traggiai, E., Chicha, L., Mazzucchelli, L., Bronz, L., Piffaretti, J.-C., Lanzavecchia, A., and Manz, M.G. (2004). Development of a human adaptive immune system in cord blood cell-transplanted mice. Science *304*, 104–107.

Uchida, M., Shimatsu, Y., Onoe, K., Matsuyama, N., Niki, R., Ikeda, J.E., and Imai, H. (2001). Production of transgenic miniature pigs by pronuclear microinjection. Transgenic Res. *10*, 577–582.

Unger, W.W.J., Pearson, T., Abreu, J.R.F., Laban, S., van der Slik, A.R., Mulder-van der Kracht, S., Kester, M.G.D., Serreze, D. V., Shultz, L.D., Griffioen, M., et al. (2012). Islet-Specific CTL Cloned from a Type 1 Diabetes Patient Cause Beta-Cell Destruction after Engraftment into HLA-A2 Transgenic NOD/SCID/IL2RG Null Mice. PLoS One *7*.

Villa, A., Santagata, S., Bozzi, F., Giliani, S., Frattini, A., Imberti, L., Gatta, L.B., Ochs, H.D., Schwarz, K., Notarangelo, L.D., et al. (1998). Partial V(D)J recombination activity leads to omenn syndrome. Cell *93*, 885–896.

De Villartay, J.-P., Poinsignon, C., de Chasseval, R., Buck, D., Le Guyader, G., and Villey, I. (2003). Human and animal models of V(D)J recombination deficiency. Curr. Opin. Immunol. *15*, 592–598.

Walker, S.C., Shin, T., Zaunbrecher, G.M., Romano, J.E., Johnson, G. a, Bazer, F.W., and Piedrahita, J. a (2002). A highly efficient method for porcine cloning by nuclear transfer using in vitro-matured oocytes. Cloning Stem Cells *4*, 105–112.

Watanabe, M., Nakano, K., Matsunari, H., Matsuda, T., Maehara, M., Kanai, T., Kobayashi, M., Matsumura, Y., Sakai, R., Kuramoto, M., et al. (2013). Generation of interleukin-2 receptor gamma gene knockout pigs from somatic cells genetically modified by zinc finger nuclease-encoding mRNA. PLoS One *8*, e76478.

Wernersson, R., Schierup, M.H., Jørgensen, F.G., Gorodkin, J., Panitz, F., Staerfeldt, H.-H., Christensen, O.F., Mailund, T., Hornshøj, H., Klein, A., et al. (2005). Pigs in sequence space: a 0.66X coverage pig genome survey based on shotgun sequencing. BMC Genomics *6*, 70.

Williams, K.M., Hakim, F.T., and Gress, R.E. (2007). T cell immune reconstitution following lymphodepletion. Semin. Immunol. *19*, 318–330.

Willinger, T., Rongvaux, A., Strowig, T., Manz, M.G., and Flavell, R. a (2011). Improving human hemato-lymphoid-system mice by cytokine knock-in gene replacement. Trends Immunol. *32*, 321–327.

Wolf, E., Schernthaner, W., Zakhartchenko, V., Prelle, K., Stojkovic, M., and Brem, G. (2000). Transgenic technology in farm animals--progress and perspectives. Exp. Physiol. *85*, 615–625.

Zanjani, E.D., Pallavicini, M.G., Ascensao, J.L., Flake, a W., Langlois, R.G., Reitsma, M., MacKintosh, F.R., Stutes, D., Harrison, M.R., and Tavassoli, M. (1992). Engraftment and long-term expression of human fetal hemopoietic stem cells in sheep following transplantation in utero. J. Clin. Invest. *89*, 1178–1188.

Zanjani, E.D., Flake, a W., Rice, H., Hedrick, M., and Tavassoli, M. (1994). Long-term repopulating ability of xenogeneic transplanted human fetal liver hematopoietic stem cells in sheep. J. Clin. Invest. *93*, 1051–1055.

APPENDIX

Materials and Methods.

TALEN Design and Construction. The design and construction of TALENs targeting *IL2RG* and *RAG1* was performed according to the protocol for the fast ligation-based automatable solid-phase high-throughput (FLASH) system described in (Reyon et al., 2012) and as summarized in Figure 54. In brief, the online ZiFiT software suite (http://zifit.partners.org) was queried to identify TALEN sequences from the ZiFiT database that will bind and mutate the target sequence. ZiFiT returns the unique FLASH IDs and linear ordering of individual modular units which are assembled to build TALENs with a customized binding specificity. The target sequences for *IL2RG* and *RAG1* and corresponding FLASH IDs of the individual units for TALEN assembly used in this study are shown in Table 7.

Pig Oocyte Collection and Maturation: Preparation for Nuclear Transfer. All chemicals were purchased from Sigma (St. Louis, MO) unless otherwise specified. Ovaries were retrieved from commercial/occidental breed sows at a slaughterhouse located one hour from the laboratory transported in 0.9% saline solution at 30–35°C. Follicular fluid from 3 to 6 mm antral follicles was aspirated with an 18 G needle attached to a 10 mL syringe. Cumulus-oocyte complexes (COCs) with uniform cytoplasm and several layers of cumulus cells were selected and rinsed twice in washing medium (Tyrode's lactate-buffered HEPES supplemented with 0.1% polyvinyl alcohol) and three times in basic maturation medium (TC199-HEPES medium supplemented with 10% porcine follicular fluid, 5 μg/ml insulin, 10 ng/ml EGF, 0.6 mM cysteine, 0.2 mM pyruvate, 25 μg/ml kanamycin). Approximately 50 to 70 COCs per well were cultured in 4-well Nunclon dishes containing 500 μl TC199-Hepes

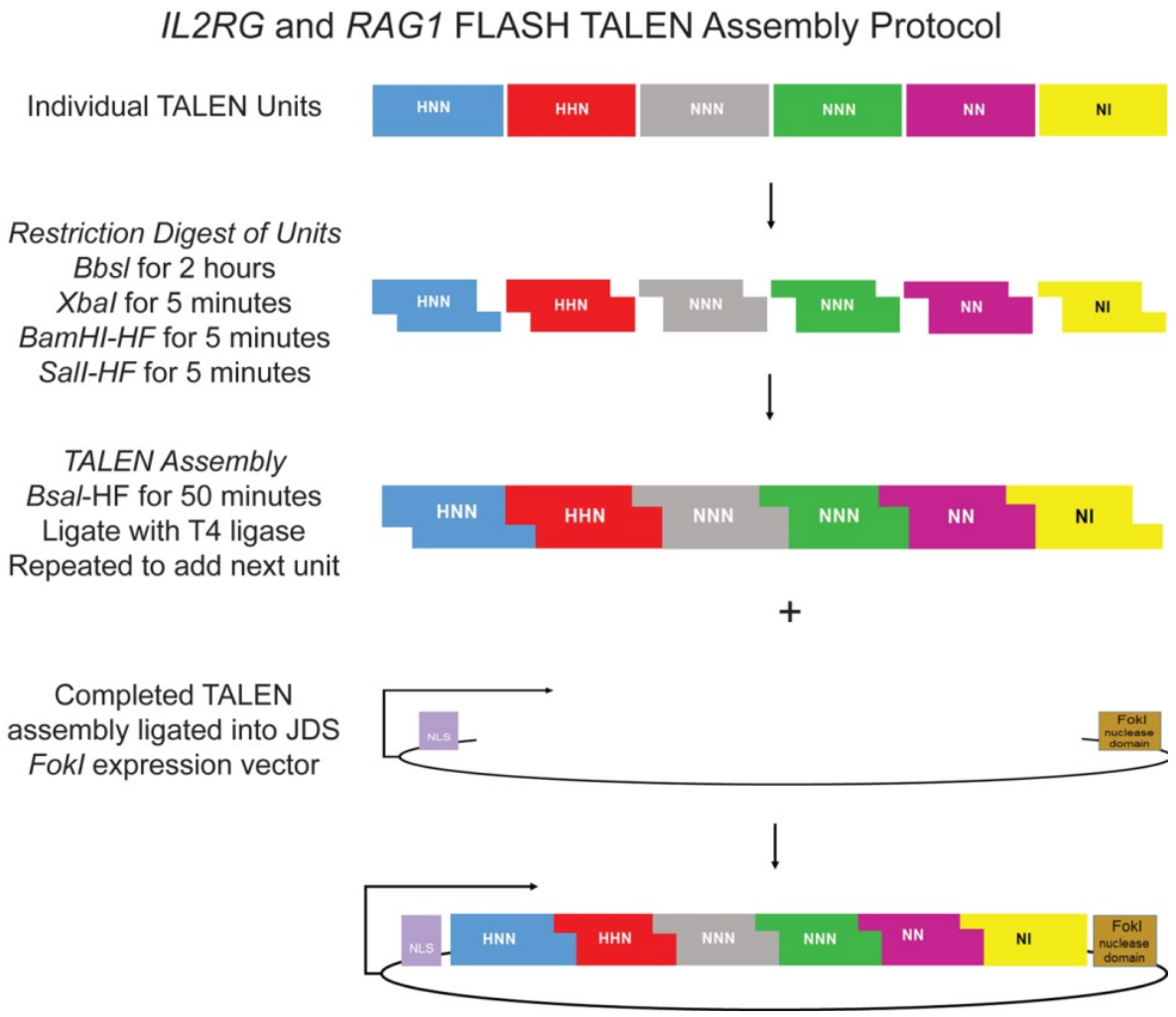

Fig. 54. Schematic of FLASH TALEN assembly.
Individual TALEN units, each encoded by a unique FLASH ID, are selected from a database and arranged in order based on analysis of the target sequence. The individual units are digested by restriction enzymes in the order shown; the initial digestion products bear sticky ends that are non-complementary. The first (5'-most) TALEN unit is ligated via its 5' end to a magnetic bead (not shown). The 3' end of the first unit is digested with *BsaI*-HF, which can hybridize with the 5' end of the second unit. The first and second units are then joined by T4 ligase, yielding a new 3' end for repeat rounds of *BsaI*-HF digestion and ligation of subsequent TALEN units. Finally, the assembled TALEN is ligated into the *FokI* expression vector, yielding the TALEN fusion protein containing the DNA recognition domain and the *FokI* endonuclease domain. A 5' and 3' TALEN pair is required for each desired cleavage target site. Adapted from (Reyon et al., 2012).

Table 7. FLASH TALEN target sequences and units.
Sequences are 5' to 3'. (*A*) TALEN target sequences and spacer regions for *IL2RG* and *RAG1*. (*B*) FLASH IDs and order of individual units used for TALEN assembly.

A

	Left binding	Spacer region	Right binding
IL2RG	TCTGCTGGGGGTGGGACT	GAACCCGAAGGTCCTC	ACGCACAGTGGGAATGAA
RAG1	TCCCAGGTACCTCAGCCA	GCATGGCTGTCTCTTT	GCCACCCACTCTGGGA

B

	Left FLASH TALENs	Right FLASH TALENS
IL2RG	374-232-171-187-306 JDS78	376-80-85-124-311 JDS78
RAG1	374-83-178-117-310 JDS70	374-83-47-175-371 JDS71

medium supplemented with 10% porcine follicular fluid (pFF), 5 µg/ml insulin, 10 ng/ml EGF, 0.6 mM cysteine, 0.2 mM pyruvate, 25 µg/ml kanamycin and 5 IU/ml each of eCG and hCG, covered with mineral oil. The oocytes are matured for 40-42 hours at 38.5 ^{o}C, 5% CO_2 in a humidified atmosphere.

Somatic Cell Nuclear Transfer (SCNT). Cumulus cells were removed from the oocytes by vortexing for 5 min in 0.1% bovine testicular hyaluronidase. Oocytes were incubated in manipulation media (Ca-free NCSU-23 with 5% FBS) containing 5 µg/ml bisbenzimide and 7.5 µg/ml cytochalasin B for 5 min. Following this incubation period, oocytes were enucleated by removing the first polar body and metaphase II plate and one single cell was

fused to each enucleated oocyte. Fusion/activation was induced by two DC pulses of 140 V for 40 μsec in 280 mM mannitol, 0.001 mM $CaCl_2$, and 0.05 mM $MgCl_2$. After fusion/activation, oocytes were placed back in NCSU-23 medium with 0.4% BSA and cultured at 38.5°C, 5% CO_2 in a humidified atmosphere, before being surgically transferred into the recipient.

Production of Pigs Carrying Targeted Mutations of IL2RG and RAG1. SCID piglets were generated via somatic cell nuclear transfer (SCNT) of primary porcine male fetal fibroblasts, which were transfected with TALENs targeting the IL2RG genomic locus. An eGFP indicator plasmid was co-transfected to assess TALEN activity and enrich for genetically modified cells by fluorescence activated cell sorting (FACS). Genomic DNA restriction screening by PCR and sequencing were used to verify the *IL2RG*$^{-/Y}$ genotype. The sequences of the PCR primers and corresponding PCR products used for colony screening are shown in Table 8. Cells with a mutated IL2RG locus were expanded from single cells and cloned via SCNT. *IL2RG*$^{-/Y}$ cell lines were generated from day 42 fetuses. The *IL2RG*$^{-/Y}$ cells were then cotransfected with RAG1 TALENs and eGFP indicator plasmid and screened to produce *IL2RG*$^{-/Y}$ *RAG1*$^{-/+}$ and *IL2RG*$^{-/Y}$ *RAG1*$^{-/-}$ fibroblasts. Genotypes of the *IL2RG*$^{-/Y}$ *RAG1*$^{-/+}$ and *IL2RG*$^{-/Y}$ *RAG1*$^{-/-}$ piglets were verified by gDNA restriction screening and sequencing. Western blotting of total protein from spleen samples was used to assess IL2RG and RAG1 protein expression in the *IL2RG*$^{-/Y}$ *RAG1*$^{-/+}$ and *IL2RG*$^{-/Y}$ *RAG1*$^{-/-}$ piglets.

Animal Care. Newborn piglets were housed with their mothers in an indoor clean environment. Piglets were fed from their mother's colostrum; if the mother was no longer producing colostrum, piglets were fed with formula. Piglets were given routine doses of

gentamycin and Excede for antimicrobial prophylaxis. Treatment with Baytril was added when piglets showed signs of infection. Animals handlers wore full body personal protective equipment with a face mask whenever they entered the animal housing area. All experiments involving animals were approved by the North Carolina State College of Veterinary Medicine Institutional Animal Care and Use Committee (IACUC Protocol 11-119-B).

Table 8. PCR primer and PCR product sequences for screening of TALEN-mediated genomic mutations in the *IL2RG* and *RAG1* loci.

	Primer sequence	PCR product
IL2RG	Left: CTGGTCTGGATTAGGTCAGAGG Right: CTCTTCCCTTCTCATACCA	CTGGTCTGGATTAGGTCAGAGGAAAGAGCTATAGATGTG CCCACAGGAGCCAAGACTGTATGTTTCATCTGGCCAAGA CAGTAGAGCTTTGATAGTGGTGTCAGTGTGATTGAGCCA AGGAAGGGGCATAGCATAGGATAGGGGGAGGTTCAGAC CCTCCACTACATGGGATTAAATAATTTAGAAGAGAGGTGG TTGGGAATGGTGGTGGTGGTGAACACATCCTTCCTGGG ATCTAGGTGGTCTGAGGATTTTTGAGCCTGTGACGATATT GGATACCCAGCTTTCGTCTCTGCTTAATACCGGTTACAGT GGTGGGGTTACATCTACAAATTAGATTAACACCTAATCTC CCAGAGGATTTAGCCTGTGTCATAGCATACATTGGCCACA CCCTCTTGTAAAGCCCTGGTTTCTAAGGTTCTTTCCACC GGAAGTCATGACAAAAGGAAATGTGTGGGTGGGGAGGG GTAGTGGGTAAGGGGCCCAGGTTCCTGACACAGTCTAC ACCCAGGAAACAAGGAGTAAGCGCCATGTTGAAGCCAC CATTGCCAGTCAAATCCCTCTTATTCCTGCAGCTGCCTCT GCTGGGGGTGGGACTGAACCCGAAGGTCCTCACGCAC AGTGGGAATGAAGACATCACAGCTGGTGGGAAACTGGG ACGTTGGGGGTAGGGTTGGTGAGCCGGGGGAGGCTGG CTGTGGGAAGGGGTCGTATAGAATTCTGGAACCTGCCAC TGGACTATTAGAAGGATGTGGGCAAAATTTTAGAGTACTG GGGGGAGGGCAAGGGGAAGGGTTCCCTGCCTAGTGCT GCTTCTTCTTCTGACCATCATGTCTTCCCTTTGCCTCCCC CACTTCATTTTCTCCCCGTCCTAGATTTCCTCCTGCTCTC TACACCCCCTGGGACTCTCAACGTTTCCACTCTACCCCT CCCAAAGGTTCAGTGTTTTGTGTTCAATGTTGAGTACATG AATTGCACTTGGAACAGCAGCTCTGAGCTCCAGCCTACC AACCTAACTCTGCACTACTGGTATGAGAAGGGAAGAG
RAG1	Left: CGGTATTGCCATGATCTGTG Right: CTCTTGCTTTCCCATCTTCG	CGGTATTGCCATGATCTGTGGTGTAGGTCGCAGATGCGG CTCAGGTCCCAAGCGGTTGTGGCTCTGGCGTAGGCCGG CGGCTGCAGCTCCCCTAGCCTGGGAACCTCTGTGTGCT GGTTCTGGAAAAAGGCAAAAAAGACAAAAAAATAAAATAA ATAATAAAATAAAATAAAAAATAAATGAATAATTGAATGTAC TAATTGGTATTCCTTCCAAGTTGCATCAGTGGGTTATTTAC ATTTTTTCCTAACCTGACTTGTCCTTATTGCTCCCAGGTA CCTCAGCCAGCATGGCTGTCTCTTTGCCACCCACTCTGG GACTCAGTTCCGCCCCAGATGAAATCCAGCACCCCCAC ATTAAATTTTCAGAATGGAAGTTTAAGCTATTCAGGGTGA GATCCTTTGAAAAGGCACCTGAAAAGGCTCAAACGGAAA AGCAGGATTCCTCCGAGGGGAAACCCTCGCTGGAGCAA TCTCCAGCAGTCCTGGACAAGCCTGGTGGTCAGAAGTC AGCCCTGCCTCAACCAGCATTCAAGCCCCATCCAAAGTT TTTAAAGGAATCCCACGAAGATGGGAAAGCAAGAG

Allogeneic Bone Marrow Transplantation into SCID Pigs. Donor pig bone marrow (BM) was aspirated from the proximal tibia and/or tuber coxae of male boars carrying either a Cre or H2B-GFP transgene. Leukocytes were purified from the donor BM using Ficoll-Paque. T cells were depleted from the bone marrow cell suspension following incubation with biotinylated anti-pig CD3 antibodies and removal using anti-biotin paramagnetic MicroBeads according to the manufacturer's protocol (Miltenyi Biotec). On postnatal day 2, prospective transplant recipient pigs were pretreated with butorphanol 0.05 mg/kg, midazolam 0.5 mg/kg, and/or ketamine 10 mg/kg depending on the amount of sedation needed for the pig to tolerate the procedure. T cell-depleted porcine bone marrow was resuspended in normal saline with penicillin and injected intraosseously at three sites – the left and right femur and the right tibia – with 1.33 x 10^7 cells per site, for a total of 4 x 10^7 cells per pig. On the day of transplant, a subgroup of pigs also underwent total body irradiation at 0.5 Gy/min up to a total dose of 1.6 Gy.

Human CD34+ Cell Transplantation into SCID Pigs by Intraosseous Injection. Donor human mobilized peripheral blood was obtained from volunteers treated with GM-CSF to increase the yield of hematopoietic progenitors prior to blood collection. Freshly collected mobilized human cells were flash-frozen for downstream applications. On the day of transplant (postnatal day 2), aliquots of human mobilized peripheral blood were rapidly warmed at 37 ^{O}C. Leukocytes were purified using Ficoll-Paque and CD34+ cells were purified from the human mobilized peripheral blood suspension using the CD34 MicroBead UltraPure Kit (Miltenyi Biotec) according to the manufacturer's instructions. CD34-enriched human cells was resuspended in normal saline with penicillin and injected intraosseously at

three sites – the left and right femur and the right tibia – with 8.3 x 10^6 cells per site, for a total of 2.48 x 10^7 cells per pig. On the day of transplant, a subgroup of pigs also underwent total body irradiation at 0.5 Gy/min up to a total dose of 1.6 Gy. On postnatal day 14, another subgroup of pigs was treated with a single dose of subcutaneous filgrastim (Neupogen) at 10 μg/kg.

Human CD34+ Cell Transplantation into SCID Pigs by *In Utero* Intrahepatic Injection. CD34-enriched human cells was prepared for transplantation as detailed above. Pregnant sows at 42 days gestation carrying *IL2RG*$^{-/Y}$ *RAG1*$^{-/-}$ fetuses were brought to the surgical suite for monitoring and anesthetized with halothane. The ventral midline region was prepped and draped in the usual sterile fashion. A ventral midline incision was performed to exteriorize the pregnant uterus. Intrahepatic injection of CD34-enriched human cells was performed under live ultrasound guidance using a SonoSite TITAN with a 5 MHz curvilinear probe and a sterile NeoGuard transducer cover (CIVCO). The injections were performed using a 25 G, 3.5 inch spinal needle (BD) with direct ultrasound visualization of the injected marrow entering the fetal liver.

Gross Pathology, Histology, and Organ Cell Suspensions. Following euthanasia of WT and mutant pigs, a complete autopsy was performed with special attention paid to the thymus, spleen, and lymph nodes. The thymus or thymic remnant was photographed *in situ* prior to removal. The body and organ weights were recorded. For all pigs, the cranial mediastinum and caudal cervical region was carefully examined for thymic tissue. Tissue from the thymus (or thymic remnant) and spleen was excised, fixed in 10% neutral buffered formalin, processed into paraffin, sectioned, and stained for microscopic examination by

routine hematoxylin and eosin staining or immunohistochemistry. Histological assessments were conducted by a veterinary pathologist blinded to genotype. To generate organ-derived single cell suspensions, 1 g of tissue was placed in a 15 ml conical with 3 ml of HBSS and triturated with cotton swabs to create a homogenous suspension. The suspension was then filtered sequentially through a 100 micron followed by a 70 micron cell strainer and pelleted by centrifugation prior to flow cytometric analysis (see below).

Cell Preparation and Staining for Flow Cytometry and Fluorescence Activated Cell Sorting. Blood from the external jugular vein was collected into EDTA-containing tubes. Plasma was separated by centrifugation and stored in aliquots at -20 ^{O}C for later ELISA analysis (see below). Cell pellets from whole blood, organ-derived single cell suspensions, or bone marrow aspirates were resuspended with antibody diluted in staining buffer and incubated at 4 ^{O}C for 1 hour. Antibodies specific for porcine CD3, CD4, CD8, SWC3, CD45RA, and CD16 were used to identify T, B, and NK lymphocytes. The cell suspension was then mixed with FACS lysis buffer and incubated for 10 minutes on a shaker at room temperature. The stained cells were pelleted by centrifugation, washed once with HBSS, then resuspended in staining buffer and stored at 4 ^{O}C in the dark until ready for flow cytometric analysis.

Immunoglobulin ELISAs. ELISA plates were coated at 10 μg/ml with antibody targeting the Ig of interest (goat anti-swine IgM, goat anti-swine IgG, goat anti-swine IgA, goat anti-human IgM) (Bethyl Labs) in carbonate bicarbonate buffer, pH 9.5, and incubated overnight at 4 ^{O}C. Plates were washed three times with PBS-T and blocked with 1% BSA in PBS-T for 2 hours at room temperature. Plates were washed once with PBS-T, then incubated with

stored plasma samples diluted 1:2000 or pooled pig sera (to calculate a standard curve) for 2 hours at room temperature. Plates were washed five times with PBS-T, then incubated for 1 hour at room temperature with the appropriate HRP-conjugated antibody targeting the antigen of interest and 10% normal goat serum (Gemini Bioproducts) in PBS-T. Plates were washed five times with PBS-T, then incubated with ABTS substrate (KPL) for 16 hours. Absorbance at 405 nm was measured on a plate reader with the Ig concentration calculated using the standard curve.

Statistical Analysis. Statistical significance was tested either by Student's *t*-test or Fisher's exact test. The *p* value for each comparison is included in the figure legends.